

*The Geological Society of America*  
*Memoir 74*

---

ORIGIN OF GRANITE  
IN THE LIGHT OF EXPERIMENTAL  
STUDIES IN THE SYSTEM  
 $\text{NaAlSi}_3\text{O}_8\text{--KAlSi}_3\text{O}_8\text{--SiO}_2\text{--H}_2\text{O}$

BY  
O. F. TUTTLE and N. L. BOWEN



---

November 21, 1958  
Reprinted 1960

*Made in the United States of America*

*The Memoir Series  
of  
The Geological Society of America  
is made possible  
through the bequest of  
Richard Alexander Fullerton Penrose, Jr.*

PRINTED BY WAVERLY PRESS, INC.  
BALTIMORE, MD.

PUBLISHED BY THE GEOLOGICAL SOCIETY OF AMERICA  
Address all communications to The Geological Society of America  
419 West 117 Street, New York 27, N. Y.

## PREFACE

This paper represents the fruit of approximately 5 years of experimental studies at the Geophysical Laboratory. When Bowen and I were contemplating this study while I was still on the staff at the Naval Research Laboratory and he at the University of Chicago, the need for it was made apparent by some results on experimental studies on obsidian-H<sub>2</sub>O which I had carried out at the Geophysical Laboratory a few months before. The results were of great importance if equilibrium were attained, but of little significance if only metastability were involved (I had heated obsidian in the presence of water, and relatively large amounts, as much as 30 per cent, apparently went into the obsidian powder at approximately 500°C. and 30,000 psi.). As we had no knowledge of the effect of water on equilibrium relations in such compositions we decided to direct our efforts toward a study of the system NaAlSi<sub>3</sub>O<sub>8</sub>-KAlSi<sub>3</sub>O<sub>8</sub>-SiO<sub>2</sub>-H<sub>2</sub>O. It was apparent that we would have to develop new experimental methods if we were to make progress in water-silicate mixtures. The hydrothermal quenching apparatus was therefore developed after many unsuccessful experiments with various types of pressure vessels then available.

Once the hydrothermal quenching apparatus was perfected we were able to begin studies on the granite-water system. As the three bounding binary systems were unknown we had first to study these. The NaAlSi<sub>3</sub>O<sub>8</sub>-KAlSi<sub>3</sub>O<sub>8</sub>-H<sub>2</sub>O system was the first, and results of this and various papers dealing with polymorphism in the feldspars, which came as by-products of these studies, have been published.

The remainder of our equilibrium studies is brought together here.

This study received a tragic blow when Bowen's health prevented him from taking an active part in the presentation and analysis of the data. However, the credit for the major contributions in this Memoir must go to Bowen, whereas I must assume full responsibility for any shortcomings in the presentation and application of the experimental results.

Unfortunately, the lucid and oft'times humorous presentation which characterizes the writing of Bowen is lacking here. I trust, however, that the controversial nature of the topics covered will provide the necessary spur to hold the reader's interest.

We are indebted to Drs. L. H. Adams and Philip H. Abelson, Directors of the Geophysical Laboratory—to the former for support of the experimental studies, and to the latter for generous support and encouragement during the difficult period while the manuscript was being prepared. I should also like to express our thanks to our colleagues at the Geophysical Laboratory without whose advice and friendly criticism this work would not have been completed. We are especially indebted to Drs. F. Chayes, W. S. MacKenzie, C. E. Tilley, and J. V. Smith for reading the first draft of the manuscript and making numerous suggestions which have greatly improved the presentation. I also wish to express particular appreciation for the many hours which Dr. J. W. Greig spent with me discussing phase-equilibrium relations in ternary systems. Finally, we are indebted to Dr. J. F. Schairer for making many runs for us and for permitting us to use the synthetic mixtures which made this study possible.

PENNSYLVANIA STATE UNIVERSITY  
DECEMBER 27, 1954

O. F. TUTTLE



# CONTENTS

	Page
ABSTRACT.....	1
INTRODUCTION.....	5
EXPERIMENTAL METHODS.....	6
Preparation of mixtures.....	6
Pressure measurement and control.....	8
Temperature measurement and control.....	8
Hydrothermal quenching apparatus.....	8
Cold-seal pressure vessel.....	10
Composition of feldspars by the (201) spacings.....	10
Determination of liquidus and solidus relations.....	11
Water determination.....	13
CRYSTALLINE PHASES.....	14
Albite.....	14
Orthoclase.....	16
Phase relations in the system $\text{NaAlSi}_3\text{O}_8$ - $\text{KAlSi}_3\text{O}_8$ .....	17
Silica.....	28
SYSTEM $\text{SiO}_2$ - $\text{H}_2\text{O}$ .....	31
SYSTEM $\text{NaAlSi}_3\text{O}_8$ - $\text{H}_2\text{O}$ .....	35
SYSTEM $\text{KAlSi}_3\text{O}_8$ - $\text{H}_2\text{O}$ .....	36
SYSTEM $\text{NaAlSi}_3\text{O}_8$ - $\text{KAlSi}_3\text{O}_8$ - $\text{H}_2\text{O}$ .....	37
Introductory remarks.....	37
Complete series of solid solutions at high temperatures.....	38
Equilibrium relations at various pressures of water vapor.....	39
Leucite field.....	41
Solvus.....	42
Behavior of natural alkali feldspars.....	43
General considerations of equilibrium.....	45
Isobars and isotherms on the saturation surfaces and courses of crystallization.....	45
Petrologic considerations.....	48
SYSTEM $\text{NaAlSi}_3\text{O}_8$ - $\text{SiO}_2$ - $\text{H}_2\text{O}$ .....	50
SYSTEM $\text{KAlSi}_3\text{O}_8$ - $\text{SiO}_2$ - $\text{H}_2\text{O}$ .....	53
SYSTEM $\text{NaAlSi}_3\text{O}_8$ - $\text{KAlSi}_3\text{O}_8$ - $\text{SiO}_2$ - $\text{H}_2\text{O}$ .....	54
Introduction.....	54
Isobaric crystallization.....	63
Isothermal crystallization.....	67
Adiabatic crystallization.....	69
Stability fields on the liquidus at various pressures.....	70
Isobaric minimum on the quartz-feldspar boundary.....	73
GRANITES, RHYOLITES, AND THE ISOBARIC MINIMA.....	75
BEGINNING OF THE MELTING OF THE WESTERLY, RHODE ISLAND, AND QUINCY, MASSACHUSETTS, GRANITES IN THE PRESENCE OF WATER VAPOR UNDER PRESSURE.....	80
CHARACTER OF RESIDUAL SOLUTIONS FORMED BY CRYSTALLIZING HYDROUS GRANITIC LIQUIDS.....	84
General considerations.....	84
Theoretical considerations.....	84
Portion of the system $\text{K}_2\text{O}$ - $\text{Al}_2\text{O}_3$ - $\text{SiO}_2$ - $\text{H}_2\text{O}$ .....	85
System $\text{Na}_2\text{O}$ - $\text{Al}_2\text{O}_3$ - $\text{SiO}_2$ - $\text{H}_2\text{O}$ .....	86
System $\text{K}_2\text{O}$ - $\text{Na}_2\text{O}$ - $\text{Al}_2\text{O}_3$ - $\text{SiO}_2$ .....	87
Alkali-alumina ratio in analyzed granitic rocks.....	88
Discussion.....	89
COMPOSITION OF THE VAPOR IN EQUILIBRIUM WITH HYDROUS GRANITIC MELTS.....	89



STABILITY OF THE AMPHIBOLES .....	91
Anthophyllite .....	91
Grunerite .....	92
Riebeckite .....	92
Amphibole from the Quincy granite .....	92
Discussion .....	92
WIBORGITE RAPAKIVI GRANITE IN THE LIGHT OF THE EQUILIBRIUM RELATIONS IN THE SYSTEM $\text{NaAlSi}_3\text{O}_8$ - $\text{KAlSi}_3\text{O}_8$ - $\text{SiO}_2$ - $\text{H}_2\text{O}$ .....	93
Previous views on the genesis of the rapakivi texture .....	93
Origin of ovoid alkali feldspar .....	95
Large size of the alkali feldspar .....	95
Origin of mantled feldspar .....	96
Origin of two generations of quartz and feldspar in rapakivi granites .....	97
Discussion .....	98
TERTIARY GRANITES OF SKYE .....	98
General discussion .....	98
Mineralogy .....	101
Modal analyses of Skye granites .....	109
Normative albite-orthoclase-quartz of Skye granites .....	116
Discussion .....	116
GEOTHERMAL GRADIENTS AND GRANITE MAGMAS .....	117
Introductory statement .....	117
Measured geothermal gradients .....	118
Temperature of the beginning of melting .....	121
Depth of the beginning of melting .....	122
Depth of complete melting .....	122
Zone of melting .....	123
Some restrictions on the movement of hydrous granite magmas .....	125
Discussion .....	125
CLASSIFICATION OF SALIC ROCKS .....	126
FELDSPAR CRYSTALLIZATION IN RHYOLITES, TRACHYTES, AND PHONOLITES .....	130
Feldspar equilibria .....	130
Solid solution in the system $\text{NaAlSi}_3\text{O}_8$ - $\text{KAlSi}_3\text{O}_8$ - $\text{CaAl}_2\text{Si}_2\text{O}_8$ .....	131
Crystallization in the system $\text{NaAlSi}_3\text{O}_8$ - $\text{KAlSi}_3\text{O}_8$ - $\text{CaAl}_2\text{Si}_2\text{O}_8$ .....	131
Effect of composition on the extent of solid solution .....	135
Summary .....	137
EVOLUTION OF THE GRANITIC TEXTURE .....	137
REFERENCES CITED .....	143
INDEX .....	147

## ILLUSTRATIONS

## PLATES

Plate	Following page
1. Intergrowths in sulfides and feldspars .....	138
2. Granite from Madoc, Ontario .....	
3. Granite from Westerly, Rhode Island .....	
4. Beinn an Dubhaich granite, Skye, Scotland .....	140
5. Beinn an Dubhaich granite, Skye, Scotland .....	
6. Hypersolvus and subsolvus granites .....	

## FIGURES

Figure	Pag
1. Cross section of microcrucibles used in this investigation .....	7
2. Cross section of the hydrothermal quenching apparatus .....	9
3. Cross section of cold-seal pressure vessel .....	11
4. Graph illustrating the relation between the (201) spacing of alkali feldspars and the (1010) spacing of quartz .....	13
5. Schematic vapor pressure-temperature diagram for albite feldspar .....	16
6. Schematic vapor pressure-temperature diagram for potassium feldspar .....	18
7. Solvus for alkali feldspar from Korea (Spencer P—Spencer, 1937) .....	20
8. Effect of temperature on the two components of a low temperature cryptoperthite (Spencer I—Spencer, 1937) .....	22
9. Graph showing the compositional changes in sodium- and potassium-rich components of orthoclase cryptoperthites on heating to various temperatures and quenching .....	23
10. Three solvuses in the alkali feldspars .....	27
11. Schematic equilibrium diagram for the system $\text{NaAlSi}_3\text{O}_8$ - $\text{KAlSi}_3\text{O}_8$ .....	28
12. Pressure-temperature diagram for $\text{SiO}_2$ .....	29
13. Pressure-temperature relations in the system $\text{SiO}_2$ - $\text{H}_2\text{O}$ .....	32
14. Schematic PTX relations in the system $\text{SiO}_2$ - $\text{H}_2\text{O}$ .....	34
15. Liquidus relations in the portion of the system $\text{NaAlSi}_3\text{O}_8$ - $\text{H}_2\text{O}$ projected onto the pressure-temperature plane .....	35
16. Saturation curves for the system $\text{KAlSi}_3\text{O}_8$ - $\text{H}_2\text{O}$ projected onto the temperature-pressure co-ordinate plane .....	37
17. Isobaric equilibrium relations in the system $\text{NaAlSi}_3\text{O}_8$ - $\text{KAlSi}_3\text{O}_8$ - $\text{H}_2\text{O}$ projected onto the Ab-Or face of the temperature-composition prism .....	40
18. Schematic TX and PX diagrams for the system $\text{NaAlSi}_3\text{O}_8$ - $\text{KAlSi}_3\text{O}_8$ - $\text{H}_2\text{O}$ to aid in the understanding of Figure 19 .....	44
19. Portion of the triangular diagram for the system $\text{NaAlSi}_3\text{O}_8$ - $\text{KAlSi}_3\text{O}_8$ - $\text{H}_2\text{O}$ .....	46
20. Isobaric equilibrium relations in the system $\text{NaAlSi}_3\text{O}_8$ - $\text{SiO}_2$ - $\text{H}_2\text{O}$ projected onto the Ab-Q face of the temperature-composition prism .....	52
21. Triangular diagram, in part schematic, for a portion of the system $\text{NaAlSi}_3\text{O}_8$ - $\text{SiO}_2$ - $\text{H}_2\text{O}$ .....	52
22. The 500 kg/cm <sup>2</sup> isobaric equilibrium diagram for the system $\text{NaAlSi}_3\text{O}_8$ - $\text{KAlSi}_3\text{O}_8$ - $\text{SiO}_2$ - $\text{H}_2\text{O}$ projected onto the anhydrous base of the $\text{NaAlSi}_3\text{O}_8$ - $\text{KAlSi}_3\text{O}_8$ - $\text{SiO}_2$ - $\text{H}_2\text{O}$ tetrahedron .....	54
23. The 1000 kg/cm <sup>2</sup> isobaric equilibrium diagram .....	55
24. The 2000 kg/cm <sup>2</sup> isobaric equilibrium diagram .....	55
25. The 3000 kg/cm <sup>2</sup> isobaric equilibrium diagram .....	56
26. Pressure-temperature projection showing the effect of water-vapor pressure on the liquidus of albite, the albite-orthoclase minimum, the albite-quartz eutectic, and the ternary minimum in the system $\text{NaAlSi}_3\text{O}_8$ - $\text{KAlSi}_3\text{O}_8$ - $\text{SiO}_2$ .....	56
27. Graph illustrating the amount of water dissolved in the various anhydrous compositions as a function of temperature .....	57

Figure	Page
28. Pressure-temperature diagram showing the general effect of pressure on the water content of liquids above the saturation temperature.	58
29. Schematic condensed equilibrium diagram for the quaternary system $\text{NaAlSi}_3\text{O}_8$ - $\text{KAlSi}_3\text{O}_8$ - $\text{SiO}_2$ - $\text{H}_2\text{O}$ .	62
30. Isobaric fractionation curves for a water-vapor pressure of 1000 kg/cm <sup>2</sup> in the system $\text{NaAlSi}_3\text{O}_8$ - $\text{KAlSi}_3\text{O}_8$ - $\text{SiO}_2$ - $\text{H}_2\text{O}$ .	65
31. Isobaric equilibrium curves for a water-vapor pressure of 1000 kg/cm <sup>2</sup> in the system $\text{NaAlSi}_3\text{O}_8$ - $\text{KAlSi}_3\text{O}_8$ - $\text{SiO}_2$ - $\text{H}_2\text{O}$ .	66
32. The 760°C. isothermal polybaric equilibrium diagram for the system $\text{NaAlSi}_3\text{O}_8$ - $\text{KAlSi}_3\text{O}_8$ - $\text{SiO}_2$ - $\text{H}_2\text{O}$ .	68
33. Stability fields at the liquidus in the system $\text{NaAlSi}_3\text{O}_8$ - $\text{KAlSi}_3\text{O}_8$ - $\text{SiO}_2$ - $\text{H}_2\text{O}$ for various pressures of water vapor.	70
34. Stability fields at the liquidus in the system $\text{NaAlSi}_3\text{O}_8$ - $\text{KAlSi}_3\text{O}_8$ - $\text{SiO}_2$ - $\text{H}_2\text{O}$ for various pressures of water vapor.	71
35. Isothermal section through the isobaric prism at a temperature above and a pressure below that at which two feldspars appear at the liquidus.	72
36. Isothermal section through the isobaric prism at a temperature below and a pressure above that at which two feldspars coexist at the liquidus.	73
37. Three-phase triangles at 500 kg/cm <sup>2</sup> water-vapor pressure and 755°C. in the system $\text{NaAlSi}_3\text{O}_8$ - $\text{KAlSi}_3\text{O}_8$ - $\text{SiO}_2$ - $\text{H}_2\text{O}$ .	74
38. Effect of water-vapor pressure on the isobaric minimum in the system $\text{NaAlSi}_3\text{O}_8$ - $\text{KAlSi}_3\text{O}_8$ - $\text{SiO}_2$ - $\text{H}_2\text{O}$ .	75
39. Section through the 1000 kg/cm <sup>2</sup> isobaric prism for $\text{Ab}_{50}$ - $\text{Or}_{50}$ to the $\text{SiO}_2$ apex.	76
40. Section through the isobaric prism along the quartz-feldspar boundary at 1000 kg/cm <sup>2</sup> .	76
41. Contour diagram illustrating the distribution of normative albite, orthoclase, and quartz in all (362) the analyzed extrusive rocks in Washington's Tables that carry 80 per cent or more normative $\text{Ab} + \text{Or} + \text{Q}$ .	78
42. Contour diagram illustrating the distribution of normative albite, orthoclase, and quartz in all (571) the analyzed plutonic rocks in Washington's Tables that carry 80 per cent or more normative $\text{Ab} + \text{Or} + \text{Q}$ .	79
43. Pressure-temperature projection of the solidus for the Westerly, Rhode Island, granite, the Quincy, Massachusetts, granite, and the isobaric minimum in the system $\text{NaAlSi}_3\text{O}_8$ - $\text{KAlSi}_3\text{O}_8$ - $\text{SiO}_2$ - $\text{H}_2\text{O}$ .	83
44. Isobaric equilibrium relations in a portion of the system $\text{K}_2\text{O}$ - $\text{Al}_2\text{O}_3$ - $\text{SiO}_2$ - $\text{H}_2\text{O}$ at a pressure of 1000 kg/cm <sup>2</sup> projected onto the anhydrous base of the tetrahedron.	87
45. Portion of the tetrahedron representing the system $\text{K}_2\text{O}$ - $\text{Na}_2\text{O}$ - $\text{Al}_2\text{O}_3$ - $\text{SiO}_2$ .	88
46. Distribution of normative $\text{Ab}$ - $\text{Or}$ - $\text{Q}$ in rapakivi granites.	96
47. Index showing the location of specimens from the Beinn an Dubhaich granite.	102
48. Inversion of quartz from granites and rhyolites.	102
49. Inversion temperatures of quartz from the Beinn an Dubhaich granite.	103
50. Graph showing the relation between optic axial angles and composition of alkali feldspars.	104
51. Histograms showing the range in $2V\alpha$ of alkali feldspars from (A) Obsidian, Mono Lake, California, (B) Beinn an Dubhaich granite, (C) Westerly, Rhode Island, granite.	105
52. Graph showing the relation between $2V\alpha$ and composition in some plagioclase feldspars (after Tuttle and Bowen, 1950).	108
53. Histogram illustrating the distribution of $2V\alpha$ in plagioclase of the Beinn an Dubhaich granite.	109
54. Graph showing the relation between the $2\theta_{(131)}-2\theta_{(1\bar{3}1)}$ X-ray reflection and composition in natural and synthetic plagioclase.	110
55. Modal plagioclase, orthoclase, and quartz in Skye granites.	110
56. Modal plagioclase, orthoclase, and quartz from 260 thin sections of granites from eastern United States.	112

Figure	Page
57. Distribution of normative $\text{Ab}$ - $\text{Or}$ - $\text{Q}$ of 12 analyzed granites from Skye.	113
58. Graph illustrating the relation between modal orthoclase and modal plagioclase in granites.	115
59. Histogram showing the range and distribution of measured geothermal gradients in the earth's crust.	118
60. Histogram showing the range and distribution of changes in the geothermal gradient with depth in degrees C/km/km.	119
61. Graph showing the effect of temperature on the thermal conductivity of quartz and calcite.	120
62. Graph showing the relations between the melting of granite and various geothermal gradients assuming the gradients are linear.	122
63. Contoured triangular diagram showing the distribution of normative $\text{Ab}$ - $\text{Or}$ - $\text{Q}$ in all analyzed rocks (1269) in Washington's Tables containing 80 per cent or more $\text{Ab} + \text{Or} + \text{Q}$ .	128
64. Ternary diagram of the system $\text{NaAlSi}_3\text{O}_8$ - $\text{KAlSi}_3\text{O}_8$ - $\text{CaAl}_2\text{Si}_2\text{O}_8$ .	132
65. Ternary diagram of the system $\text{NaAlSi}_3\text{O}_8$ - $\text{KAlSi}_3\text{O}_8$ - $\text{CaAl}_2\text{Si}_2\text{O}_8$ .	133
66. Ternary diagram illustrating the probable extent of solid solution in the system $\text{NaAlSi}_3\text{O}_8$ - $\text{KAlSi}_3\text{O}_8$ - $\text{CaAl}_2\text{Si}_2\text{O}_8$ at four different temperature ranges.	135
67. Contour diagram illustrating the distribution of normative $\text{Ab}$ , $\text{Or}$ , $\text{An}$ in all the analyzed rocks in Washington's Tables (1269) that carry 80 per cent or more normative $\text{Ab} + \text{Or} + \text{Q}$ .	136

## TABLES

Table	Page
1. Orthoclase content of alkali feldspars as a function of the difference between $2\theta_{(201)}$ spacing of feldspar and $2\theta_{(10\bar{1}0)}$ spacing of quartz using $\text{CuK}\alpha$ radiation.	12
2. Results of heating experiments on high-temperature cryptoperthitic alkali feldspars.	21
3. Results of heating experiments on low-temperature cryptoperthitic alkali feldspars.	24
4. Results of quenching experiments on the effect of pressure on the quartz-tridymite inversion.	30
5. Results of quenching experiments in the system $\text{SiO}_2$ - $\text{H}_2\text{O}$ .	33
6. Results of quenching experiments in the system $\text{NaAlSi}_3\text{O}_8$ - $\text{H}_2\text{O}$ .	34
7. Results of quenching experiments in the system $\text{NaAlSi}_3\text{O}_8$ - $\text{SiO}_2$ - $\text{H}_2\text{O}$ .	51
8. Results of quenching experiments in the system $\text{KAlSi}_3\text{O}_8$ - $\text{SiO}_2$ - $\text{H}_2\text{O}$ .	53
9. Results of water determinations at various pressures and temperatures.	57
10. Results of quenching experiments in the system $\text{NaAlSi}_3\text{O}_8$ - $\text{KAlSi}_3\text{O}_8$ - $\text{SiO}_2$ - $\text{H}_2\text{O}$ .	59
11. Chemical, normative, and modal composition of the Quincy and Westerly granites.	81
12. Beginning of melting at various pressures of water vapor.	82
13. Results of quenching experiments in the system $\text{K}_2\text{O}$ - $\text{Al}_2\text{O}_3$ - $\text{SiO}_2$ - $\text{H}_2\text{O}$ .	86
14. Normative corundum, alkali metasilicates and acmite in 1016 salic rocks.	88
15. Compositional changes in vapor-loss experiments.	91
16. Normative and modal composition of the Westerly granite.	99
17. Specimen localities.	100
18. Orthoclase content of alkali feldspars from the Beinn an Dubhaich granite.	106
19. Modal analyses of Skye granites.	111
20. Chemical, normative, and modal composition of granites from Skye.	114

## ABSTRACTS

This paper deals with the experimental determinations of phase-equilibrium relations in the system  $\text{NaAlSi}_3\text{O}_8$ (albite)- $\text{KAlSi}_3\text{O}_8$ (orthoclase)- $\text{SiO}_2$ - $\text{H}_2\text{O}$  and with the application of these results to some petrologic problems.

The laboratory experiments can be divided into two categories: (1) study of the liquidus, solidus, and subsolidus phase relations in synthetic mixtures, and (2) study of natural minerals and rocks. Phase relations in the binary systems  $\text{SiO}_2$ - $\text{H}_2\text{O}$ ,  $\text{NaAlSi}_3\text{O}_8$ - $\text{H}_2\text{O}$ ,  $\text{KAlSi}_3\text{O}_8$ - $\text{H}_2\text{O}$ , the ternary systems  $\text{NaAlSi}_3\text{O}_8$ - $\text{KAlSi}_3\text{O}_8$ - $\text{H}_2\text{O}$ ,  $\text{NaAlSi}_3\text{O}_8$ - $\text{SiO}_2$ - $\text{H}_2\text{O}$ ,  $\text{KAlSi}_3\text{O}_8$ - $\text{SiO}_2$ - $\text{H}_2\text{O}$ , and the quaternary system  $\text{NaAlSi}_3\text{O}_8$ - $\text{KAlSi}_3\text{O}_8$ - $\text{SiO}_2$ - $\text{H}_2\text{O}$  were investigated with the aid of synthetic mixtures. Analyzed natural feldspars were used for subsolidus studies in the system  $\text{NaAlSi}_3\text{O}_8$ - $\text{KAlSi}_3\text{O}_8$ , and the beginning of melting temperatures of natural granites were studied and compared with synthetic granites.

Heating experiments with natural alkali feldspars demonstrated that sanidine cryptoperthites could be made homogeneous by heating at  $700^\circ\text{C}$ ., whereas orthoclase cryptoperthites could not be homogenized by heating at any temperature below the solidus of the binary system ( $1060^\circ\text{C}$ .) unless the heating was carried out for such a long time that the material inverted to sanidine. A solvus or miscibility gap was determined for each series, and both differed from the solvus for synthetic mixtures (high albite-high sanidine series). Only a portion of each of these solvuses is believed to represent stable equilibria.

Phase-equilibrium relations in the system  $\text{SiO}_2$ - $\text{H}_2\text{O}$  were considered in detail because the relations in this system are representative of those expected in all systems involving a rock-forming silicate and water. There are at least five invariant points in the binary system of which three involve liquid carrying 90 per cent silica. The effect of pressure on the high quartz-tridymite inversion was investigated; 1000  $\text{kg}/\text{cm}^2$  pressure raised the inversion temperature approximately  $180^\circ\text{C}$ . to  $1050^\circ\text{C}$ .

Melting relations in the system  $\text{NaAlSi}_3\text{O}_8$ - $\text{H}_2\text{O}$  were determined by methods used throughout this investigation, and it was gratifying to find that the results were in good agreement with those obtained by Goranson (1938) using a different apparatus and method. The discovery of high-temperature albite was a by-product of this study.

Experimental studies in the system  $\text{NaAlSi}_3\text{O}_8$ - $\text{KAlSi}_3\text{O}_8$ - $\text{H}_2\text{O}$  demonstrated that the alkali feldspars form a complete series of solid solutions above  $660^\circ\text{C}$ ., and below this temperature a solvus or miscibility gap is present. Homogeneous synthetic feldspars formed above  $660^\circ\text{C}$ . unmixed when held at lower temperatures, a confirmation of the accepted theory for the origin of most natural perthites. The composition of the two alkali feldspars in the synthetic mixtures can be determined with considerable accuracy by means of X-ray diffraction patterns. With certain limitations, the X ray can be used to determine the composition of the two phases of natural perthitic alkali feldspars. Unmixing of alkali feldspars in the presence of water vapor under pressure was so rapid that it is surprising that fine perthitic intergrowths and homogeneous feldspars are found in nature. They must have formed in a dry environment.

Tridymite and albite are the stable crystalline phases at the liquidus below 300  $\text{kg}/\text{cm}^2$  pressure, whereas at higher pressures high quartz and albite are the stable phases. The change from tridymite to quartz is a consequence of the liquidus lowering by water dissolving in the melt together with the pressure raising of the quartz-tridymite inversion; at about 300  $\text{kg}/\text{cm}^2$  the pressure-temperature curve of the quartz-tridymite inversion intersects the liquidus.

Phase studies in the quaternary system  $\text{NaAlSi}_3\text{O}_8$ - $\text{KAlSi}_3\text{O}_8$ - $\text{SiO}_2$ - $\text{H}_2\text{O}$  provided quantitative data on the melting relations in these granitic compositions as well as



information on fractional and equilibrium crystallization. At constant pressure, the system is characterized by a minimum melting temperature on the boundary between quartz and feldspar solid solutions. Liquids throughout the system move toward this minimum on crystallization, and if fractionation is pronounced most liquids will reach the minimum. A plot of the normative albite, orthoclase, and quartz in all analyzed granites and rhyolites from Washington's Tables (1917) demonstrates that the minimum at low water-vapor pressure, corresponding to a water content of 1-2 per cent, falls at the composition of the average granite and rhyolite. It is suggested that this demonstrates that crystal-liquid equilibria control granite compositions; therefore granites not formed at magmatic temperatures will be rare and will not have compositions related to the minimum. The liquids can originate by fractional crystallization of more basic liquids (*i.e.*, basalts) or by fractional melting of appropriate sedimentary and metamorphic rocks.

The beginning of melting of two granites—The Westerly, Rhode Island, and the Quincy, Massachusetts—one a normal calc-alkaline granite, and the other an alkaline granite, was determined at a series of water-vapor pressures; a PT curve for the beginning of melting of the two granites corresponds within the experimental error to the beginning of melting at the isobaric minimum in the quaternary system.

Evidence is presented to show that a continuous gradation from magma to hydrothermal solution will obtain in hydrous granitic compositions if the alkali to alumina ratio is such that crystallization results in concentration of alkali silicates in the residual liquids.

The vapor in equilibrium with hydrous granitic liquids can remove the silica, feldspars, and quartz from the liquid phase by vapor transport or by diffusion through the vapor, and in long runs these materials were transferred to the cooler part of the pressure vessel. CaO, MgO, FeO, and P<sub>2</sub>O<sub>5</sub> were concentrated by this process, and in one experiment with the Westerly granite the vapor removed essentially all the feldspar and quartz, leaving a residue of garnet, pyroxene, and apatite. This tendency for the oxides abundant in the basic and ultrabasic rocks to be relatively insoluble in the vapor suggests that such a mechanism may produce the basic zones commonly found at granite contacts.

The amphiboles anthophyllite, grunerite, and riebeckite appeared to be unstable in the presence of water vapor under pressure, and the absence of amphiboles in the granite pegmatites and their almost universal presence in the perthite-quartz granites indicate that the pegmatites were produced in a water-rich environment while the perthite-quartz granites crystallized in a water-deficient environment.

The rapakivi granite problem has been reviewed in the light of the experimental results, and it is pointed out that normal crystallization of magmas containing somewhat more potassium than the average granite can produce the rapakivi texture, providing water is concentrated during crystallization and the liquidus is depressed below the feldspar miscibility gap.

The Tertiary granites of Skye are normal granites, chemically, and to some extent texturally; mineralogically, however, they are similar to rhyolitic rocks. The quartz and feldspars resemble in many respects the corresponding phenocrysts of extrusive rocks. It is suggested that these young granites represent quenched granites which, as a consequence, have some properties of both granites and rhyolites.

Melting is expected in the earth's crust at depths of 12-21 km in geosynclinal areas where the initial gradient is on the order of 30°C./km. Complete melting will take place if 9-10 per cent water is available. If the water content is 2 per cent, melting will still begin at the same depth; complete melting will not take place until some greater depth has been reached. This range of melting will produce a zone in the earth's crust which may range in thickness from a few to 20 km with the amount of liquid increasing downward. It is proposed that this zone of melting, where temperatures are high enough to melt granite completely and more basic compositions

at least partially, may offer a mechanism for producing large batholithic masses of granite.

A classification of salic rocks based on the nature of the alkali feldspar is proposed. The classification has two major divisions: (1) subsolidus, and (2) hypersolvus, depending on the whereabouts of the soda feldspar. In the hypersolvus rocks all the soda feldspar is or was in solid solution in the potash feldspar whereas in the subsolvus rocks the plagioclase is present as discrete grains. The two major divisions are further subdivided according to the nature of the alkali feldspar modification.

The suggestion that most granites finished crystallization with a single alkali feldspar precipitating has been questioned by some petrologists because rhyolites commonly carry phenocrysts of plagioclase and sanidine feldspar. A study of the feldspars of extrusive rocks indicates that the plagioclase phenocrysts may react with the liquid during crystallization leaving a single alkali feldspar. If fractionation takes place, the tendency to complete crystallization with only a single feldspar crystallizing from the liquid is greatly enhanced.

The proposition that two-feldspar granites may have gone through a one-feldspar stage has been examined in the light of experimental studies, and it was concluded that the required adjustments in mineral composition and texture are reasonable.

## INTRODUCTION

Judging from the voluminous literature on the subject, the origin of granite is one of the most controversial topics in petrology today. Much of the controversy has arisen from the conflicting evidence submitted by field investigators. Field studies of granites deal with end products of processes long since completed, and the most detailed mapping and study of these products may fail to give convincing evidence concerning the exact nature of the processes responsible for the relations. Laboratory studies, under controlled and measured conditions, of the common minerals of granites and of the nature of the melting relations in compositions approaching those of granites are natural avenues of attack on the granite problem.

A great deal of the geologists' criticism of laboratory research on chemical systems has resulted from the fact that the laboratory investigator must select simple systems in order to understand the phase equilibria involved, whereas the rocks are very complex chemically and cannot in general be represented on a ternary diagram. The system to be considered here is an exception, as the granites commonly contain only minor amounts of oxides in addition to those found in albite, orthoclase, and quartz. The average granite contains less than 10 per cent of normative constituents other than Ab, Or, and Q, and it is therefore expected that equilibrium relations in this system will yield information directly applicable to the granite problem.

It has long been realized that studies of dry silicate systems do not yield exactly the conditions of formation of the igneous rocks because the salic<sup>1</sup> rocks contain volatile ingredients, principally water. Hydrous minerals occur in nearly all granites, syenites, and nepheline syenites and as phenocrysts in many rhyolites, trachytes, and phonolites. Volatile materials emanating from volcanic rocks have been carefully analyzed chemically, and in them also water is the predominant volatile constituent. It is thus natural that water should be added to the feldspars and to mixtures of feldspars and quartz—the principal constituents of granite.

A preliminary report on the system  $\text{NaAlSi}_3\text{O}_8$  (nepheline)– $\text{KAlSi}_3\text{O}_8$  (kalsilite)– $\text{SiO}_2$  was published by Schairer and Bowen (1935). The system  $\text{NaAlSi}_3\text{O}_8$ – $\text{KAlSi}_3\text{O}_8$ – $\text{SiO}_2$  is a portion of this studied system, and it is interesting to note that there are no determined points in the vicinity of the boundary between the silica field and the feldspar field. There is a very good reason for this lack of data—the mixtures in the critical region near the center of this system are so viscous that crystallization in the dry way is impossible. Additional information has been added by Schairer since 1935, but the “dry” melting relations in the critical region still remain unknown. This then is the reason why this ternary system ( $\text{NaAlSi}_3\text{O}_8$ – $\text{KAlSi}_3\text{O}_8$ – $\text{SiO}_2$ )—petrologically the most important system that could be studied—has not long ago been worked out and the results applied to the granite problem. Reaction between liquid and crystals in compositions approximating those of the granites is so sluggish that crystalline mixtures can be held for long periods above the melting temperature without the formation of appreciable liquid, and liquids

<sup>1</sup> The term salic will be used throughout to indicate rocks rich in the salic components, quartz albite, orthoclase, nepheline, leucite, and kalsilite, the constituents of petrogeny's residua system.

can be held at temperatures below which crystallization should take place, with or without seeds of the proper kind, for periods of 10 years and longer with no evidence of crystallization.

The presence of water vapor under pressure greatly increases the rate of crystallization so that for most of the compositions in this system equilibrium between liquid and crystals can be attained in a reasonable length of time.

#### EXPERIMENTAL METHODS

##### PREPARATION OF MIXTURES

In nearly all experiments made in connection with this study the initial material was a glass previously prepared by Schairer for work in the dry system. The preparation of these viscous glasses was an extraordinarily difficult and time-consuming process, and their availability was of inestimable value in the present study. We are consequently greatly indebted to Schairer for making them available for this investigation.

The glasses were prepared from the following raw materials:  $\text{SiO}_2$ —crushed quartz treated with  $\text{HCl}$ ; Insoluble residue after treating with  $\text{H}_2\text{SO}_4$  and  $\text{HF}$  0.030 per cent;  $\text{Al}_2\text{O}_3$ —tabular alumina T-61 from the Aluminum Company of America, impurities 0.075 per cent ( $\text{SiO}_2$  0.020,  $\text{Na}_2\text{O}$  0.020,  $\text{Fe}_2\text{O}_3$  0.030,  $\text{TiO}_2$  0.005);  $\text{NaHCO}_3$ —Impurities 0.037 per cent (Insoluble 0.015,  $\text{CaO} + \text{MgO}$  0.002,  $\text{Fe}$  0.020); and  $\text{KHCO}_3$ —Impurities 0.005 per cent ( $\text{SiO}_2$  0.003,  $\text{Al}_2\text{O}_3 + \text{Fe}_2\text{O}_3$  0.001,  $\text{CaO}$  0.001).

The glasses were not made up directly from these materials because appreciable alkali would have been lost on heating to the high temperatures necessary to dissolve alumina in a reasonable time; instead, potassium silicate and sodium silicate glasses were first prepared, and these in turn were used to prepare the appropriate glasses by addition of the alumina. Some alkalies were lost even under these circumstances, but the losses were replaced, and the errors arising from volatilization were certainly very small. Fairbairn and Schairer (1952) discuss the possible sources of error and their influence on the final compositions.

At the beginning of this study the charges were placed in open crucibles inside the pressure vessels. This proved to be satisfactory for the early experiments of short duration (15–30 minutes), but as more viscous mixtures were used the times required to attain equilibrium were increased to several hours, and the quenched liquids (glasses) commonly showed a blue color in the upper exposed portion of the charge. This was obviously the result of vapor transport of material (possibly cobalt) from the walls of the pressure vessel. The transport was prevented by placing a second, snug-fitting crucible over the first. As still more viscous compositions were studied this arrangement did not satisfactorily prevent loss of material by vapor transport as the charges lost weight in runs of several days. This was minimized by placing the crucible containing the charge (with a tight-fitting lid) in a larger crucible and filling the space between the two with material (buffer) of the same composition. This outer crucible was then covered with a still larger crucible in the same manner as the inner pair (Fig. 1).

The crucibles were made of platinum foil (0.01 mm). They were fabricated by wrapping a small sheet of platinum of the proper dimensions about a mandrel of

the appropriate size and welding a slight overlap by heating to red heat and tapping the overlap with a tiny hammer. One end of this cylinder was then folded over by placing it over a mandrel with a section extending over the end and “spinning” the overhang about the end of the mandrel while turning in a lathe. Dimensions of

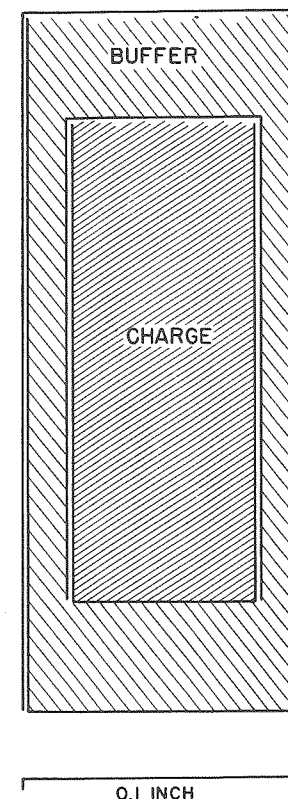


FIGURE 1.—Cross section of microcrucibles used in this investigation

The crucibles are made of platinum foil, and although they are reasonably tight fitting there is free access for water vapor between the crucibles and through pin holes in the foil.

the mandrels, foil, and the amount of overhang for the four sizes of crucibles were as follows:

MANDREL			
Drilled rod size	Size in inches	Size of Pt sheet in inches	Amount of overhang in inches
52	.0635	$\frac{3}{16} \times \frac{1}{4}$	$\frac{1}{32}$
50	.0700	$\frac{3}{16} \times \frac{1}{4}$	$\frac{3}{64}$
40	.0980	$1\frac{1}{32} \times \frac{3}{8}$	$\frac{7}{64}$
37	.1040	$1\frac{1}{32} \times \frac{3}{8}$	$\frac{7}{64}$

Mandrels were made of a heat-resistant alloy, such as Nichrome, and tapered slightly to facilitate removal of the crucibles. They were heated with a small gas-air torch.



These precautions against compositional changes caused by loss via the vapor were inadequate for some long runs (1 month or longer), and it was necessary to use the sealed-tube technique described in detail by Goranson (1931, p. 486). The charge was sealed in a platinum tube with a known amount of water and welded shut. The pressure was applied to the charge by the collapse of the tube on the contents.

#### PRESSURE MEASUREMENT AND CONTROL

Pressure was generated by pumping water directly into the pressure vessels by means of a piston-type pump manufactured by the American Instrument Company. These pumps are rated at 30,000 psi, but by using a more powerful motor they will operate satisfactorily at pressures up to 60,000 psi. The pressure was maintained at any preset value by a simple regulating device attached to the Bourdon gauge. A decrease in pressure was detected by an adjustable pointer made of fine wire attached to the gauge in such a manner that an electrical contact was made as the gauge hand touched the wire. The resulting contact activated a thyatron tube which in turn operated a relay that started the pump motor. A sudden loss of pressure resulting from failure of a pressure connection or the pressure vessel caused the gauge hand to pass the fine wire, thereby stopping the pump.

Bourdon-type gauges were used to measure pressure. The gauges were calibrated against a dead-weight gauge. Pressure measurements are believed to be accurate to within  $\pm 10$  per cent of the stated value.

#### TEMPERATURE MEASUREMENT AND CONTROL

The experimental method did not lend itself to accurate measurement of the temperature of the charges because the thermocouple was located some distance (about 3 mm) from the charge (Fig. 2). The error introduced by this uncertainty made it futile to measure the temperature closer than within  $\pm 2^\circ\text{C}$ . Consequently, it was convenient to use strip-chart recorders to measure and record the temperature. Chromel-Alumel thermocouples were used at all temperatures between  $500^\circ\text{C}$ . and  $1200^\circ\text{C}$ ., and iron constantan thermocouples between  $0^\circ\text{C}$ . and  $500^\circ\text{C}$ . The thermocouple wire was periodically calibrated at the melting point of lead, antimony, and silver, and the recorder was frequently checked against a potentiometer. Temperature measurements are believed to be accurate within  $\pm 5^\circ\text{C}$ .

Temperatures were controlled with Brown indicating controllers which normally maintain the temperature within  $\pm 2^\circ\text{C}$ . All temperatures were continuously recorded during the runs.

#### HYDROTHERMAL QUENCHING APPARATUS

This apparatus was first described by Tuttle (1948) and has been used since that time with only a few minor changes. Most of the experiments described here were carried out in this apparatus. The principal advantages of the equipment over previous apparatus are: (1) simple design that permits making quenching experiments as rapidly as with the conventional methods used for anhydrous silicate studies at atmospheric pressure, and (2) the design provides a continuous thrust for maintaining the seal, thereby permitting use of the equipment at temperatures

well above the elastic limit of the alloys used for the pressure vessel. Deformation of the pressure vessel amounting to more than 10 per cent vertical shortening took place without causing rupture and loss of the run.

The apparatus is illustrated in Figure 2. The pressure vessel (B) was supported

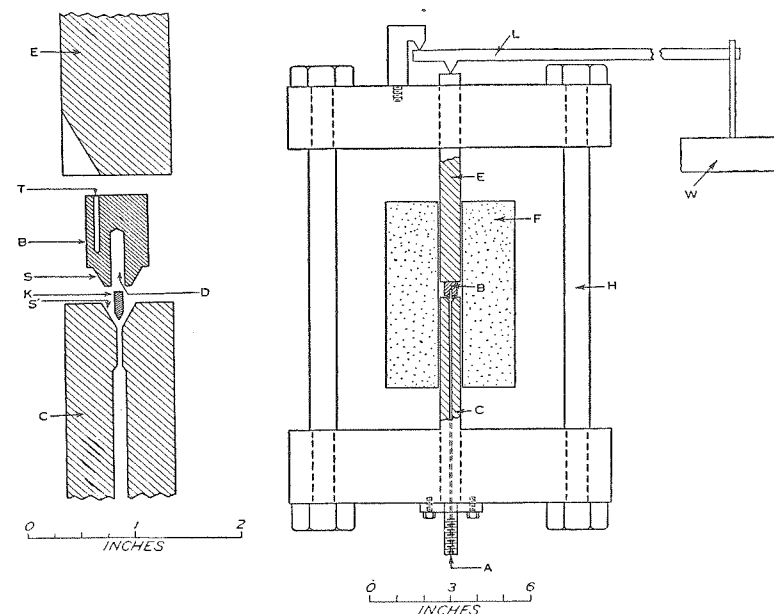


FIGURE 2.—Cross section of the hydrothermal quenching apparatus

The microcrucibles illustrated in Figure 1 are placed in the chamber (D). The support for the furnace (F) is not shown.

by the rod (C), and the seal was maintained by a downward thrust on the rod (E) by means of a lever arm (L) and weight (W). The lower end of the pressure vessel was a cone (S) with an included angle of  $59^\circ$  that fitted into the top of the lower plunger (C) which had a  $60^\circ$ -degree cone seat. The ring seal resulting from the pressing together of these two surfaces produced incipient welding in most runs especially if the cones were resurfaced before the experiment. At temperatures above  $800^\circ\text{C}$ . and pressures above  $2000\text{ kg/cm}^2$ , the surfaces of the cones were normally remachined for each run. At lower temperatures and pressures many experiments were carried out without resurfacing the cones. Water was introduced through a small axial bore in the lower supporting rod (C), the lower end (A) of which was attached to high-pressure tubing, which was in turn connected to a pump that supplied the desired pressure. The pressure vessel and the portion of the upper and lower (C, E) plungers were heated by means of a split furnace such as is commonly used in combustion analysis, but mounted in a vertical instead of the usual horizontal position. The furnace was hinged about a vertical axis and supported on a sleeve (not shown) about (H) that permitted the furnace to swing about (H). Temperatures were measured by a thermocouple inserted in the well (T) in the pressure vessel. On comple-

tion of a run the furnace was quickly swung aside, and the stream of air directed against the pressure vessel. In this manner charges were cooled  $300^{\circ}$  in 10 seconds.

A typical experiment was carried out as follows: The charge, consisting of 10 to 12 mg of material, was placed in the pressure vessel with a small pedestal which supported the charge in a position directly opposite the thermocouple junction. The pressure vessel was then placed on the lower support rod, the thermocouple inserted in the well, and the upper support rod put into place. The thermocouple leads were fastened to the lower support rod and insulated with suitable small ceramic tubing. The furnace was then swung into place about the assembly, and the temperature was brought to the desired value at which time the lever arm ( $L$ ) was put in place, the appropriate weight added, and the water admitted. If necessary, the pressure was applied before heating.

Pressure-temperature limitations of the equipment depended on the hot strength of the alloy used. Stellite alloy No. 25 was the most satisfactory material used. Runs were made at  $1150^{\circ}\text{C}$ . and  $500\text{ kg/cm}^2$  pressure using this alloy. At  $800^{\circ}\text{C}$ . pressures up to  $4000\text{ kg/cm}^2$  were used.

#### COLD-SEAL PRESSURE VESSEL

This pressure vessel (Tuttle, 1949) has proved to be very useful for preparing large amounts of material for subsequent use in the quenching apparatus and for sealed-tube experiments. Some slight modifications have been made which simplify fabrication; the most recent design is shown in Figure 3. The pressure vessel is simply a 7-inch rod of Stellite with a quarter-inch axial hole bored to within half an inch of one end. The closed end is placed in a furnace, and the threaded portion ( $B$ ) with the pressure connection (which is made by the cone on  $A$  being pressed into the cone on  $C$ ) is kept at low temperatures at all times. Charges are supported by the support rod ( $D$ ) near the closed end which is adjusted in the furnace so that it lies in the position of maximum temperature ("hot spot" of the furnace). Convection and danger due to explosive failure are minimized by having the support for the charge ( $D$ ) fill most of the internal volume of the vessel. For temperature measurement a thermocouple is placed in the small well opposite the charge.

#### COMPOSITION OF FELDSPARS BY THE $(\bar{2}01)$ SPACINGS

Use of the  $(\bar{2}01)$  spacing to determine the "orthoclase" content of alkali feldspars was described in an earlier paper on the ternary system  $\text{NaAlSi}_3\text{O}_8\text{--KAlSi}_3\text{O}_8\text{--H}_2\text{O}$  (Bowen and Tuttle, 1950). The  $(\bar{2}01)$  spacing was determined by mixing with the feldspar of known composition some olivine which has a strong reflection near by; the difference between the two peaks is then a measure of the composition. In the present study, the  $(10\bar{1}0)$  spacing of quartz was used as a standard, principally because quartz appeared in many of our preparations along with the feldspars. In these preparations the standard was "built in". As the  $(10\bar{1}0)$  reflection may be convenient for others to use in determinations of feldspar compositions, the values for the difference in  $2\theta$  between the  $(10\bar{1}0)$  of quartz and the  $(\bar{2}01)$  of the alkali feldspars from albite to orthoclase are given in Table 1 and are shown graphically in Figure 4. Quartz is not suitable for those feldspars having compositions near orthoclase because the quartz reflection is very near the  $(\bar{2}01)$  of pure potassium

feldspar. However, for these compositions a sodic plagioclase can be used after calibrating with quartz.

The  $(\bar{2}01)$  spacing can also be used to determine the "orthoclase" content of natural feldspars after they have been rendered homogeneous by a suitable heat treat-

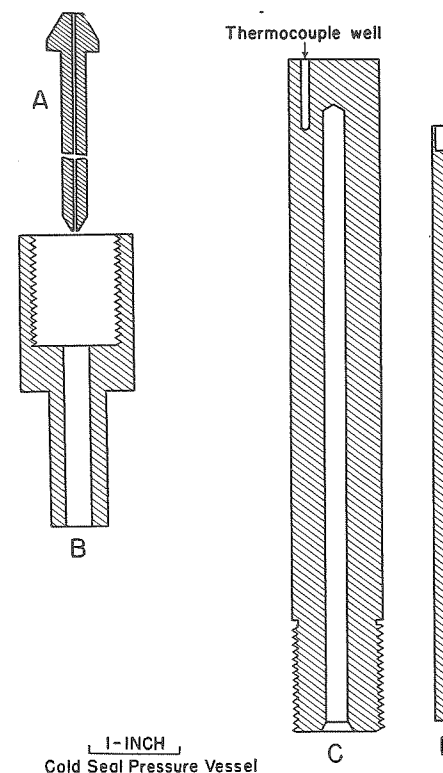


FIGURE 3.—Cross section of cold-seal pressure vessel

Used for all sealed-tube experiments and for preparing large batches for subsequent treatment in the hydrothermal quenching apparatus. Charges are placed in the cup on the upper end of the support rod ( $D$ ) which is then supported in the pressure vessel in such a way that the center of the charge is opposite the thermocouple junction.

ment. Natural alkali feldspars belonging to the sanidine-high albite series can be readily homogenized by heating for a few minutes at a temperature between  $700^{\circ}$  and  $1000^{\circ}\text{C}$ . Feldspars of the orthoclase-low albite series having compositions between approximately  $\text{Or}_{30}$  and  $\text{Or}_{55}$  cannot be homogenized until they have been changed to the sanidine modification which may take several weeks at  $1050^{\circ}\text{C}$ .

#### DETERMINATION OF LIQUIDUS AND SOLIDUS RELATIONS

Initial material for runs on synthetic compositions was in all cases a glass of known composition. The glass was used directly for water-determination runs, but for all liquidus and solidus experiments it was found necessary to crystallize the

glass, in some cases completely, in others only partially. Liquidus determinations were made on either wholly or partially crystallized material whereas determinations of beginning of melting required completely crystalline materials. Completion

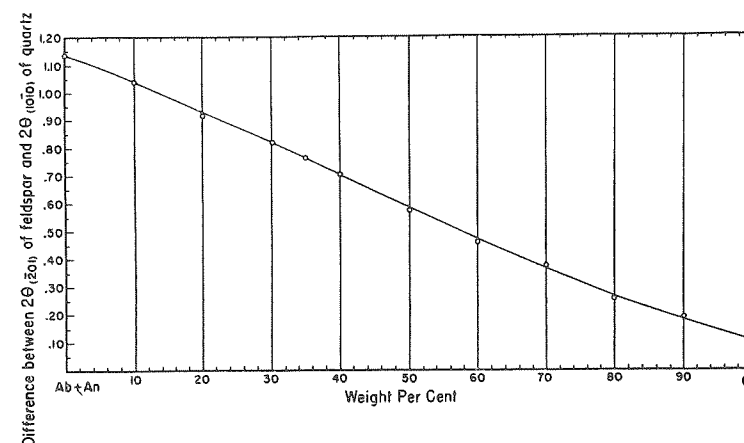
TABLE 1.—Composition of the alkali feldspars by X ray

$2\theta$ (201) Feldspar-(10 $\bar{1}0$ ) quartz	Or content of Feldspar	$2\theta$ (201) Feldspar-(10 $\bar{1}0$ ) quartz	Or content of Feldspar
.10	100	.59	50
.11	98	.61	48
.12	96	.64	46
.14	94	.66	44
.16	92	.68	42
.18	90	.71	40
.19	88	.73	38
.21	86	.76	36
.23	84	.78	34
.25	82	.80	32
.27	80	.82	30
.28	78	.85	28
.30	76	.87	26
.32	74	.89	24
.34	72	.91	22
.36	70	.93	20
.38	68	.96	18
.41	66	.98	16
.43	64	1.00	14
.45	62	1.02	12
.47	60	1.04	10
.50	58	1.06	8
.52	56	1.08	6
.54	54	1.10	4
.57	52	1.12	2
		1.14	0

of melting is best determined on very finely crystalline material because coarse crystals greatly delay the attainment of equilibrium. Experience showed that the size of crystals was influenced by the particle size of the initial glass. Large fragments tend to give large crystals, so all crystallizations were carried out on finely ground materials. A temperature of 700°C. was satisfactory for obtaining finely crystalline products; below 700°C. two feldspars were produced, and at higher temperatures large crystals tended to grow despite the fine grinding of the glass.

The time required for complete crystallization of the glasses varies greatly with composition. Mixtures of orthoclase and albite crystallize completely in 30 minutes or less, as do quartz and albite compositions. Orthoclase-quartz mixtures and the ternary compositions rich in orthoclase are most difficult to crystallize, and in some cases it was necessary to crystallize for a day or so, remove the charge and grind fine again, then crystallize for another day or two. With one or two exceptions this treatment resulted in a crystalline product in which no glass could be detected with

the petrographic microscope. In most of the mixtures, the crystalline product consisted of feldspar and quartz, but occasionally a minute amount of tiny needles of a high-index phase appeared which was probably mullite, indicating that the composition of the mixture was slightly off the Ab-Or-SiO<sub>2</sub> section.

FIGURE 4.—Graph illustrating the relation between the (201) spacing of alkali feldspars and the (10 $\bar{1}0$ ) spacing of quartz

Quartz is used as an X-ray standard. The graph may be used to determine composition of alkali feldspars belonging to the high-temperature series only. If it is impossible to invert the feldspars to the high form the graph will give a rough estimate of the composition if the material is homogeneous or nearly so.

Liquidus determinations are accomplished by holding the previously crystallized charge at a constant temperature and pressure for the desired time, then quenching and examining the product with the petrographic microscope. If crystals appeared in the glass the temperature of the subsequent run was raised until that temperature is reached above which all glass is obtained and below which crystals remain and appear to be growing. Solidus determinations were carried out by heating completely crystalline material and observing the temperature at which glass appeared in the quenched product.

#### WATER DETERMINATION

Discrepancies in the determinations of the water content of the silicate glasses were one of the most perturbing problems encountered in this investigation. Water determinations were made by measuring ignition loss of the hydrous glasses after heating them at a temperature and pressure just above the liquidus. The charges were removed from the crucibles, weighed, placed in a loose-fitting crucible, reweighed, and ignited to constant weight. The heating rate was carefully controlled to prevent vesiculation, which may rupture the crucible and cause loss of part of the charge. A heating rate of 2°C. per minute is slow enough to prevent vesiculation in most compositions. Charges varied in weight from 10 to 50 mg, and weighings were made on a microbalance to the nearest 0.01 mg.



The discrepancies are believed to be due largely to the fact that we were unable to free the charges from bubbles. The bubbles were not formed by vesiculation on quenching, as there was no evidence of an increase in volume, and it was concluded that they represent water trapped in the powdered glass initially (Bowen and Tuttle, 1950, p. 498). As the bubbles were filled with water which was not dissolved in the glass, loss of weight on ignition tended to give a high value for the water content of the charge. The number and size of the bubbles varied from one run to another and consequently produced erratic results. The lowest value obtained, assuming no other source of error, would then be a maximum value somewhat higher than the true water content.

If the bubbles represent water trapped in the powdered glass, a variation in the grain size of glass particles used initially should influence the final water content. Accordingly the following set of runs was made to evaluate any relation between initial grain size of the glass powder and the water content of the final hydrous glass (at constant pressure and temperature).

Charge	Water content (Per cent)
Random size, fine-grained ( <i>i.e.</i> , <.001 mm)	9.14
Random size, coarse-grained ( <i>i.e.</i> , <1.0 mm)	8.47
>.03 mm <.08 mm	6.43
>.001 mm <.08 mm	7.20
A few large fragments ( <i>i.e.</i> , approximately 1 mm or larger)	5.86

These experiments appear to confirm the suspicion that the water was trapped in the powdered glass at the beginning of the runs. Additional experiments showed that it is not practicable to determine the water content with great precision as the glass fragments themselves contain air bubbles trapped during the preparation of the anhydrous charge; these acquire water during the subsequent hydrothermal run. Ideally it would be desirable to have the initial charge in the form of a single cylinder, free from bubbles, but to obtain such cylinders would be a very difficult and time-consuming task.

## CRYSTALLINE PHASES

### ALBITE

One of the most interesting results of the study of albite-water equilibria was the discovery that albite crystallized hydrothermally was different from natural albite (Tuttle and Bowen, 1950). The first clue to this difference was noted when the orientation of the optic plane and the optic axial angle were measured and found to differ from those given for albite. At first the differences were attributed to lack of precision because of twinning in the imperfectly crystallized material, but X-ray diffraction studies confirmed the optical indications that our products contained a new form of  $\text{NaAlSi}_3\text{O}_8$ . Synthetic albite encountered in this study is a high-temperature modification of  $\text{NaAlSi}_3\text{O}_8$ . Low-temperature albite from pegmatites such as that from Amelia, Virginia, can be changed by long heating at high temperatures (*i.e.*, 1050°–1100°C.) to a modification having X-ray and optical properties essentially identical with those of the synthetic material. Final confirmation of the high-tempera-

ture stability of the modification produced synthetically was found in rhyolitic rocks where high albite has been found (Tuttle and Bowen, 1950, p. 580). In contrast, the low-temperature form is found in rocks in which the temperature of formation is known to be well below that of rhyolites.

The exact temperature of the inversion is not known, but it is believed to be near 700°C. Low-temperature albite has not been synthesized, and the temperature of the inversion will remain in doubt until the low form is produced in the laboratory. Low albite can be changed to a high-temperature modification by heating at temperatures near the liquidus, and in the presence of water vapor and sodium disilicate, as a flux, the transformation can be brought about at temperatures as low as 720°C. These experiments suggest that the transformation temperature is near 700°C., but there is no certainty that prolonged heating at still lower temperatures will not change the low-temperature to the high-temperature form.

The possibility that the change produced by the flux at 720°C. is metastable must also be considered although this appears unlikely. For example, albite crystallized from a liquid rich in sodium disilicate and water at temperatures well below 720°C. would almost certainly be the high-temperature form, and the change brought about in low albite at 720°C. may be a recrystallization below the maximum temperature of stability of the low form. The authors are unaware of any experimental results indicating this possibility, but the very strong tendency for these silicates to grow as metastable phases suggests that such a behavior must be considered.

Recent studies on high albite by W. S. MacKenzie (1952) have shown that this "modification" consists of two and possibly three phases which may have a stable range of existence. Evidence for these phases was found by observing changes in the difference in  $2\theta$  between the (111) and ( $\bar{1}\bar{1}1$ ) reflections as a function of temperature. Donnay and Donnay (1952) showed that these two reflections could be used to determine the symmetry of alkali feldspars from X-ray powder diffraction patterns. These two reflections coincide when the symmetry is monoclinic, and if they are separated the difference between the two represents a measure of departure from monoclinic symmetry.

MacKenzie found that albite which had been heated for long periods at high temperatures becomes monoclinic at about 920°C. The change from triclinic symmetry at room temperature to monoclinic symmetry at 920°C. is gradual and nonquenchable and would, presumably, be classified as a displacive transformation by Buerger (1948). No heat effect was found at the temperature of the symmetry change.

High albite synthesized below 800°C. does not become monoclinic on heating to the melting temperature, but apparently becomes monoclinic metastably above the liquidus (MacKenzie, 1952, p. 324). The situation is further complicated by the inversion in low albite reported by Bakken and Rosenqvist (1952) at 835°C. This inversion is probably metastable in view of the fact that low albite has been transformed to high at 720°C.

These studies suggest four forms of albite with stable ranges of existence and two forms which must be metastable at atmospheric pressure. Figure 5 shows the interrelations among the various modifications.

As the silicates are subjected to closer examination by modern X-ray techniques

and optical and thermal studies, more and more will be learned of their stability relations, and many new modifications will probably be found. The custom of naming each new modification seems unwarranted; therefore a system of symbols is here used to identify each polymorph (Fig. 5). As three principal forms of albite are now be-

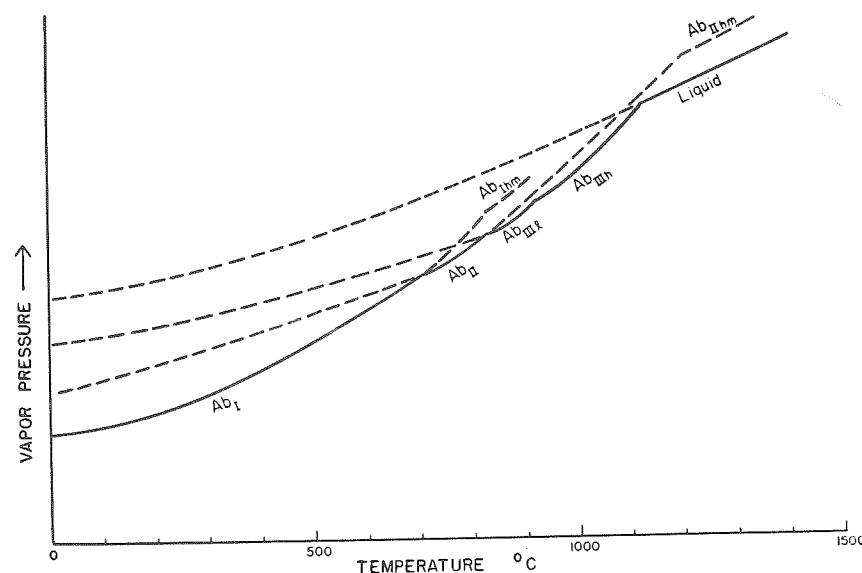


FIGURE 5.—Schematic vapor pressure-temperature diagram for albite feldspar

Shows theoretical interrelations among the various modifications.  $Ab_I$  = low-temperature albite;  $Ab_{II}$  = high-temperature albite which becomes monoclinic only above 1120°C. on heating ( $Ab_{IIhm}$ ),  $Ab_{III}$  = high-temperature albite which becomes monoclinic at about 920°C. on heating ( $Ab_{IIIh}$ ),  $Ab_{IIIhm}$  = a modification of the low albite discovered by Bakken and Rosenqvist (1952).

lieved to have a stable range of existence they are designated  $Ab_I$ ,  $Ab_{II}$ , and  $Ab_{III}$ .  $Ab_{III}$  changes to  $Ab_{IIIh}$  at 920°C., and as this is a nonquenchable inversion  $l$  and  $h$  are used as subscripts. If a form is metastable at atmospheric pressure or under all known conditions it is followed by the subscript  $m$ . For example, Bakken and Rosenqvist (1952) report a metastable transformation in low albite—this form is designated  $Ab_{Ihm}$ . MacKenzie (1952) reported that  $Ab_{II}$  becomes monoclinic at about 1200°C.; this form is then  $Ab_{IIhm}$  as the change is nonquenchable.  $Ab_I$ ,  $Ab_{II}$ , and  $Ab_{III}$  are triclinic, whereas  $Ab_{IIIh}$  is monoclinic.

#### ORTHOCLASE

Stability relations of the various modifications of potassium feldspar are less well known than are those of albite. The high-temperature forms have long been distinguished from the low by optical tests, but the range of temperatures and pressures in which the various modifications are stable remains unknown. Spencer (1937) has shown that microcline and orthoclase cryptoperthites can be changed to sanidine by heating for long periods at temperatures near the incongruent melting point of

orthoclase. The rate of change varies from one specimen to another, but there is little doubt that the change to sanidine can be brought about if the heating is continued for long periods. In general, the change from microcline to sanidine appears to be more difficult to produce than the change from orthoclase to sanidine.

Sanidine is found in nature with two different optical orientations, and it has been suggested (Tuttle, 1952) that the orientation with the optic plane approximately perpendicular to the symmetry plane be called low sanidine since heating causes the optic axial angle to change to 0° and open out in the symmetry plane (high sanidine). This change takes place at about 800°C. in the Eifel sanidine studied by Spencer (1937, p. 466).

Optical studies, then, indicate that potassium feldspar may occur in four modifications: microcline, orthoclase, low sanidine, and high sanidine. Adularia, considered by some a polymorph of potassium feldspar, may well represent a microcline with +10 per cent albite in solid solution (MacKenzie, 1954). Aside from the change from low- to high sanidine at approximately 800°C., the heating experiments and synthesis of potassium feldspars have provided little information on their stability. Sanidine is found as phenocrysts in the glassy rocks and may therefore be considered to be the high-temperature form. Both high- and low sanidine have been reported, and MacKenzie (1952) has described zoning from high- to low sanidine in a single phenocryst. In view of the change from low- to high sanidine at 800°C. (Spencer, 1937, p. 466) we may tentatively place the inversion at 800°C. High sanidine is then stable from 800°C. up to a temperature at which melting occurs (this will vary somewhat with solid solution of albite). The lower limit of stability of low sanidine is at least as low as 650°C. as there are good reasons for believing that some rhyolites were not far from this temperature when low sanidine was precipitated, suggesting that low sanidine may be the stable form from 650°C. to 800°C. Orthoclase and microcline must be stable below this temperature. Laves (1952) maintains that orthoclase has no stable range, but he has not cited convincing evidence to support this view. A final solution to this problem of the stability of orthoclase awaits further experimental studies. A schematic diagram showing possible interrelations among the four polymorphs is presented in Figure 6.

The system of symbols used for the albite polymorphs is also used for the potassium feldspars.

#### PHASE RELATIONS IN THE SYSTEM $NaAlSi_3O_8$ - $KAlSi_3O_8$

This system is characterized by an unbroken series of solid solutions at high temperatures (Bowen and Tuttle, 1950; Schairer, 1950). Many petrologists have considered this relation the most probable from the relations found in the natural minerals, but others have suggested that a hiatus exists near the sodium end of the series. One feature of the synthetic and natural minerals, the change in symmetry from monoclinic to triclinic, had been most perplexing until the discovery by MacKenzie (1952) that one modification of high albite is monoclinic above 920°C. All the high-temperature triclinic sodium-rich (anorthoclases) alkali feldspars become monoclinic on heating, as discovered independently by MacKenzie and Laves in 1952.

**HIGH SANIDINE-HIGH ALBITE SERIES:** Optical study of synthetic potassium feldspar (Tuttle, 1952) indicated that this material was high sanidine, and the synthetic materials could be considered to represent a complete series of solid solutions between high sanidine and high-temperature monoclinic albite. At temperatures below 660°C.

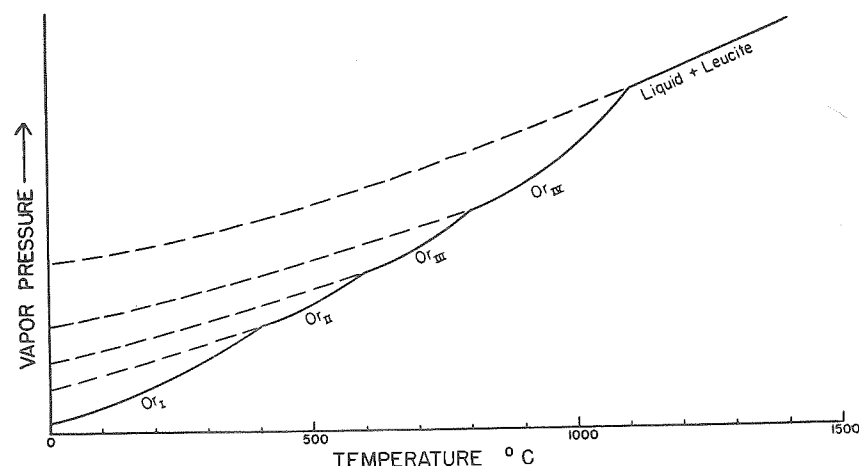


FIGURE 6.—Schematic vapor pressure-temperature diagram for potassium feldspar

Shows theoretical interrelations among the various modifications. Or<sub>I</sub> = microcline, Or<sub>II</sub> = orthoclase, Or<sub>III</sub> = low sanidine, Or<sub>IV</sub> = high sanidine.

two phases appeared in this system. This was first discovered by crystallizing glasses of the appropriate compositions below 660°C. and noting the presence of two peaks on the X-ray diffraction pattern for the (201) reflection. When the two peaks indicate compositions considerably different, two phases can be recognized optically. The composition of the two phases can be estimated by measuring the exact position of the two reflections, using the graph shown in Figure 4 (Bowen and Tuttle, 1950). Thus the compositions of two co-existing feldspars in equilibrium were determined at several temperatures. The miscibility gap or solvus had a maximum temperature of 660°C. at a composition near 55 per cent albite. The minimum temperature of stable existence of a feldspar having this composition is therefore 660°C. If the composition of the feldspar lies on either side of this point its minimum temperature of stable existence will be lower, as indicated by the solvus. When a homogeneous feldspar is cooled to the appropriate temperature indicated by the solvus, unmixing will take place if opportunity for equilibrium prevails. In the presence of water vapor under pressure this reaction can be made to go in both directions. A feldspar held below the solvus will unmix in a few days to two phases, and if these are heated above the solvus they will combine into a single feldspar.

A portion of the solvus determined with our synthetic mixtures may represent metastable equilibria. For example, the sodium-rich feldspar which we obtain at 500°C. may be metastable as it is common for silicates to crystallize in a high-temperature form metastably at low temperatures. The inversion from low albite to the

high form is believed to be below 720°C. for pure albite, and as potassium is more soluble in the high form the inversion will be lowered by the presence of orthoclase in solid solution. If the lowering is rapid the portion of the solvus determined experimentally (*i.e.*, 500°C. and above) may well represent stable equilibria. The solvus determined by direct crystallization of glasses, by unmixing the homogeneous material, and by crystallization at the liquidus at 4000 kg/cm<sup>2</sup> water pressure in the presence of excess silica gave a maximum at 660°C.; this adds considerable support to our belief that the determined solvus represents the stable condition at these temperatures.

**LOW SANIDINE-HIGH ALBITE CRYPTOPERTHITES:** The optical properties of alkali feldspar phenocrysts of most rhyolites (Tuttle, 1952b) differ slightly from the high-sanidine-high-albite (Or<sub>IV</sub>-Ab<sub>IIIh</sub>) series, but here also there is a complete series of solid solutions. The albite end member of this series may be the form Ab<sub>II</sub> which is obtained synthetically below 800°C.; the potassium end member is low sanidine (Or<sub>III</sub>). If this is the correct relation, the possibility of a slight discontinuity near the albite composition must be considered because of the symmetry change from monoclinic to triclinic.

Examples of this series were not prepared synthetically, and our study was restricted to natural materials. Nearly all phenocrysts from rhyolites, as well as the alkali feldspars of certain high-temperature pegmatites and granites, fall into this series. All samples which we examined that contain 30-60 per cent albite are perthitic. Many specimens showed a strong schiller (moonstone), and in some a fine intergrowth could be resolved by the microscope. Usually there was no optical evidence of the two phases, and the perthitic character could be determined only by X-ray studies.

As with the synthetic materials, compositions of the two phases in these natural crystals could be estimated by using the (201) spacing, and after suitable heating the total composition could be determined with an accuracy which may well surpass that of a routine chemical analysis. Most specimens become homogeneous after heating a few minutes at 900°C. Anorthite in solid solution in these sanidines apparently behaves exactly like albite as far as the (201) spacing is concerned, and potassium (orthoclase) content is given by the curve of Figure 4.

Phenocrysts having compositions near Ab<sub>50</sub>Or<sub>50</sub> are usually unmixed to nearly pure albite and pure potassium feldspar. For example, the (201) of the sanidine from the Mitchell Mesa rhyolite (Or<sub>66</sub>) indicates Or<sub>0</sub> for the sodium phase and Or<sub>98</sub> for the potassium phase. In general, sanidines richer than this in potassium show a corresponding increase in the sodium content of the potassium phase, and sanidines having an orthoclase content of 80 per cent or more may show no second phase. Also, anorthoclases rich in sodium may have no unmixed potassium phase. In other words, the unmixing appears to be complete to "pure" end members only when the sodium and potassium are present in nearly equal amounts. It is expected that sodium-rich anorthoclases and potassium-rich sanidines should show less unmixing than intermediate compositions because on cooling they reach the solvus at a considerably lower temperature (and therefore have less opportunity for ordering) than do the intermediate compositions; but it is not apparent why the compositions of the un-



mixed phases in the intermediate sanidine should be nearly pure albite and pure potassium feldspar.

Those specimens which are more nearly unmixed have been used to determine a solvus for this feldspar series. The determinations were made by heating the crystals

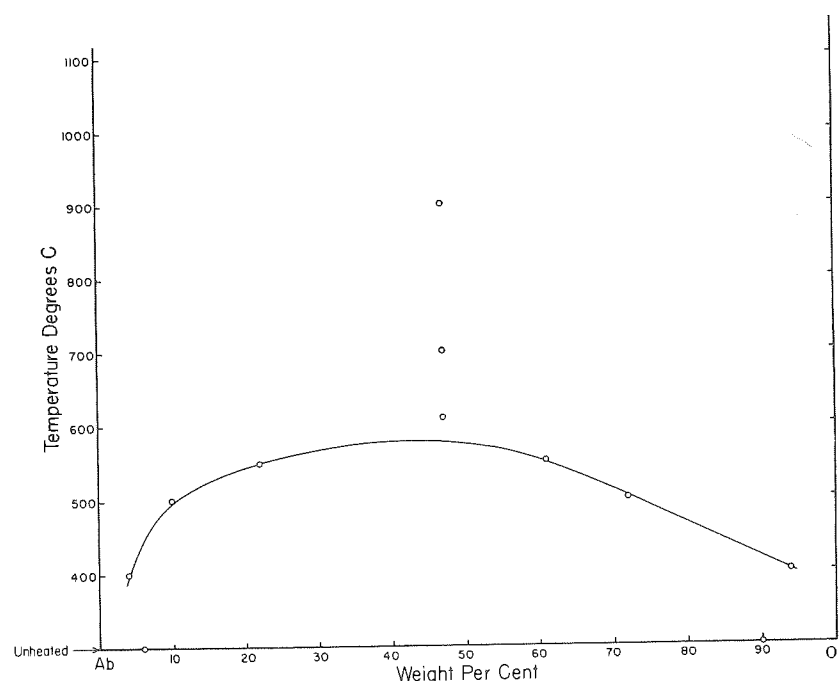


FIGURE 7.—Solvus for alkali feldspar from Korea (Spencer P—Spencer, 1937)

The compositions of the sodium and potassium-rich phases have been determined by the X ray using the (201) spacing.

at various temperatures and estimating the composition of the phases as described above by using the (201) spacing. The method can be illustrated by results on a sanidine from Korea (Spencer P<sup>2</sup>) (Fig. 7). The chemical composition of this feldspar is  $\text{Ab}_{52}\text{Or}_{47}\text{An}_1$ . The first heating at 400°C. apparently resulted in a slight additional unmixing as the two (201) peaks moved apart somewhat from the unheated condition. Heating at 500°C. and 550°C. resulted in marked changes in the compositions of the two phases (Fig. 7; Table 2). At 625°C., only one phase could be recognized, and its position nearly coincides with the chemical composition given by analysis. Additional heating at 700°C. and 900°C. caused no further change in the (201) spacing, and the composition indicated by the (201) is essentially the same as the composition determined by chemical analysis.

Similar results for other specimens are shown in Table 2. The exact position of the

<sup>2</sup> Spencer (1930, 1937, 1938) collected and studied a series of alkali feldspars from a variety of host rocks, and his analyzed specimens have become "type specimens" for many mineralogists studying alkali feldspars. It has become customary to refer to these specimens by the letters that Spencer used (1937, Table I).

TABLE 2.—Results of heating experiments on high-temperature alkali feldspars

Sample	Analyzed composition Or	Temperature °C.	Time	Potassium phase	Sodium phase	One phase present
Spencer P	47.4	unheated	.....	Or <sub>90</sub>	Or <sub>6</sub>	.....
		400	105 days	Or <sub>94</sub>	Or <sub>4</sub>	.....
		500	95 days	Or <sub>72</sub>	Or <sub>10</sub>	.....
		550	4 days	Or <sub>61</sub>	Or <sub>22</sub>	.....
		610	60 hours	.....	.....	Or <sub>47</sub>
		700	2 hours	.....	.....	Or <sub>47</sub>
		900	4 hours	.....	.....	Or <sub>47</sub>
Spencer Sparling Gulch	46.6	unheated	.....	Or <sub>89</sub>	Or <sub>0</sub>	.....
		400	105 days	Or <sub>90</sub>	Or <sub>0</sub>	.....
		500	95 days	Or <sub>72</sub>	Or <sub>13</sub>	.....
		548	4 days	Or <sub>62</sub>	Or <sub>21</sub>	.....
		610	60 hours	.....	.....	Or <sub>46</sub>
		900	1 hour	.....	.....	Or <sub>46</sub>
		900	140 hours	.....	.....	Or <sub>47</sub>
Mitchell Mesa rhyolite	43.3	unheated	.....	Or <sub>98</sub>	Or <sub>2</sub>	.....
		400	105 days	Or <sub>94</sub>	Or <sub>3</sub>	.....
		500	95 days	Or <sub>80</sub>	Or <sub>10</sub>	.....
		548	4 days	Or <sub>63</sub>	Or <sub>19</sub>	.....
		610	60 hours	.....	.....	Or <sub>45</sub>
		900	140 hours	.....	.....	Or <sub>44</sub>
Grant County, New Mexico	59.2	unheated	.....	Or <sub>89</sub>	Or <sub>0</sub>	.....
		400	105 days	Or <sub>85</sub>	Or <sub>3</sub>	.....
		500	95 days	Or <sub>72</sub>	.....	.....
		548	4 days	Or <sub>62</sub>	.....	.....
		900	140 hours	.....	.....	Or <sub>62</sub>
Victoria, Australia	23.4	unheated	.....	.....	Or <sub>7</sub>	.....
		500	95 days	.....	Or <sub>14</sub>	.....
		900	16 hours	.....	.....	Or <sub>23</sub>

solvus for these natural materials varies somewhat from one specimen to another, perhaps because of slight variations in anorthite content, but taken together the specimens studied give a solvus considerably different from the solvus determined for the synthetic materials.

ORTHOCLASE CRYPTOPERTHITES: Alkali feldspars from many pegmatites, granites, and associated metamorphic rocks are commonly identified as orthoclase or as orthoclase cryptoperthites. Spencer (1930; 1937; 1938) demonstrated that an unbroken series of alkali feldspars extends from orthoclase to compositions containing up to 60 per cent albite. Extrapolation of the optical properties to the sodium end of the series coincides with the values for low-temperature albite. Most representatives of this series are perthitic. The size of the perthite lamellae varies from sub-optical to lamellae large enough to identify optically as low albite. This series then represents intergrowths of low-temperature albite and a potassium feldspar which

may be called orthoclase although single-crystal studies of the unmixed materials may show the presence of a triclinic potassium phase. In general, however, the potassium phase is monoclinic.

As with the high-temperature series, the  $(\bar{2}01)$  spacing indicates the presence of

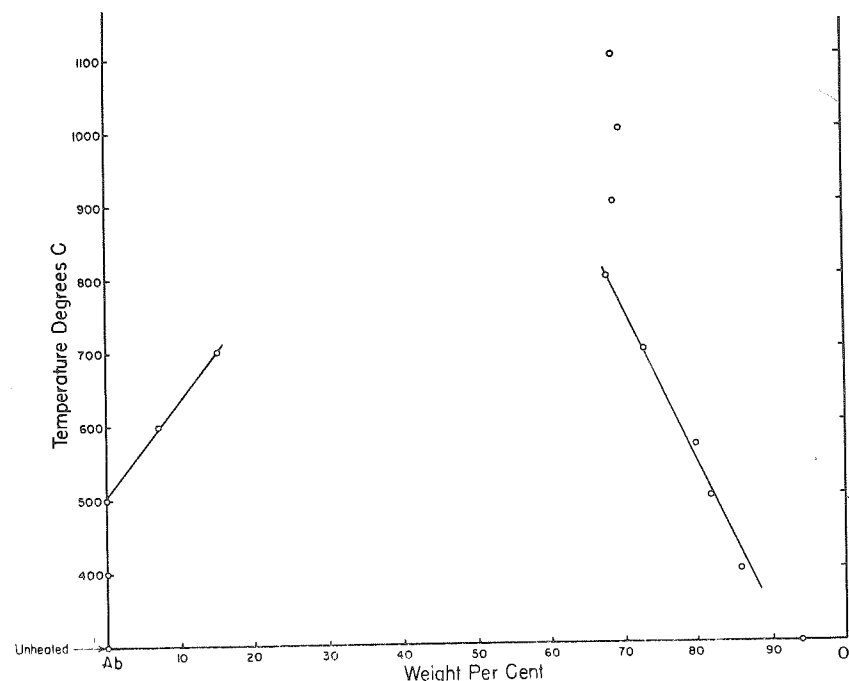


FIGURE 8.—Effect of temperature on the two components of a low temperature cryptoperthite (Spencer I—Spencer, 1937)

The compositions of the sodium- and potassium-rich phases have been determined by the X ray using the  $(\bar{2}01)$  spacing.

two phases. However, determination of the position of the  $(\bar{2}01)$  reflections commonly indicates albite with a negative quantity of orthoclase and orthoclase with a negative amount of albite, when using the curve prepared from synthetic materials. This indicates that the  $(\bar{2}01)$  of the two phases is different from the same spacing in high albite and sanidine; the  $(\bar{2}01)$  of low albite is different from high albite in the right direction to explain part of the discrepancy. A possible explanation is that the two phases are interacting in some fashion to give anomalous results for the  $(\bar{2}01)$  spacing. This difficulty does not arise in the cryptoperthites of the low-sanidine-high-albite series, and there is no obvious reason why the representatives of this series should behave in this fashion.

Despite this uncertainty, the  $(\bar{2}01)$  gave approximate compositions, and the heated materials behaved much like the sanidine-high albite cryptoperthites—that is, on heating the potassium phase took up sodium, and the sodium phase became richer in potassium. To determine compositions in this series, the two phases in Spencer M were considered pure orthoclase and pure albite, and a curve was drawn

using these as end members. Spencer M was chosen because the difference between the  $(\bar{2}01)$  of the sodium and potassium phases was slightly greater than the other specimens studied (Spencer R and O are essentially the same as M).

Figure 8 illustrates the results of heating Spencer I at various temperatures. At

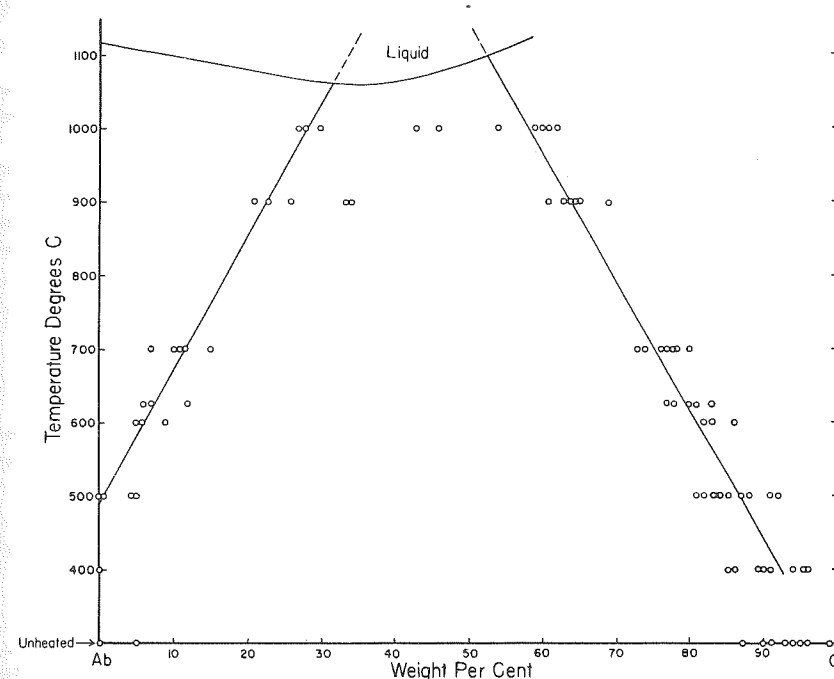


FIGURE 9.—Graph showing the compositional changes in sodium- and potassium-rich components of orthoclase cryptoperthites on heating to various temperatures and quenching

The compositions were determined by the X ray using the  $(\bar{2}01)$  spacing. The results indicate that there is a metastable miscibility gap in these feldspars which extends to the liquidus. Prolonged heating at 900°C., for example, will sanidinize these feldspars, and in this condition they are completely miscible above approximately 660°C.

500°C. the albite phase is represented by a rather strong  $(\bar{2}01)$  reflection which has not changed from the original position, but the intensity is somewhat less. At 600°C. the albite  $(\bar{2}01)$  has moved appreciably, and the intensity has fallen considerably. The  $(\bar{2}01)$  for the sodium-rich phase at 700°C. is very weak, but it has moved to the composition illustrated. Above 700°C. the  $(\bar{2}01)$  for the sodium phase is no longer recognized, and at 800°C. and higher the potassium phase remains unchanged in composition, indicating that the material is homogeneous. The slope of the two lines for the sodium and potassium phases, projected to higher temperatures, suggests that the liquidus will be intersected before the material becomes homogeneous. This is the relation found for the specimens richer in sodium than Spencer I. Orthoclase cryptoperthites containing approximately 50 per cent albite do not homogenize below the liquidus. They apparently become homogeneous only after inverting to the high-temperature form. The results of the heating experiments are shown in Figure 9 and Table 3.

TABLE 3.—Results of heating experiments on low-temperature alkali feldspars

Sample	Analyzed composition Or	Temperature °C.	Time	Potassium phase	Sodium phase	One phase only
Spencer E	83.3	unheated	.....	Or <sub>87</sub>	.....	.....
		400	105 days	Or <sub>85</sub>	.....	.....
		500	95 days	.....	.....	Or <sub>84</sub>
		890	4 days	.....	.....	Or <sub>80</sub>
Spencer F	78.7	unheated	.....	.....	.....	Or <sub>77</sub>
		400	105 days	.....	.....	Or <sub>74</sub>
		500	95 days	.....	.....	Or <sub>71</sub>
		700	4 days	.....	.....	Or <sub>71</sub>
Spencer H	72.5	unheated	.....	Or <sub>91</sub>	Or <sub>0</sub>	.....
		400	105 days	Or <sub>91</sub>	Or <sub>0</sub>	.....
		500	95 days	Or <sub>88</sub>	Or <sub>0</sub>	.....
		625	92 days	Or <sub>78</sub>	?	.....
		700	4 days	Or <sub>77</sub>	?	.....
		900	4 hours	.....	.....	Or <sub>74</sub>
		1000	21 hours	.....	.....	Or <sub>73</sub>
Spencer I	69.4	unheated	.....	Or <sub>94</sub>	Or <sub>0</sub>	.....
		400	105 days	Or <sub>86</sub>	Or <sub>0</sub>	.....
		500	95 days	Or <sub>82</sub>	Or <sub>5</sub>	.....
		625	92 days	Or <sub>80</sub>	Or <sub>12</sub>	.....
		700	125 hours	Or <sub>73</sub>	?	.....
		800	125 hours	Or <sub>68</sub>	?	.....
		900	40 hours	.....	.....	Or <sub>69</sub>
		1000	21 hours	.....	.....	Or <sub>70</sub>
Spencer J	66.6	unheated	.....	Or <sub>96</sub>	Or <sub>0</sub>	.....
		400	105 days	Or <sub>96</sub>	Or <sub>0</sub>	.....
		500	95 days	Or <sub>85</sub>	Or <sub>0</sub>	.....
		625	92 days	Or <sub>81</sub>	Or <sub>7</sub>	.....
		700	125 hours	Or <sub>77</sub>	Or <sub>16</sub>	.....
		900	4 hours	Or <sub>69</sub>	?	.....
Spencer K	64.5	unheated	.....	Or <sub>93</sub>	Or <sub>0</sub>	.....
		400	105 days	Or <sub>90</sub>	Or <sub>0</sub>	.....
		500	95 days	Or <sub>81</sub>	?	.....
		625	92 days	Or <sub>77</sub>	?	.....
		700	102 hours	Or <sub>74</sub>	?	.....
		900	54 hours	Or <sub>69</sub>	?	.....
		1080	15 hours	.....	.....	Or <sub>65</sub>

TABLE 3.—Continued

Sample	Analyzed composition Or	Temperature °C.	Time	Potassium phase	Sodium phase	One phase only
Spencer M	57.3	unheated	.....	Or <sub>100</sub>	Or <sub>0</sub>	.....
		400	105 days	Or <sub>96</sub>	Or <sub>0</sub>	.....
		500	105 days	Or <sub>87</sub>	Or <sub>5</sub>	.....
		625	92 days	Or <sub>84</sub>	Or <sub>5</sub>	.....
		700	144 hours	Or <sub>80</sub>	Or <sub>11</sub>	.....
		900	4 hours	Or <sub>64</sub>	Or <sub>34</sub>	.....
		900	40 hours	Or <sub>66</sub>	Or <sub>36</sub>	.....
		900	136 hours	Or <sub>64</sub>	Or <sub>25</sub>	.....
		1000	8 hours	Or <sub>62</sub>	Or <sub>43</sub>	.....
Spencer N	53.7	unheated	.....	Or <sub>90</sub>	Or <sub>0</sub>	.....
		400	105 days	Or <sub>90</sub>	Or <sub>0</sub>	.....
		500	95 days	Or <sub>84</sub>	Or <sub>0</sub>	.....
		600	82 days	Or <sub>82</sub>	Or <sub>5</sub>	.....
		700	120 hours	Or <sub>76</sub>	Or <sub>11</sub>	.....
		900	5 hours	Or <sub>63</sub>	Or <sub>34</sub>	.....
		900	160 hours	Or <sub>63</sub>	Or <sub>32</sub>	.....
		1000	21 hours	Or <sub>61</sub>	Or <sub>46</sub>	.....
Spencer O	48.5	unheated	.....	Or <sub>98</sub>	Or <sub>0</sub>	.....
		400	105 days	Or <sub>94</sub>	Or <sub>0</sub>	.....
		500	95 days	Or <sub>92</sub>	Or <sub>0</sub>	.....
		600	89 days	Or <sub>86</sub>	Or <sub>5</sub>	.....
		700	13 days	Or <sub>77</sub>	Or <sub>7</sub>	.....
		900	40 hours	Or <sub>64</sub>	Or <sub>23</sub>	.....
		1000	8 hours	Or <sub>59</sub>	Or <sub>28</sub>	.....
Spencer Q	45.6	unheated	.....	Or <sub>95</sub>	Or <sub>5</sub>	.....
		900	21 hours	Or <sub>65</sub>	Or <sub>21</sub>	.....
		1000	21 hours	Or <sub>60</sub>	Or <sub>27</sub>	.....
Spencer R	44.1	unheated	.....	Or <sub>99</sub>	Or <sub>0</sub>	.....
		400	105 days	Or <sub>100</sub>	Or <sub>0</sub>	.....
		500	95 days	Or <sub>91</sub>	Or <sub>0</sub>	.....
		600	89 days	Or <sub>83</sub>	Or <sub>9</sub>	.....
		700	14 days	Or <sub>78</sub>	Or <sub>10</sub>	.....
		900	10 days	Or <sub>61</sub>	Or <sub>26</sub>	.....
		1000	21 hours	Or <sub>54</sub>	Or <sub>30</sub>	.....

The metastable mixing of these orthoclase cryptoperthites was readily reversed by slow cooling or by first heating to high temperatures and then at lower temperatures. The unmixing could be produced more readily than in the high-temperature series. For example, Spencer M, first heated to 1000°C., unmixed at 700°C. in 3 hours to the same composition obtained on heating to 700°C. This was the shortest time used, and it is likely from Spencer's (1937) slow-cooling experiments that the un-

mixing will take place even more rapidly. Nearly complete unmixing took place in Spencer M in 60 days at 500°C. after heating at a higher temperature.

The greater part of the solvus determined on the orthoclase cryptoperthites is almost certainly metastable, and probably the entire solvus as determined is metastable. At the higher temperatures the mixing is certainly metastable as continued heating will sanidinize the intergrowth, and complete mixing will take place. After sanidinization, the unmixing observed at, say, 700°C. in the unsanidinized material will not take place.

**MICROCLINE CRYPTOPTHITES:** Cryptoperthites in which the potassium component is microcline were not studied in detail because analyzed materials of suitable compositions were not available. However, the microclines studied by Spencer were subjected to the same heating experiments described above for orthoclase cryptoperthites, and in all cases the (201) spacing changed in the same fashion as the members of the other series. Some of the feldspars which have been called orthoclase cryptoperthites contain a triclinic potassium phase. If the potassium phase is microcline, then the general relations described above for the orthoclase cryptoperthites will also hold for the microcline-low albite series.

**DISCUSSION:** All the low-temperature cryptoperthites having compositions near  $Ab_{50}Or_{50}$  refused to mix completely on heating near the liquidus, and in this respect our results differ from the proposal of Laves (1952) that there is a complete, although metastable, series of solid solutions between microcline and low albite. Possibly all the specimens we studied represent orthoclase-low albite cryptoperthites rather than microcline-low albite mixtures, but the fact that the potassium phase in some of our specimens was triclinic suggested that the metastable miscibility gap at high temperatures might well exist for the microcline-low-albite series also.

Laves (1952, p. 567) has proposed that the failure of these low-temperature cryptoperthites to homogenize readily is due to different Al-Si distributions in the two unmixed phases and that the changes observed are a result of the development of a distribution equilibrium of Na and K ions between the two Al-Si frameworks of the two phases. We prefer to regard this as a metastable equilibrium, and the miscibility gap which we have determined indicates the limited solubility of the two metastable phases in one another.

The three miscibility gaps determined for the three series (orthoclase, sanidine, and synthetic feldspar) are shown in Figure 10. The solvus determined on the synthetic material is believed to represent the stable relationship above approximately 550°C. This is supported by the fact that the temperature of 660°C. for the top of this solvus was found by three different methods.

Composition of the perthitic components of orthoclase cryptoperthites as a function of temperature showed a considerably greater spread than would be expected from experimental error alone (Fig. 9). The spread may result from small differences in the calcium or barium content of the specimens, or it may be related to the nature of the potassium feldspar which can vary continuously from orthoclase to maximum microcline.

The complexity of the phase relations between the sodium and potassium feldspars can be illustrated by a schematic TX phase diagram (Fig. 11). The relations are further complicated by the fact that the inversions are sluggish; as a result it is possible that two to five phases can coexist in a cryptoperthite which appears op-

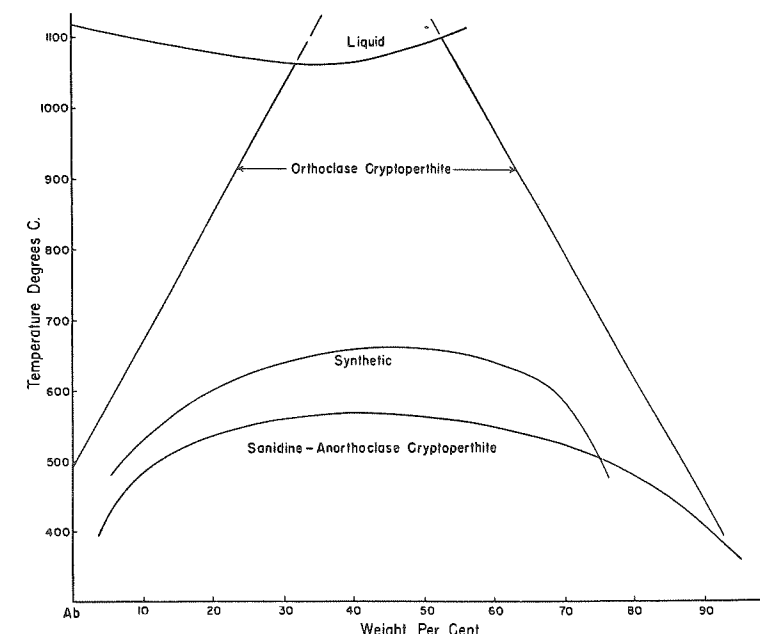


FIGURE 10.—Three solvuses in the alkali feldspars

It is believed that the miscibility gap for the low-albite-microcline series will be little different from the low-albite-orthoclase series when suitable material is discovered to determine these relationships for microcline cryptoperthites.

tically homogeneous. For example, optical and X-ray studies indicate that the following phases may coexist in a single crystal:

- High sanidine-low sanidine
- Low sanidine-microcline
- Low sanidine-orthoclase
- Orthoclase-microcline
- High albite-low sanidine
- High albite-orthoclase
- High albite-microcline
- Low albite-orthoclase
- Low albite-microcline
- High albite-low albite-low sanidine
- High albite-low albite-orthoclase
- High albite-low albite-microcline
- High albite-low albite-orthoclase-microcline
- Low albite-orthoclase-microcline



With these possible complications it is not difficult to envisage the tremendous storage capacity of the feldspars for information concerning their thermal history and the thermal and chemical history of the rocks in which they are found. The door to this storehouse of information is slowly being opened, and the geological

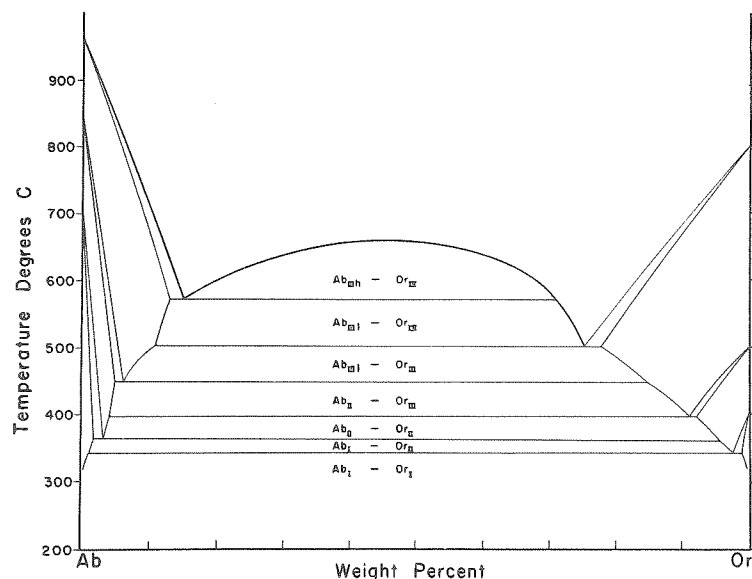


FIGURE 11.—Schematic equilibrium diagram for the system  $\text{NaAlSi}_3\text{O}_8$ - $\text{KAlSi}_3\text{O}_8$

The solvuses of Figure 10 probably represent metastable extensions of the stable relations depicted in this figure, at least for the orthoclase and sanidine cryptoperthites.

thermometer will soon have many new divisions to aid in deciphering the history of the feldspar-bearing rocks.

#### SILICA

The stable form of  $\text{SiO}_2$  encountered at the liquidus throughout most of the system is high ( $\beta$ ) quartz which is invariably found as doubly terminated hexagonal pyramids. The prism faces were not observed on the synthetic material. Low ( $\alpha$ ) quartz is the stable form below 575°C. at atmospheric pressure, and the temperature of the inversion ( $\alpha \rightleftharpoons \beta$ ) is raised approximately 25°C. for each 1000 kg/cm<sup>2</sup> hydrostatic pressure (Yoder, 1950). This modification, then, occurs at the liquidus at 4000 kg/cm<sup>2</sup> below approximately 675°C.

Above 870°C. and below 1470°C. tridymite is the stable form of silica at atmospheric pressure. The influence of pressure on the temperature of the  $\beta$  quartz  $\rightleftharpoons$  tridymite transformation has been calculated from thermodynamic data (Mosesman and Pitzer, 1941), but apparently direct determinations of this univariant equilibrium have not been carried out. As tridymite was encountered at the liquidus at low pressures in some experiments, the PT relations of this transformation were experimentally determined up to 1000 kg/cm<sup>2</sup>.

The inversion temperature for each pressure was determined by placing a charge,

consisting of quartz surrounded by a buffer of tridymite (or vice versa), in the quenching apparatus and heating at a known temperature and pressure of water vapor until one of the phases changed, completely or in part, to the other phase. By repeating at constant pressure, a temperature above which quartz changed to

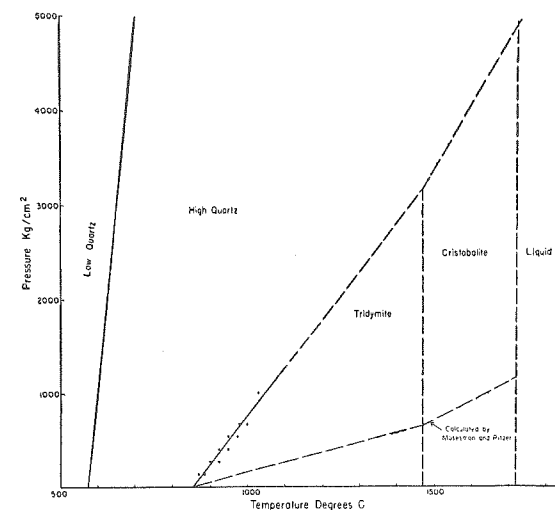


FIGURE 12.—Pressure-temperature diagram for  $\text{SiO}_2$

tridymite and below which tridymite changed to quartz could be readily determined. The quartz and tridymite were prepared from pure silica glass (a 0.5 gm sample gave less than 0.001 gm residue on treatment with sulfuric acid and hydrogen fluoride) by crystallizing in the presence of water vapor.

Results of the determinations are shown in Table 4 and Figure 12. The inversion is indeed sensitive to pressure. A pressure of 1000 kg/cm<sup>2</sup> raises the inversion temperature approximately 180°C. Extrapolation of this curve to high temperatures indicated that quartz will melt directly to a liquid at moderate pressures. If the extrapolation is made without considering the cristobalite field, quartz will melt directly to a liquid at about 4500 kg/cm<sup>2</sup>, assuming the liquidus temperature is not greatly raised by this pressure. The slope of the cristobalite  $\rightleftharpoons$  quartz curve will, of course, not coincide with the tridymite  $\rightleftharpoons$  quartz curve; however, in all probability their slopes will not differ greatly, and the cristobalite  $\rightleftharpoons$  quartz curve will be the steeper. Our knowledge of the density of tridymite and cristobalite at elevated temperatures is so meager that the sign of the slope of the curve for tridymite  $\rightleftharpoons$  cristobalite reaction cannot be predicted with confidence, and in Figure 12 it is shown as being vertical.

The general relations shown in Figure 12 were first pointed out by Mosesman and Pitzer (1941) on the basis of thermodynamic calculations. Their calculations gave the quartz  $\rightleftharpoons$  tridymite and tridymite  $\rightleftharpoons$  cristobalite curves shown in Figure 12. The discrepancies between the calculated and observed results are rather large, but the general character of the phase relations is changed but little by the direct determination of the quartz  $\rightleftharpoons$  tridymite inversion. Mosesman and Pitzer concluded that

quartz would melt directly and stably to a liquid at pressures above 1170 atmospheres hydrostatic pressure. The present results suggest that the pressure must be considerably higher, probably greater than 5000 atmospheres.

Geologically, the fact that quartz may melt directly to a liquid at 5000 kg/cm<sup>2</sup>

TABLE 4.—Results of quenching experiments on the effect of pressure on the quartz-tridymite inversion

Starting material	Temperature °C.	Pressure psi	Time	Result
Quartz	885	2000	2 days	Tridymite
Tridymite	885	2000	2 days	Tridymite
Quartz	870	2000	2 days	Quartz
Tridymite	870	2000	2 days	Tridymite partially changed to quartz
Quartz	925	4000	16 hours	Quartz partially changed to tridymite
Tridymite	925	4000	16 hours	Tridymite
Quartz	900	4000	16 hours	Quartz
Tridymite	900	4000	16 hours	Tridymite partially changed to quartz
Quartz	950	6000	16 hours	About 50% of quartz changed to tridymite
Tridymite	950	6000	16 hours	Tridymite
Quartz	925	6000	16 hours	Quartz
Tridymite	925	6000	16 hours	Tridymite partially changed to quartz
Quartz	975	8000	20 hours	Quartz partially changed to tridymite
Tridymite	975	8000	20 hours	Tridymite
Quartz	950	8000	20 hours	Quartz
Tridymite	950	8000	20 hours	Quartz
Quartz	1000	10,000	6 hours	Tridymite
Tridymite	1000	10,000	6 hours	Tridymite
Quartz	980	10,000	5 hours	Quartz
Tridymite	980	10,000	5 hours	Tridymite partially changed to quartz
Quartz	1050	15,000	2 hours	Quartz partially changed to tridymite
Tridymite	1050	15,000	2 hours	Tridymite
Quartz	1030	15,000	2 hours	Quartz
Tridymite	1030	15,000	2 hours	Quartz

and 1720°C. is of very little importance, as such conditions are not to be expected in the earth's crust. The quartz  $\rightleftharpoons$  tridymite inversion falls in a different category, as tridymite is found as phenocrysts in some rhyolitic rocks, and the PT curve gives a minimum temperature for various pressures at which the phenocrysts could have formed under equilibrium conditions.

Using the slope of the inversion temperature versus pressure curve, the heat of transformation can be calculated using the Clapeyron equation:

$$\frac{dT}{dP} = \frac{T\Delta V}{\Delta H}$$

$$\frac{dT}{dP} = .18^\circ/\text{bar using the PT curve}$$

$$T = 1143^\circ\text{K}$$

$$\Delta V = 3.75 \text{ cc/mole}$$

$$\text{then } \Delta H = 560 \text{ cal/mole}$$

This value for  $\Delta H$  is to be compared with  $120 \pm 50$  cal/mole calculated by Mosesman and Pitzer (1941). As the same value for  $\Delta V$  has been used in both calculations the discrepancy can be attributed to three possible sources of error: (1) heat of solution measurements, (2) heat-capacity measurements used by Mosesman and Pitzer in their calculations, or (3) the present results are in error because of solid solution of water in either high quartz or tridymite or both. It seems unlikely that appreciable solubility of water in quartz or tridymite could escape detection, and therefore it appears that the discrepancy is likely to be discovered in the calorimetric determinations or the thermodynamic calculations.

The value of  $\Delta V$  used in both calculations is subject to a considerable uncertainty and should be checked by X-ray measurements of the cell dimensions of quartz and tridymite at 870°C.

#### SYSTEM $\text{SiO}_2\text{-H}_2\text{O}$

During the study of the effect of pressure on the quartz-tridymite inversion it was noted that at the highest pressures and temperatures used the quartz grains appeared to have melted some during the experiment. Although the quartz melted metastably, it nevertheless suggested that we might very well be approaching the liquidus in the binary system  $\text{SiO}_2\text{-H}_2\text{O}$ . Accordingly, an attempt was made to determine the liquidus relations in the silica-rich portion of the system.

A preliminary report has been made on these studies (Tuttle and England, 1955). The experiments were carried out by J. L. England using the Goranson apparatus (see Goranson, 1931, for a description of this equipment) which is internally heated and therefore permits use of higher temperatures and pressures than does the equipment used for most of this study. Unfortunately, the equipment failed before we could check the reproducibility, but as the results are of general interest it was thought desirable to publish the tentative diagram for the silica-rich part of the system (Fig. 13; Table 5).

The effect of water on the silica liquidus was considerably greater than expected. The liquidus of cristobalite was lowered rapidly by water vapor under pressure; the first 1000 kg/cm<sup>2</sup> of water vapor lowered the liquidus nearly 500°C. Geologists have long known that water is a potent flux for the alkali silicates, but apparently it has not been suspected that the liquidus of silica itself would be profoundly affected by water vapor under pressure.

A water determination carried out on one charge which had been heated at 1306°C. and 1200 kg/cm<sup>2</sup> gave 2.3 weight per cent water. This value appears to be low considering the amount of lowering of the liquidus produced by 1200 kg/cm<sup>2</sup> water-vapor pressure.

This information on the effect of water on the liquidus of silica permitted construction of a PTX diagram for the system (Fig. 14). The diagram is schematic in part because certain triple and quadruple points have not been precisely located. In this system there are at least 15 triple points involving unary equilibria, and 5 quadruple points involving binary equilibria.

As silica is only slightly soluble in water at low temperatures the critical point ( $K_{\text{H}_2\text{O}}$ ) will be only slightly raised by the presence of silica ( $K_1$ ), and a second critical end point must lie at high pressure unless decomposition intervenes. As there is no

evidence of decomposition of silica by water vapor it is assumed that a second critical end point ( $K_2$ ) lies at high pressure and at a temperature somewhat above the first critical end point. The proportion of water and silica in the liquid at the second critical end point is unknown.

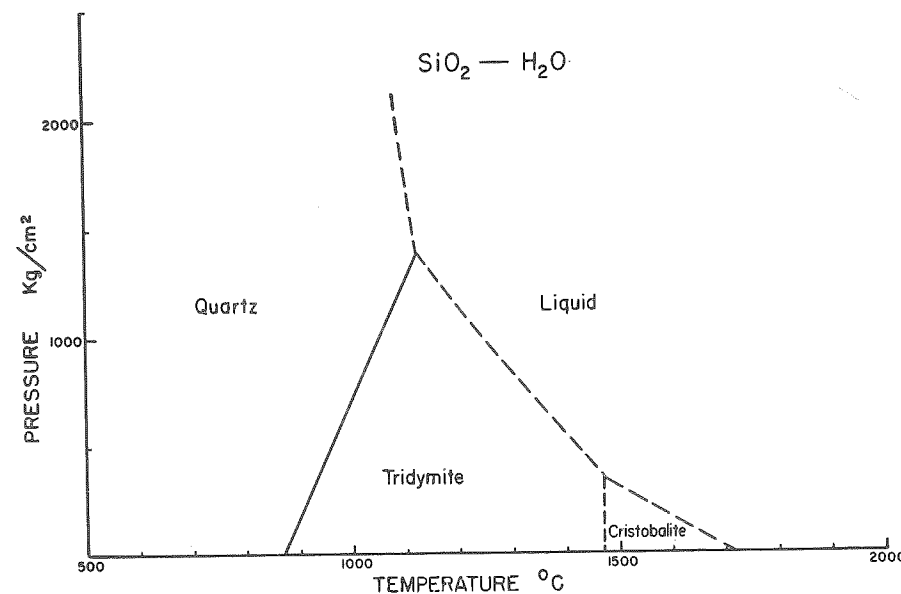


FIGURE 13.—Pressure-temperature relations in the system  $\text{SiO}_2\text{-H}_2\text{O}$   
(After Tuttle and England, 1955)

It is assumed that low quartz is slightly soluble in water, and therefore the liquidus of water will be lowered to the eutectic  $E$ . The curve  $E\text{-}K_1$  represents the pressures and temperatures along which low quartz was in equilibrium with hydrous liquids. From the above experimental studies it is known that water under pressure lowers the liquidus of silica along the curve  $T_{\text{SiO}_2}\text{-}Q_1$  (Fig. 14). At  $Q_1$  the saturation surface of cristobalite intersects the stability field of tridymite, and tridymite becomes the primary phase at lower temperatures. The PT curve for the univariant transition  $\text{tridymite} \rightleftharpoons \text{cristobalite}$  is unaffected by the intersection of the liquidus, because there is no solid solution in either phase, and the curve deals only with unary relationships.

As the temperature was lowered from  $Q_1$  into the tridymite stability field the saturation surface of tridymite rose in pressure along the curve  $Q_1\text{-}Q_2$ . The amount of water dissolved in the liquid steadily increased as can be seen in the TX and PX projections. At  $Q_2$  the stability field of high quartz was reached, and we now had four phases in equilibrium—tridymite, high quartz, liquid, and vapor. Continued lowering of the temperature, although not experimentally studied, will cause additional water to dissolve in the liquid phase, and this in turn requires higher pressure until at  $Q_3$  the stability field of low quartz will be reached. The temperature and

pressure of this quadruple point are unknown, but they probably lie well within the experimental range of present-day apparatus.

The next quadruple point ( $Q_4$ ) to be reached by the saturation surface will involve low quartz, silica<sub>c</sub>, liquid, and vapor. Silica<sub>c</sub>, which has been produced at high pres-

TABLE 5.—Experiments on the system  $\text{SiO}_2\text{-H}_2\text{O}$

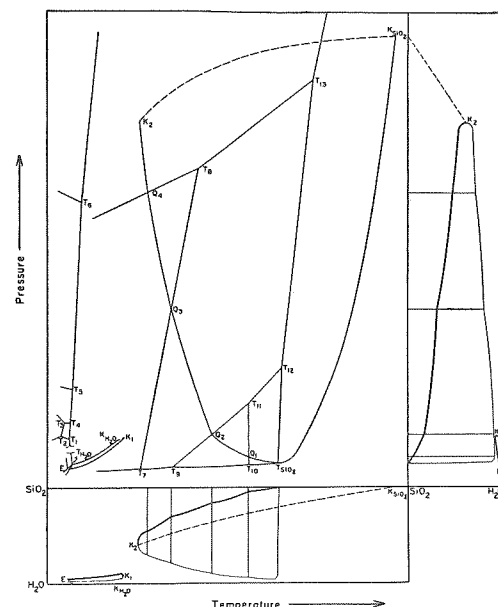
Experimental number	Initial material	Temp. °C.	Pressure kg/cm²	Time Hours	Result
Q2-33D	Tridymite	1306	1200	1	All glass
	Quartz	1306	1200	1	All glass
	$\text{SiO}_2$ glass	1306	1200	1	All glass
Q2-33E	Tridymite	1200	1200	1	All glass
	$\text{SiO}_2$ glass	1200	1200	1	All glass
Q2-34A	Tridymite	1156	1200	1½	Tridymite
	$\text{SiO}_2$ glass	1156	1200	1½	Largely tridymite
Q2-34C	Quartz	1000	2000	2	Quartz
	$\text{SiO}_2$ glass	1000	2000	2	Largely quartz
Q2-34D	Quartz	1075	2000	2	Quartz
	$\text{SiO}_2$ glass	1075	2000	2	Quartz

ures (Coes, 1953), has not been discovered in nature. The high density of this phase suggests that the slope of the PT curve for the reactions  $\text{low quartz} \rightleftharpoons \text{silica}_c$  and  $\text{high quartz} \rightleftharpoons \text{silica}_c$  will have a strong positive slope and that silica<sub>c</sub> will probably appear at the liquidus at extreme pressures.

One feature of the PX and TX projections which differs from previously suggested relationships for such systems consisting of a volatile and a nonvolatile substance is the manner in which the vapor composition changes when water is added to liquid silica. In Figure 14 the vapor composition varies rapidly for slight changes in pressures of water vapor, whereas previous investigators have indicated that the vapor composition is changed only slightly initially (*i.e.*, Morey and Ingerson, 1937, p. 615; Ricci, 1951, p. 87, etc.). It is believed that the vapor in any such system will consist largely of the volatile component at very low pressures. In other words the vapor in equilibrium with liquid silica will consist largely of water when the pressure is only a fraction of 1 kg/cm², and the concentration of silica in the vapor will become appreciable again only at very high pressures of water vapor.

The triple points are:  $T_1 = \text{Ice}_I + \text{Ice}_{III} + \text{liquid}$ ,  $T_2 = \text{Ice}_I + \text{Ice}_{II} + \text{Ice}_{III}$ ,  $T_3 = \text{Ice}_{II} + \text{Ice}_{III} + \text{Ice}_V$ ,  $T_4 = \text{Ice}_{III} + \text{Ice}_V + \text{liquid}$ ,  $T_5 = \text{Ice}_V + \text{Ice}_{VI} + \text{liquid}$ ,  $T_6 = \text{Ice}_{VI} + \text{Ice}_{VII} + \text{liquid}$ ,  $T_7 = \text{low quartz} + \text{high quartz} + \text{vapor}$ ,  $T_8 = \text{silica}_c + \text{low quartz} + \text{high quartz}$ ,  $T_9 = \text{high quartz} + \text{tridymite} + \text{vapor}$ ,  $T_{10} = \text{tridymite} + \text{cristobalite} + \text{vapor}$ ,  $T_{11} = \text{high quartz} + \text{tridymite} + \text{cristobalite}$ ,  $T_{12} = \text{high quartz} + \text{cristobalite} + \text{liquid}$ ,  $T_{13} = \text{silica}_c + \text{low quartz} + \text{liquid}$ ,  $T_{\text{H}_2\text{O}} = \text{Ice}_I + \text{liquid} + \text{vapor}$ ,  $T_{\text{SiO}_2} = \text{cristobalite} + \text{liquid} + \text{vapor}$ .

<sup>3</sup>  $\text{Ice}_{IV}$  is apparently a metastable modification which is obtained along the metastable prolongation of the curve  $T_6\text{-}T_5$  to lower pressures and temperatures. A metastable triple point can be realized involving  $\text{Ice}_{IV} + \text{Ice}_V + \text{liquid}$ .

FIGURE 14.—Schematic PTX relations in the system  $\text{SiO}_2\text{-H}_2\text{O}$ 

The new form of silica discovered by L. Coes (1953) is shown as being stable only at high pressures as is indicated by the experimental studies of Coes. Point  $T_8$  is then the triple point involving silica<sub>c</sub>, low quartz, and high quartz.

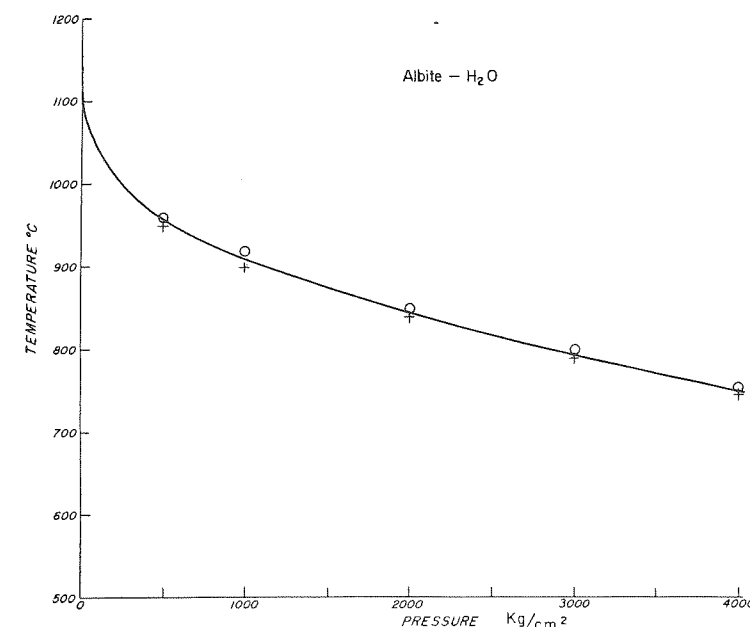
TABLE 6.—Results of quenching experiments in the system  $\text{NaAlSi}_3\text{O}_8\text{-H}_2\text{O}$   
All material was crystalline at beginning of experiment

Run number	Pressure kg/cm <sup>2</sup>	Temp. °C.	Time Hours	Results
Q2-25B	500	950	1	No glass
Q2-25A	500	960	1	50% glass
Q1-28B	1000	900	24	No glass
Q1-28E	1000	920	22	90+ % glass
Q1-30A	2000	840	3	No glass
Q1-29E	2000	850	3	75% glass
Q1-29A	3000	790	3	No glass
Q1-29B	3000	800	3	90+ % glass
Q2-25H	4000	745	1	No glass
Q2-25G	4000	755	1	50% glass
*	5291	760	1	Largely glass
*	5632	727	½	No glass

\* These runs were kindly made for us by Dr. H. S. Yoder.

The quadruple points are:  $Q_1$  = cristobalite + tridymite + liquid + vapor,  $Q_2$  = tridymite + high quartz + liquid + vapor,  $Q_3$  = high quartz + low quartz + liquid + vapor,  $Q_4$  = silica<sub>c</sub> + low quartz + liquid + vapor, and E = low quartz + Ice<sub>1</sub> + liquid + vapor.

This somewhat detailed discussion of the system silica-water has been included to familiarize the reader with the general nature of silicate-water equilibria, for this system is much like the systems  $\text{NaAlSi}_3\text{O}_8\text{-H}_2\text{O}$ ,  $\text{KAlSi}_3\text{O}_8\text{-H}_2\text{O}$ , and  $\text{CaAl}_2\text{Si}_2\text{O}_8\text{-H}_2\text{O}$ . Also, it is well to realize the complexities introduced by volatile material and

FIGURE 15.—Liquidus relations in a portion of the system  $\text{NaAlSi}_3\text{O}_8\text{-H}_2\text{O}$  projected onto the pressure-temperature plane

pressure before proceeding into the more complex systems involving two or more silicates.

The application of these results on the silica-water system to the problems of silica migration, the quartz veins, and the quartz cores of pegmatites is a very attractive objective, but until the system is studied at higher pressures and lower temperatures and the water content of the liquids is known as a function of pressure it is futile to attempt to so apply the results.

#### SYSTEM $\text{NaAlSi}_3\text{O}_8\text{-H}_2\text{O}$

Liquidus relations in the system albite-water have been studied by Goranson (1938), using the sealed-tube technique (Goranson, 1931, p. 486). We restudied this system using the hydrothermal quenching apparatus, and it is gratifying to report that the two methods give comparable results. Liquidus determinations by the two methods were identical up to 2000 kg/cm<sup>2</sup>, within the stated limits of error in pressure and temperature measurements. At 2700 kg/cm<sup>2</sup>, the highest pressure used by Goranson, the quenching apparatus gave a slightly lower temperature for the liquidus than that reported by Goranson (approximately 822°C. for the sealed-tube method versus 810°C. for the quenching apparatus). This discrepancy was probably due to



slight errors in temperature measurement. Our results for the liquidus relations are shown in Table 6 and Figure 15.

Figure 15 is a projection of the system  $\text{NaAlSi}_3\text{O}_8\text{-H}_2\text{O}$  on the PT co-ordinate plane. The projections involving composition are not known with the certainty of the PT relations because of experimental difficulties in determining the water content of the liquid phase.

One feature of the liquidus determinations which is not readily explained is the apparent melting interval of albite. Theoretically if the albite glass is made up to be stoichiometrically correct and if there are no other oxides present albite should melt sharply at each pressure. We found, however, that, although the beginning of melting is easily and accurately located, the completion of melting is not so readily fixed. As the albite used for these determinations was made from a glass which was very carefully prepared it is unlikely that the melting interval can be due to a difference between the initial composition and that of albite. If alumina or silica were present in excess they would be readily detected in the completely crystalline material and if sodium were present in excess the hydrothermal crystallization would quickly remove it during crystallization.

It would appear therefore that the melting interval is a result of: (1) the liquid and/or the vapor having compositions off the binary join albite-water, (2) the runs not representing equilibrium conditions, or (3) solid solution of water in albite. As the beginning of melting is sharp, and approximately 90 per cent glass is formed (Table 5) in a temperature interval of  $10^\circ$ , no great error was introduced in our studies by the failure to melt completely in this temperature range. A thorough check on these various possible explanations would be a major research in itself.

The PT composition relations for albite-water are undoubtedly similar to those shown in some detail for the system  $\text{SiO}_2\text{-H}_2\text{O}$ . The critical temperature of water is only slightly raised by the presence of albite, and therefore a critical end point must lie near the critical point for pure water. A second critical end point must therefore lie at very high pressures and at a temperature below  $700^\circ\text{C}$ . The composition of the liquid and vapor must be identical at the end point, but the concentration of water in the liquid is unknown.

#### SYSTEM $\text{KAlSi}_3\text{O}_8\text{-H}_2\text{O}$

This system was not investigated because the high temperatures and pressures at the liquidus were above the usual range for our equipment. However, Goranson (1938) studied the phase relations up to approximately 4000 bars, and his results are reproduced in Figure 16. This system is complicated by the fact that orthoclase melts incongruently to leucite and liquid, a situation that is changed markedly upon addition of water under pressure. The effect of water on the liquidus temperature of leucite in this system is remarkable; the temperature lowering by the first 1000 bars pressure is approximately  $550^\circ\text{C}$ . This amounts to about twice the lowering (for the first 1000 bars) observed in the  $\text{NaAlSi}_3\text{O}_8\text{-H}_2\text{O}$  system. At a pressure of approximately 2500 bars the incongruent melting to leucite and liquid is eliminated, and the system becomes binary for all higher pressures.

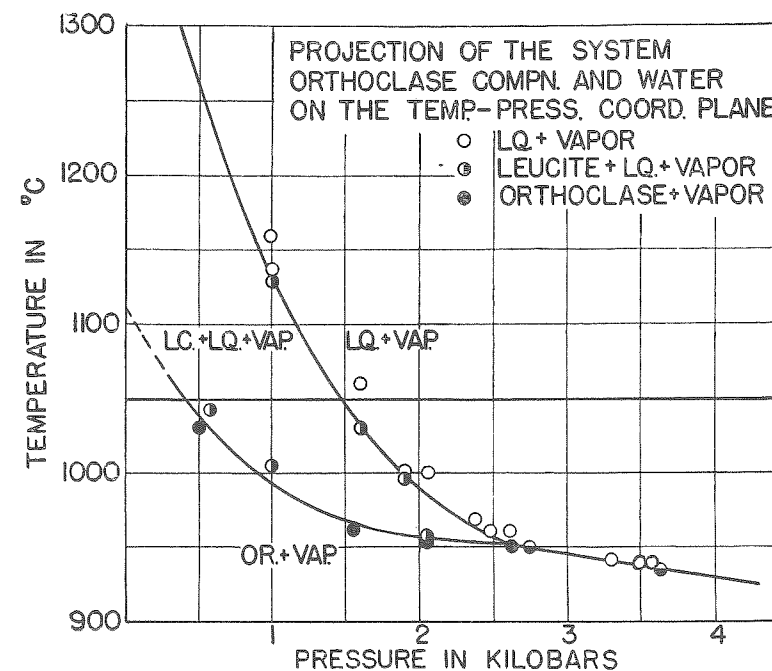


FIGURE 16.—Saturation curves for the system  $\text{KAlSi}_3\text{O}_8\text{-H}_2\text{O}$  projected onto the temperature-pressure co-ordinate plane

The lower curve is the incongruent melting curve of orthoclase (after Goranson, 1938, p. 89).

#### SYSTEM $\text{NaAlSi}_3\text{O}_8\text{-KAlSi}_3\text{O}_8\text{-H}_2\text{O}$

##### INTRODUCTORY REMARKS

This ternary system is one "face" of the quaternary tetrahedron representing the system  $\text{NaAlSi}_3\text{O}_8\text{-KAlSi}_3\text{O}_8\text{-SiO}_2\text{-H}_2\text{O}$ . As the feldspars are very important constituents of the igneous rocks, and as compositions in this system are not far from the compositions of the syenites and trachytes, this system was selected as a door through which we might gain access into the formidable "granite-water" tetrahedron. The results of this study have been published but, inasmuch as additional data have been obtained at higher pressures and as certain minor corrections are necessary, particularly in the water contents of the liquids, it appears desirable to present the full picture here again.

The results of Goranson (1938) on the sodium and potassium feldspars with water served as a guide for our preliminary experiments. It turned out that these early results were a very good guide indeed for work with mixtures of these feldspars as Goranson's results need little or no correction to fit into the picture which was found for the quaternary system.

These compositions also turned out to be the best compositions for obtaining equilibrium rapidly in the entire quaternary system. Without the background of experi-

ence gained on these compositions, which are relatively good crystallizers, it would have been impossible to work within the tetrahedron. It is likely that if the study had been started with mixtures near the average granite composition the results would have been so confusing and unreproducible that we would have become discouraged and turned our efforts to other less important systems.

#### COMPLETE SERIES OF SOLID SOLUTIONS AT HIGH TEMPERATURES

In the dry way, glasses of the composition of the alkali feldspars refuse to yield a completely crystalline product at any temperature, even if crystallization is continued for years. Without completely crystalline material, temperatures of beginning of melting cannot be determined in these viscous mixtures. Partial crystallization can, however, be realized, with sufficient patience and persistence, and the resulting crystals plus glass can be used to determine the temperature of completion of melting. The most recent results on dry studies in this system are by Schairer (1950). The best interpretation of the results is that sodium and potassium feldspars form a complete series of solid solutions of the type with a minimum-melting composition; the diagram is complicated toward the potassium-rich side by the incongruent relations resulting from the separation of leucite. However, three compositions give an identical liquidus temperature, within the error of measurement, and the possibility remains that we are dealing not with a very flat minimum but with a eutectic, which would necessitate a hiatus in the solid-solution series. Further evidence is desirable, and, indeed, conclusive evidence is found through studies in the presence of water.

When glasses of the system are crystallized at 900°C. under a pressure of water vapor of 300 kg/cm<sup>2</sup>, complete crystallization of all compositions is readily attained. X-ray studies of these fully crystalline mixtures indicated a complete series of solid solutions. The ( $\bar{2}01$ ) spacing was found to be very suitable for a quantitative test of the complete solubility relations between sodium and potassium feldspar because it shifted rapidly with compositional changes. By mixing a standard material with the crystalline powders the change in the ( $\bar{2}01$ ) spacing with composition could be measured with an accuracy of  $\pm 1$  per cent orthoclase. Altogether 15 compositions were studied, and a plot of the composition versus the difference between the ( $\bar{2}01$ ) of the feldspar and the ( $10\bar{1}0$ ) of a standard quartz is illustrated in Figure 4. Quartz can be used as an internal standard for all but the extremely potassium-rich members of the series.

The continuous change in spacing from one end member to another is convincing evidence of complete solid solution. If there were a hiatus in the solid-solution series, two peaks would appear, or, if the break were too small for the peaks to be resolved, a broadening of the resultant peak would be readily observed.

There was no escaping the conclusion that we were dealing with a complete series of solid solutions between a triclinic and a monoclinic substance. The problem was further outlined by Donnay and Donnay (1952) who carried out a careful X-ray study of our synthetic materials and found that the symmetry change took place at a composition of Ab<sub>67</sub>Or<sub>33</sub>. All compositions in the range Ab<sub>67</sub> to Ab<sub>100</sub> were triclinic, whereas the others were monoclinic. These puzzling relations were finally cleared up after Dr. W. S. MacKenzie (1952) carried out X-ray studies at elevated

temperatures and found that albite was monoclinic above 940°C. All compositions between Ab<sub>67</sub> and Ab<sub>100</sub> change to monoclinic symmetry on heating.

It will be recalled that the foregoing apparently complete series of solid solutions was obtained by crystallizing at 900°C. At low temperatures very different results were obtained; before describing these, we shall first consider further evidence indicating the existence of a complete series of solid solutions at high temperatures. This comes from the determination of the melting relations in the presence of water vapor at high pressures. As has been stated already, only the liquidus curve can be determined in dry melts, and some doubt is left as to the exact relations between the feldspars; but the determination of both solidus and liquidus which is readily accomplished under pressure of water vapor leaves little room for doubt. The foregoing X-ray data obtained on crystals of known compositions were of great service in establishing the solidus curves at different pressure, as we shall see.

#### EQUILIBRIUM RELATIONS AT VARIOUS PRESSURES OF WATER VAPOR

We found it convenient to investigate equilibrium at isobars—that is, to work at constant pressure with various compositions and then to repeat at other constant pressures. Such a procedure yielded diagrams so simply related to the “binary” diagram for the dry melts that they are readily understood. Indeed, the diagram for the dry melts is itself the isobaric diagram for the pressure of water vapor in the atmosphere which is, for practical purposes, zero.

In an individual run with any mixture the initial material was always a glass of known composition. By experience it was found necessary to grind the glass very fine and then to crystallize at a temperature of 700°C. and 1000 kg/cm<sup>2</sup> water pressure for 30 minutes to 1 hour. This procedure gave a very fine-grained, completely crystalline product of uniform composition for all alkali feldspar mixtures. The uniformity of composition was determined with the X-ray spectrometer, which gave only one sharp ( $\bar{2}01$ ) peak for each mixture so treated. If this preliminary crystallization was carried out at a higher temperature, large crystals grew in the glass, and their size greatly delayed the attainment of equilibrium in the subsequent run. If the glass was not ground to a very fine powder, very large crystals grew, even at 700°C., and again there was the same difficulty in the subsequent run. If crystallization was carried out below 700°C., two feldspars resulted, as indicated by the presence of two peaks for ( $\bar{2}01$ ). But, by following the procedure indicated and obtaining a very fine-grained product consisting of one feldspar of uniform composition, it was possible with this material to determine the temperature of beginning of melting, the temperature of completion of melting, and other relations to be mentioned. This was accomplished by holding the charge thus pre-treated at a constant temperature and pressure for the desired period, quenching it, and then examining the product with the petrographic microscope and the X-ray spectrometer. For all runs the charge was approximately 10 mg in weight. The results of the runs are shown in Figure 17.

The figure needs no explanation, but some further details of procedure may be given that are most readily appreciated with the aid of the diagram. The liquidus curve for each pressure was, of course, determined by finding for each feldspar com-

position the temperature at which the last crystals disappear. The solidus curve was determined by finding the temperature at which the first liquid appears. At one composition the two curves coincided, and at this composition both liquidus and solidus curves had a temperature minimum. For all other compositions there was a

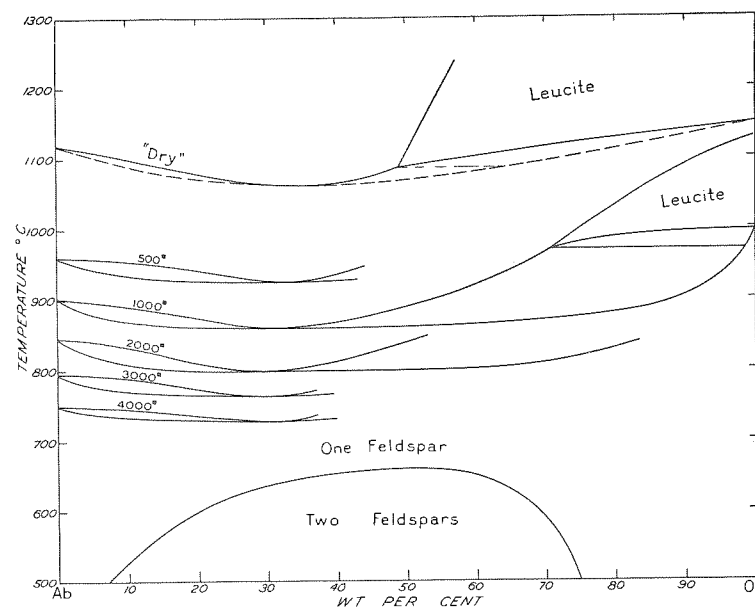


FIGURE 17.—Isobaric equilibrium relations in the system  $\text{NaAlSi}_3\text{O}_8\text{--KAlSi}_3\text{O}_8\text{--H}_2\text{O}$  projected onto the Ab-Or face of the temperature-composition prism

Portions of the 500, 1000, 2000, 3000, and 4000  $\text{kg/cm}^2$  isobars are shown as well as the solvus which is not measurably affected by these pressures. Pressures are indicated thus, 500<sup>\*</sup> = 500  $\text{kg/cm}^2$ .

temperature difference between the two curves which was the melting interval for that feldspar composition. A charge held in this interval gave crystals and glass upon quenching; the composition of the glass (in proportions of the feldspar components) was indicated by a point on the liquidus curve at the temperature of the run, and the composition of the crystals was the point on the solidus curve at the same temperature. This fact enabled the fixing of the solidus curve much more accurately by merely observing the temperature at which liquid first appears, for it was difficult to detect a small proportion of glass in a fine crystalline aggregate. It was necessary only to hold a charge at a measured temperature in the melting interval, quench it, and then determine the composition of the crystals by means of the X rays, using the method outlined above. A point on the solidus for the temperature of the run was thus determined. This, which may be termed the "composition method", is much more accurate than the temperature method of determining the solidus.

The minimum on the solidus (and liquidus) curve was determined by applying the same principle. A glance at the equilibrium diagrams showed that the lower part

of the solidus was so flat that only a very rough approximation to the composition of the minimum could be reached by the temperature method. On the other hand, the minimum could be located very accurately by the composition method. If the composition chosen for investigation lay to the right of the minimum, the crystals moved in composition to the right as melting proceeded; if the composition lay to the left of the minimum, they moved to the left; and, if it lay at the minimum and was heated for a time which was insufficiently long for complete melting, the composition of the crystals remained as it was initially. Crystals with 70 per cent sodium feldspar melted without measurable change of composition at both 1000 and 2000  $\text{kg/cm}^2$  pressure of  $\text{H}_2\text{O}$ ; in all other compositions the crystals changed in composition in one direction or the other, according to composition, as indicated above. The composition of the minimum was therefore placed at this value for both these pressures. The actual minima could depart from one another by about 2 per cent without detection, but not by any significantly greater value.

In the diagram for the dry melts there are three compositions—60, 65, and 70 per cent sodium feldspar—all of which melt at  $1063^\circ\text{C}$ ., within the limits of error of measurement, and the minimum was placed at the intermediate value, 65 per cent. Experimentation with the dry melts is so difficult, and the placing of our minima at both pressures at 70 per cent has so small a probable error, that we at first supposed the minimum probably should be at the same value in the dry melts also. To test this possibility, we made a run with the 70 per cent composition at a low pressure of water vapor (500  $\text{kg/cm}^2$ ). At this pressure the 70 per cent composition was to the right of the minimum, for the crystals now moved unmistakably to the right. Accordingly, the 65 per cent composition must actually be very close to the minimum for the dry melts.

The composition of the minimum thus behaved much like the temperature of the minimum. With the first increments of water pressure, the minimum changed in composition rather markedly, but with increasing pressure the amount of change decreased rapidly.

The similar behavior of the temperature of the minimum is brought out in the equilibrium diagrams, but some comment may be desirable. The first 1000  $\text{kg/cm}^2$  water pressure lowered the minimum about  $250^\circ\text{C}$ ., but an additional 1000  $\text{kg/cm}^2$  gave a further lowering of only  $50^\circ\text{C}$ .. Although we did not determine a complete diagram at 500  $\text{kg/cm}^2$  pressure, we did determine (in addition to the composition relations at the minimum just noted for this pressure) the temperature of the minimum. For this the lowering was  $170^\circ\text{C}$ . It is thus clear that the lowering effect for equal increments of pressure rapidly decreases with increasing pressure.

#### LEUCITE FIELD

Leucite is the primary phase in the composition  $\text{KAlSi}_3\text{O}_8$  and is the stable phase in contact with liquid through an interval of more than  $400^\circ\text{C}$ . It is not surprising, therefore, that the field of leucite extends far out on the feldspar join. Actually, it extends to 51 per cent albite in the dry melts (Fig. 17). Goranson (1938) found that in  $\text{KAlSi}_3\text{O}_8$  water greatly diminishes the temperature interval in which leucite forms. At 1000  $\text{kg/cm}^2$  pressure of water the interval is reduced to about  $135^\circ\text{C}$ .



In correspondence with this, we found that the leucite field extends only to 29 per cent albite at 1000 kg/cm<sup>2</sup>. At 2000 kg/cm<sup>2</sup> pressure of water, the leucite field is reduced to very small dimensions, so that nearly the whole feldspar diagram shows simple congruent relations. According to Goranson's determination, at or near 2500 kg/cm<sup>2</sup> pressure of water the leucite field is suppressed entirely in KAlSi<sub>3</sub>O<sub>8</sub>. At this pressure of water, therefore, the whole feldspar diagram should become simple; we have not thought it necessary to confirm this since the trend is clear.

#### SOLVUS

When alkali feldspar glasses are crystallized at low temperatures with water vapor under pressure to facilitate crystallization, instead of a single homogeneous feldspar, two feldspars are formed. This fact is established from the observation that two maxima or peaks of X-ray reflection from (201) are shown; by measuring the exact position of these peaks and referring them to the curve of Figure 4, the composition of the two feldspars in equilibrium at any temperature can be determined. Thus a homogeneous feldspar formed at high temperatures should unmix at lower temperatures, a relation long ago deduced from natural materials (perthites), but now we have a means of establishing the position of the unmixing curve or solvus.

The solvus is shown in Figure 17. Unlike the solidus and liquidus curves, the solvus did not change its position measurably with change of pressure of water vapor because water did not participate in the equilibria involved at the solvus, whereas it did participate in the solidus-liquidus equilibria by entering into the composition of the liquid phase. Pressure as such had, of course, some effect on the solvus, but the magnitude of the effect was relatively very small because it depended on the small volume change attending mutual solution (solid solution) of the two feldspars.

Figure 17 shows that, unless some new factor intervenes—for example, critical phenomena—there will be a pressure of water vapor which will lower the solidus-liquidus curves to temperatures at which they will intersect the solvus. At this isobar, and for all isobars corresponding to higher pressures, the feldspar diagram will cease to show complete solid solution. Instead, two series of solid solutions will form with a hiatus and a eutectic or a reaction relation, depending on the manner of encounter of the solidus and solvus.

The solvus has its maximum temperature at 660°C.  $\pm$  10°, at a composition close to 50 per cent sodium feldspar. Thus 660°C. is the minimum temperature of stable existence of a feldspar of that composition, and each composition of feldspar has its own minimum temperature of stable existence at which it will, if opportunity for equilibrium prevails, begin to break up or unmix into two feldspars. These depart more and more widely in composition as the temperature falls. Of course, when crystallized at 700°C. or higher, any feldspar can be cooled rapidly to room temperature and will remain a single homogeneous feldspar—indeed, that is the method whereby we determined that a complete series exists at 700°C. and higher. If any feldspar is held at a temperature where it should form two feldspars, however, as indicated by the solvus, unmixing will occur within a few days if water vapor under pressure is present to facilitate mobility. This behavior confirms the results obtained by direct crystallization of glass at various temperatures, which is the method whereby the solvus was determined. The presence of two feldspars in the product obtained

by thus inducing unmixing from an originally homogeneous feldspar cannot, to be sure, be observed with the petrographic microscope. The intergrowth is submicroscopic and is revealed only by the X rays.

An intergrowth of two feldspars thus obtained by unmixing from a single feldspar was rehomogenized by heating for about 24 hours at 700°C. even in the absence of water vapor, and at higher temperatures homogenization was accomplished in shorter times (1 hour at 950°C., *e.g.*).

The mixing and unmixing of alkali feldspars was thus readily reversible, as is shown by the behavior of the microscopic intergrowths, and their behavior is altogether in accord with the determined solvus. One feature of the solvus thus determined in the laboratory must, however, be emphasized: At least some part of our solvus may pertain to metastable equilibrium. All the feldspars obtained synthetically in these studies were high-temperature varieties, and the solvus was the unmixing curve of these high-temperature feldspars. At 500°C., for example, our solvus showed that the sodium-rich feldspar had a composition approaching that of pure albite, but the sodium-rich feldspar stable at 500°C. may be the low-temperature variety rather than the high-temperature form we obtained. It is a common experience with silicates to obtain a high-temperature form metastably at low temperatures. The only indication we had as to the inversion temperature of albite was obtained by finding the lowest temperature at which natural low albite could be transformed to high albite with the aid of a flux; this temperature is 700°C. The inversion temperature, then, is not higher than 700°C. but may be lower. If it is as low as 500°C., then our solvus, as determined down to 500°C., represents stable equilibrium. If the inversion is really as high as 700°C., then the lower-temperature part of the sodium-rich limb of the solvus may refer to metastable equilibrium.

However, even if the inversion of albite is as high as 700°C., it is not necessary that any part of the sodium-rich limb of our solvus be metastable. It is highly probable that the addition of potassium feldspar to albite will lower its inversion temperature, for, almost certainly, at any temperature potassium feldspar is less soluble in low albite than in high albite.

#### BEHAVIOR OF NATURAL ALKALI FELDSPARS

In rocks of appropriate composition which are believed on geologic grounds to have crystallized at high temperatures, a single feldspar with high content of both alkalies is normally found, whereas in rocks believed to have formed at low temperatures a sodium-rich feldspar and a potassium-rich feldspar are found side by side. These observations, together with other supporting evidence, have led to the conclusion that the alkali feldspars form a nearly, if not entirely, complete series of solid solutions at high temperatures but have only limited miscibility in the crystal state at low temperatures. This conclusion is now demonstrated to be true by our investigation of synthetic feldspars.

The existence in nature of perthitic, microperthitic, and cryptoperthitic intergrowths of the two feldspars supported the early conclusion and indicated also that, even when a homogeneous feldspar is first formed, it may unmix in the solid state at lower temperatures, giving an intergrowth of the two feldspars. X-ray studies have revealed that the two feldspars exist in the "crypto" varieties of these inter-



grown feldspars, such as the moonstones (Kôzu and Endô, 1921), and by heat treatment some investigators (Kôzu and Endô, 1921; Spencer, 1930; 1937) have shown that the feldspars will again form a homogeneous solid solution.

These conditions and changes of condition are all readily produced in the synthetic

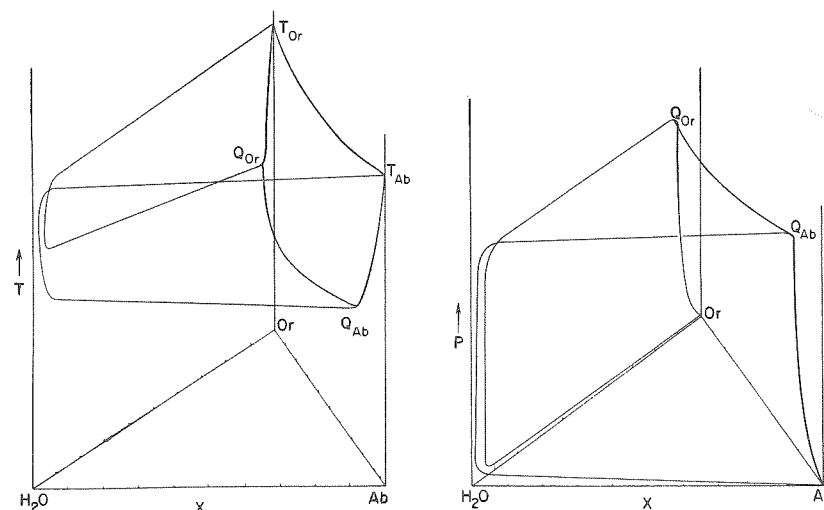


FIGURE 18.—Schematic TX and PX diagrams for the system  $\text{NaAlSi}_3\text{O}_8\text{--KAlSi}_3\text{O}_8\text{--H}_2\text{O}$  to aid in the understanding of Figure 19

$T_{\text{Ab}}\text{--}T_{\text{Or}}\text{--}Q_{\text{Or}}\text{--}Q_{\text{Ab}}$  is the temperature-saturation surface of alkali feldspar crystals, and  $\text{Ab}\text{--}\text{Or}\text{--}Q_{\text{Or}}\text{--}Q_{\text{Ab}}$  is the pressure-saturation surface of those crystals.

feldspars, as we have seen, and we have also been able to determine by X rays the composition of each of the feldspars in the synthetic intergrowths. This, too, we do with the natural crypto-intergrowths. X rays revealed that a sanidine or an orthoclase which appeared to be a single feldspar under the highest power of the microscope and gave the optical properties ordinarily regarded as those of a homogeneous feldspar could nevertheless be an intergrowth of nearly pure end members.

When examined further, however, the actual relations in the natural feldspars were considerably more complex than were those in our synthetic analogues. These latter, throughout all the changes to which we subjected them, retained their characteristics as high-temperature feldspars. The only change in a synthetic intergrowth on heating was homogenization, presumably accomplished merely by mobilization and diffusion of the cations.

The natural intergrowths, on the other hand, were, in many instances, low-temperature feldspars. When these feldspars were heated, the cations were readily mobilized, and they gave, within certain limits of composition, a homogeneous feldspar after a short period of heating; but the feldspar so produced was quite different from one grown at a high temperature or produced by rehomogenizing an intergrowth of two high feldspars. Further details on the natural feldspars are presented in the section on the Crystalline Phases.

#### GENERAL CONSIDERATIONS OF EQUILIBRIUM

For convenience we may, for the moment, neglect the incongruent melting of  $\text{KAlSi}_3\text{O}_8$  and assume that with water it would give a diagram analogous to that for  $\text{NaAlSi}_3\text{O}_8$ . Then in the ternary system we would have the relations shown in Figure 18.

In a discussion of equilibrium between crystals and liquids in a dry system, it is customary to speak of a liquidus surface or a fusion surface, but in a system with water these terms are not entirely satisfactory. In the system with water, interest is focused upon a very special fusion surface—namely, that representing the composition of liquids in equilibrium at any temperature, not only with crystals but with water vapor. For the surface representing liquids that are thus saturated both with crystals and with water vapor, the term “saturation surface” is appropriate. The general form of the TX saturation surface is shown in Figure 18. There is an infinite number of liquidus or fusion surfaces between the saturation surface and the liquidus surface for an extremely small water content in the liquid; each represents a definite water content, from nearly zero to the saturation value.

In the foregoing remarks we have emphasized the temperature aspects of saturation because it is easy to pass to them from the familiar considerations applicable to dry melts. But saturation has pressure aspects as well, and the PX diagram of Figure 18 shows the PX saturation surface. A knowledge of at least the pertinent parts of these two saturation surfaces is necessary for a discussion of courses of crystallization. For an understanding of the general relations, reference should be made to the legend of Figure 18.

#### ISOBARS AND ISOTHERMS ON THE SATURATION SURFACES AND COURSES OF CRYSTALLIZATION

The PX and TX surfaces are utterly unlike and are not usable in themselves, but one can obtain a most useful diagram by projecting them, or that part of them which has been experimentally determined, upon the composition triangle, representing the one by isotherms and the other by isobars. This has been done in Figure 19, which enables one to describe completely the crystallization of any liquid within the limits of our determinations. The isobaric sections of Figure 17, which represent the simplest experimental approach to the solution of the problems of the system, nevertheless do not describe crystallization completely because the water content of the liquid is not shown in such sections, although it was, of course, the data shown in these sections plus the determination of water in the quenched glasses that enabled us to construct Figure 19, showing saturation isobars and isotherms on the composition triangle.

The “composition triangle” presented here is really only a part of that triangle, and it is constructed in an unusual manner, which requires some description. Although it is customary to represent ternary compositions on an equilateral triangle, one can use a triangle of any shape with co-ordinates drawn parallel to its sides. It is convenient here to use a triangle in which the water ordinate is greatly exaggerated, and, accordingly, we have constructed an isosceles triangle with an altitude five times that of an equilateral triangle. Water is plotted at its apex, and one of the feldspars at each end of its base. Of this triangle we show only the lower portion in

Figure 19 because only this portion is required to represent the experimental results. The proportion of water is read in the ordinary manner with the aid of lines parallel to the base, but, as it is desirable to know the feldspar proportions apart from water content, instead of drawing co-ordinates parallel to the other two sides of the tri-

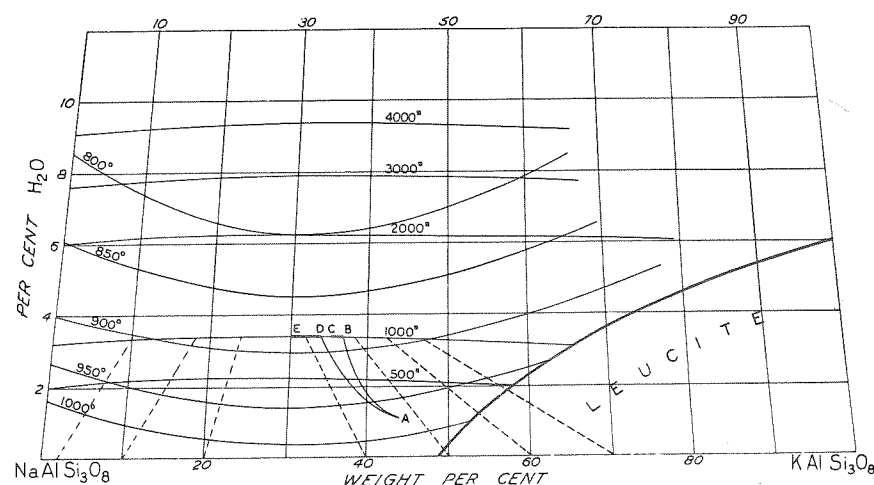


FIGURE 19.—Portion of the triangular diagram for the system  $\text{NaAlSi}_3\text{O}_8$ - $\text{KAlSi}_3\text{O}_8$ - $\text{H}_2\text{O}$

Illustrates the courses of crystallization for equilibrium and fractional crystallization. Both the temperature-saturation surface and the pressure-saturation surface are projected on the triangle and are represented by isotherms and isobars, respectively. Pressures are illustrated thus:  $500^\circ = 500 \text{ kg/cm}^2$ . Additional details of the method of construction of diagram in text.

angle, lines radiating from the  $\text{H}_2\text{O}$  apex are drawn. The feldspar proportions represented by any point can then be read directly, whatever the water content.

The isobars and isotherms are then plotted with the aid of the data on which the diagrams in Figure 18 are based and also the determined water contents of the liquids (glasses), including Goranson's (1938) determinations. The significance of these curves is simply stated. The isobar of  $1000 \text{ kg/cm}^2$ , for example, represents the composition of all liquids that are saturated with feldspar crystals and with water vapor at a pressure of  $1000 \text{ kg/cm}^2$ , and an isotherm, for example, that for  $950^\circ\text{C}$ . represents the composition of all liquids that are just saturated with feldspar crystals and water vapor at  $950^\circ\text{C}$ . Tie lines may now be added, joining the composition of any liquid represented by a point on an isobar with the particular feldspar in equilibrium with it. These tie lines are given only for the  $1000 \text{ kg/cm}^2$  isobar. An attempt to show them for more than one isobar would result in a confusion of lines. Figure 17 supplies this information also, for horizontal lines on Figure 17 are such tie lines.

Figure 19 is now ready for use to describe the course of crystallization of a liquid (magma) of any composition in the system. We shall bring out the principles involved by discussing crystallization of only one composition.

Composition A contains  $\text{NaAlSi}_3\text{O}_8$  and  $\text{KAlSi}_3\text{O}_8$  in the relative proportions 55:45 with 1 per cent  $\text{H}_2\text{O}$ . We shall assume that a liquid of that composition exists

under an external pressure of  $1000 \text{ kg/cm}^2$  and at a temperature of  $1000^\circ\text{C}$ . Crystallization of this liquid will begin, if it is cooled, at approximately the temperature of the isotherm passing through A. It will not be exactly at the temperature of that isotherm, because the isotherms locate a saturation surface, and the liquids are saturated with both water vapor and crystals. At  $1000 \text{ kg/cm}^2$  this liquid A is not saturated with water vapor; the saturation pressure is about  $250 \text{ kg/cm}^2$ . Accordingly, the temperature of initial crystallization at the higher pressure of  $1000 \text{ kg/cm}^2$  will be raised slightly above that indicated by the saturation surface. This effect of pressure in raising the crystallization temperature in the condensed system is slight. Therefore, the liquid will begin to crystallize at a temperature slightly higher than that indicated by interpolation between isotherms on the saturation surface; but the actual difference is very small, and, for all practical purposes, isotherms on the saturation surfaces can be used.

Crystallization will therefore begin at approximately  $975^\circ\text{C}$ . The first crystals formed will have the composition  $\text{Ab}_{14}$ ; if the perfect equilibrium type of crystallization prevails, the first part of the course of crystallization is given by the curve AB. At B, which is a point on the  $1000 \text{ kg/cm}^2$  isobar, the liquid is saturated with water vapor. The temperature, indicated precisely by the isotherm through B, is, by interpolation,  $885^\circ\text{C}$ . The position of the point B is determined by the tie line (three-phase boundary) which passes through A. The mass now consists of liquid B, which contains nearly 3.5 per cent  $\text{H}_2\text{O}$ , and crystals of  $\text{Ab}_{52}$ . The proportion of liquid to crystals is approximately 30:70.

As the assumed external pressure is  $1000 \text{ kg/cm}^2$ , further abstraction of heat will result in boiling, accompanied by crystallization, and the composition of the liquid will now move along the isobar until the liquid reaches the point C; the temperature falls very slightly between B and C. At C crystallization will be complete; the mass will have boiled dry and be made up entirely of crystals of composition  $\text{Ab}_{55}$ . Compared with the rate of cooling during earlier stages, that during the boiling stage is so slow that it may be referred to as semi-isothermal. During the period of boiling, the water content of the residual liquid increases slightly, but the amount of residual liquid decreases markedly and is finally reduced to zero. The point indicating the total composition of the mass does not remain at A but migrates to the feldspar side of the diagram during the boiling.

With crystallization of the perfect fractionation type, initial formation of crystals will be as above, but thereafter the liquid will follow the course ADE, boiling will begin at D, a significantly lower temperature than B, and both boiling and crystallization will be completed at E, which is the point of minimum temperature on the isobar ( $840^\circ\text{C}$ ). The crystals in this case are continuously zoned, with compositions ranging from  $\text{Ab}_{14}$  to  $\text{Ab}_{70}$ . For a similar system the principles controlling crystallization by these two contrasted methods are discussed in a theoretical paper by Bowen (1941).

The assumed pressure of  $1000 \text{ kg/cm}^2$  prevailing during the crystallization of the liquid A corresponds with the weight of overburden at a depth of 2.2 miles in the earth, assuming a rock density of 2.7. With the aid of Figure 19, crystallization for a pressure and, therefore, a depth twice as great ( $2000 \text{ kg/cm}^2$ ) can be described in

a similar quantitative manner on the basis of our results. Indications are that at a pressure twice as great again—namely, 4000 kg/cm<sup>2</sup>—corresponding with a depth of 8.9 miles, the general situation will not be greatly different. The boiling away of the water in the last residual liquid will take place in a manner similar to that described; the only difference will be that the last liquid will persist to a significantly lower temperature (estimated by extrapolation to be approximately 700°C.), and the content of water in the final liquid will probably be about 11 per cent. No reliance can be placed on more extended extrapolation, and it is futile to attempt to estimate the pressure (and depth), if any, at which critical phenomena would intervene and the final liquid (fluid), instead of boiling, would pass into the vapor (fluid) state without change of volume or discontinuity of any kind, including composition.

In the foregoing it is assumed that the vapor escapes from the system, in which case the crystalline feldspar will cool indefinitely without undergoing any change except the unmixing into two feldspars. If, however, the system could increase its volume—say by arching its roof—and thus retain the vapor as the filling of miarolitic cavities, then at a temperature around 400°C. or somewhat lower a liquid would form again. This would be a liquid very rich in water (hydrothermal solution) but would contain in solution some feldspar or, more probably, decomposition products of the feldspar, as the relationships might be incongruent. A notable recrystallizing effect may be expected of this liquid, but, of course, the retained vapor itself, existing in the temperature interval between that of magmatic liquids and that of hydrothermal solutions, would also have a similar effect. The unmixing of the feldspar to give two feldspars is one phenomenon that would be notably facilitated by the presence of water in either form.

The reverse process, the heating of feldspar to a high temperature in the presence of some water, has some suggestive significance in connection with the problem of palingenesis. In a feldspar mass under a load of 1000 kg/cm<sup>2</sup> and with sufficient pore space to contain 2 per cent water, the effects of heating would be the reverse of the cooling effects described if the volume relations are correct—that is, if the pore space is such that the 2 per cent water by weight fills or nearly fills it. If the feldspar is assumed to have the same composition (Ab<sub>55</sub>) as that whose crystallization was discussed, a magmatic liquid will first form at *C*, and further melting will be the exact reverse of crystallization. Even a minute trace of water filling the pore space in such a feldspar mass would induce the formation of a little magmatic liquid at *C*, if the pressure is again assumed as 1000 kg/cm<sup>2</sup>. This liquid would, however, move along the isobar only a minute distance from *C* and then would leave the isobar and go to higher temperatures, with solution of more feldspar. In other words, no more than a very small quantity of liquid is formed unless the temperature is raised well above that of point *C*.

#### PETROLOGIC CONSIDERATIONS

The present investigation of crystallization equilibrium of the alkali feldspars definitely confirms the indications of dry-melt studies that these feldspars form a complete series of solid solutions of the type with a minimum-melting member. Many petrologists have considered this relation the most probable, solely from examination of the relations of the natural minerals.

The existence of the lowest-melting composition at 65–70 per cent NaAlSi<sub>3</sub>O<sub>8</sub> agrees with the indications of natural rocks; viewed in reverse, the relations of natural rocks approaching the synthetic mixtures in composition confirm the view that crystal-liquid equilibrium is the dominant control in the development of these rocks. It has long been argued that the presence of even moderate quantities of water in the natural magmas would completely change the relations found in dry melts, even to the extent of reversing the order of crystallization, and that studies of dry melts can therefore give no indication of the crystallization behavior of magma. No one having any real familiarity with equilibrium diagrams could adhere to such views, and here we have a concrete illustration of the fact that the principal function of water is as a flux, in which capacity it is indeed very powerful, but it affects equilibrium positions progressively and only moderately when present in moderate amounts. The result is that, in investigated compositions containing water up to 10 per cent, crystallization equilibria are nearly the same as in the dry melts except that they go forward at much lower temperatures. Water does have an outstanding effect on one equilibrium—the incongruent melting of KAlSi<sub>3</sub>O<sub>8</sub>. Only about 6 per cent H<sub>2</sub>O is sufficient to nullify this behavior, but its great fluxing power is probably at the root of this effect. Albite gives the same result eventually, but it requires 50 per cent albite to prevent formation of leucite. The difference is one of degree rather than of kind.

Those intergrowths of the alkali feldspars known as perthites, microperthites, and cryptoperthites have long been interpreted by petrologists as the result of the unmixing of a homogeneous solid solution. Our results confirm unmixing and supply information on its quantitative aspects, especially in indicating the minimum possible temperature of crystallization of a feldspar of a given composition.

It is not surprising that syenites and trachytes should be the principal abode of perthitic, and especially of microperthitic and cryptoperthitic, feldspars. In such magmas there is practically no constituent that induces a lowering of the melting temperatures of the feldspars except water, and the water content must be rather high to lower the whole crystallization range to such a temperature that two feldspars will form throughout the period of primary crystallization. Therefore, we may expect that the bulk of the crystallization of such rocks took place at a temperature at which a single homogeneous alkali feldspar is formed. This feldspar later unmixes to give a cryptoperthite, or a coarser intergrowth, according to the rate of cooling.

If the pressure is high enough, however—that is, if crystallization takes place at sufficient depth in the crust—even a magma with a small initial percentage of water will eventually develop a residual liquid containing an appreciable amount. Thus a magma initially containing 1.2 per cent of water will have 12 per cent when the residual liquid is 10 per cent of the mass, unless notable amounts of water enter into hydrous minerals.

At this stage the rate of heat flow from a deep-seated rock mass will be very low and consequently the boiling away of water and accompanying crystallization will proceed very slowly. The residual liquid, amounting at first to 10 per cent and slowly decreasing, will be present for an excessively long period. By virtue of its high water content, it is a very active liquid and may be expected to effect complete recrystalli-



zation of the early-formed feldspar, with formation of those with which it is in equilibrium. To be sure, if only the feldspars and water are present, the temperature, while liquid persists, will not go far down into the range of two feldspars—that is, the feldspars will not be of extreme composition—but in the natural system residual liquids will have potent fluxes in addition to water, and this recrystallization may be expected to be carried to significantly lower temperatures. Through this action the typical deep-seated syenite may be formed. At very high pressures approaching critical end points the vapor phase formed is not greatly different in composition from the liquid phase (Figs. 17, 18), and this vapor phase, filling minute interstices, will also induce recrystallization even after the exhaustion of all liquid.

Such vapors and the vapors boiling off at earlier stages introduce material into surrounding rocks, with resultant "granitization" of these rocks.

The fact that homogeneous feldspars can be unmixed in a few hours in the laboratory in the presence of water vapor under pressure leads one to wonder how the cryptoperthites manage to persist in nature at all. They must have been in an extremely dry environment during cooling, otherwise unmixing on a much greater scale would have certainly taken place.

#### SYSTEM $\text{NaAlSi}_3\text{O}_8\text{--SiO}_2\text{--H}_2\text{O}$

The system  $\text{NaAlSi}_3\text{O}_8\text{--SiO}_2\text{--H}_2\text{O}$  is one face of the tetrahedron  $\text{Ab--Or--Q--H}_2\text{O}$ , which is the principal subject of this investigation, and it is therefore desirable to study this ternary system before proceeding into the more complicated quaternary system.

We did not investigate this system as extensively as the  $\text{NaAlSi}_3\text{O}_8\text{--KAlSi}_3\text{O}_8\text{--H}_2\text{O}$  system principally because no extrusive rocks have these compositions, and the rare plutonic rocks with compositions approaching a mixture of albite and quartz probably owe their origin to metasomatic processes. The detailed X-ray studies carried out on the feldspar solid solutions in the system  $\text{NaAlSi}_3\text{O}_8\text{--KAlSi}_3\text{O}_8\text{--H}_2\text{O}$  are unnecessary here as there is no solid solution between silica and albite. The petrographic microscope is the only tool needed to identify the various phases of this system.

It was found convenient to study the equilibrium at constant pressure, varying the composition and temperature, and then to repeat at another pressure. The resulting temperature-composition diagrams are similar to an ordinary binary diagram and are easily understood. Our results are shown in the TX diagram of Figure 20 and in Table 7. In projection the system is simple "binary" with only the polymorphism of silica complicating the equilibrium relations (the polymorphism of albite is not well enough understood, particularly when pressure is added as another variable, to include it at this time). At pressures above approximately 1500 kg/cm<sup>2</sup> quartz melts directly to a hydrous liquid so that at higher pressures the TX projection is similar to a simple binary system. Above approximately 5000 kg/cm<sup>2</sup> pressure the silica field is further complicated by the appearance of low quartz at the liquidus (the inversion temperature of quartz at 5000 bars pressure is 704°C., and

TABLE 7.—Results of quenching experiments in the system  $\text{NaAlSi}_3\text{O}_8\text{--SiO}_2\text{--H}_2\text{O}$

Run number	Composition Wt. % Ab	Temperature °C.	Time	Pressure kg/cm <sup>2</sup>	Result
Q1-27E	82.7	960	2 days	500	All glass
Q1-26E	82.7	940	2 days	500	Albite + glass
Q1-27C	82.7	900	1 day	1000	All glass
Q1-28A	82.7	880	1 day	1000	Albite + glass
Q1-27D	82.7	850	1 day	2000	All glass
Q1-27A	82.7	830	10 hours	2000	Albite + glass
Q1-27B	82.7	795	1 day	3000	All glass
Q1-26D	82.7	775	1 day	3000	Albite + glass
B2-94D	73.5	860	7 days	1000	All glass
B2-94C	73.5	840	4 days	1000	Albite + glass
Q1-21A	69.0	900	1 day	500	All glass
Q1-19C	69.0	890	7 days	500	Albite + glass
Q1-51B	69.0	740	4 days	3000	All glass
Q1-51C	69.0	730	3 days	3000	Albite + glass
Q1-49H	69.0	720	2 days	4000	All glass
Q1-51E	69.0	710	2 days	4000	Albite + glass
Q1-10C	64.5	760	4 days	2000	All glass
Q1-10D	64.5	750	7 days	2000	Albite + glass
Q1-16C	64.5	730	4 days	3000	All glass
Q1-17B	64.5	715	5 days	3000	Quartz + glass
Q1-52E	64.5	720	2 days	4000	All glass
Q1-52D	64.5	710	2 days	4000	Quartz + glass
Q1-49G	64.5	700	4 hours	4000	Albite + quartz + glass
Q1-29D	59.8	870	3 days	500	All glass
Q1-17C	59.8	860	7 days	500	Albite + glass
Q1-20D	59.8	840	4 days	500	Albite + quartz + glass
Q1-22B	59.8	770	4 days	2000	All glass
Q1-18C	59.8	755	7 days	2000	Quartz + glass
Q1-25F	59.8	915	2 days	350	All glass
Q1-25C	59.8	895	5 days	350	Albite + glass
Q1-21B	59.8	760	4 days	3000	Quartz + glass
Q1-19D	55.2	900	22 hours	500	All glass
Q1-14E	55.2	880	6 days	500	Quartz + glass
B2-92E	55.2	850	7 days	1000	All glass
B2-92D	55.2	825	1 day	1000	Quartz + glass
Q1-14B	55.2	800	7 days	2000	Quartz + glass
Q1-21D	55.2	810	14 hours	3000	All glass
Q1-24B	55.2	790	43 hours	3000	Quartz + glass
Q1-20C	55.2	935	24 hours	350	All glass
Q1-42C	55.2	915	4 days	350	Quartz + glass

the "eutectic" between albite and quartz will be at a slightly lower temperature than this at 5000 kg/cm<sup>2</sup> water-vapor pressure).

The eutectic between albite and cristobalite which was located in the dry way represents a metastable extension of the cristobalite liquidus to lower temperatures



as a result of the failure of tridymite to crystallize. This failure to reach equilibrium is common in the dry systems but was not encountered in this study. The stable

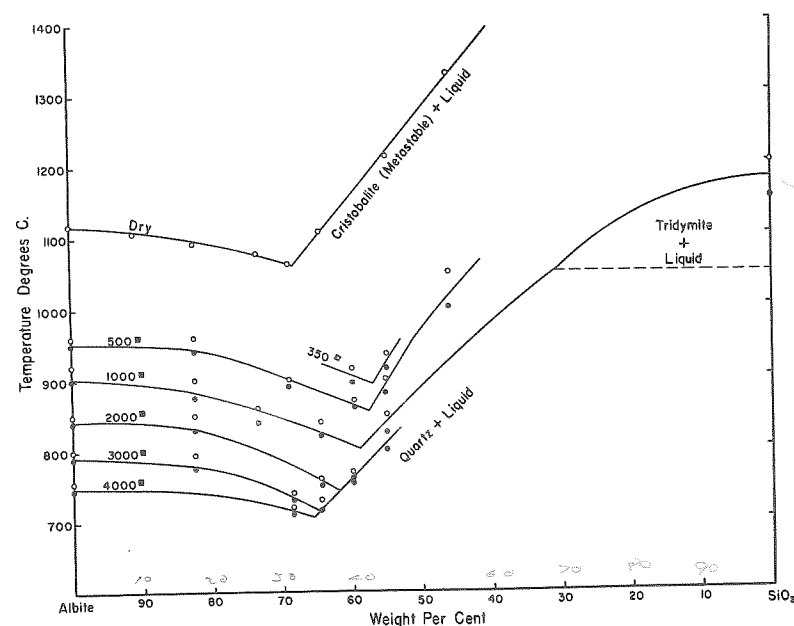


FIGURE 20.—Isobaric equilibrium relations in the system  $\text{NaAlSi}_3\text{O}_8\text{-SiO}_2\text{-H}_2\text{O}$  projected onto the Ab-Q face of the temperature-composition prism

Portions of the 350, 500, 1000, 2000, and 4000  $\text{kg/cm}^2$  isobars are shown with the 1000  $\text{kg/cm}^2$  isobar complete. Pressures are indicated thus: 500# = 500  $\text{kg/cm}^2$ .

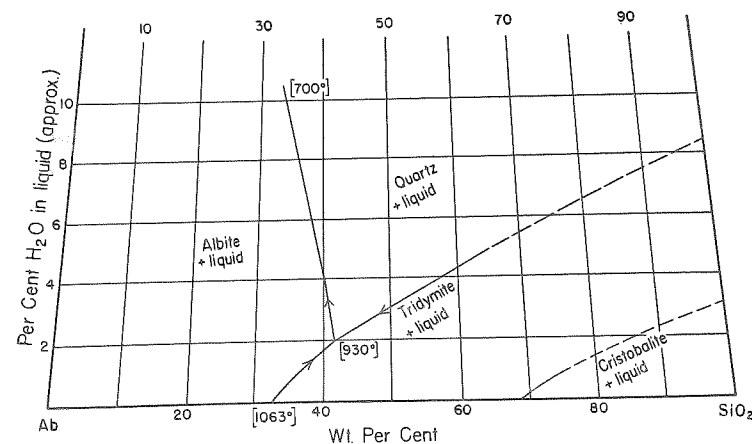


FIGURE 21.—Triangular diagram, in part schematic, for a portion of the system  $\text{NaAlSi}_3\text{O}_8\text{-SiO}_2\text{-H}_2\text{O}$   
Shows the stability fields of albite, quartz, tridymite, and cristobalite

tridymite-albite eutectic must lie on the albite side but very near the metastable cristobalite-albite eutectic. At first glance it appeared that the eutectic is changed with pressure in a very peculiar manner; with the first few hundred  $\text{kg/cm}^2$  pressure the "eutectic" moved toward the silica side, whereas further increase of pres-

TABLE 8.—Results of quenching experiments on the system  $\text{KAlSi}_3\text{O}_8\text{-SiO}_2\text{-H}_2\text{O}$

Run number	Composition Wt. % Or	Tem- perature °C.	Time	Pressure	Result
Q1-33A	61.5	850	16 hours	1000	All glass
Q1-33D	61.5	830	16 hours	1000	Feldspar + glass
Q1-35D	61.5	870	2 days	500	All glass
Q1-36D	61.5	855	2 days	500	Feldspar + glass
Q1-13I	56.0	770	7 days	2000	All glass
Q1-13E	56.0	760	7 days	2000	Quartz + glass
Q1-23D	56.0	825	5 days	500	All glass
Q1-25D	56.0	810	5 days	500	Feldspar + glass
B2-93F	50.0	850	6 days	1000	All glass
B2-93A	50.0	800	7 days	1000	Quartz + glass
Q1-26B	50.0	890	4 days	500	All glass
Q1-25E	50.0	870	2 days	500	Quartz + glass
Q1-35B	50.0	825	1 day	2000	Quartz + glass

sure caused the "eutectic" to move toward albite. Figure 21 illustrates the probable explanation of these changes. The water apex of the triangular diagram has been greatly exaggerated, and as in the case of Figure 19 we have shown only the lower portion. The initial slope of the eutectic toward the silica side took place while tridymite was the primary phase, and the reversal took place when the tridymite-albite boundary curve reached the invariant point albite-tridymite-quartz-liquid-vapor. The albite-quartz boundary line extending from the invariant point to higher pressures then sloped toward the albite-water side line. This diagram is in part schematic because we have determined the water content of the liquids at only a few points.

#### SYSTEM $\text{KAlSi}_3\text{O}_8\text{-SiO}_2\text{-H}_2\text{O}$

We did not study this system in detail principally because the compositions involved are not particularly interesting geologically, and after studying the  $\text{NaAlSi}_3\text{O}_8\text{-KAlSi}_3\text{O}_8\text{-H}_2\text{O}$  and  $\text{NaAlSi}_3\text{O}_8\text{-SiO}_2\text{-H}_2\text{O}$  systems we were anxious to proceed into the tetrahedron and the granite compositions. This system is similar to the  $\text{NaAlSi}_3\text{O}_8\text{-SiO}_2\text{-H}_2\text{O}$  system in that at low pressures there are complications in the crystalline phases (polymorphism in silica and incongruent melting of orthoclase), but at higher pressures the isobaric diagram looks like a simple binary system involving quartz and potassium feldspar.

Results of quenching experiments in this system are given in Table 8.

SYSTEM  $\text{NaAlSi}_3\text{O}_8\text{--KAlSi}_3\text{O}_8\text{--SiO}_2\text{--H}_2\text{O}$ 

## INTRODUCTION

In the quaternary system  $\text{NaAlSi}_3\text{O}_8\text{--KAlSi}_3\text{O}_8\text{--SiO}_2\text{--H}_2\text{O}$ , as in the ternary systems, we found it convenient to carry on our experimental studies at constant

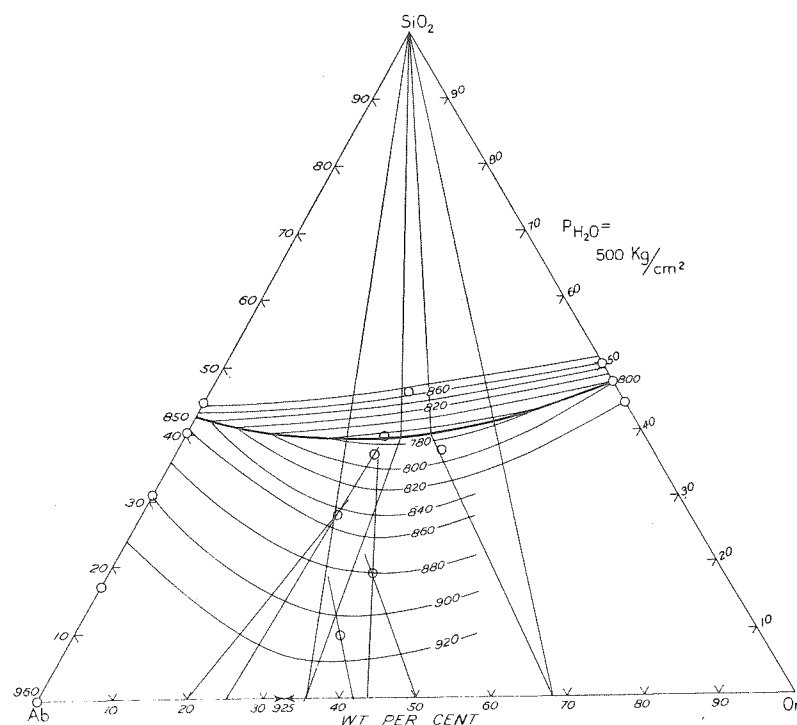


FIGURE 22.—The 500 kg/cm<sup>2</sup> isobaric equilibrium diagram for the system  $\text{NaAlSi}_3\text{O}_8\text{--KAlSi}_3\text{O}_8\text{--SiO}_2\text{--H}_2\text{O}$  projected onto the anhydrous base of the  $\text{NaAlSi}_3\text{O}_8\text{--KAlSi}_3\text{O}_8\text{--SiO}_2\text{--H}_2\text{O}$  tetrahedron

Two three-phase triangles are shown which locate the position of the isobaric minimum on the quartz-feldspar boundary. The straight lines emanating from the Ab-Or sideline are tie lines giving the compositions of liquids in equilibrium with various feldspar solid solutions.

pressure giving isobaric diagrams similar in many respects to the ternary condensed diagram. These "ternary" diagrams can then be used to illustrate the crystallization paths and other phase relations. These isobaric diagrams are not truly ternary in that a considerable amount of water was present in the liquid, and the vapor, although extremely poor in dissolved nonvolatile material, could not be entirely neglected. More properly, the isobaric diagrams represent an isobaric section through the tetrahedron at approximately constant water content. For example, the water content of the liquids at 500 kg/cm<sup>2</sup> pressure of water vapor ranged from 2.3 to 2.9 per cent at the liquidus for all compositions investigated; as the water content could vary this amount in repeated determinations on the same sample, the actual variation of the water content throughout the investigated portion of the 500 kg/cm<sup>2</sup> isobaric diagram (Figs. 22, 26, 27) may well be less than 0.6 per cent

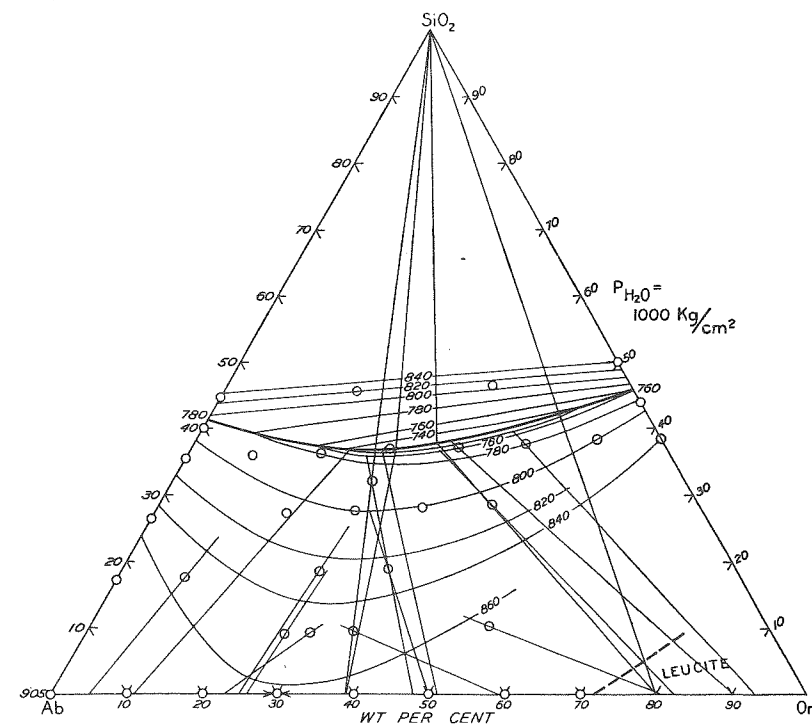


FIGURE 23.—The 1000 kg/cm<sup>2</sup> isobaric equilibrium diagram

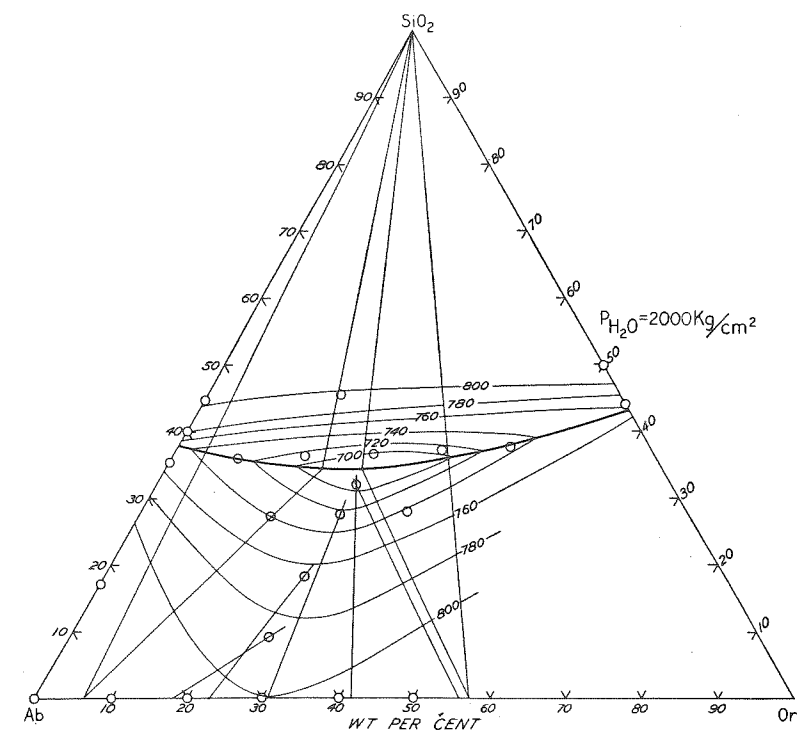


FIGURE 24.—The 2000 kg/cm<sup>2</sup> isobaric equilibrium diagram

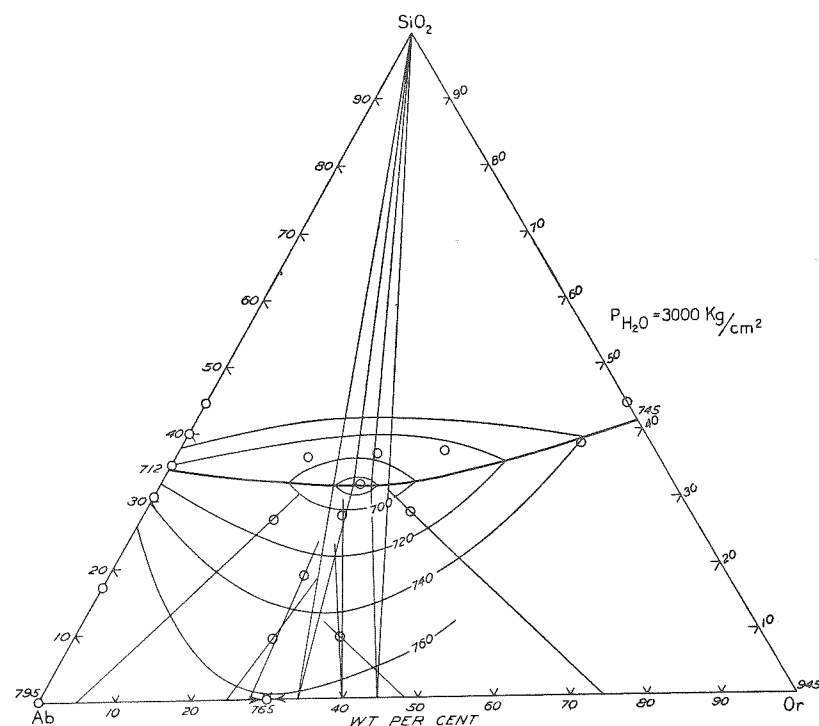
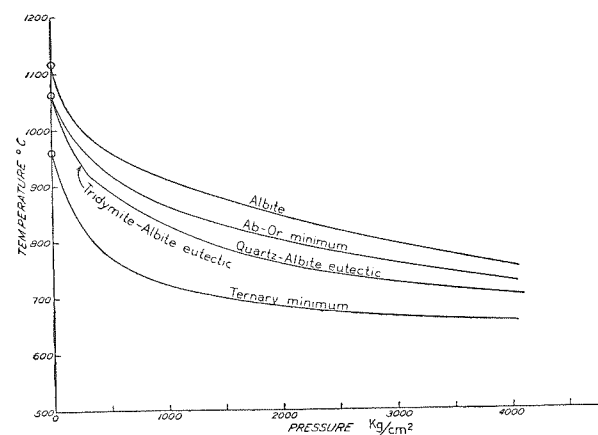


FIGURE 25.—The 3000 kg/cm² isobaric equilibrium diagram

FIGURE 26.—Pressure-temperature projection showing the effect of water-vapor pressure on the liquidus of albite, the albite-orthoclase minimum, the albite-quartz eutectic, and the ternary minimum in the system  $\text{NaAlSi}_3\text{O}_8\text{-KAlSi}_3\text{O}_8\text{-SiO}_2$ 

Compare with Figure 27

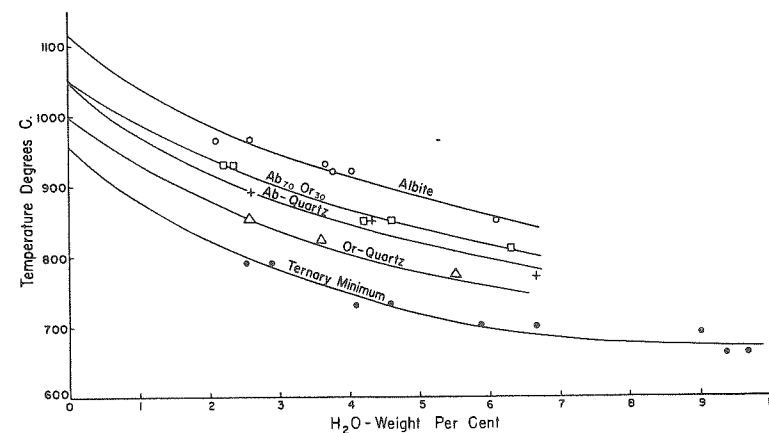


FIGURE 27.—Graph illustrating the amount of water dissolved in the various anhydrous compositions as a function of temperature

TABLE 9.—Results of water determinations at various pressures and temperatures

Run number	Initial composition	Pressure kg/cm²	Tem- perature °C.	Time	% H <sub>2</sub> O	
					Charge	Buffer
Q1-41B	Albite	1000	930	4 hours	3.65	4.38
Q1-41C	Albite	1000	920	4 hours	3.76	4.18
Q1-43C	Albite	1000	920	16 hours	4.04	5.19
Q1-42C	Albite	500	965	6 hours	—	2.58
Q1-43D	Albite	500	965	4 hours	2.08	2.66
Q1-41E	Albite	2000	850	4 hours	6.50	6.08
Q1-46B	Ab <sub>70</sub> Or <sub>30</sub>	500	930	4 hours	2.49	2.23
Q1-46E	Ab <sub>70</sub> Or <sub>30</sub>	500	930	4 hours	2.45	2.36
Q1-42F	Ab <sub>70</sub> Or <sub>30</sub>	1000	850	4 hours	4.18	4.52
Q1-47E	Ab <sub>70</sub> Or <sub>30</sub>	2000	810	4 hours	6.30	6.29
Q1-40C	Ab <sub>70</sub> Or <sub>30</sub>	1000	870	4 days	—	4.61
Q1-47D	Or <sub>56</sub> Q <sub>44</sub>	500	850	4 days	2.49	2.60
Q1-48B	Or <sub>56</sub> Q <sub>44</sub>	1000	825	4 days	3.59	4.10
Q1-47F	Or <sub>56</sub> Q <sub>44</sub>	2000	770	4 days	5.65	5.50
Q1-47G	Or <sub>56</sub> Q <sub>44</sub>	500	850	4 days	2.23	2.03
Q1-47A	Ab <sub>64.5</sub> Q <sub>35.5</sub>	2000	770	4 days	7.29	6.68
Q1-48C	Ab <sub>64.5</sub> Q <sub>35.5</sub>	1000	850	4 days	4.34	5.30
Q1-47B	Ab <sub>55.2</sub> Q <sub>44.8</sub>	500	890	4 days	2.04	2.60
Q1-38A	Ab <sub>36.8</sub> Or <sub>26.4</sub> Q <sub>36.8</sub>	2000	700	1 hour	5.86	6.46
Q1-38B	Ab <sub>36.8</sub> Or <sub>26.4</sub> Q <sub>36.8</sub>	1000	730	1 hour	4.19	4.08
Q1-38D	Ab <sub>36.8</sub> Or <sub>26.4</sub> Q <sub>36.8</sub>	2000	700	16 hours	6.66	7.00
Q1-38F	Ab <sub>36.8</sub> Or <sub>26.4</sub> Q <sub>36.8</sub>	500	790	16 hours	2.91	2.98
Q1-39B	Ab <sub>36.8</sub> Or <sub>26.4</sub> Q <sub>36.8</sub>	1000	730	4 hours	4.78	4.56
Q1-39C	Ab <sub>36.8</sub> Or <sub>26.4</sub> Q <sub>36.8</sub>	500	740	4 hours	2.88	2.92
Q1-38C	Ab <sub>36.8</sub> Or <sub>26.4</sub> Q <sub>36.8</sub>	3000	690	16 hours	9.96	9.00
Q1-46C	Ab <sub>47</sub> Or <sub>23</sub> Q <sub>30</sub>	4000	660	4 hours	9.36	9.68
Q1-46F	Ab <sub>47</sub> Or <sub>23</sub> Q <sub>30</sub>	4000	660	4 hours	10.26	9.66

H<sub>2</sub>O (Table 9). In other words at constant pressure the liquids encountered did not deviate appreciably in composition from a plane parallel to the anhydrous Ab-Or-SiO<sub>2</sub> base of the tetrahedron, and no great error was introduced by assuming a constant water content.

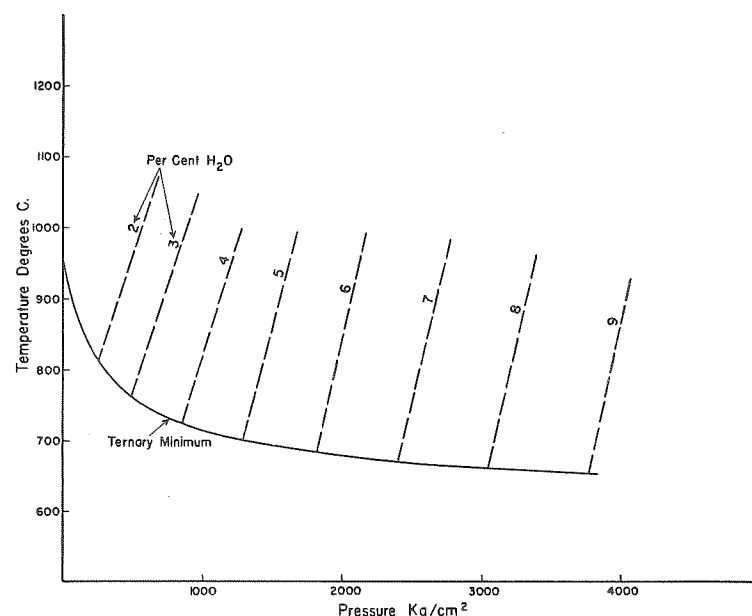




TABLE 10.—Continued

Run number	Initial composition			Temperature °C.	Time	Initial material	Result	Composition of crystals by X ray
	SiO <sub>2</sub>	Or	Ab					
B2-100B	28.1	35.2	36.7	800	5 days	Partially crystalline	Feldspar + glass	....
B2-100C	28.1	35.2	36.7	820	4 days	Partially crystalline	All glass	....
B2-99F	27.7	26.4	46.0	800	5 days	Partially crystalline	All glass	....
Q2-32F	27.7	26.4	46.0	790	1 day	Glass	Feldspar + glass	....
Q1-4F	36.0	8.8	55.2	790-800	11 days	Partially crystalline	All glass	....
Q1-5D	36.0	8.8	55.2	780	7 days	Partially crystalline	Feldspar + glass	....
B2-83D	36.4	17.7	46.0	790	3 days	Partially crystalline	All glass	....
B2-85E	36.4	17.7	46.0	735	3 days	Partially crystalline	Quartz + feldspar + glass	Or <sub>11</sub>
Q2-23H	36.9	26.4	36.7	725	41 days	All crystalline	Quartz + feldspar + glass	Or <sub>39</sub>
Q2-16D	36.9	26.4	36.7	740	7 days	Partially crystalline	All glass	....
Q2-33A	36.9	26.4	36.7	730	1 day	Partially crystalline	Quartz + glass	....
Q2-4E	36.9	26.4	36.7	730	1 day	All crystalline	10% glass	....
Q2-4D	36.9	26.4	36.7	715	1 day	All crystalline	No glass	....
Q2-22A	36.9	26.4	36.7	720	17 days	All crystalline	Glass present	....
Q1-1D	37.1	35.2	27.7	765	6 days	Partially crystalline	All glass	....
Q1-1A	37.1	35.2	27.7	745	6 days	Partially crystalline	Feldspar + glass	....
B2-86C	37.1	35.2	27.7	725	3 days	Partially crystalline	Feldspar + quartz + glass	Or <sub>80</sub>
Q1-3D	37.6	44.0	18.4	790	7 days	Partially crystalline	All glass	....
Q1-1F	37.6	44.0	18.4	770	6 days	Partially crystalline	Feldspar + glass	Or <sub>93</sub>
B2-94E	45.6	17.7	36.7	840	7 days	Partially crystalline	All glass	....
B2-95B	45.6	17.7	36.7	820	7 days	Partially crystalline	Quartz + glass	....
B2-95C	46.4	35.2	18.4	820	7 days	Partially crystalline	All glass	....
B2-95E	46.4	35.2	18.4	800	4 days	Partially crystalline	Quartz + glass	....
B2-97A	28.3	44.0	27.7	815	6 days	Partially crystalline	All glass	....
B2-96B	28.3	44.0	27.7	795	6 days	Partially crystalline	Feldspar + glass	....
B2-85D	28.3	44.0	27.7	755	3 days	Partially crystalline	Feldspar + glass	Or <sub>88</sub>
P <sub>H<sub>2</sub>O</sub> = 2000 kg/cm <sup>2</sup>								
Q1-1E	9.1	26.4	64.5	780	8 days	Partially crystalline	Feldspar + glass	Or <sub>18</sub>
Q1-2B	9.1	26.4	64.5	800	6 days	Partially crystalline	All glass	....
Q1-2E	18.4	26.4	55.2	780	7 days	Partially crystalline	All glass	....
Q1-3A	18.4	26.4	55.2	760	7 days	Partially crystalline	Feldspar + glass	Or <sub>28</sub>
Q1-12B	27.1	17.7	55.2	745	5 days	Partially crystalline	All glass	....
Q1-11D	27.1	17.7	55.2	730	7 days	Partially crystalline	Feldspar + glass	....
Q1-3F	27.7	26.4	46.0	730	7 days	Partially crystalline	All glass	....
Q1-4A	27.7	26.4	46.0	710	7 days	Partially crystalline	Feldspar + glass	Or <sub>31</sub>
Q1-11F	28.1	35.2	36.7	740	7 days	Partially crystalline	Very rare feldspar in glass	....
Q1-13H	32.3	26.4	41.3	680	7 days	Partially crystalline	Feldspar + glass	Or <sub>42</sub>
Q1-14A	32.3	26.4	41.3	700	7 days	Partially crystalline	All glass	....
Q1-9B	36.0	8.8	55.2	730	7 days	Partially crystalline	All glass	....
Q1-8D	36.0	8.8	55.2	720	7 days	Partially crystalline	Quartz + feldspar + glass	....

TABLE 10.—Continued

Run number	Initial composition			Temperature °C.	Time	Initial material	Result	Composition of crystals by X ray
	SiO <sub>2</sub>	Or	Ab					
Q1-7C	36.4	17.7	46.0	720	7 days	Partially crystalline	All glass	....
Q1-44B	36.4	17.7	46.0	690	4 days	Partially crystalline	Quartz + feldspar + glass	Or <sub>6</sub>
Q1-44D	36.9	26.4	36.7	690	4 days	Glass	Quartz + feldspar + glass	Or <sub>57</sub>
Q2-19E	36.9	26.4	36.7	710	10 days	Partially crystalline	Crystals growing	....
Q2-21C	36.9	26.4	36.7	720	7 days	Partially crystalline	Crystals dissolving	....
Q1-9F	37.1	35.2	27.7	710	4 days	Partially crystalline	All glass	....
Q1-10A	37.1	35.2	27.7	700	7 days	Partially crystalline	Quartz + glass	....
Q1-13D	37.6	44.0	18.4	735	7 days	Partially crystalline	Feldspar + glass	....
Q1-7A	45.6	17.7	36.7	800	1 day	Partially crystalline	All glass	....
Q1-6B	45.6	17.7	36.7	780	4 days	Partially crystalline	Quartz + glass	....
P <sub>H<sub>2</sub>O</sub> = 3000 kg/cm <sup>2</sup>								
Q2-5E	9.1	26.4	64.5	765	10 hrs.	Partially crystalline	All glass	....
Q2-5D	9.1	26.4	64.5	750	20 hrs.	Partially crystalline	Feldspar + glass	....
Q2-20E	9.5	35.2	55.3	740	20 hrs.	Partially crystalline	Feldspar + glass	Or <sub>48</sub>
Q2-20F	9.5	35.2	55.3	720	20 hrs.	Glass	Feldspar + glass	Or <sub>40</sub>
Q2-5C	18.4	26.4	55.2	740	20 hrs.	Partially crystalline	All glass	....
Q2-5B	18.4	26.4	55.2	730	20 hrs.	Partially crystalline	Feldspar + glass	....
Q2-5A	18.4	26.4	55.2	720	20 hrs.	Partially crystalline	Feldspar + glass	Or <sub>28</sub>
Q1-31E	27.1	17.7	55.2	700	2 days	Partially crystalline	Feldspar + glass	Or <sub>13</sub>
Q1-10B	27.6	26.4	46.0	710	7 days	Partially crystalline	All glass	....
Q1-9E	27.6	26.4	46.0	690	7 days	Partially crystalline	Feldspar + glass	Or <sub>60</sub>
Q1-10F	28.1	35.2	36.7	690	7 days	Partially crystalline	Feldspar + glass	Or <sub>75</sub>
Q1-11C	28.1	35.2	36.7	710	7 days	Partially crystalline	All glass	....
Q2-21A	36.9	26.4	36.7	710	3 days	Partially crystalline	All glass	....
Q1-8E	36.9	26.4	36.7	700	6 days	Partially crystalline	Feldspar + glass	....
Q1-13F	37.1	35.2	27.7	720	4 days	Partially crystalline	All glass	....
Q1-13C	37.1	35.2	27.7	710	5 days	Partially crystalline	Quartz + glass	....
Q1-18A	38.0	52.8	9.2	745	4 days	Partially crystalline	All glass	....
Q1-20A	38.0	52.8	9.2	730	4 days	Partially crystalline	Feldspar + glass	....
Q2-32A	27.1	17.7	55.2	670	30 days	Glass	Feldspar + quartz + glass	Or <sub>34</sub>
Q2-32A	38.9	26.4	36.7	670	30 days	All crystalline	Feldspar + quartz + glass	Or <sub>44</sub>
P <sub>H<sub>2</sub>O</sub> = 4000 kg/cm <sup>2</sup>								
Q1-32D	27.7	26.4	46.0	650	2 days	Partially crystalline	Crystals + glass	Or <sub>72</sub>
Q1-35A	32.3	26.4	41.3	660	1 day	Partially crystalline	Quartz + feldspar + glass	Or <sub>39</sub>
Q1-39A	30.0	23.0	47.0	650	1 day	Partially crystalline	Feldspar + glass	Or <sub>81</sub>
Q2-22B	36.9	26.4	36.7	710	4 days	Partially crystalline	All glass	....
Q2-21F	36.9	26.4	36.7	700	3 days	Partially crystalline	Quartz growing	....
Q2-1D	36.9	26.4	36.7	650	2 days	All crystalline	No glass	....
Q2-1E	36.9	26.4	36.7	660	2 days	All crystalline	50% glass	....

ample, the tie line intersecting the Ab-Or side line at Or<sub>50</sub> (Fig. 22) gives the following information: 15 per cent crystals having a composition Or<sub>50</sub> are in equilibrium with 85 per cent liquid having the composition Ab<sub>46</sub>Or<sub>32</sub>Q<sub>22</sub> at 870°C. and 500 kg/cm<sup>2</sup> water vapor pressure with an initial composition shown by the circle

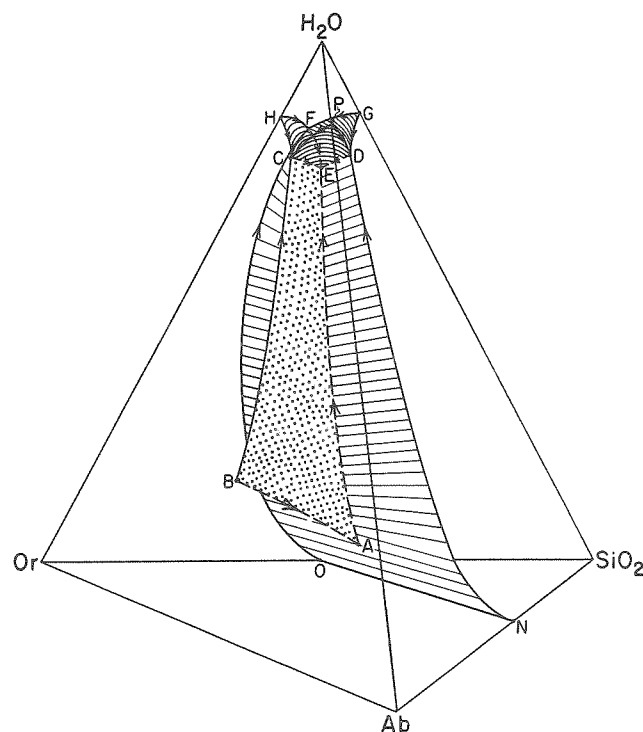


FIGURE 29.—Schematic condensed equilibrium diagram for the quaternary system  $\text{NaAlSi}_3\text{O}_8\text{--KAlSi}_3\text{O}_8\text{--SiO}_2\text{--H}_2\text{O}$

Shows the phase relations assuming no critical phenomena. See text for details.

through which the tie line passes. This tie line was experimentally located by heating the charge, whose composition is indicated by the circle, at 870°C., quenching, and determining the composition of the crystals by the X-ray method, using quartz as a standard. The composition of the liquid is given by the intersection of the tie line drawn from the feldspar composition through the initial composition to the appropriate isotherm.

Another type of straight line shown in the isobaric diagrams represents one side of a three-phase triangle. Just as the tie lines discussed above give the direction in which the liquid is changing composition with respect to the crystalline phase in the field of a single crystalline phase, so the three-phase triangle gives the direction in which the liquid is changing composition with respect to two crystalline phases. For example, the two three-phase triangles illustrated in Figure 22 show that the

temperature minimum on the boundary between the feldspar and quartz fields lies between the two obtuse apices of the three-phase triangles. The three-phase boundaries are experimentally located by finding the temperature at which feldspar is joined by quartz on lowering the crystallization temperature and determining the composition of the feldspar at that temperature.

Before taking up details of crystallization it may be desirable to have a bird's-eye view of the system via a schematic perspective sketch of the quaternary tetrahedron showing the phase relations in the condensed system. Figure 29 is such a sketch in which the critical phenomena have been ignored and it is assumed that each of the three ternary systems containing water has a ternary eutectic involving ice at compositions near pure water.

All heavy full lines lie on the face of the tetrahedron, whereas the dashed lines are within the tetrahedron. The arrows indicate falling temperatures.

The curve *ON* is the field boundary between silica and feldspar solid solutions. As the water content is increased this boundary moves into the tetrahedron, generating a curved surface which develops a crease at *A* as it is intersected by the surface *ABCE* representing the compositions in which potassium feldspar solid solutions, sodium feldspar solid solutions, and liquid are in equilibrium. This intersection becomes a univariant line (*AE*) in the tetrahedron representing the compositions of all liquids that are in equilibrium with the three solid phases—potassium feldspar solid solutions, sodium feldspar solid solutions, and quartz. The point *B* lies in the ternary system  $\text{NaAlSi}_3\text{O}_8\text{--KAlSi}_3\text{O}_8\text{--H}_2\text{O}$  and represents the composition of the liquid in equilibrium with the feldspar at the maximum on the solvus. Point *E* is a quaternary invariant point involving Ab-Or-SiO<sub>2</sub>-Ice-liquid and vapor. All relations at compositions having a water content greater than point *A* are schematic.

#### ISOBARIC CRYSTALLIZATION

Two types of isobaric crystallization will be considered, fractional and equilibrium crystallization; each represents limiting cases for crystallization in natural systems. In fractional crystallization there is no interaction between the crystals and liquid during crystallization. An element of fractional crystallization is provided in natural systems when zoning is produced in solid-solution series, when crystals settle during growth, and when the liquid is squeezed out of a crystal-liquid mush. Equilibrium crystallization requires that the crystals being precipitated react continuously with the liquid when the liquid and crystals are of variable composition. If the composition of the solid phase is fixed the crystallization paths for either type of crystallization radiate in straight lines away from the composition of the solid phase.

Representation of fractional crystallization can be illustrated by a series of curves on the composition plane. Equilibrium crystallization cannot be so readily illustrated because each composition within the field of a solid-solution series has a unique crystallization path. Although there is only a single equilibrium tie line for each composition at the liquidus in the field of a solid-solution series, the path which the liquid will follow on cooling will be influenced by the relative amounts of the solid and liquid phases present. In other words, a liquid will follow one path if it

has an opportunity to react with, say, an equal amount of crystals of a given composition, and still a different path if it can react with a larger amount of crystals having the same composition.

Despite these differences, the two types of curves are geometrically related, and one type can be derived from the other. A detailed discussion of fractionation and equilibrium curves can be found in papers by Bowen (1941) and by Osborn and Schairer (1941).

Isobaric crystallization in this system requires that the water dissolved in the silicate liquid escape by boiling during crystallization, for the water content of the liquid remains nearly constant throughout, and no hydrous phases are being formed to use up the water concentrated by separation of the anhydrous silicate phases. In natural systems this escaping water is introduced into the surrounding rocks where it may be the agent responsible for recrystallization, granitization, and the hydrothermal ore deposits.

**FRACTIONAL CRYSTALLIZATION:** In the following example it will be assumed that the liquid is saturated with water at the beginning of crystallization. Osborn and Schairer (1941) and Bowen (1941) have treated crystallization in a system of this type, and the reader is referred to their papers for details of the complications introduced when the fractionation curve extending from the binary minimum into the ternary system does not intersect the boundary curve at the ternary minimum and when this particular fractionation curve is not a straight line. In general, except for Osborn and Schairer (1941), those who have considered crystallization in a system of this type, in which there is complete solid solution between two phases and no solid solution between either of the two and the third component, have shown the "thermal valley" extending from the binary minimum into the ternary system as intersecting the field boundary at the ternary minimum. Such a situation seemingly is a unique case, and in general the intersection may occur at any place along the field boundary.

There is, of course, a somewhat different set of fractionation curves for each pressure, but at pressures up to approximately 3500 kg/cm<sup>2</sup> they differ only slightly, and the 1000 kg/cm<sup>2</sup> isobar will be used to illustrate the relationships. Figure 30 illustrates the general nature of the fractionation curves at 1000 kg/cm<sup>2</sup> water-vapor pressure. These curves were located by interpolation between the established tie lines shown in Figure 23. The most important region is that near the "thermal valley" running from the binary minimum into the boundary at *P* (Fig. 30), and in this area the curves are determined with reasonable accuracy.

In the area *OrAME*, liquids follow the curved paths to the quartz boundary *EE'* and move along the boundary to *M* where crystallization is completed. If the liquid is not used up during crystallization all liquids will reach the minimum *M*. Crystallization in the area *QME* results in a change of composition of the liquid along straight lines radiating from the quartz apex. These liquids crystallize quartz until the boundary *EE'* is reached; feldspar then begins to crystallize, and the liquid behaves as above. Fractional crystallization by zoning results in continuous zoning of the crystals with the albite content increasing until the outermost composition reaches *N*. Crystallization in the area *OrAMPm* is slightly more complex as the

zoning is reversed. For example, a liquid at *F* will begin to crystallize feldspar having the composition *F'* at 850°C., and the liquid will move along its fractionation curve to the boundary *EE'* at *G*, at which time the crystals will be continuously zoned from *F'* to *G'*. As the liquid at *G* crystallizes further and quartz and feldspar

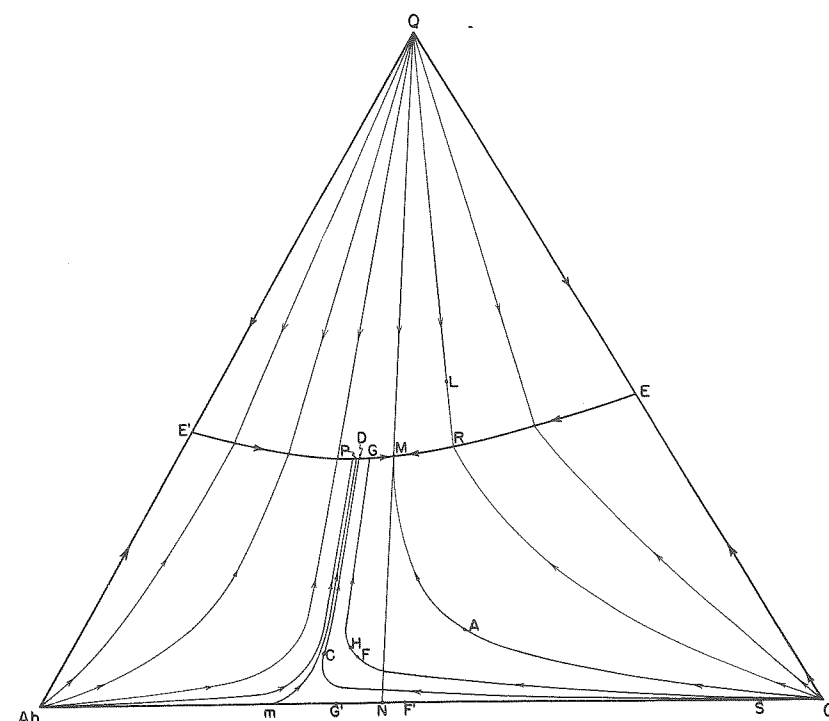


FIGURE 30.—Isobaric fractionation curves for a water-vapor pressure of 1000 kg/cm<sup>2</sup> in the system  $\text{NaAlSi}_3\text{O}_8\text{--KAlSi}_3\text{O}_8\text{--SiO}_2\text{--H}_2\text{O}$

The relations are projected onto the anhydrous base of the tetrahedron.

are both being precipitated, the crystals now change composition from *G'* toward *N*, and the final outermost zone will have the composition *N*. These crystals will now have two zones having the composition *N*, one formed when the temperature was at *H* and the outer zone at the temperature of the ternary minimum *M*. In the area *OrAMGF* the reversal of the zoning will take place when the liquid reaches the quartz-feldspar boundary, whereas in the area *OrCDPm* the reversal of zoning takes place at the inflection point on the fractionation curve such as at *C*. Fractionation of liquids in the quartz field will not produce a reversal of zoning in the feldspar solid solution. For example, a liquid having the composition *L* will precipitate quartz on cooling at 840°C., and its composition will change along the straight line away from *Q* to *R* where a feldspar having the composition *S* (the composition of the feldspars given by the three-phase triangle *QSR*) will join the quartz, and on further cooling the liquid will move along the boundary to the minimum *M* where

crystallization will be completed. The feldspar will be continuously zoned from  $S$  to  $N$ . If the initial composition is on the line  $QM$  the quartz will be joined by a feldspar having the composition  $N$ , and at  $M$  crystallization will be completed with a homogeneous feldspar of composition  $N$  and quartz as the final products.

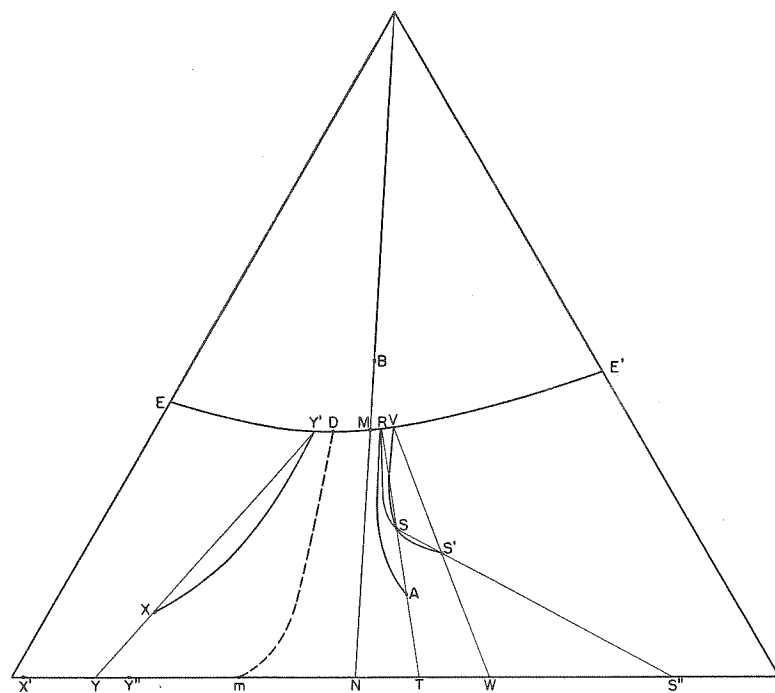


FIGURE 31.—Isobaric equilibrium curves for a water-vapor pressure of 1000 kg/cm<sup>2</sup> in the system  
NaAlSi<sub>3</sub>O<sub>8</sub>-KAlSi<sub>3</sub>O<sub>8</sub>-SiO<sub>2</sub>-H<sub>2</sub>O

The relations are projected onto the anhydrous base of the tetrahedron.

Fractional crystallization in the areas *AbmPE'* and *E'QP* is similar to crystallization in the areas *OrAME* and *MQE* respectively except that any zoning in the first areas will be from sodic cores to outer layers richer in potassium, whereas in the latter areas the cores will be rich in potassium and the outer layers richer in sodium.

Fractional crystallization, then, tends to change the composition of all liquids toward the minimum at  $M$ .

EQUILIBRIUM CRYSTALLIZATION: A group of typical equilibrium curves is illustrated in Figure 31. In contrast to fractionation curves an infinite number of equilibrium curves pass through each point in the feldspar field. This difference is brought about by the fact that each liquid in the feldspar field must continuously react with the solid-solution crystals, and the path which the liquid follows is consequently dependent on the amount of the solid phase present. For example, equilibrium curves for all compositions lying on the tie line  $SS''$  must pass through the

point  $S$ ;  $S'$  is an example. Thus a family of curves beginning along the tie line  $SS''$  will pass through  $S$  and reach the boundary curve  $EE'$  at slightly different points which are fixed by the three-phase boundary lines extending from the Ab-Or side line through the point representing the total composition of the mixtures to the quartz-feldspar boundary  $EE'$ . The line  $RST$  is such a three-phase boundary for the composition  $S$ . Also, since  $RT$  is a tie line as well as a three-phase boundary a series of equilibrium curves originating along  $RT$  converges to  $R$ ; the curve  $AR$  is an example.

Crystallization of a liquid such as  $X$  will begin at  $840^{\circ}\text{C}.$ , and the first crystals to separate will have the composition  $X'$  ( $XX'$  is a tie line). On further crystallization the liquid moves along the curved path to  $Y'$ . The composition of the crystals has now changed by reaction with the liquid until at  $Y'$  the crystals have the composition  $Y$  ( $YY'$  is a three-phase boundary). Further crystallization causes the liquid to move along the boundary to  $D$ , and quartz separates with the feldspar solid solution. At  $D$  the liquid will be used up, and the final crystals will have the composition  $Y''$ .

## ISOTHERMAL CRYSTALLIZATION

Crystallization in silicate systems is so intimately tied to temperature that the possibility of isothermal crystallization is rarely considered; yet complete crystallization, starting with a liquid containing no crystals, can take place with no drop in temperature. This is possible because of the manner in which the water affects the liquidus and because the amount of water held in the silicate melts is a function of pressure. Many of the effects normally considered to be due to temperature variations, such as zoning in the feldspars and other solid-solution series, the appearance of new phases etc., can be the result of pressure changes which in turn alter the water content of the melts.

Isothermal polybaric crystallization can be treated quantitatively in the same fashion as the isobaric polythermal crystallization discussed above. However, as we carried out our experimental studies at only a few pressures, detailed information was not gathered on any one isothermal section. Crystallization takes place with falling pressure in the same manner as with falling temperature in isobaric crystallization. Heat must be dissipated just as in polythermal crystallization, but, in general, in isothermal crystallization considerably less heat must be dissipated. In isothermal crystallization the only heat to be dissipated is the heat of melting, whereas in isobaric crystallization the heat of melting plus the heat released by the temperature lowering of the rock during crystallization must be dissipated. If the temperature interval of crystallization is on the order of 200° to 300°C. the heat that must be expelled during isobaric crystallization may be twice that released during isothermal crystallization.

An isothermal section is illustrated in Figure 32. At 760°C. and 3000 kg/cm<sup>2</sup> water-vapor pressure the mixture represented by *A* will be entirely liquid. If the pressure is lowered crystals of nearly pure albite will begin to separate, and the liquid will move along the curved line toward *B*. As the pressure is lowered the water content of the liquid must decrease by boiling. (At 2000 kg/cm<sup>2</sup> the liquid



will contain about 6 per cent water, whereas at 1000 kg/cm<sup>2</sup> water-vapor pressure the water content will have fallen to about 4 per cent.) When the pressure has fallen to just below 1000 kg/cm<sup>2</sup> the liquid will have the composition *B*, and quartz will begin to crystallize. At *B* the feldspar composition will have changed, by reaction

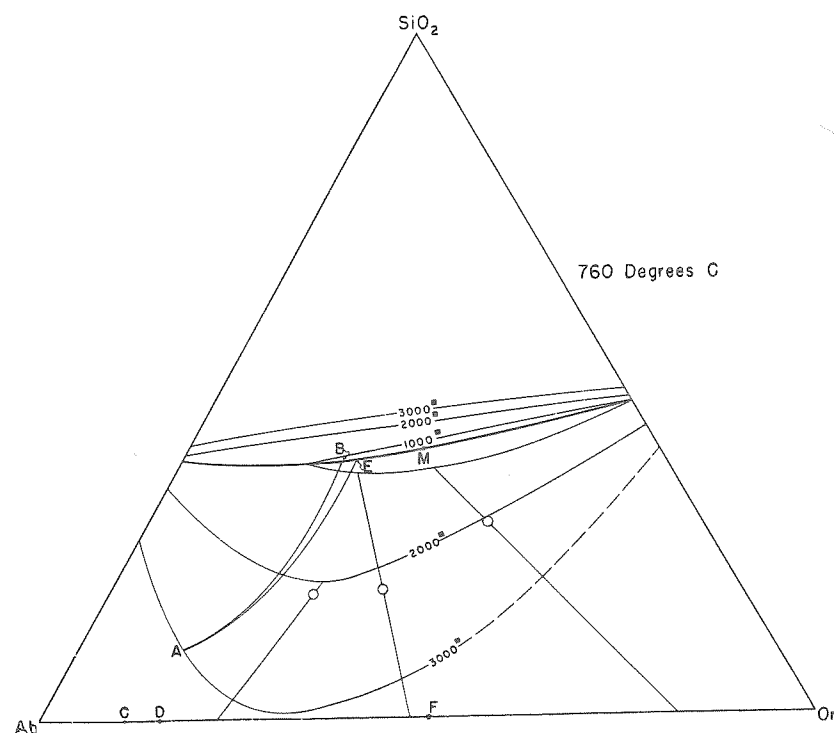


FIGURE 32.—The 760°C. isothermal polybaric equilibrium diagram for the system  $\text{NaAlSi}_3\text{O}_8\text{--KAlSi}_3\text{O}_8\text{--SiO}_2\text{--H}_2\text{O}$

Projected onto the anhydrous base of the tetrahedron

with the liquid, to *C* (assuming the perfect-equilibrium type of crystallization). At a pressure of about 700 kg/cm<sup>2</sup> the liquid will be used up, and the final product will be quartz plus feldspar of composition *D*. The final liquid will have a composition *E*. If the pressure drop is too rapid for equilibrium to be maintained the feldspar will zone, and the liquid will move along the curve *AE*; the final liquid could then reach the composition represented by *M*, and the last feldspar to crystallize would have the composition *F*. The pressure at final crystallization would under these circumstances be approximately 500 kg/cm<sup>2</sup>, somewhat lower than with equilibrium crystallization. The temperature remains at 760°C. throughout crystallization.

To have the temperature remain constant throughout crystallization the rate of heat loss from the system must just balance, at all times, the heat evolved as a result of crystallization. Of course such a fine balance of heat generation and loss is

unlikely in a crystallizing magma, but a near approach to this type of crystallization is not unreasonable in hydrous granite magmas.

Those hydrous granite magmas which have been moved to higher levels in the earth's crust may crystallize by loss of pressure rather than by a drop in temperature. Usually it is considered that a loss of pressure produces melting (Yoder, 1952) because the slope of the liquidus PT curve for most substances is positive. The different behavior here described is due to the dissolved volatile material, and even a basaltic liquid may crystallize rather than melt if the pressure is released and volatiles escape.

#### ADIABATIC CRYSTALLIZATION

Crystallization in these hydrous systems can be promoted by temperature lowering, pressure lowering, or pressure increase. In general, the liquid must be undersaturated with respect to the volatile component in order to crystallize as a result of a pressure increase.

Crystallization in "dry" systems usually takes place in response to heat loss from the system with consequent temperature drop—if the heat is not lost crystallization will not proceed. In systems in which a volatile substance is held in solution by pressure, as in the present system, a release of pressure with concomitant loss of volatile material will promote crystallization *whether or not heat is lost from the system*. In other words crystallization can proceed adiabatically.

At first thought it would appear absurd to suggest that a molten silicate liquid could crystallize while the temperature is being raised, but this is exactly what must happen if the water content of the liquid is decreased and if the heat generated by the induced crystallization cannot escape. Not all the heat needs to be used in raising the temperature of the system, but a large portion may be so expended. The heat required to vaporize the water dissolved in the melts may take up a considerable portion of the heat of crystallization. Also, there are several possible polymorphic transitions in the general temperature range of hydrous granite liquids that may take up a considerable amount of heat (e.g., the high-low quartz inversion, the quartz  $\rightleftharpoons$  tridymite inversion, and the high  $\rightleftharpoons$  low albite inversion). If these are taken together, it is unlikely that these heat "sinks" could use all the heat generated on crystallizing, and possibly the temperature will rise on the order of 100° to 300°C. during adiabatic crystallization of a hydrous granite liquid, assuming that the liquid is saturated with water vapor at the higher pressure and no heat is lost from the system.

The versatility introduced into crystallization by volatile constituents dissolved in the liquid phase is most remarkable. Complicated oscillatory zoning, for example, is no longer so formidable a problem when we realize that both pressure and temperature changes can produce zoning. The ubiquitous zoning in the plagioclase feldspars of the igneous rocks must now be studied with these facts in mind. Zoning heretofore interpreted as a result of repeated movement of crystals from one part of a magma chamber to another may well be due in part to pressure changes with consequent loss of volatiles.

## STABILITY FIELDS ON THE LIQUIDUS AT VARIOUS PRESSURES

The polymorphism of silica, the miscibility gap in the feldspars, and the incongruent melting of orthoclase tend to complicate the saturation surface in this system. Figures 33 and 34 illustrate these relationships for various water-vapor pressures.

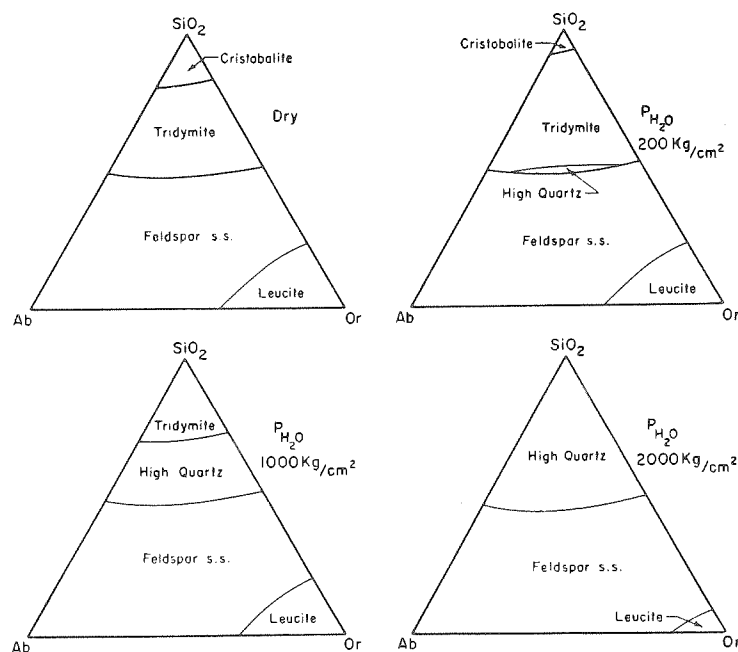


FIGURE 33.—Stability fields at the liquidus in the system  $\text{NaAlSi}_3\text{O}_8\text{--KAlSi}_3\text{O}_8\text{--SiO}_2\text{--H}_2\text{O}$  for various pressures of water vapor

tures. The diagrams are in part schematic since many of the field boundaries lie at temperatures above, and at compositions outside, the range in which we worked.

Changes in the stability fields at various pressures are the result of two opposing tendencies: (1) the tendency for water to lower the liquidus of all compositions as the solution of water is promoted by pressure, and (2) the tendency for pressure *per se* to raise the various inversion and liquidus temperatures. The effect of these two opposing factors can be readily seen in the PT relations of Figure 14 in which the inversions in silica are raised by pressure, and the water vapor lowers the liquidus of silica in such fashion that the liquidus intersects the stability field of all the modifications of silica.

At very low water pressures, as in the "dry" system, four phases appear on the isobaric saturation surface. They are cristobalite, tridymite, feldspar solid solutions, and leucite (Fig. 33). As the water-vapor pressure is increased (*i.e.*,  $P_{\text{H}_2\text{O}} = 200 \text{ kg/cm}^2$ ) the resulting liquidus lowering brings high quartz to the liquidus surface. Further increase in the water-vapor pressure results in the lowering of the liquidus of silica below the stability field of cristobalite, and as a result this phase is absent on the isobaric liquidus diagrams for all higher pressures. At  $2000 \text{ kg/cm}^2$  water-

vapor pressure tridymite is no longer stable, and quartz melts directly to a liquid. At the next highest pressure (Fig. 34),  $3000 \text{ kg/cm}^2$ , the field of leucite is missing, and only two stable phases are left at the saturation surface. The system is now entirely quaternary. As long as leucite appears on the liquidus surface the system

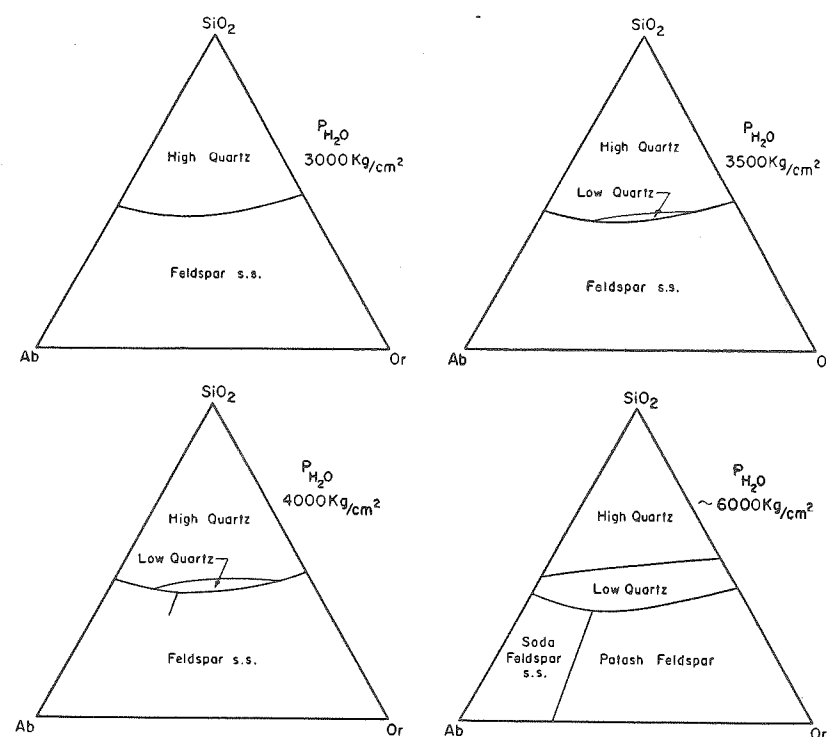


FIGURE 34.—Stability fields at the liquidus in the system  $\text{NaAlSi}_3\text{O}_8\text{--KAlSi}_3\text{O}_8\text{--SiO}_2\text{--H}_2\text{O}$  for various pressures of water vapor

is not quaternary because the composition of leucite lies outside the tetrahedron. Up to this pressure ( $3000 \text{ kg/cm}^2$ ) the effect of water vapor has been to make the liquidus surface less complicated. This trend is now changed, and increasing water-vapor pressure brings in new phases. At approximately  $3500 \text{ kg/cm}^2$  low quartz makes an appearance at the liquidus. The minimum on the boundary between the feldspar and silica fields becomes, isobarically, a "ternary" eutectic at approximately the same pressure because the temperature of the minimum has fallen below the top of the feldspar miscibility gap (*i.e.*, below  $660^\circ\text{C}$ ). At a pressure between  $3000$  and  $4000 \text{ kg/cm}^2$  and at a temperature of  $660^\circ\text{C}$ . the quaternary divariant plane representing the compositions of the liquids which are in equilibrium with quartz and feldspar solid solutions is intersected by the divariant plane representing the composition of the liquids which are in equilibrium with two-feldspar solid solutions, one rich in sodium and the other in potassium. At pressures below this intersection only one feldspar solid solution is in equilibrium at the liquidus with quartz,

whereas above this pressure two feldspars, quartz, and liquid coexist. This is a unique point in the tetrahedron, but it cannot be considered an invariant point because the maximum number of phases which coexist at one temperature and pressure is only five—two feldspars, quartz, liquid, and vapor. At pressures above and

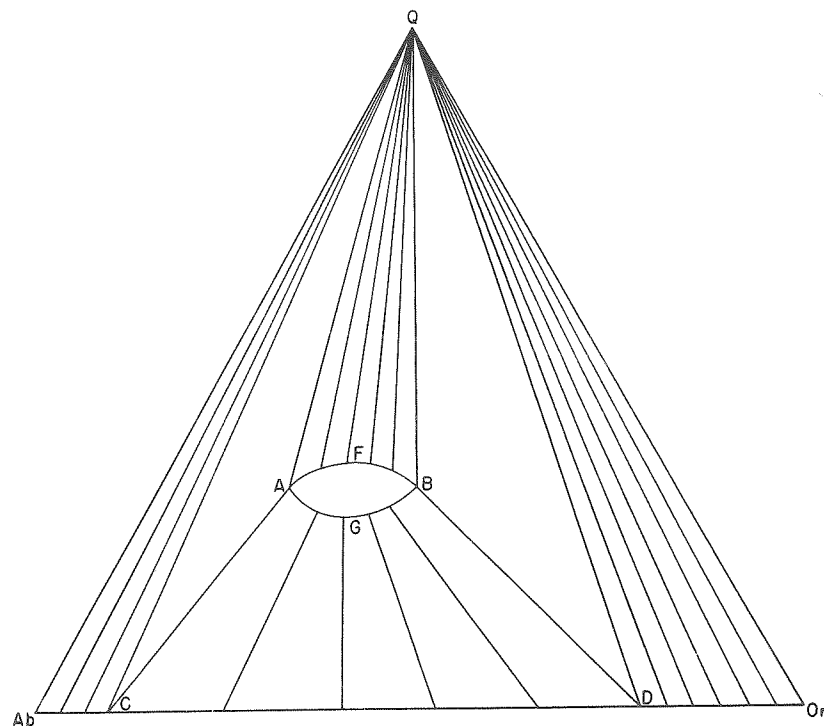


FIGURE 35.—Isothermal section through the isobaric prism at a temperature above and a pressure below that at which two feldspars appear at the liquidus

temperatures below this point these five phases coexist along a univariant line in the tetrahedron (Fig. 29). At about this same pressure and temperature low-temperature quartz appears at the liquidus because pressure has raised the high-low inversion of quartz, and dissolved water vapor in the liquid has lowered the liquidus. It is not certain whether the low quartz makes its appearance at the liquidus at a pressure just above or below this unique point in the tetrahedron (it is shown in Fig. 34 as being present at 3500 kg/cm<sup>2</sup>).

The relations just above and below this unique point in the tetrahedron can perhaps be better understood with the aid of two isothermal sections through the isobaric prism, one above and one below the critical pressure and temperature. In Figure 35, which is at a temperature above and a pressure below the critical point, only one feldspar can exist in equilibrium with liquid or vapor or quartz. The stable phases in the various fields are as follows: In *QAbC*, quartz with a feldspar whose composition lies along *AbC*; in *QCA*, quartz, feldspar having the composition *C* and the liquid *A*; in *QAFB*, liquids *AFB* with quartz; in *CAGBD* feldspar solid solu-

tion with compositions ranging from *C* to *D* in equilibrium with liquids *AGB*; in *QDB*, feldspar *D*, quartz and liquid *B*; in *QOrD*, feldspar *Or* to *D* with quartz. Figure 36 represents the relations at a pressure above and a temperature below the critical point. The coexisting phases are: In the area *AbQF*, feldspar

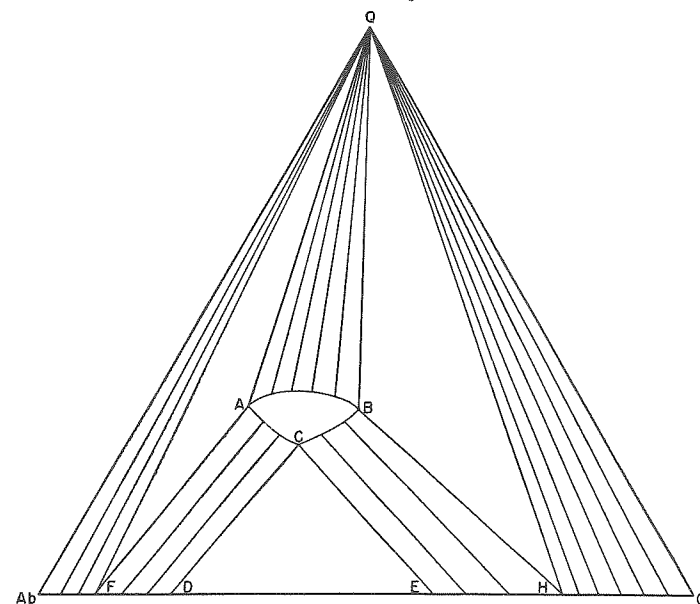


FIGURE 36.—Isothermal section through the isobaric prism at a temperature below and a pressure above that at which two feldspars coexist at the liquidus

*Ab* to *F* with quartz; in *QFA*, feldspar *F*, quartz, and liquid *A*; in *FACD*, feldspars *F* to *D* with liquids *AC*; in *QAB*, quartz with liquids *A* to *B*; in *DCE*, feldspars *D* and *E* with liquid *C*; in *ECBH*, feldspars *E* to *H* with liquids *C* to *B*; in *HQB* feldspar *H*, quartz, and liquid *B*; in *HQOr*, feldspars *H* to *Or* with quartz.

At pressures above 6000 kg/cm<sup>2</sup> many additional phase changes undoubtedly take place on the saturation surface. High-density silica will probably appear on the liquidus at pressures above 10,000 kg/cm<sup>2</sup>, for example. Nothing has been said about the various modifications of the potassium and sodium feldspars, principally because little is known about the effect of pressure on these transitions; however, it is certain that several modifications of these feldspars will appear at the liquidus at high pressures. The coexistence of high- and low sanidine (MacKenzie, 1952) in a single phenocryst suggests that this transition lies at a temperature and pressure in the range which has been discussed above, but as many of these transitions are extremely sluggish experimental determination of this pressure dependence is difficult.

#### ISOBARIC MINIMUM ON THE QUARTZ-FELDSPAR BOUNDARY

Petrologically the minimum on the isobaric diagrams is the most important feature of the system, as the compositions of the minimum at various pressures give the compositions toward which liquids move when they crystallize.

The minimum was located by finding the direction in which liquids moved along the boundary when the temperature was lowered and pressure was constant. For example, the mixture  $x$  (Fig. 37) held at 500 kg/cm<sup>2</sup> water-vapor pressure and 775°C. consisted of approximately 50 per cent glass, quartz, and feldspar (Or<sub>36</sub>). This

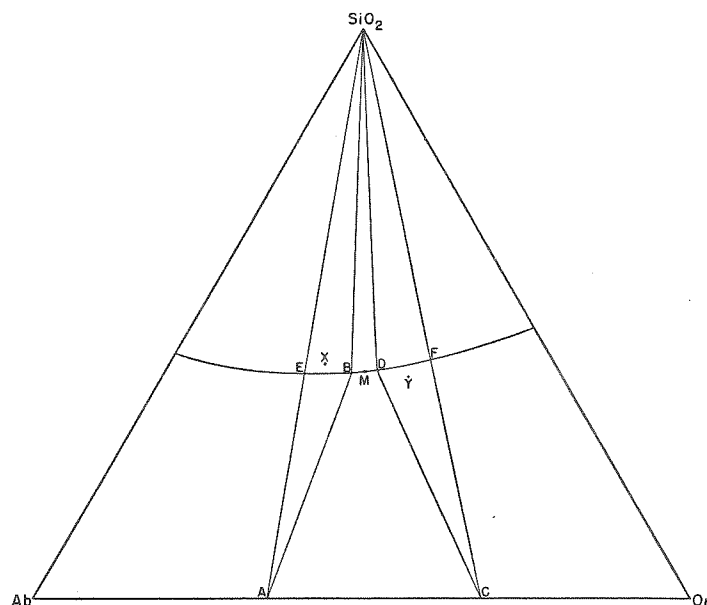


FIGURE 37.—Three-phase triangles at 500 kg/cm<sup>2</sup> water-vapor pressure and 755°C. in the system  
NaAlSi<sub>3</sub>O<sub>8</sub>-KAlSi<sub>3</sub>O<sub>8</sub>-SiO<sub>2</sub>-H<sub>2</sub>O

located the three-phase triangle  $ABSiO_2$ . All compositions lying in  $ABSiO_2$  are, then, partially liquid under these conditions; the amount of liquid ranges from 100 per cent at  $B$  to 0 per cent at  $E$ . It follows that  $B$  lies on the boundary at a lower temperature than  $E$ , and therefore the minimum must lie to the right of  $B$ . Similar relations hold for the composition  $V$  and the three-phase triangle  $CDSiO_2$ . These two determinations place the minimum between  $B$  and  $D$  on the feldspar-quartz boundary. These relations were further checked by running three mixtures corresponding to the compositions  $B$ ,  $M$ , and  $D$  simultaneously and observing that there is a temperature at which  $M$  is partially liquid, while  $B$  and  $D$  show no liquid.

The position of the "ternary" minimum for various pressures of water vapor is shown in Figure 38. The most conspicuous feature of this diagram is the shift of the minimum toward the albite apex with increased water-vapor pressure. This shift is accompanied by an increase in the water content of the silicate melts. The relation between water content and temperature is illustrated in Figures 27 and 28, and the relation between pressure and temperature in Figure 26. At some pressure between 3000 and 4000 kg/cm<sup>2</sup> the minimum becomes an isobaric "ternary" eutectic as the temperature has now fallen below the top of the binary solvus in the albite-orthoclase system. Strictly speaking this eutectic is one point on a line which is the intersection of

three quaternary surfaces representing the following equilibria: (1) sodium feldspar solid solution + potassium feldspar solid solutions + liquid, (2) sodium feldspar solid solutions + quartz + liquid, and (3) potassium feldspar solid solutions + quartz + liquid (Fig. 29).

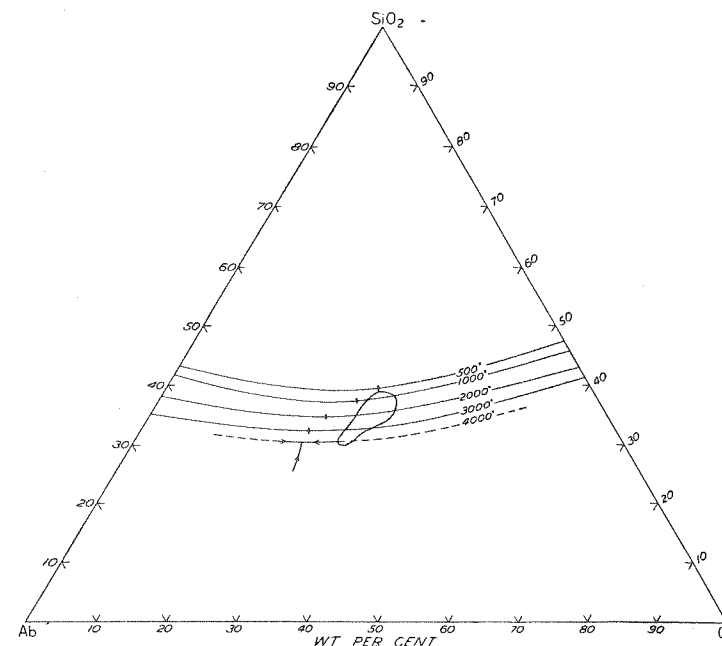


FIGURE 38.—Effect of water-vapor pressure on the isobaric minimum in the system  $NaAlSi_3O_8$ - $KAlSi_3O_8$ - $SiO_2$ - $H_2O$

The minimum becomes, isobarically, a ternary eutectic at pressures above approximately 3600 kg/cm<sup>2</sup>. The outline of the maximum of Figure 42 is superimposed to illustrate the close relationship between the ternary minimum for low water-vapor pressures and the normative compositions of granites.

## GRANITES, RHYOLITES, AND THE ISOBARIC MINIMA

The most striking feature of the isobaric diagrams for the system is the pronounced trough along the boundary between the feldspar and quartz fields. The nature of the trough can be seen from the isotherms of Figure 23, for example, but perhaps the general character can be illustrated better by vertical sections. Figure 39 represents a section through the 1000 kg/cm<sup>2</sup> isobaric diagram from Ab<sub>50</sub>-Or<sub>50</sub> to SiO<sub>2</sub>, and Figure 40 is a section along the quartz-feldspar boundary. This thermal deep is particularly pronounced in the sections extending toward the silica apex, and consequently the temperature of beginning of crystallization varies markedly with slight changes in silica content. For example, a change of less than 10 per cent in the silica content of the liquid may affect the temperature of beginning of crystallizing over 100°C. at constant pressure.

Another significant feature of the isobaric diagrams is the direction in which the liquids change composition during crystallization. In the field of silica all liquids move



directly away from the  $\text{SiO}_2$  apex in straight lines during crystallization because there is no solid solution in the crystalline phases, whereas in the feldspar field the relations are much more complicated because of the complete solid solution between albite and orthoclase. In this field the general nature of the direction of change of the compo-

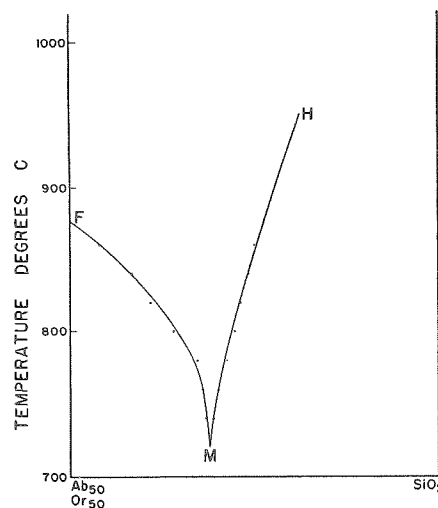


FIGURE 39.—Section through the 1000 kg/cm<sup>2</sup> isobaric prism from Ab<sub>50</sub>-Or<sub>50</sub> to the  $\text{SiO}_2$  apex

The nature of the thermal valley along the quartz-feldspar boundary is brought out well by this section.

sition of the liquids is shown by the fractionation curves of Figure 30. The shallow trough extending from the binary minimum on the Ab-Or sideline to the center of the diagram is a region toward which feldspar-rich liquids change their composition on crystallization. This subsidiary trough together with the principal trough along the quartz-feldspar boundary constitutes a thermal deep of great importance to the petrologist because together they prescribe the compositions toward which all rhyolitic and syenitic liquids will change on fractionation, and one can predict that, if the granitic and syenitic rocks have been through a liquid state, and if there has been opportunity for fractionation, their composition will be controlled by this thermal deep. The glassy rocks testify to the common occurrence of liquids of these compositions, and the numerous descriptions throughout the literature of crystal settling and compositional zoning provide unequivocal evidence that fractionation takes place in these liquids.

Viscosity may play an important role in controlling crystal fractionation in these hydrous silicate liquids, and it would be desirable to measure it in our synthetic liquids. Such experimental determinations have not been undertaken, and our knowledge of the viscosity is only indirect and is based on the assumption that viscosity is related to ease of crystallization. Mixtures whose compositions lie along

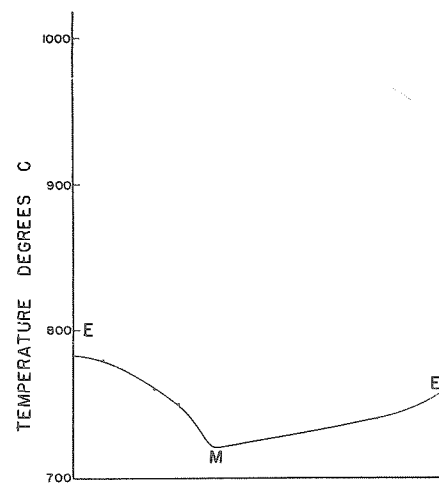


FIGURE 40.—Section through the isobaric prism along the quartz-feldspar boundary at 1000 kg/cm<sup>2</sup>

the Ab-Or sideline are the least viscous in the system, whereas those compositions near the quartz-orthoclase eutectic are the most viscous. Compositions near the isobaric "ternary" minima are much more viscous than the feldspar and albite-quartz mixtures, but they are not so difficult to crystallize as the Or-Q eutectic mixtures. For example, near the Ab-Or sideline, equilibrium between liquid and crystals can be attained in a few hours, whereas compositions near the isobaric "ternary" minima require weeks, and mixtures of orthoclase and quartz may require months to attain equilibrium. In a very rough way the viscosity is inversely proportional to the liquidus temperatures except near the Or-Q eutectic. Thus the thermal deep becomes a viscosity maximum.

With this understanding of the crystallization trends and viscosity of the liquids it can be predicted that these features control the compositional variations in rhyolitic and trachytic lavas. For example, if the viscosities were low and uniform the rocks should show compositional variations controlled largely by the isobaric "ternary" minimum with a very subsidiary influence of the trough extending from the Or-Ab minimum to the quartz-feldspar boundary. On the other hand, with the viscosity increasing toward the minimum it is expected that many of the rocks would have compositions lying along the subsidiary trough extending from the Or-Ab sideline to the minimum because the increasing viscosity would tend to inhibit the separation of crystals from liquid.

The compositional variations in the extrusive rocks themselves are shown in Figure 41 which has been constructed by plotting the normative quartz + albite + orthoclase in all the extrusive rocks in Washington's Tables (1917) that contain 80 per cent or more of these constituents. The only rocks omitted from this compilation are those which contain nepheline in the norm. The resulting point diagram was then contoured using the method commonly used in contouring petrofabric diagrams (Chayes, 1950a, p. 147).

The compositional variations in the rhyolites and trachytes are exactly as would have been predicted from the experimental results in the system quartz-orthoclase-albite-water. The concentration of analyses near the minimum on the isobaric diagram for water-vapor pressures of 500 kg/cm<sup>2</sup> is indeed striking. More than one-third of all the analyses lie within the two innermost contours. This represents a concentration of points far greater than is normally found in petrofabric diagrams of the minerals of well-foliated metamorphic rocks such as schists and gneisses.

Figure 42 has been prepared in the same fashion by taking all the plutonic rocks in Washington's Tables (1917). Here also the concentration is extremely high, and the maximum coincides with that found for the extrusive rocks. The coincidence between the maxima for rhyolites and granites and the thermal deep of the isobaric equilibrium diagram for lower water-vapor pressures is far too strong to be fortuitous. There can be little doubt that magmatic liquids are involved in the genesis of the granitic rocks, and those who propose that the granites are formed primarily by solid diffusion, hydrothermal replacement, or by any other mechanism not involving a magma must demonstrate an alternative method of controlling, to such a strong degree, the composition of the granites.

Although a liquid phase is necessary to explain the compositional variations in the granites, the liquid can originate either by remelting of salic rocks or by fractional crystallization of more basic liquids.

The position of the maximum for the rhyolites and granites suggests another feature

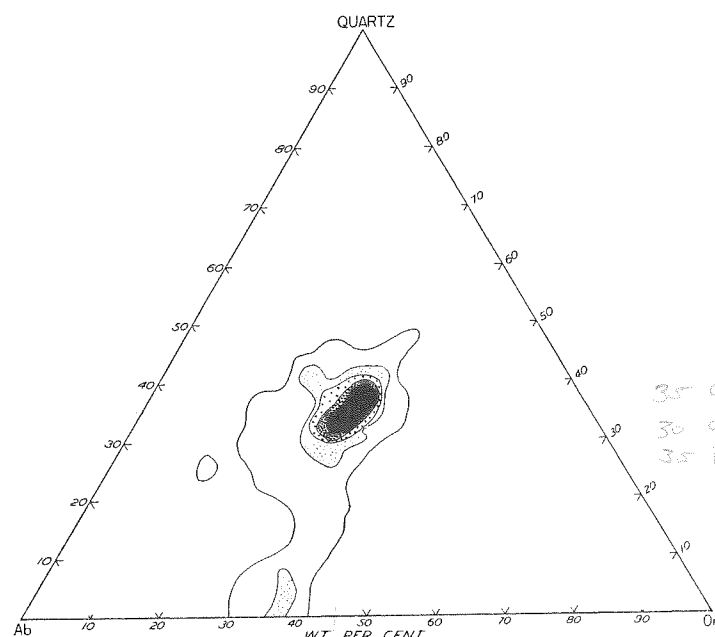


FIGURE 41.—Contour diagram illustrating the distribution of normative albite, orthoclase, and quartz in all (362) the analyzed extrusive rocks in Washington's Tables that carry 80 per cent or more normative  $Ab + Or + Q$

The concentration of extrusive rocks near  $\frac{1}{3} Ab$ ,  $\frac{1}{3} Or$ ,  $\frac{1}{3} Q$  is most remarkable, and in view of the phase relations previously described there is little doubt that this concentration is a result of the operation of liquid  $\rightleftharpoons$  crystal equilibria. The diagram has been contoured much like the familiar petrofabric diagrams after the method developed by Chayes (1949). Contours more than 1, 2, 3, 4, and 5 per cent. 0.25 per cent counter.

of importance to the petrologists; the water content of the liquids which would be expected to produce the maxima shown by the rocks must necessarily be low, probably less than 2 per cent by weight. This is in agreement with the actual water content found in the glassy rocks. Some glassy rocks (pitchstones) do contain more than this amount of water, but by and large the glassy rocks hold less than 2 per cent water. Daly's (1914, p. 19) average for rhyolites is 1.5 per cent. If melting of hydrous sediments were responsible for the origin of granites, the maximum for the granites (Fig. 42) should lie considerably nearer the quartz-albite sideline (note the position of the eutectic at 4000 kg/cm<sup>2</sup> in Figure 38 with respect to the position of the granite maxima also shown on this figure) because the isobaric minimum moves in this direction with increasing water-vapor pressure. The fact that few granites have compositions near the "ternary" eutectic at 4000 kg/cm<sup>2</sup> water-vapor pressure, or near the

minimum at 3000 kg/cm<sup>2</sup>, suggests that granitic magmas are probably rarely saturated with water. If granite liquids are commonly formed by selective melting of hydrous sediments, many of the liquids should be saturated with water. The amount of water necessary to saturate the liquid phase at 4000 kg/cm<sup>2</sup> is approximately 10

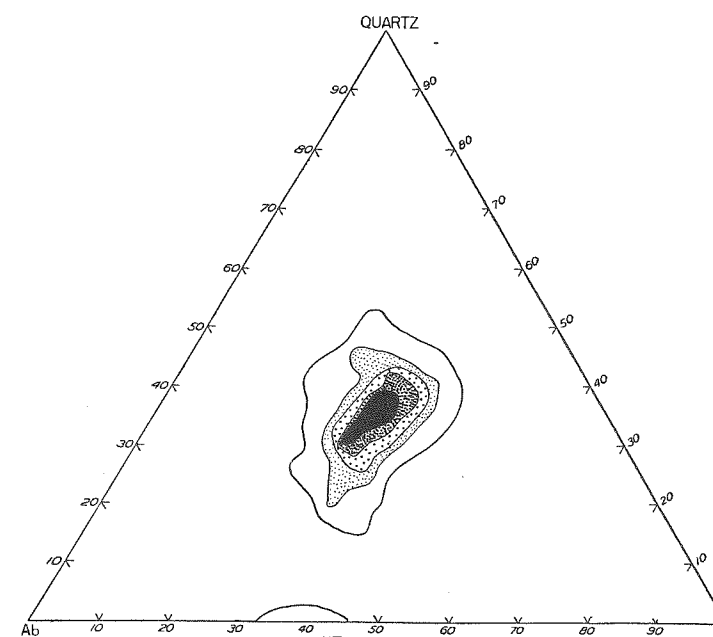


FIGURE 42.—Contour diagram illustrating the distribution of normative albite, orthoclase, and quartz in all (571) the analyzed plutonic rocks in Washington's Tables that carry 80 per cent or more normative  $Ab + Or + Q$

To be compared with Figures 38 and 41. The concentration of analyses near the center of the diagram is readily explained if a magmatic history is involved in the origin of most granites. On the other hand, no method of arriving at such a composition by solid diffusion or hydrothermal metasomatism has been discovered. Contours more than 1, 2, 3, 4, 5, 6-7 per cent. 0.25 per cent counter.

per cent. However, this value of 10 per cent water represents only the water present in the liquid phase and not the water content of the entire rock. In other words, a sedimentary rock containing 5 per cent water would give 50 per cent liquid containing 10 per cent water at 4000 kg/cm<sup>2</sup> water-vapor pressure at 640°C. This is equivalent to approximately 15 km depth in the earth's crust. If the water content of the rock were only 2.5 per cent, approximately 25 per cent of the rock would melt, giving a liquid containing 10 per cent water. This assumes that the anhydrous composition of the rock falls near the minimum of the isobaric sections. Under these conditions it would, of course, be impossible to produce melting in a quartzite or a limestone.

We can thus conclude that the chemical composition of the granites and rhyolites is controlled by liquid  $\rightleftharpoons$  crystal equilibria. Chayes (1952) has arrived at the same

conclusion by the results of a quantitative study of the mineralogical variations in the granites of New England. Chayes found that the distribution of the modal composition of various granite masses, as estimated by thin-section analysis, was related to the thermal valley described by Bowen (1937) in a simple fashion. The silica-rich portion of this thermal valley is the low-melting region of the isobaric sections. It was located by Bowen on the basis of the incomplete knowledge of the melting relations in the system  $\text{NaAlSi}_3\text{O}_8\text{--KAlSi}_3\text{O}_8\text{--SiO}_2$  together with the distribution of the compositions of the volcanic rocks. The determination of melting relations in the silica-rich portion of the system kalsilite-nepheline-silica reported here has made it clear that the thermal valley as outlined by Bowen need not be altered by the new data.

Chayes (1952) has plotted the results of modal analyses of 12 New England granites on the ternary diagram Ab-Or-Q on which the thermal valley of Bowen (1937) is outlined (Chayes, 1952, Figs. 11, 12, 13, 14). He found:

"For certain granites, as shown in Figure 11, all results lie in the valley. There are three examples of this type in the sample: Westerly and Bradford, Rhode Island, and Milford, New Hampshire. In each of the other nine New England granites for which sufficient data are available, some points lie outside the valley, but in only one (Westwood, Massachusetts) are they all outside. Thus in light of the nine cases there is some overlap of the valley boundaries, and the nature of this overlap is highly critical, for, in any particular granite, values lying outside the valley are all on the same side of the valley.

"In the granites of North Jay-Hallowell, Maine, Westwood, Massachusetts, and Pownal, Maine, outlying values are all on the orthoclase side of the valley (Fig. 12). In the granites of Fitzwilliam and Concord, New Hampshire, and Clark Island, Maine, overlap is in the quartz field (Fig. 13). In the granites of North Sullivan, Maine, and Barre and Woodbury, Vermont, overlap is exclusively on the plagioclase border of the valley (Fig. 14).

"In every one of these nine cases, a reasonable shift of the ternary mean would have generated overlap on two sides of the valley. In three of the nine, dispersion is easily large enough that a rather small shift of the ternary mean, depending on its sense, would have generated either a two- or threefold overlap. Yet the single overlap is the only type so far observed.

"By any of the nonmagmatic hypotheses, this effect can only be regarded as a chance event. So far as these hypotheses are concerned, there is no reason for the points to be concentrated in the center of the diagram at all, and values for any particular granite might fall outside the valley on any one side, on any two sides, or on all three sides.

"For magmatic hypotheses, however, the situation is entirely different. The observed distribution of Q-Or-Pl values is reasonable and almost necessary. If exceptions to it were anything but rare magmatists would have to conclude that either their theories were wrong or their experimental techniques faulty. Crystallization of a liquid whose initial composition lies in the diagram generates a liquid residue which approaches and finally enters the thermal valley; and, unless heat is added, the liquid cannot escape from the valley, once it has entered. The composition of adequate samples of such a crystallizing mass would necessarily fall either in the valley or outside it on the side nearest the initial composition. The observed distribution is thus thoroughly compatible with the hypothesis that granites form by crystallization of magmas (liquids) of granitic composition. . . ."

In summary, the compositional variations of the analyzed rocks containing 80 per cent or more albite + orthoclase + quartz are so closely related to the thermal valley on the liquidus surface in the system  $\text{NaAlSi}_3\text{O}_8\text{--KAlSi}_3\text{O}_8\text{--SiO}_2$  that there is little doubt that crystal  $\rightleftharpoons$  liquid equilibria are involved in the origin of the bulk of the granites. The quantitative modal study of granites by Chayes demonstrates that, modally, granites are related to the thermal valley in a fashion that strongly suggests a magmatic origin for the granites studied.

#### BEGINNING OF THE MELTING OF THE WESTERLY, RHODE ISLAND, AND QUINCY, MASSACHUSETTS, GRANITES IN THE PRESENCE OF WATER VAPOR UNDER PRESSURE

Having determined the beginning of melting for synthetic mixtures whose compositions closely approach those of the average granite, we selected two granites for a

TABLE 11.—Chemical, normative, and modal composition of the Quincy and Westerly granites

	Quincy	Westerly
	<i>Chemical Analysis</i>	
SiO <sub>2</sub>	72.26	72.34
Al <sub>2</sub> O <sub>3</sub>	13.18	14.34
Fe <sub>2</sub> O <sub>3</sub>	0.24	0.68
FeO	2.77	1.13
MgO	0.20	0.37
CaO	1.10	1.52
Na <sub>2</sub> O	3.99	3.37
K <sub>2</sub> O	5.01	5.47
H <sub>2</sub> O+	0.20	0.30
H <sub>2</sub> O—	0.08	0.06
CO <sub>2</sub>	0.04	N.D.
TiO <sub>2</sub>	0.36	0.26
P <sub>2</sub> O <sub>5</sub>	0.07	N.D.
MnO	0.10	0.02
	99.60	99.86
	<i>Norm</i>	
Q	26.10	26.24
Or	29.47	32.80
Ab	34.06	28.82
An	3.06	7.23
Di	1.16	0.24
Hy	3.84	1.47
Mt	0.23	0.93
Il	0.76	0.61
Ap	1.01	.....
Cc	0.10	.....
H <sub>2</sub> O	.20	0.30
	100.01	98.34
	<i>Mode*</i>	
Quartz	21.7	27.1
Microcline	.....	35.0
Perthite	69.1	.....
Plagioclase	.....	32.2
Others	9.1	5.8
	99.9	99.9

\* Mode of the Westerly after Chayes (1952)

similar set of experiments to test the possible effect of constituents other than the feldspars and quartz in lowering the temperature of beginning of melting. The Westerly and Quincy granites were selected as they represent two different types of granites. The Westerly is a plagioclase-microcline-quartz granite with biotite and muscovite, whereas the Quincy is a perthite-quartz granite carrying a sodium-iron

TABLE 12.—Beginning of melting at various pressures of water vapor

Run no.	Temperature °C.	Pressure kg/cm <sup>2</sup>	Time	Result
<i>Westerly Granite</i>				
Q2-10C	760	500	7 days	No glass
Q2-9F	780	500	7 days	10% glass
Q2-10B	710	1000	7 days	No glass
Q2-8C	725	1000	7 days	10% glass
Q2-13C	690	2000	7 days	No glass
Q2-8B	700	2000	5 days	80% glass
Q2-15D	660	3000	7 days	No glass
Q2-14D	670	3000	7 days	10% glass
Q2-6A	650	4000	20 hours	No glass
Q2-6B	680	4000	20 hours	75% glass
Q2-6E	665	4000	3 days	10% glass
<i>Quincy Granite</i>				
Q2-10E	760	500	7 days	No glass
Q2-10F	780	500	12 days	50% glass
Q2-13B	715	1000	7 days	No glass
Q2-12D	725	1000	6 days	10% glass
Q2-11C	680	2000	7 days	No glass
Q2-8B	700	2000	5 days	90% glass
Q2-12E	660	3000	6 days	No glass
Q2-13D	670	3000	7 days	90% glass
Q2-10A	650	4000	5 days	No glass
Q2-10D	660	4000	2 days	10% glass
<i>"Ternary" Minimum</i>				
.....	950	0	35 days	No melting
.....	970	0	35 days	Some glass
Q2-9G	760	500	7 days	No glass
Q2-9A	780	500	10 days	Glass + crystals
Q2-8D	715	1000	7 days	No glass
Q2-4E	725	1000	1 day	10% glass
Q2-15E	680	2000	7 days	No glass
Q2-16E	690	2000	7 days	Glass + crystals
Q2-6H	660	3000	7 days	No glass
Q2-16B	670	3000	7 days	50% glass
Q2-1D	650	4000	2 days	No glass
Q2-1E	660	4000	2 days	10% glass

amphibole as the principal dark mineral. Chemical and modal compositions of the two granites are given in Table 11.

Results of the experiments are given in Table 12 and Figure 43. In all runs the initial material was completely crystalline, and the presence or absence of glass was determined by examination with the petrographic microscope. There are two possible sources of error in these determinations: (1) the composition of the charge may change somewhat during the experiment, and (2) minute traces of glass may escape notice.

Compositional changes have to be very large to give significantly different results, and changes of such magnitude are unlikely. The presence of small traces of glass which have escaped detection might result in materially lower temperatures, but the values given certainly indicate the minimum temperature at which a significant amount of melting takes place.

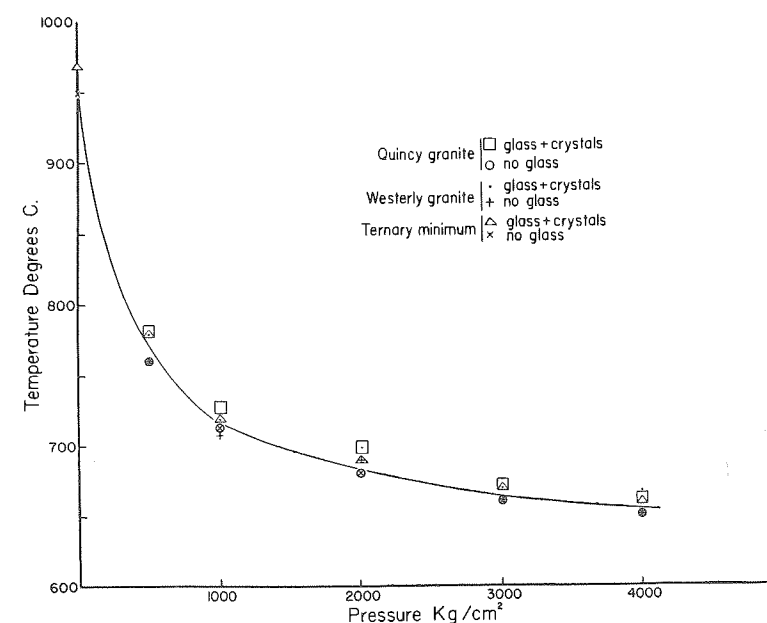


FIGURE 43.—Pressure-temperature projection of the solidus for the Westerly, Rhode Island, granite, the Quincy, Massachusetts, granite, and the isobaric minimum in the system  $\text{NaAlSi}_3\text{O}_8\text{--KAlSi}_3\text{O}_8\text{--SiO}_2\text{--H}_2\text{O}$

The minimum becomes an isobaric ternary eutectic above 3600 kg/cm<sup>2</sup> water vapor pressure as the temperature is then below the top of the albite-orthoclase solvus.

At atmospheric pressure anhydrous synthetic granites begin to melt at about 960°C. This value is in notable disagreement with the previous determination on dry granite reported by Greig, Shepherd, and Merwin (1931), who reported that a granite became half liquid in one week at 800°C. The only explanation we can offer for this difference is that the granite used by Greig, Shepherd, and Merwin melted metastably because the crystalline phases were unstable at the temperature of their experiments. For example, the granite consisted essentially of quartz, microcline, and plagioclase, whereas the stable assemblage at 800°C. would be quartz and sanidine.

The primary phase in both granites appears to be biotite. No special effort was made to study the liquidus relations of these granites, but those runs which were nearly completely liquid gave indications that the biotite was growing (recrystallizing). The amphibole of the Quincy granite apparently is unstable under these conditions, and the primary phase is probably biotite. Pyroxene was also present in most of the runs and under some circumstances may be the primary phase. The presence of



hematite, which was reported to be the primary phase by Goranson (1932), was not noted in our experiments. Here the difference in results is probably due to the oxidizing atmosphere in Goranson's experiments as a result of the escape of hydrogen, whereas in our runs the hydrogen apparently could not escape readily if at all.

Within the experimental error the two contrasted natural granites begin to melt at the same temperature as synthetic mixtures having compositions near the ternary minimum. The PT curve for the ternary minimum may then be used with confidence to indicate the pressures and temperatures at which natural granites begin to melt in the presence of water vapor.

#### CHARACTER OF RESIDUAL SOLUTIONS FORMED BY CRYSTALLIZING HYDROUS GRANITIC LIQUIDS

##### GENERAL CONSIDERATIONS

Some recent papers dealing with the residual solutions of crystallizing granite magmas have stressed the view that there is a hiatus between granite magmas and hydrothermal solutions (Eskola, 1939, p. 378; Turner and Verhoogen, 1951, p. 315; Ramberg, 1952, p. 3). These views can be illustrated by a quotation from Ramberg (1952, p. 3):

"According to Goranson's experiments, water and rock making silicate melts are only partly miscible, showing that no continuity exists between magmatic melts and hydrothermal solutions. It is therefore impossible, although it has often been assumed, that a gradually increasing concentration of water can depress the crystallization temperatures of a magma down to any value convenient for the interpretation of metamorphism as a secondary effect of magmas".

It is the purpose of this section to demonstrate that it is possible to have a continuous gradation between granite magmas and hydrothermal solutions and that under certain circumstances equilibrium relations could, in fact, demand continuous solubility between silicate melts and water.

Results of equilibrium studies in the system  $K_2O-Al_2O_3-SiO_2-H_2O$  indicate that continuous solubility can be expected at low pressure if the initial composition is such that liquids rich in alkali silicates are concentrated during crystallization.

##### THEORETICAL CONSIDERATIONS

The solubility of feldspars and quartz in water is relatively slight at temperatures up to the critical temperature of water, and it can be assumed that the critical temperature of water is therefore not greatly affected by the presence of alkali feldspar or quartz. On the other hand, Goranson (1938) has shown, and it has been confirmed in the present study, that the solubility of water in albite and orthoclase liquids is slight, and a reasonable extrapolation of the data indicates that a solubility greater than 10 per cent water is unlikely at pressures prevailing in the outer 20 km of the earth's crust. It is reasonable to assume therefore that these compositions will not have a continuous solubility relation with water. These studies support the view expressed by Ramberg (1952).

A different relationship was found for the alkali silicates. For example, the potassium silicates exhibited continuous solubility with water at moderate pressures (Morey and Fenner, 1917). The vapor-pressure curve for these silicates had a maxi-

mum, and the critical curve did not intersect the solubility curve. The maximum pressure on the saturation surface for all compositions in the system  $K_2SiO_3-SiO_2-H_2O$  in which an alkali silicate was the stable phase is probably less than 200 kg/cm<sup>2</sup>. Similar relations undoubtedly exist in the system  $Na_2SiO_3-SiO_2-H_2O$  (Tuttle and Friedman, 1948). At first glance these compositions appear far removed from expected liquids formed by crystallizing granite magmas, but, as there are no known compounds intermediate between these alkali silicates and the feldspars, liquids rich in these components are possible and in fact very probable.

Granitic magmas containing water and other volatiles tend to concentrate these constituents in the liquid phase during crystallization if they are present in amounts greater than that taken up by hydrous phases (amphiboles and micas). Water so concentrated will dissolve in the silicate melt as crystallization proceeds unless critical phenomena intervene or unless the pressure generated exceeds the strength of the magma chamber. The compositions studied by Goranson probably fall in the latter category as he discovered no evidence of critical phenomena at pressure up to 4000 kg/cm<sup>2</sup> (equivalent to a depth of about 15 km, rock density 2.7).

##### PORTION OF THE SYSTEM $K_2O-Al_2O_3-SiO_2-H_2O$

The orthoclase-quartz join in this system is one of the sidelines in the  $NaAlSi_3O_8-KAlSi_3O_8-SiO_2-H_2O$  system which embraces the principal compositions under investigation. As the system  $NaAlSi_3O_8-KAlSi_3O_8-SiO_2$  is ternary, compositions studied in this system do not give information on crystallization of compositions in which the alkalies and alumina are present in ratios different from that found in feldspars. It is to be expected that magmas will commonly contain an excess of either alkalies or alumina above that in the ratio required by the feldspars, and it is therefore desirable to learn the effects of such compositional variations on the course of crystallization. The system  $K_2O-Al_2O_3-SiO_2-H_2O$ , which was studied at 1000 kg/cm<sup>2</sup> water-vapor pressure (Table 13), illustrates the nature of liquids formed by crystallization when the initial alkali and alumina content are different from the stoichiometric proportions of the feldspars.

The orthoclase-quartz eutectic appears in this system (Fig. 44) as a maximum on the boundary between the quartz and orthoclase fields. On the alumina side of the join this boundary falls a few degrees to a near-by isobaric "ternary" eutectic involving quartz, orthoclase, and mullite. The boundary falls on the potassium side to much lower temperatures and reaches compositions rich in potassium silicate. In the presence of water vapor at a pressure of 1000 kg/cm<sup>2</sup>, this boundary falls to temperatures below 400°C., and the liquid probably contains more than 30 per cent water. Reasonable extrapolation of the experimentally determined values leads to liquids rich in potassium silicates and water. These liquids are so near those known to exhibit a continuous solubility with water that there is little doubt that similar relations exist when the liquids contain a small amount of alumina.

Thus liquids whose compositions may be represented as a mixture of quartz and orthoclase, but having an excess of potassium over the ratio of potassium to alumina in orthoclase, must, on crystallization in the presence of water under pressure, give rise to residual liquids which have a continuous solubility relation with water.



## ALKALI-ALUMINA RATIO IN ANALYZED GRANITIC ROCKS

The question now arises: Do any granitic liquids contain alkalis in excess of that required to combine with all the alumina to form feldspars? Fortunately, for all practical purposes, the normative classification (Cross, Iddings, Pirsson, Washington,

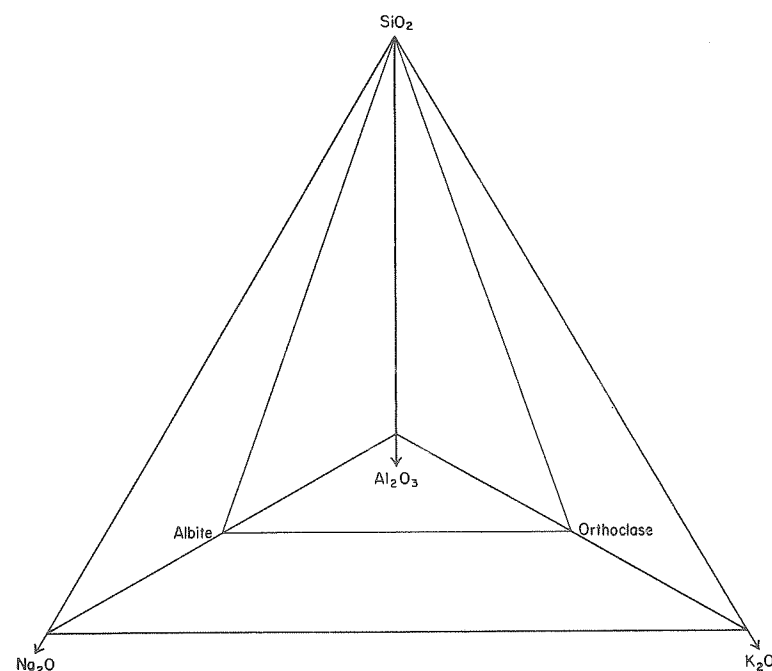


FIGURE 45.—Portion of the tetrahedron representing the system  $K_2O-Na_2O-Al_2O_3-SiO_2$

Shows the position of the ternary plane Ab-Or- $SiO_2$  within the tetrahedron

TABLE 14.—Normative corundum, alkali metasilicates, and acmite in 1016 analyzed silic rocks

	Corundum	Alkali metasilicate	Acmite	Total*
Granites	348	4	34	575
Rhyolites	216	24	69	441

\* 189 granites and 133 rhyolites do not have corundum, alkali metasilicates, or acmite in their norms.

1902) of the granitic rocks gives this information directly. If alumina is present in excess of that required to satisfy all the alkalis and lime as feldspars, it appears as corundum in the norm. If the alkalis are present in excess of that required to combine with the alumina as feldspars, acmite and/or alkali metasilicates appear in the norm. Table 14 shows these relations in 1016 analyses of rocks from Washington's Tables (1917) that contain 75 per cent or more normative albite + orthoclase + quartz. The analyses are divided into two groups, granites and rhyolites.

Less than 1 per cent of the granites have alkali metasilicate in the norm, whereas 5.4 per cent of the rhyolitic rocks carry normative metasilicate.

There is little doubt that some of the extrusive rocks carry considerably more alkalis in proportion to alumina than do the intrusive granites. This relationship is to be expected as the granitic rocks crystallized under conditions which permit alkalis to be expelled during the final stages of crystallization; this does not occur in rhyolitic extrusives. Those who maintain that rhyolites are merely melted granites which have in turn formed by granitization are confronted with the problem of explaining this excess of alkalis in the rhyolites. On the other hand, those who accept fractional crystallization as a method of forming granitic liquids are not faced with this problem; the alkali-alumina ratio in a liquid formed by fractional crystallization of a basaltic parent need not correspond to the ratio of alkalis to alumina in the feldspars.

## DISCUSSION

Evidence has been presented to show that residual solutions developed during the crystallization of hydrous granitic magmas may exhibit a continuous gradation from hydrous silicate liquid to hydrothermal solution. Evidence for the gradation is based on experimental data on portions of the system  $K_2O-Na_2O-Al_2O_3-SiO_2-H_2O$ . It is concluded that continuous gradation from magma to hydrothermal solution will obtain in hydrous liquids if the alkali to alumina ratio is such that crystallization results in concentration of alkali silicates in the residual liquids. This restriction may not apply to a complex system such as a granite magma in which many volatiles in addition to water are concentrated. Such a system concentrating lithia, carbon dioxide, sulfur, chlorine, fluorine, and many other materials may exhibit a continuous gradation even when alumina is present in excess of that amount required to combine with the alkalis to form feldspar.

## COMPOSITION OF THE VAPOR IN EQUILIBRIUM WITH HYDROUS GRANITIC MELTS

Early in this study it was noted that material was added to the charges from the walls of the pressure vessel by transport through the vapor phase. This transfer was inhibited by a tight-fitting lid (Fig. 1). Later it became necessary to make longer runs, and as the time was lengthened from a few minutes to a few days it was discovered that the charges had lost considerable weight during the experiment. The loss of material from the charge is presumably due to the diffusion of vapor through "pin holes" and other minute openings in the platinum foil crucibles and deposition of crystalline material in the cooler parts of the pressure apparatus. Such deposition sets up a concentration gradient in the vapor and promotes transport of a considerable amount of material.

It would be desirable to collect the vapor that is in equilibrium with synthetic and natural granites and to determine its composition directly. This, however, would be a very difficult task as the vapor is largely water, and a relatively large amount would have to be collected at the pressure and temperature of the experiment to permit accurate determinations of the composition of the silicate fraction. A less satisfactory and indirect method was adopted because of this difficulty.

Runs in the  $\text{NaAlSi}_3\text{O}_8\text{-SiO}_2\text{-H}_2\text{O}$  system gave indications that the anhydrous portion of the vapor was considerably richer in silica than the original material was. For example, in one experiment the buffer, which initially contained 40 per cent silica and 60 per cent albite, consisted largely of albite crystals at the end of the run.

This experiment suggested a qualitative method of ascertaining the composition of the silicate component of vapors in equilibrium with hydrous synthetic granites. The experiments were carried out by permitting the liquid to change composition by escape of the vapor; the change was measured by the X ray after crystallizing the liquid completely to feldspar and quartz. The method involved estimating the composition of the feldspar in completely crystallized synthetic granite by means of the (201) reflection and at the same time determining the amount of quartz present by the intensity of the (10 $\bar{1}$ 1) reflection of quartz relative to the intensity of the (201) reflection of the feldspar. In order to use the relative intensities of the (10 $\bar{1}$ 1) reflection of quartz and the (201) reflection of the feldspars to estimate the proportion of quartz present, it was first necessary to calibrate the relative intensities against known quartz-feldspar ratios. This was carried out by crystallizing completely six glasses having known compositions, ranging between 46 per cent feldspar and 100 per cent feldspar, and measuring the relative intensities of the two reflections on the X-ray spectrometer. The measurements gave a curve showing the percentage of silica versus the ratio of the intensities (201) feldspar to (10 $\bar{1}$ 1) of quartz. This curve was then used to determine approximately the composition of quartz-feldspar mixtures.

Results of five such runs are shown in Table 15. The principal change in composition was the loss of silica. At 725°C. and 3000 kg/cm<sup>2</sup> water-vapor pressure a synthetic granite containing 37.1 per cent quartz lost approximately 22 per cent of the quartz in 8 days (Table 15). The feldspar changed only from Or<sub>56.1</sub> to Or<sub>51</sub>.

The feldspar changed composition in three of the runs; all three showed an increase in the albite content. The feldspars of the other two changed less than 2 per cent in orthoclase content and could not be considered significant.

If these measurements represent a change in composition by vapor loss it is certain that the vapor is richer than the liquid in silica, and there is a tendency for it also to be richer than the liquid in "orthoclase". Apparently the vapor is congruent—that is, it contains alkalis, alumina, and silica in the same ratio as the feldspars, because a slight loss of alkalis over alumina and silica would result in the appearance of aluminum silicates such as mullite in the final crystalline product. Extremely small amounts of mullite would be readily detected by the microscope.

Possibly the compositional changes were due to diffusion through the vapor rather than actual movement of the vapor *per se*. If so the compositional changes are a function of diffusion rates rather than vapor composition.

Rapidity of transfer at high pressures was illustrated by one experiment at 4000 bars pressure. A sample of Westerly granite (approximately 1 gm) was held in a cold-seal pressure vessel for 36 days at a temperature of 700°C. and 4000 bars pressure. On quenching, the platinum-foil crucible contained only about 50 mg of material, which was largely monoclinic pyroxene and garnet with accessory alkali feldspar and apatite. The quartz and feldspar components had been almost completely ab-

stracted from the liquid and deposited in the cooler portions of the pressure vessel (initially the granite was completely liquid). The pyroxene was badly corroded, and it, too, would probably have been removed if the run had been prolonged. In contrast the garnet dodecahedra showed no evidence of attack.

In summary, it can be said that the vapor in equilibrium with hydrous granite

TABLE 15.—Compositional changes in vapor-loss experiments

Sample no.	Initial composition		Temperature °C.	Pressure kg/cm <sup>2</sup>	Length of run (Days)	Final Composition	
	% Or	% Q				% Q	% Or
VC-7A	56.1	37.1	750	2000	21	17	58
VC-7C	41.8	36.9	800	2000	21	26	41
VC-6D	56.1	37.1	725	2000	8	19	50
VC-4A	56.1	37.1	725	3000	8	15	51
VC-5A	56.1	37.1	775	1000	8	31	53

liquids is rich in silica. The few experiments undertaken also indicated that the feldspars are a major constituent of the vapor, but quantitative data are lacking. The experiment with the Westerly granite suggested that lime and magnesia, as well as  $\text{P}_2\text{O}_5$ , were relatively insoluble in the hydrous-vapor phase. The relatively minute amounts of lime, magnesia, and  $\text{P}_2\text{O}_5$  present in the initial melted granite stayed behind presumably because they were essentially insoluble in the hydrous vapor. This tendency for the oxides which are abundant in the "basic" rocks to be relatively insoluble in the hydrous vapor suggests a possible mechanism for producing the basic zones commonly found at granite contacts. If hydrous vapor, escaping from a cooling granite intrusive, passes along the contact the vapor at certain places can selectively dissolve feldspars and quartz and leave behind lime, magnesia,  $\text{P}_2\text{O}_5$ , and perhaps iron. Such residual basic zones would not be expected to develop as complete shells around intrusives, but rather they would presumably develop in structurally favorable parts of the contact zone where relatively "open" areas permit movement by vapor transfer.

#### STABILITY OF THE AMPHIBOLES

##### ANTHOPHYLLITE

The magnesian amphibole, anthophyllite, was synthesized (Bowen and Tuttle, 1949) by decomposing talc in the presence of water vapor, but continued heating under the same conditions of pressure and temperature caused the amphibole to break down to a pyroxene and quartz. This behavior indicated that the amphibole was unstable in the presence of excess water vapor, or that the pure magnesian anthophyllite was unstable, and small amounts of cations other than Mg were necessary to stabilize the structure. Experiments now indicate that the first suggestion is correct.

Anthophyllite was synthesized by heating a charge of  $\text{MgO-SiO}_2\text{-H}_2\text{O}$  in the stoichiometric proportions of anthophyllite in a sealed capsule at 810–820°C. with 1000 kg/cm<sup>2</sup> external pressure. This temperature was just above the breakdown



temperature of talc at this pressure. In all cases the product consisted of anthophyllite, enstatite, and quartz. A large yield of anthophyllite was not obtained in any of these experiments. Under these same conditions of temperature and pressure anthophyllite broke down to enstatite and quartz if an excess of water vapor was present.

#### GRUNERITE

Flaschen and Osborn (1953) reported the ferrous-iron amphibole, grunerite, as a decomposition product of minnesotite, the ferrous-iron analogue of talc. As with anthophyllite, this amphibole also formed on short runs and decomposed on continued heating under the same conditions. In the long runs grunerite was replaced by fayalite and silica.

#### RIEBECKITE

This amphibole has been synthesized by J. L. England (Personal communication) using the sealed-tube technique. The amphibole was obtained in runs in which the water content was less than 3.9 per cent at temperatures less than 610°C. If the water content was greater than approximately 4 per cent, acmite was the major phase. At and above a temperature of 610°C. only acmite was present. These results are similar to those for the amphibole from the Quincy granite. There are some indications that the amphibole will be replaced by acmite even below 610°C., if the environment is not reducing. For example, at 512°C. and 1350 bars external pressure only the amphibole was obtained in runs in which metallic iron was present, whereas amphibole plus acmite was present only if FeO was initially present. Presumably dissociation of H<sub>2</sub>O and escape of H<sub>2</sub> at these temperatures were sufficient to oxidize some of the FeO to Fe<sub>2</sub>O<sub>3</sub>.

#### AMPHIBOLE FROM THE QUINCY GRANITE

The principal amphibole from the Quincy granite has been identified as the soda-iron amphibole, riebeckite (Warren, 1913). Several grams of this material were separated by heavy liquids and purified by magnetic treatment. The purified fraction was heated in the presence of excess water vapor in an attempt to determine its stability. At 600°C. and water-vapor pressure of 1000 kg/cm<sup>2</sup> no change was noted after 25 days, whereas at 625°C. and the same pressure considerable decomposition took place in 9 days. This indicates that this amphibole also is unstable at magmatic temperatures in the presence of water vapor at 1000 kg/cm<sup>2</sup> pressure.

The decomposition at 625°C. could conceivably be due to factors other than the presence of excess water, but previous study of other amphiboles suggests this is the most likely explanation. If this is the correct interpretation we may conclude that the water-vapor pressure in the Quincy granite magma was relatively low as this is a perthite-quartz granite and therefore must have crystallized well above 650°C.

#### DISCUSSION

Experimental results indicate that at least some of the amphiboles may well be unstable in the presence of a moderate or high water-vapor pressure. If so these amphiboles and perhaps others will not be found in rocks formed in the presence of an excess of water. Perhaps the only common rock type in this category is the granite pegmatite, and the absence of amphiboles in these rocks appears to support this

interpretation. This is not to suggest that all pegmatites lack amphiboles, but certainly these minerals are rare in the zoned pegmatites associated with the granites. Where granite pegmatites cut amphibolites, there is commonly a zone of biotite between the pegmatite and amphibolite (Jahns, 1955, p. 1069).

It has been suggested (Tuttle, 1952) that the rate of cooling of a granite pluton will control the character and amount of unmixing of the alkali feldspar. Studies of contacts of one-feldspar granite indicate that other factors are operative as well, because relatively large plutons such as the Madoc, Ontario, granite show little change in the character of the perthite near contacts. Most perthite-quartz granites carry amphibole as the principal dark mineral, suggesting that the lack of extensive unmixing of the alkali feldspars in these granites may well be a result of the low water content of the magma. In contrast, the two-feldspar granites (microcline-plagioclase-quartz) carry mica (known to be stable in the presence of excess water vapor) as the principal dark mineral.

Laboratory studies of feldspars have shown that unmixing and recrystallization are greatly accelerated by the presence of water vapor under pressure and suggest that the presence of excess water vapor may control to a large extent the unmixing and recrystallization of the two-feldspar granites. Field studies of the metamorphic effects of these two types of granite on their wall rocks, particularly those granites that have not been subjected to a later metamorphism, should provide evidence as to the validity of these suggestions. Perthite-quartz granites, if they are relatively anhydrous, should produce only local thermal effects on the surrounding rocks, whereas the two-feldspar granites may have a considerable excess of water which would produce marked metamorphism of the country rocks with considerable metasomatic granitization. The magnitude of the metamorphic effects of such granites will doubtless vary with the amount of water in excess of that taken up in the hydrous minerals. } #440

#### WIBORGITE RAPAKIVI GRANITE IN THE LIGHT OF THE EQUILIBRIUM RELATIONS IN THE SYSTEM NaAlSi<sub>3</sub>O<sub>8</sub>-KAlSi<sub>3</sub>O<sub>8</sub>-SiO<sub>2</sub>-H<sub>2</sub>O PREVIOUS VIEWS ON THE GENESIS OF THE RAPAKIVI TEXTURE

To many petrographers the name rapakivi has come to signify granite in which potassium feldspar is mantled, in part at least, by plagioclase feldspar (usually oligoclase). This restriction of the term is unfortunate as many geologists include under the classification of rapakivi granites (*see* Sahama, 1945) granites which do not carry mantled alkali feldspar.

Granite containing ovoidal alkali feldspar with plagioclase rims is particularly well developed in the Wiborg (or Viipuri) area in southeast Finland. Wahl (1925) proposed that this type of granite be called wiborgite rapakivi. Although there has been some objection to this nomenclature it has, in general, been accepted. The following discussion is concerned with this type of rapakivi granite.

There have been at least six principal theories advanced to account for the rapakivi texture as typified by the granite at Wiborg, Finland.

One of the earliest attempts to explain the texture was that of Holmqvist (1899) who suggested that liquid immiscibility caused drops of a different composition to

separate from the magma; these drops later crystallized as feldspar. Experimental studies on silicate systems have shown that such an immiscibility is highly unlikely if not impossible, and field studies have revealed no instance of immiscibility in such compositions although, as pointed out by Bowen (1928), such evidence would undoubtedly be readily discovered if such a process were operative.

A second theory was advanced by Popoff in 1903. He noted the variable size of the oval feldspars and suggested that they must have crystallized at different places and that subsequent movements of the magma mixed them. He also suggested that, once crystallized, feldspar may sink in the magma; at lower levels the increased temperature may dissolve a portion of the crystals and thus produce the oval shape. These rounded potassium feldspars thus provide a nucleus for the precipitation of oligoclase. The concentric rims (in places as many as 10 rims) were believed due to repeated resolution and redeposition by alternate cooling of the magma and sinking of the crystals. Later investigators have not supported this concept because of the complexity of the theory and because it fails to explain mantling in certain localities where movement of the feldspar was impossible.

Vogt (1906) suggested that the oval shape of the potassium feldspar was due to resorption when the composition of the liquid crossed the orthoclase-plagioclase field boundary by undercooling and the consequent supersaturation of plagioclase caused the plagioclase to crystallize as mantles around the partially resorbed orthoclase. This theory fails, as do all the others, to explain why only some of the potassium feldspars have mantles of plagioclase.

A fourth theory was proposed by Wahl (1925) who stressed the feature of two generations of quartz and feldspar. He suggested that the oval shape was due to the high temperature of crystallization and that the early-formed crystals were later reformed into drops of liquid feldspar by the release of pressure. Crystallization then produced the second generation of quartz and feldspar as well as the oval potassium feldspars from the drops of liquid feldspar.

A fifth explanation of the oval feldspar was proposed by Sederholm (1928). He writes (p. 92):

"It is perhaps possible to assume that the zone of magma rich in oligoclase that has originated by the crystallization of the potash feldspars and has not been removed at once by diffusion, has caused by its high viscosity, an internal friction hindering the diffusion, and gradually causing the cessation of the crystallization of the potash feldspar. Therefore, spheroidal crystals instead of those with a perfect crystal form have originated".

This explanation of the oval shape of the feldspars does not account for the fact that not all the large potassium feldspar crystals have a plagioclase mantle.

The sixth proposal for the origin of the rapakivi texture, metasomatic replacement, has little to commend it and, like the other theories, fails to explain why only some of the potassium feldspar exhibits plagioclase rims. It would be a remarkable feat for a hydrothermal solution to deposit a plagioclase rim around an alkali feldspar grain, leaving a similar grain a few hundredths of a millimeter away without any suggestion of a mantle. Other hypotheses for the origin of rapakivi texture have been proposed, but to our knowledge no theory has been advanced which adequately

accounts for the presence of alkali feldspar grains with rims of plagioclase side by side with unmantled grains.

The four most characteristic features of wiborgite rapakivi are (1) oval shape of the alkali feldspars, (2) large size of the alkali feldspars, (3) mantles of oligoclase on some of the alkali feldspars, and (4) the ubiquitous occurrence of two generations of quartz and alkali feldspar. Any theory explaining these features must also account for the coexistence of alkali feldspar "phenocrysts" with and without mantles of oligoclase.

#### ORIGIN OF OVOID ALKALI FELDSPARS

Many petrologists have attributed the lack of crystal faces on the ovoidal feldspar to resorption, apparently because such a rounding of crystals takes place when crystals are dissolved. Sederholm (1928, p. 91) noted that alternating oligoclase-alkali feldspar rims are regular and without embayments such as resorption would cause. This observation led Sederholm to suggest that high viscosity, and not resorption, was responsible for the lack of crystal faces. Crystals without faces have been observed in numerous silicate systems and are particularly common in metals where the liquid and crystals have very similar physical properties. Buerger (1947, p. 601) discusses this problem as follows:

"Crystals without faces would be anomalous to some crystallographers, yet they are not only possible but normal under certain circumstances. From the last section it is evident that the stability of a face is the function of surface energy. Furthermore, the very existence of crystal faces depends on surface energy. Therefore, if a crystal is grown in a medium whose surface tension is equal to its own, no faces can develop. . . . The condition is nearly realized when a close packed crystal forms from a melt of pure metal. In this case the melt is nearly close packed, and the forces on an atom at a metal-melt interface are nearly alike on both sides, thus causing the interfacial tension to nearly vanish."

#### LARGE SIZE OF THE ALKALI FELDSPAR

There is a consensus among those who have studied rapakivi granite that alkali feldspar crystallized early in these rocks. This view is supported by our equilibrium studies. Figure 46 illustrates the relation of the normative amount of quartz, albite, and orthoclase in rapakivi granites as compared with the average or normal granite as shown by the outline of the maxima for all granites. The 37 analyses compiled by Sahama (1945) were selected as typical of rapakivi granites. The rapakivi granites are richer in potassium feldspar than is the average granite. This places the composition of the rapakivi granites in the alkali-feldspar field. If the composition of the average Fennoscandian rapakivi granite is compared with the 500 kg/cm<sup>2</sup> isobar (Fig. 22), for the synthetic granites it will be seen that a potassium feldspar is expected to crystallize early, and the amount of albite in solid solution in the alkali feldspar will be about 25-30 per cent.

Inasmuch as alkali feldspar is the first mineral to crystallize it is expected that, given adequate time, large phenocrysts will form. Now if we assume that the amount of water present is approximately 3 per cent, the field boundary will then be very near that shown for the 500 kg/cm<sup>2</sup> isobar; if the amount is less than this, as it probably is, the boundary will be somewhat nearer the quartz apex. Given these conditions approximately 15 per cent of the liquid will crystallize to alkali feldspar

before the quartz field is reached; if the amount of water is less than this more feldspar will crystallize before the quartz boundary is reached. This amount of alkali feldspar crystallizing early provides an opportunity for large phenocrysts to grow before the quartz or plagioclase fields are reached.

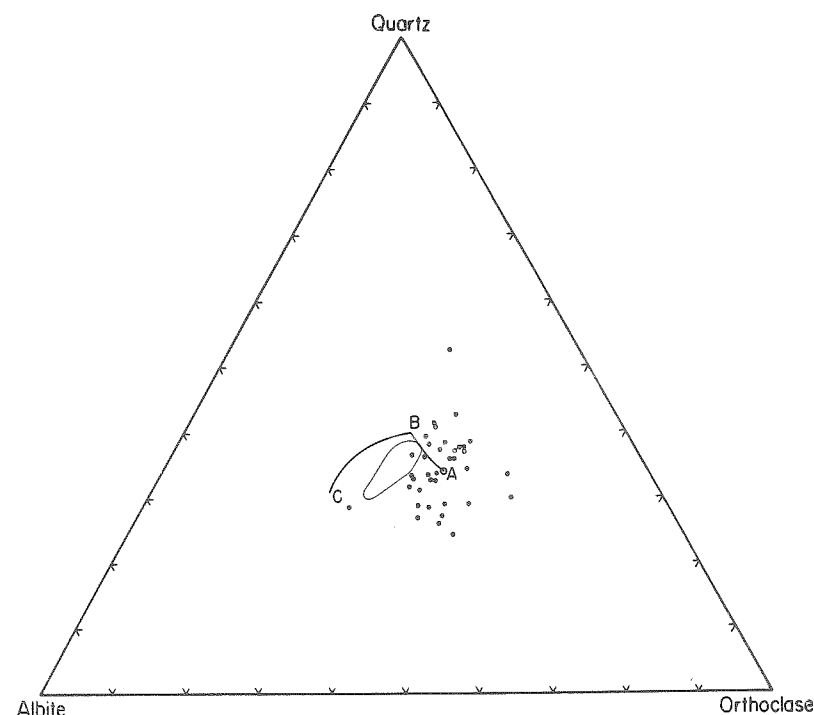


FIGURE 46.—Distribution of normative Ab-Or-Q in rapakivi granites

The circle at A represents the "average" rapakivi as computed by Sahama (1945).

#### ORIGIN OF MANTLED FELDSPAR

The explanation of the origin of the mantles must also indicate how unmantled feldspars can exist in the immediate vicinity of the mantled crystals. The coexistence of these two types of alkali feldspar has not gone unnoticed; Sederholm (1928, p. 92) described them in some detail and reported that the alkali feldspars without the mantles are commonly euhedral and that both types occur side by side. He also noted that the oligoclase mantles may have exterior crystal faces and anhedral development toward the alkali-feldspar core.

These relationships may be explained by considering crystallization of liquid having the composition of the normative quartz + albite + orthoclase of the average for the Fennoscandian rapakivi granites. Considering a liquid whose composition is represented by A, containing 2 per cent water (Fig. 46), the first crystals to separate will be potassium-rich feldspar. If equilibrium is maintained as crystallization proceeds, the liquid will move along AB, and the feldspar will become progressively

richer in the albite molecule. At B quartz will begin to crystallize, the liquid will contain approximately 15 per cent feldspar phenocrysts whose composition will be approximately  $Ab_{25}Or_{75}$ , and the water content, assuming there has been no escape of water vapor, will now be about 2.4 per cent. Initial crystallization will have begun at a temperature slightly above  $800^{\circ}C$ ., and when the quartz field is reached the temperature will have fallen about  $30^{\circ}C$ . With further crystallization of quartz and feldspar the liquid will move along BC as the quartz-alkali feldspar field boundary moves toward the Ab-Or sideline with increasing water content of the liquid (and increasing pressure). If the overburden withstands the pressure being generated by crystallization and concomitant increase in water content, the liquid will reach point C when the temperature has fallen to  $660^{\circ}C$ . At this temperature 78 per cent of the original liquid will have crystallized to quartz and alkali feldspar. The remaining 22 per cent of liquid will contain 10 per cent water, and the vapor pressure will be nearly  $4000 \text{ kg/cm}^2$ . At this temperature the top of the solvus in the binary system Ab-Or will be intersected, and the two feldspars will crystallize together with quartz; the isobaric "ternary" minimum now becomes an isobaric "ternary" eutectic. At all lower temperatures two feldspars and quartz will crystallize simultaneously. At first the two feldspars will have nearly identical compositions, but as the temperature is lowered one will become richer in potassium, and the other richer in sodium. Now, if this were an abrupt change such as occurs when a liquid reaches the stability field of a new phase, it would be expected that plagioclase would precipitate as new centers of crystallization forming small plagioclase crystals along side the large alkali feldspar phenocrysts. However, as the change is not abrupt it is expected that the already present alkali feldspar will zone in such a way that the two feldspars will both be accommodated by the zoning. In other words, some of the alkali phenocrysts will zone toward oligoclase, and others toward orthoclase. This, then, is the typical rapakivi texture.

The above relations are for a hypothetical magma consisting of quartz, albite, and orthoclase. The actual temperatures and pressures will, of course, be somewhat different in a magma containing other constituents, but the principles involved and the general trend of crystallization will differ only slightly. The melting relations of the Quincy and Westerly granites indicate that the difference will indeed be small. The presence of lime will raise the temperature at which the two feldspars begin to crystallize, and, if the top of the solvus is flattened by the addition of lime, the two feldspars will diverge in composition rapidly with a slight drop in temperature. The average rapakivi granites contain 1.59 per cent lime, and 10 of the 37 analyses have less than 1 per cent lime indicating the equilibrium relations will be little different in many of the rapakivi granites from those determined experimentally in the  $NaAlSi_3O_8-KAlSi_3O_8-SiO_2-H_2O$  system.

#### ORIGIN OF THE TWO GENERATIONS OF QUARTZ AND FELDSPAR IN RAPA KIVI GRANITES

The build-up of the vapor pressure of a crystallizing hydrous granite will eventually result in pressure greater than that which the overburden can withstand, and

<sup>4</sup> The points A, B, and C are actually quaternary but for the purpose of illustration may be considered a projection onto the Ab-Or-Q plane.

the pressure will be released by escape of the water vapor. If the release of pressure is rapid because of fracturing of the roof, crystallization will proceed rapidly, and it is not unreasonable to expect that many new centers of crystallization will be set up, resulting in a "second generation" of quartz and feldspar. The texture seen in some rapakivi granites suggests rapid crystallization and may be the result of a relatively sudden escape of water vapor.

#### DISCUSSION

The question now arises: Why are mantled alkali feldspars not found in granites having an Ab-Or-Q ratio falling at the maximum for all granites? The answer would seem to be that these granites are richer in sodium feldspar, and these compositions may crystallize a plagioclase early in their crystallization history. Sederholm noted (1928, p. 95): "In granites where oligoclase has been the first to crystallize, we never observe any ovoidal feldspars". If the water content of a granite liquid is extremely low or if the depth of burial at the time of crystallization is too shallow to permit the water pressure to build up to where the solvus is intersected, mantling of the feldspar cannot occur by the process outlined above even though the composition is appropriate.

#### TERTIARY GRANITES OF SKYE

##### GENERAL DISCUSSION

In an earlier publication (Tuttle, 1952) it was suggested that the quartz and feldspars of salic plutonic rocks may have undergone considerable recrystallization during initial cooling. Evidence from inversion studies, from inclusions, and from petrofabric studies indicates that the quartz of plutonic rocks is different from the quartz phenocrysts of extrusive rocks, and the differences can be attributed to recrystallization. Similarly the plagioclase feldspars of extrusive rocks show significant differences from the plagioclase feldspars of the plutonic rocks. Alkali feldspars are so strikingly different in the two rock types that one may conclude that they are very sensitive indicators of the changing stability relations in a cooling granite. It was suggested that a study of unmetamorphosed chilled contacts of granites might provide information on the intermediate stages of the change from high- to low-temperature assemblages.

The potassium feldspar of many granites is microcline. For example, Chayes (1952, p. 212) reported as follows on the potassium feldspar of New England granites:

"Potash feldspar seems to be mostly, and is perhaps entirely microcline. Grains devoid of optical complexity occur in almost every thin section but are, on the whole, uncommon. Usually a wavy or indistinct grid can be made out under crossed nicols and often—in some rocks, almost invariably—the familiar microcline grill is clear and sharp."

Many authors have reported microcline and orthoclase coexisting in granites, apparently on the basis of the presence or absence of polysynthetic twinning; in fact, some have reported Rosiwal analyses in which the orthoclase and microcline were differentiated. This criterion for distinguishing the two types is not reliable as untwinned microcline is common, and if some of the grains show a microcline grill probably all the potassium feldspar is microcline.

In contrast, the potassium feldspars of the extrusive salic rocks are usually identified as sanidine or anorthoclase. A study of the compositional variations in these feldspars (Tuttle, 1952) indicated that the potassium feldspars of rhyolites are usually richer in sodium than are the microcline and orthoclase of the granites.

Equilibrium studies in the system  $\text{NaAlSi}_3\text{O}_8\text{--KAlSi}_3\text{O}_8\text{--H}_2\text{O}$  (Bowen and Tuttle, 1950) provide quantitative information on the stability relations of these alkali

TABLE 16.—*Normative and modal composition of the Westerly granite*

	Norm	Mode
Quartz	28.6	27.5
Orthoclase	32.5	35.4
Plagioclase	33.7	31.4

feldspars and show that a single feldspar is stable at high temperature, but at lower temperatures this single phase breaks up into two phases, albite and potassium-rich feldspar. This breakup of the single phase takes place in the laboratory in a few days in the presence of water vapor under pressure and provides quantitative information on the process of unmixing, a process long recognized as the mechanism by which many perthites have formed. It is not surprising then that homogeneous sanidine and anorthoclase are rare in the plutonic rocks, where prolonged cooling through the temperature range, which demands unmixing, has taken place. This unmixing process is well illustrated in the granites which consist essentially of perthite and quartz. Here there is little reason to doubt that the perthite was originally homogeneous sanidine or anorthoclase which has unmixed to an intergrowth of orthoclase (or microcline) and albite. In addition to unmixing, the feldspars have changed to low-temperature modifications, the potassium feldspar from sanidine to orthoclase or microcline, and the sodium feldspar from high albite to low albite. At the same time the quartz has suffered a change in inversion properties which is probably due to recrystallization.

These "one"-feldspar granites may have chemical compositions very similar and perhaps identical with the common two-feldspar granites which contain microcline and plagioclase in approximately equal amounts. It was suggested that the presence of two feldspars may be due to unmixing beyond the perthite stage, as the possibility of relatively pure microcline and albite crystallizing from a granitic magma is not in accord with the experimental facts. Earlier studies appear to demand that some of the plagioclase, and perhaps most of it, must have been in solid solution in the potassium feldspar if these two-feldspar granites have a magmatic history.

The Westerly, Rhode Island, granite is a prime example of a two-feldspar granite and illustrates the necessity of unmixing at least a portion of the plagioclase from the potassium feldspar. The average norm and mode of the Westerly granite is listed in Table 16 (after Chayes, 1952, p. 229). Approximately 93 per cent of the normative plagioclase is present as plagioclase in the mode, leaving less than 7 per cent as a component of the orthoclase. Crystallization of these two minerals side by



TABLE 17.—*Specimen localities*(For a description of the granites of Skye, see Wager *et al.* (1948))

F2-129	Granite G-1	Collected 150 feet from contact with marscoite on west side of Glamaig (Marscoite is believed to be later)
F2-130	Granite G-1	Collected 3 feet from F2-129
F2-131	Granite G-1	150 feet from F2-130 (300 feet from contact)
F2-133	Granite G-1	Contact with gabbro on west side of Glamaig
F2-134		Dike offshoot from Granite G-1 in gabbro
F2-135	Granite G-1	10 inches from contact and F2-133
F2-136	Granite G-1	30 inches from contact and F2-133
F2-138	Granite G-1	10 feet from contact and F2-133
F2-139	Granite G-1	80 feet from contact and F2-133
F2-140	Granite G-1	Contact specimen at lower granite-gabbro contact on south side of Glamaig
F2-141	Granite G-1	5 feet from contact and F2-140
F2-142	Granite G-1	10 feet from contact and F2-140
F2-152		Riebeckite granophyre collected 1000 feet east of the summit of Meall Dearg
F2-153		Perthite-quartz granite dike in Torridonian sandstone (specimen at contact) collected in Broadford road 5 miles east of Sligachan Inn
F2-154		Perthite-quartz granite dike (locality same as F2-153) collected 1 foot from contact
F2-155		Contact specimen, perthite-quartz granite, Torridonian sandstone
F2-156		Perthite-quartz granite collected 150 feet from contact
F2-157		Perthite-quartz granite collected in road cut (locality near F2-153)

The following specimens are from the Beinn an Dubhaich granite.  
Specimen localities are shown in Figure 47.

F2-159	Small dike in limestone
F2-160	Contact specimen, thin section cut 1 inch from contact
F2-161	6 inches from contact and F2-160
F2-162	2 feet from contact and F2-160
F2-163	6 feet from contact and F2-160
F2-164	30 feet from contact and F2-160
F2-165	Contact specimen, thin section 2 inches from contact
F2-166	1 foot from contact and F2-165
F2-167	6 feet from contact and F2-165
F2-177	Contact specimen thin section cut 1 inch from contact
F2-178	6 inches from contact and F2-177
F2-179	1 foot from contact and F2-177
F2-180	6 feet from contact and F2-177
F2-181	30 feet from contact and F2-177
F2-182	1000 feet from contact and F2-177
F2-183	1500 feet from contact
F2-184	18-inch dike in limestone
F2-185	Contact between diabase and granite (granite later)
F2-186	1 foot from contact and F2-185
F2-187	2 feet from contact and F2-185
F2-188	10 feet from contact and F2-185
F2-189	20 feet from contact and F2-185
F2-191	Center of 20-foot lens in limestone

TABLE 17.—*Continued*

F2-192	Small vein of granite in diabase
F2-193	Center of the Beinn an Dubhaich pluton
F2-227	Cambridge University No. S.38 ( <i>see</i> Tilley, 1951, Analysis No. 4, p. 661)
F2-228	Cambridge University No. KCI.11 ( <i>see</i> Tilley, 1951, Analysis No. 1, p. 661)
F2-229	Cambridge University No. 28520 Dun Beag, Loch Slapin
F2-232	Cambridge University No. G.S. 55 ( <i>see</i> Tilley, 1951, Analysis No. 2, p. 661)
F2-233	Cambridge University No. C.M. 70 ( <i>see</i> Tilley, 1951, Analysis No. 3, p. 661)
F2-234	Analyzed granite G-1 (*No. H-857)
F2-235	Analyzed granite G-2 (*No. H-932)
F2-236	Analyzed granite G-4 (*No. H-817)
F2-237	Analyzed perthite-quartz granite (G) from same road cut as F2-157 (*No. H-984)
F2-238	Analyzed granite (Harker, 1904, p. 153, No. 1)
F2-239	Analyzed granite (Harker, 1904, p. 153, No. 2)

\* These numbers refer to unpublished analyses of Skye granites kindly made available by Prof. L. R. Wager of Oxford University.

side from a granite magma would require a temperature far below that at which this rock begins to melt in the laboratory with 4000 bars water-vapor pressure. Either this granite is a metamorphic rock, or a considerable amount of the plagioclase has unmixed from the potassium feldspar after crystallization. The Westerly granite occurs in an area of schistose and gneissic metamorphic rocks, and more than likely it has been metamorphosed; this would promote unmixing of the feldspars. Chayes (1952) has presented evidence that the mineralogical homogeneity of this granite demands a magmatic history.

If the perthite-quartz and the two-feldspar granites are magmatic, it should be possible to find young unmetamorphosed granites intermediate between these extreme types—that is, granites that contain potassium feldspar and plagioclase feldspar, but in which the potassium feldspar carried more plagioclase in solid solution than did the potassium feldspar of Westerly granite. Also, if chilled contacts of the one-feldspar granites can be found, the phase changes that have taken place in these rocks (*i.e.*, sanidine to orthoclase or microcline, and high to low plagioclase) should be arrested at intermediate states recognizable as such.

A collection of specimens from granite contacts has been made with these problems in mind. At the suggestion of Prof. C. E. Tilley of Cambridge University, some of the Tertiary granites of Skye, Scotland, were collected. The following is a report on studies of these young granites. The location of the specimens is illustrated in Figure 47 and described in Table 17.

## MINERALOGY

QUARTZ: Keith and Tuttle (1952) have shown that the temperature of the high-low inversion of quartz varies with the geological history of the quartz. One of the most interesting features of these studies was the discovery that the inversion temperature of quartz from rhyolites differs from the inversion temperature of quartz from granites. The differences can be best illustrated on a graph of the beginning of inversion on heating versus the beginning on cooling through the inversion (Fig. 48).

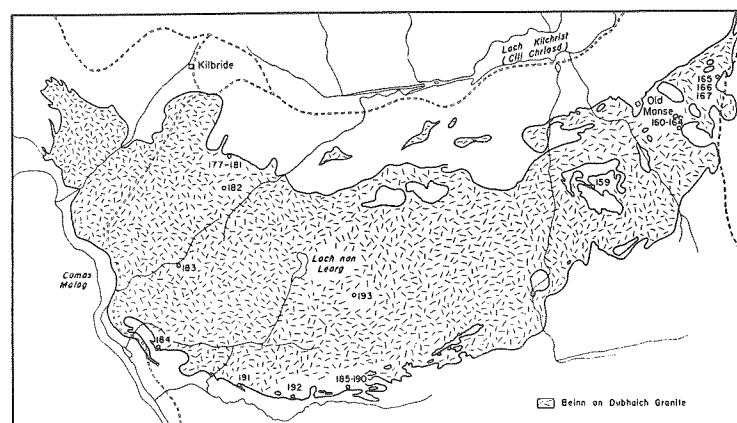


FIGURE 47.—Index showing the location of specimens from the Beinn an Dubhaich granite  
Map after C. E. Tilley (1951)

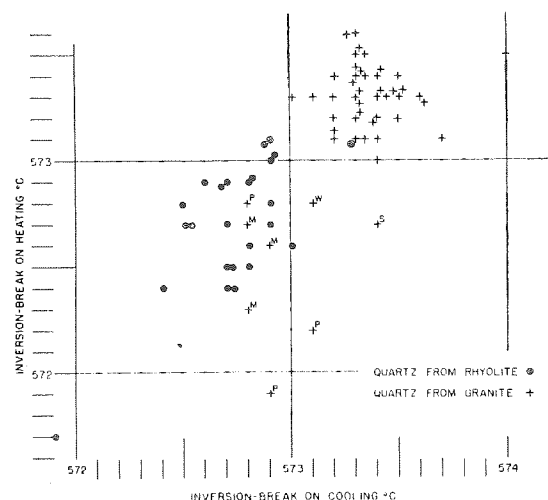


FIGURE 48.—Inversion of quartz from granites and rhyolites

The higher temperature of inversion of most granitic quartz studied is believed to indicate that the quartz recrystallized at relatively low temperatures. M = granites from three localities in Maine: North Sullivan, Jonesport, and Wallace Cove. P = Pikes Peak granite. W = granite from Westwood, Massachusetts. S = White Silver Plume granite, Colorado. (After Keith and Tuttle, 1952, p. 231)

A plot of inversion temperatures of quartz from most granites places them in an area on this graph in which quartz from rhyolites is absent. The inversion temperatures of quartz from cavities in limestone and quartz veins, where the geological environment indicates a low temperature of crystallization, fall in the general area of the quartz from granites. In contrast, quartz from rhyolites has a somewhat lower inversion temperature. These differences were attributed to recrystallization

of the quartz from granite, perhaps during the final stages of crystallization when the residual fluids become potent fluxes by virtue of their increased volatile content.

A study of the inversion characteristics of quartz from the Beinn an Dubhaich granite (Tuttle and Keith, 1954) revealed that the quartz from this granite was

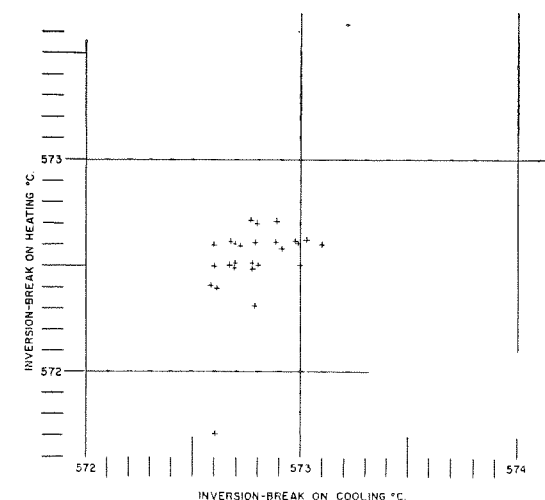


FIGURE 49.—Inversion temperatures of quartz from the Beinn an Dubhaich granite

Compare with Figure 48. (After Tuttle and Keith, 1954, p. 67). Note that the inversions fall in the area of rhyolite quartz of Figure 48. It is believed that this quartz has not recrystallized as has the quartz of most granites.

similar to rhyolitic quartz in inversion properties (Fig. 49). Not one of the quartz specimens from the Beinn an Dubhaich granite falls in the principal area of granites previously investigated. These results are attributed to the lack of recrystallization of the quartz from the Beinn an Dubhaich granite. The granites previously studied are older (Paleozoic and Precambrian), and many—perhaps all—were metamorphosed to some extent.

**ALKALI FELDSPARS:** Optically the alkali feldspars from the Beinn an Dubhaich range from a rather coarse perthite to orthoclase cryptoperthite to sanidine cryptoperthite (Tuttle, 1952), and in some specimens a considerable portion of the alkali feldspar is optically homogeneous. The homogeneous material ranges in optical properties from orthoclase to sanidine. X-ray studies of the optically homogeneous material revealed that it is a suboptical intergrowth of a nearly pure potassium and sodium feldspar and may be called an X-ray perthite (Tuttle, 1952).

This gradation from a rather coarse perthite to optically homogeneous material may be found within a single grain. At first glance the cores of the alkali feldspar grains seemed to be optically homogeneous with a gradation to micropertthite at the border. Detailed study revealed, however, that many grains are homogeneous at the border as well as in the core. The outer border tends to be perthitic, but in many specimens the border on one side of a grain is perthitic, whereas the homogeneous

core extends to the opposite border. These grain-boundary relations might be very useful in interpreting the history of these complex crystals, if the grains could be observed in three dimensions.

The coarse perthitic portions of some of the grains, when properly oriented, are

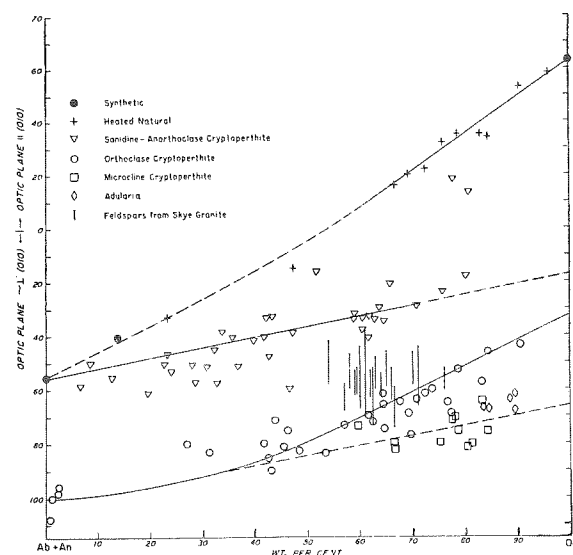


FIGURE 50.—Graph showing the relation between optic axial angles and composition of alkali feldspars

Vertical lines illustrate the range in  $2V\alpha$  of 23 alkali feldspars from the Beinn an Dubhaich granite. (After Tuttle, 1952). All the alkali feldspars are cryptoperthitic, and the gradational optics are a reflection of the variable amounts of the various modifications of sodium- and potassium-rich phases present. The gradation, then, is not due to gradual structural changes but to abrupt structural changes in the unmixed phases which are partially inverted (*i.e.*, high and low albite, but not intermediate albites).

intricately twinned; and, when the section is parallel or nearly parallel to the planar direction of the perthite lamellae, the perthite has a patchy appearance with fairly large irregular areas of sodium feldspar set in potassium feldspar.

The optic axial angle of alkali feldspars distinguishes high-temperature modifications from low-temperature forms (Tuttle, 1952) if the chemical composition is known. On the basis of optic axial angle and position of the optic plane, the alkali feldspars may conveniently be divided into four series: high sanidine-high albite, low sanidine-high albite, orthoclase-low albite, and microcline-low albite. Previous studies indicated that all gradations between the first two and last two series could be expected. The present study suggests that all gradations between the high sanidine-high albite and microcline-low albite series exist, and the optic axial angle will serve to place an alkali feldspar in or intermediate between these series. The high sanidine-high albite and low sanidine-high albite series are high-temperature modifications since they are found in volcanic and other high-tempera-

ture rocks. The other two series are representative of low-temperature rocks as they do not occur in the volcanic rocks and they can be changed to the high-temperature series by heating (Spencer, 1937).

Optic axial angle measurements on the alkali feldspars from the Skye granites

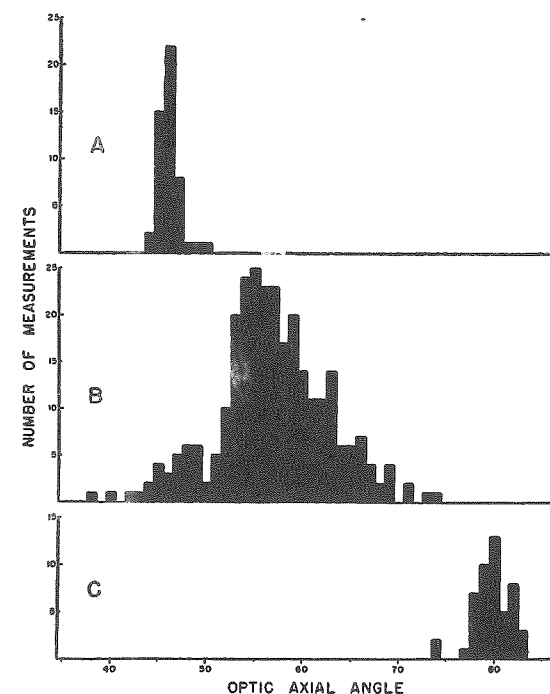


FIGURE 51.—Histograms showing the range in  $2V\alpha$  of alkali feldspars from (A) Obsidian, Mono Lake, California, (B) Beinn an Dubhaich granite, and (C) Westerly, Rhode Island granite

This illustrates that the feldspars of the Beinn an Dubhaich granite are transitional between those of the rhyolites and the microcline granites.

are shown in Figure 50. In all cases (except F2-229 in which 50 grains were measured) 10 grains from each specimen were measured. Most of the measurements are reproducible to within  $\pm 1^\circ$ ; a few are less accurate because of incipient alteration which results in poor resolution of the isogyres. All measurements were made on the universal stage using the interference-figure method. The conoscopic method permits more accurate results and is far less tedious than extinction methods. It is surprising that this method is not more widely used in conjunction with the universal stage. Excellent interference figures can be obtained on feldspar grains 0.10 mm in diameter, and grains as small as 0.04 mm yield satisfactory figures.

Variations in the optic axial angle from grain to grain in the same hand specimen (Fig. 51B) are probably a result of partial inversion from sanidine to orthoclase cryptoperthite (or X-ray perthite). A portion of the range in  $2V$  may result from

zoning, but measurements of index of refraction on grains with low and high  $2V$  from the same sample indicate only small compositional variations. The transitional nature of the feldspars from the Beinn an Dubhaich granite is further illustrated by optic axial angle measurements on the alkali feldspar from a rhyolite (A) and from

TABLE 18.—Orthoclase content of alkali feldspars from the Beinn An Dubhaich granite  
(Determined by the  $\bar{2}01$  spacing)

Specimen No.	Or Content
F2-159	71
F2-160	60
F2-161	76
F2-162	62
F2-163	61
F2-164	61
F2-166	66
F2-167	58
F2-178	66
F2-179	64
F2-180	66
F2-181	58
F2-182	65
F2-183	59
F2-184	63
F2-185	61
F2-186	61
F2-187	61
F2-188	59
F2-189	62
F2-191	60
F2-192	57
F2-193	70
F2-229	55

a two-feldspar granite (C), containing microcline (Fig. 51). The relatively rapid cooling of the rhyolite has prevented partial inversion, and the values of  $2V$  fall within a very narrow range; 90 per cent of the measurements gave  $2V = 46^\circ \pm 1^\circ$ . Similar measurements on microcline also fall within a fairly narrow range; 88 per cent of these results gave  $2V = 80^\circ \pm 2^\circ$ . As microcline is the low-temperature modification it is to be expected that the optic axial angle would be uniform if inversion is complete. However, the value for the optic axial angle of microcline which has reached equilibrium, structurally and chemically, at  $300^\circ\text{C}$ ., for example, is not necessarily the same as for microcline which has reached equilibrium at  $100^\circ\text{C}$ ., although the difference should not be great. It is therefore not to be expected that microcline will show the same uniformity as the alkali feldspars from the quenched rhyolites. Results of optic axial angle measurements on specimens whose compositions have been determined by use of the  $\bar{2}01$  spacing (Table 18) are shown in Figure 50. They fall in the interval between the sanidine and orthoclase cryptoperthite

series. This supports the contention that the range in  $2V$  is a result of partial inversion. Such transitional optics are to be expected in materials renowned for their sluggish transitions.

Single-crystal X-ray studies of these feldspars support the conclusions reached from the optical studies. We are indebted to Drs. W. S. MacKenzie and W. H. Taylor of Cambridge University for the following single-crystal X-ray data. Single-crystal oscillation photographs of an alkali feldspar crystal ( $2V = 53^\circ$ ) from specimen F2-229 show a sodium-feldspar phase twinned after the albite and pericline laws and a monoclinic potassium-feldspar phase. Measurements of the reciprocal-lattice angles of the sodium feldspar reveal that the albite-twinned part represents low albite and the pericline-twinned part represents high albite. Further confirmation of this was obtained by heating for a short period at  $700^\circ\text{C}$ . At this temperature high-albite-sanidine cryptoperthite will homogenize readily (Bowen and Tuttle, 1950), but low-albite-orthoclase cryptoperthites resist homogenization (Tuttle, 1951). The pericline twinning of high albite disappeared leaving only the low albite and a monoclinic potassium-rich phase.

Furthermore, the relative amounts of high- and low-albite as estimated from the intensities of the X-ray reflections are directly related to the optic axial angle ( $2V$ ). Four alkali feldspar grains were selected from specimen F2-229 with  $2V = 45^\circ, 49^\circ, 54^\circ$ , and  $58^\circ$ , and single-crystal oscillation photographs were taken about the b axis with the X-ray beam parallel to (001) in the center of the oscillation. High-temperature albite predominates in the crystal with  $2V = 45^\circ$ , whereas the crystal having  $2V = 58^\circ$  shows largely low-temperature albite. Optically, the grain with  $2V = 45^\circ$  is very near the curve for sanidine-high albite, whereas that with  $2V = 58^\circ$  is about midway between the orthoclase-low-albite and sanidine-high-albite series. This confirms the optical studies and emphasizes the usefulness of the optic axial angle as an indicator of the type of feldspar. The potassium phase shows slight differences in the four crystals; it is monoclinic in the  $2V = 45^\circ$  grain, whereas it may be triclinic in the crystal having  $2V = 58^\circ$ .

**PLAGIOCLASE FELDSPARS:** The plagioclase feldspar from the Beinn an Dubhaich granite appears at first glance to be normal sodium-calcium feldspar. However, the optic axial angle is abnormally low, and X-ray studies indicate that it too is a high-temperature modification. As with the alkali feldspar, there is probably a gradation from high oligoclase to "normal" oligoclase.

In thin section the plagioclase is very fresh and free of clouding in some specimens; in others some type of incipient alteration has clouded the grains with minute crystals of an unknown phase. Some of the clear fresh grains have a peculiar texture, as though the crystals have been fractured, perhaps by contraction; the fractures are filled by a low-refractive-index material and a platy high-birefringent phase. All grains of plagioclase are profusely twinned polysynthetically. Compositional zoning is common.

High-temperature modifications of sodium-rich plagioclase feldspar can be distinguished from the low-temperature polymorphs by the optic axial angle and by X-ray methods if the composition is known. Results of  $2V$  measurements are shown in Figure 52. Compositions were determined by refractive-index measurements using



the determinative curves prepared by Chayes (1950). Optic axial angles of the Skye plagioclase are certainly abnormal; many of the values are too low for "normal" plagioclase of any composition. Optic axial angles of plagioclase from the Skye granite fall between the curve for the high-temperature series and that of the low-

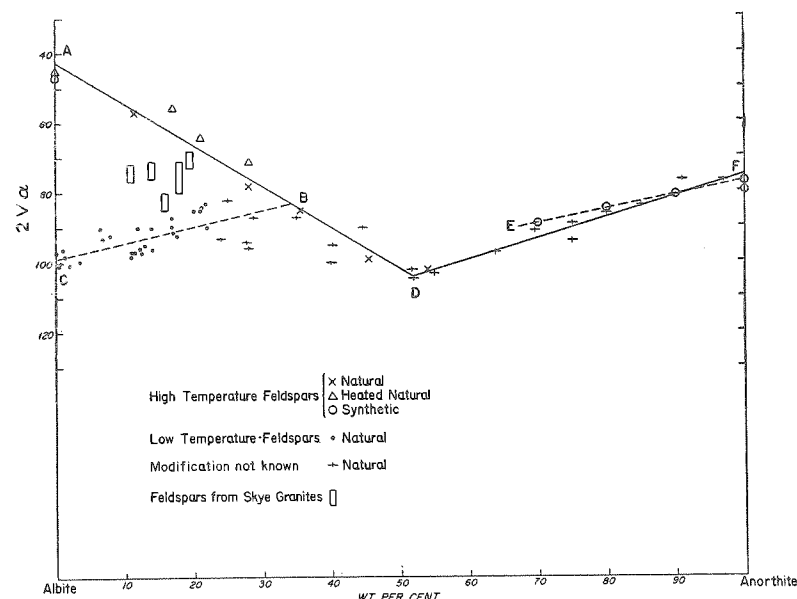


FIGURE 52.—Graph showing the relation between  $2V\alpha$  and composition in some plagioclase feldspars

(After Tuttle and Bowen, 1950). The plagioclase feldspar from the Beinn an Dubhaich granite falls between the high- and low-temperature series. It is believed that this represents partial inversion, but the exact nature of the change awaits single crystal X-ray studies. It is possible that the potassium content of these plagioclase feldspars is abnormally high and that this is the cause of the unusual optics.

temperature series. Results of 104 measurements of  $2V\alpha$  of plagioclase from the Beinn an Dubhaich granite are shown in Figure 53.

Optic axial angle measurements on analyzed low-temperature sodic plagioclase indicate that a  $2V\alpha$  of less than  $80^\circ$  is "abnormal" (Fig. 53). Heating the low-temperature crystals decreases the optic axial angles, and, as phenocrysts from lavas also give values less than  $80^\circ$ , it can be assumed that those specimens with  $2V\alpha = 40^\circ$ – $75^\circ$  belong to the high-temperature series or are between the high and low series. The optic axial angle ( $2V\alpha$ ) of high albite is decreased by the presence of potassium feldspar in solid solution, and perhaps potassium has a similar effect on low-temperature sodic plagioclase; if so some proportion of the "abnormal" plagioclase may carry orthoclase in solid solution as a contributing cause of the low  $2V\alpha$ . (As potassium in appreciable amounts is rare—or unknown—in low-temperature plagioclase it is probable that if potassium is present in the abnormal feldspars it is as unmixed perthitic intergrowths.)

High- and low-temperature sodic plagioclase can also be distinguished by X-ray methods. The angular difference between  $2\theta$  (131) and  $2\theta$  ( $1\bar{3}1$ ) reflections is particularly suitable for this purpose as the difference is  $1.06^\circ$  for low-temperature albite and  $2.03^\circ$  in high-temperature albite. When these spacing differences are

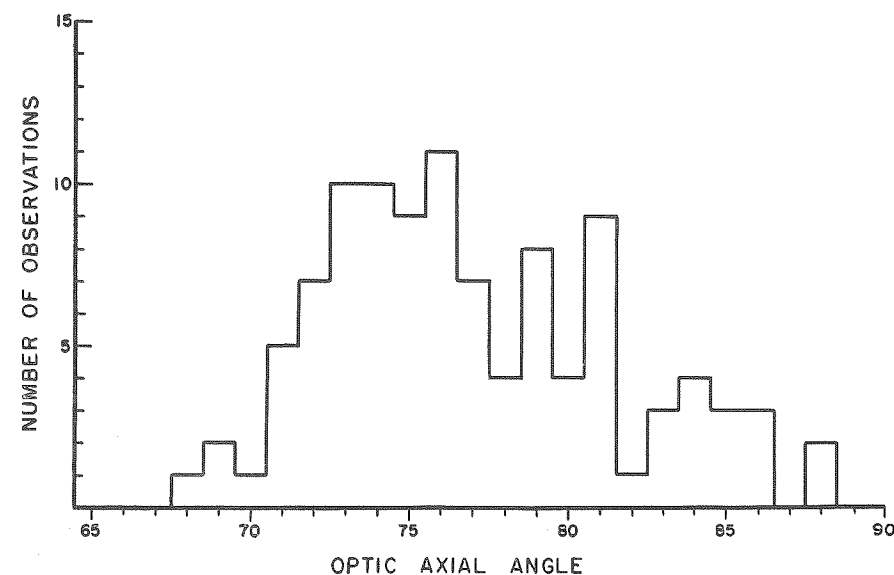


FIGURE 53.—Histogram illustrating the distribution of  $2V\alpha$  in plagioclase of the Beinn an Dubhaich granite

plotted against anorthite content, high- and low-temperature modifications appear as two curves (Fig. 54) which approach each other as the anorthite content increases. Values of  $2\theta$  ( $1\bar{3}1$ )– $2\theta$  (131) for plagioclase of the Skye granite are shown as solid bars in Figure 54. These results confirm the optical data and suggest that the plagioclase is high-temperature oligoclase partially transformed toward low-temperature oligoclase.

**OTHER MINERALS:** Biotite is perhaps the most abundant dark mineral in most specimens, although in numerous specimens amphibole exceeds mica. Certain contact facies carry an alkali pyroxene (Tilley, 1949). These minerals are represented by fine-grained alteration products in several specimens. No special study was made of these minerals although it is believed that much useful information will be forthcoming when such a study is undertaken, particularly when contrasted with the same minerals in two-feldspar granites.

#### MODAL ANALYSES OF SKYE GRANITES

Modal analyses were made on 44 specimens of Skye granites, using the Chayes point counter (Chayes, 1949; 1951). Each analysis was made by traversing thin sections and identifying the mineral at the intersection of the crosshair at 0.3-mm

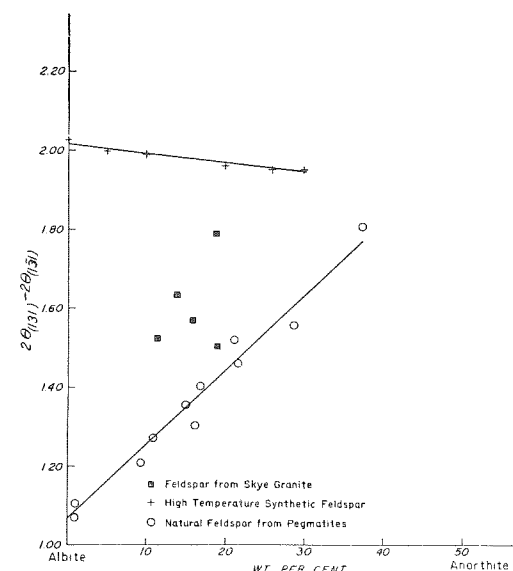


FIGURE 54.—Graph showing the relation between the  $2\theta_{(131)}-2\theta_{(\bar{1}31)}$  X-ray reflection and composition

The plagioclase from the Skye granites falls intermediate between the high- and low-temperature series.

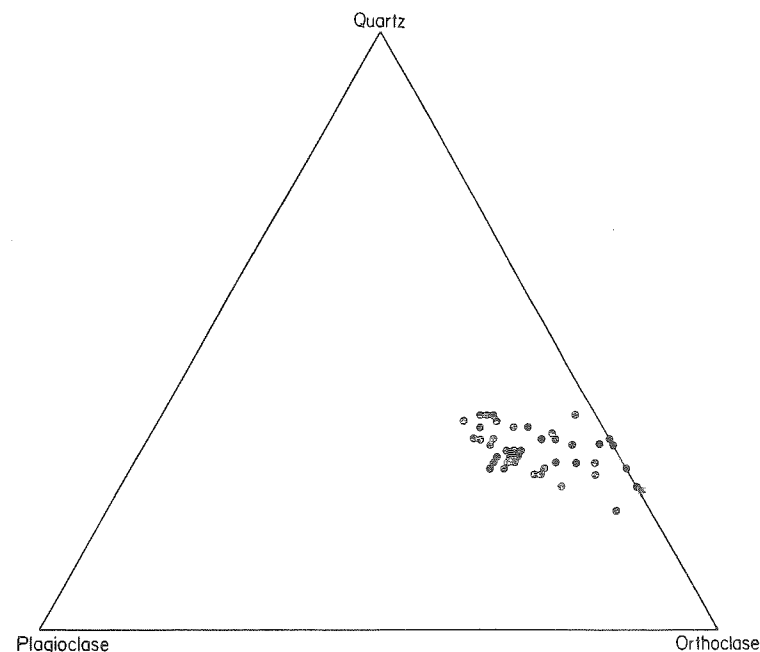


FIGURE 55.—Modal plagioclase, orthoclase, and quartz in Skye granites

This is to be compared with Figure 56 which shows the distribution of these constituents in granites from eastern United States. (After Chayes, 1951).

TABLE 19.—Modal analyses of Skye granites

Specimen no.	Q	Or	Pl	Others
F2-129	25.6	56.7	11.3	6.4
F2-130	23.9	56.6	12.3	7.2
F2-131	24.8	56.2	12.8	6.2
F2-133	30.6	44.7	19.2	5.5
F2-135	25.2	48.9	18.7	7.2
F2-136	26.9	51.6	15.5	6.0
F2-138	27.7	52.8	13.0	6.5
F2-139	26.0	51.4	16.1	6.5
F2-140	26.4	50.3	17.6	5.7
F2-141	27.0	50.0	16.6	6.4
F2-142	24.0	48.6	16.3	11.1
F2-143	29.9	52.7	15.6	1.8
F2-152	21.9	38.5	34.1	5.5
F2-153	30.3	60.9	6.4	2.4
F2-154	31.1	66.8	0.0	2.1
F2-155	35.3	59.2	2.8	2.7
F2-156	27.4	69.8	0.0	2.8
F2-157	32.9	63.9	0.0	3.2
F2-159	26.3	70.2	0.0	3.5
F2-160	26.6	52.2	16.2	5.0
F2-161	28.6	53.4	15.0	3.0
F2-162	30.0	49.2	17.6	3.2
F2-163	33.7	47.4	14.4	4.5
F2-164	34.6	46.7	15.7	3.0
F2-165	30.8	65.9	0.0	3.3
F2-166	22.6	71.6	0.3	5.5
F2-167	33.3	51.6	12.2	2.9
F2-177	30.4	64.9	2.1	2.6
F2-178	18.8	69.0	5.2	7.0
F2-179	22.4	61.4	10.9	5.3
F2-180	24.4	64.9	4.3	6.4
F2-183	34.7	44.5	15.8	5.0
F2-184	28.9	53.9	14.9	2.3
F2-185	33.2	53.5	10.3	3.0
F2-186	27.1	59.7	9.7	3.5
F2-187	30.8	47.0	18.6	3.6
F2-188	31.3	56.0	9.4	3.3
F2-189	33.2	42.6	19.2	5.0
F2-191	32.7	57.2	7.9	2.2
F2-193	30.7	43.8	17.4	8.1
F2-227	30.1	67.0	0.0	2.9
F2-228	32.0	49.0	17.4	1.6
F2-229	33.2	45.7	14.4	6.7
F2-232	29.7	45.0	21.6	3.7

intervals. The traverses were spaced 0.5 mm apart. In all cases 2000 points were counted over one or more thin sections, representing a line 600 mm in total length. If a "hole" was encountered in the section during a traverse, the counting was stopped and a new traverse begun. With this grid each point counted could be con-

sidered to represent an area of 0.15 sq mm, and the total area traversed was 300 sq mm.

Quartz, alkali feldspar, and plagioclase feldspar were in all cases recorded separately, whereas the other constituents were lumped together. The alkali feldspar

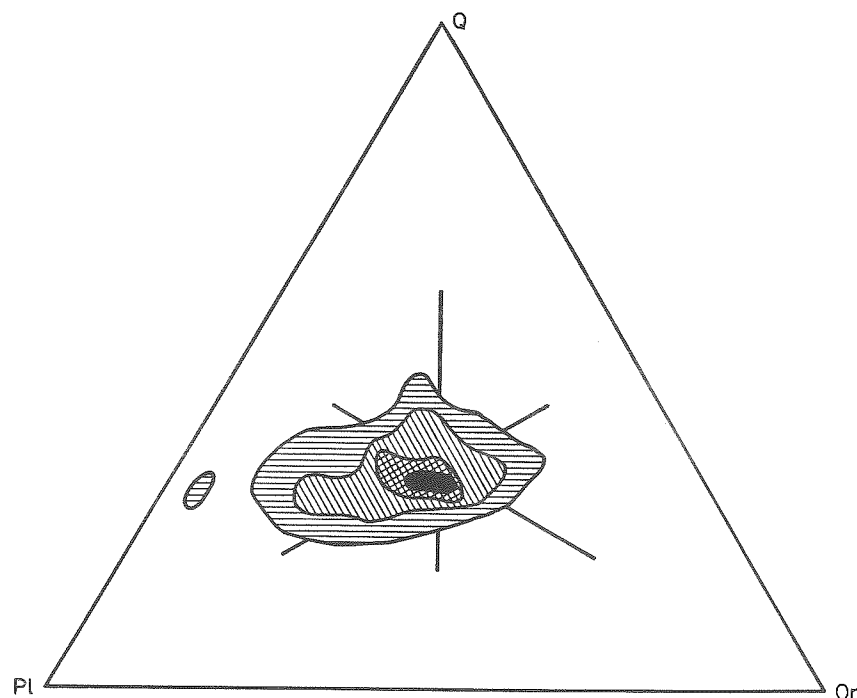


FIGURE 56.—Modal plagioclase, orthoclase, and quartz from 260 thin sections of granites from eastern United States

(After Chayes, 1951). Contours more than 0, 2, 5, and 7 per cent. 0.25 per cent counter

was stained to facilitate identification. All specimens but one contained more than 90 per cent quartz + alkali feldspar + plagioclase feldspar (Table 19; Fig. 55).

**QUARTZ CONTENT:** Of the 44 specimens studied only 1 contained less than 20 per cent quartz, and none carried more than 35 per cent; the average quartz content was 28.7 per cent. This variation is considerably greater than was found by Chayes (1952) in any single New England granite. The average, however, is essentially the same as that for all New England granites combined. The spread in quartz values may be in part due to less accurate analysis, but a more likely cause of the wider dispersion is the location of the specimens—a large proportion of the Skye specimens were taken near contacts, whereas Chayes made no such selection of specimens. The Skye granites may then be considered “normal” granites as far as the quartz content is concerned.

**ALKALI FELDSPARS:** Alkali feldspar is the most abundant mineral in the Skye granites; it makes up 39–72 per cent of the specimens studied. Only 1 of the Skye

specimens contains less than 42 per cent potassium feldspar, and, of the 145 specimens of New England granites studied by Chayes (1952, Table 18), only 1 specimen contains more than 42 per cent potassium feldspar. The significance of this difference will be discussed later.

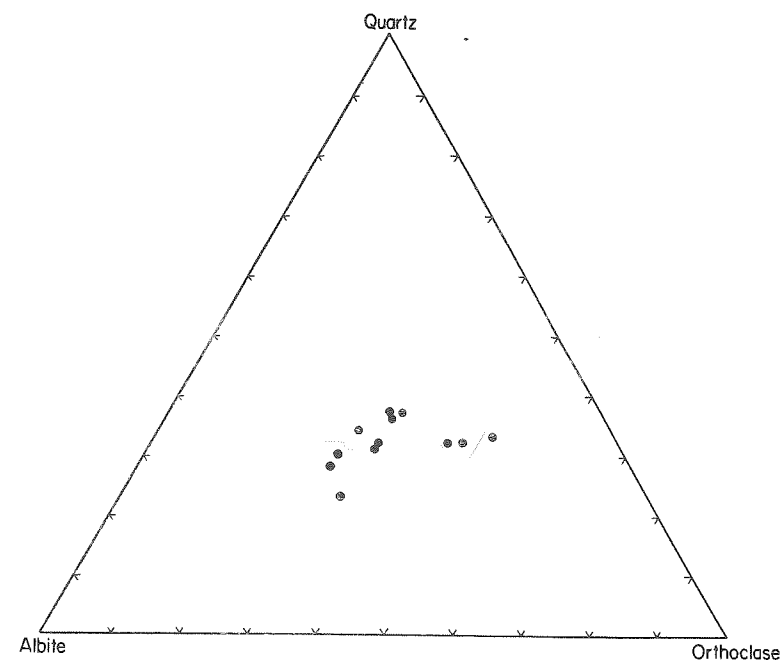


FIGURE 57.—Distribution of the normative Ab-Or-Q of 12 analyzed granites from Skye

The three orthoclase-rich granites are contact specimens taken within 1 foot of the contact. Compare with Figure 42 which illustrates the distribution of Ab-Or-Q in 571 granites from Washington's Tables. Chemically, the Skye granites are normal granites, with the exception of the contact facies.

Much of the alkali feldspar is perthitic, and no attempt has been made to estimate the plagioclase content of the perthite. Perthite is counted as alkali feldspar, even though the plagioclase lamellae are coarse enough to be recognized occasionally as such.

**PLAGIOCLASE FELDSPAR:** Plagioclase content of the Skye granites ranges from 19.2 per cent to 0.0 per cent and varies inversely with the alkali feldspar content. The average plagioclase content of the 44 Skye specimens is 11.4 per cent. Again, if these results are compared with those of Chayes for eastern United States granites, the differences are striking. The average plagioclase content in 225 analyses of United States granites is 30.1 per cent. These differences cannot be attributed to chemical variations, as the Skye granites contain approximately 30 per cent normative plagioclase. The modal differences can be due only to the variations in the amount of “plagioclase” held in solid solution in the alkali feldspar. This is perhaps the most significant feature of the modal analyses.

TABLE 20.—Chemical, normative, and modal composition of Skye granites

	F2-165	F2-187	F2-232	F2-228	F2-233	F2-227	F2-234	F2-235	F2-236	F2-237	F2-238	F2-239
SiO <sub>2</sub>	76.00	75.71	73.99	74.88	75.33	74.69	69.62	71.68	71.14	74.31	70.34	71.98
Al <sub>2</sub> O <sub>3</sub>	12.20	12.61	13.02	12.73	11.88	12.00	13.91	12.55	12.82	11.71	13.16	13.13
Fe <sub>2</sub> O <sub>3</sub>	0.56	0.73	0.76	0.53	0.43	0.44	1.18	2.29	1.17	1.63	2.65	1.33
FeO	0.22	1.09	1.60	1.33	0.95	0.71	3.01	2.40	3.48	1.67	2.24	1.64
MgO	0.20	0.20	0.31	0.25	0.08	0.12	0.46	0.24	0.29	0.04	0.40	0.56
CaO	0.60	0.73	1.22	1.12	0.92	1.66	1.73	0.92	1.36	0.61	1.24	1.15
Na <sub>2</sub> O	2.97	3.49	3.43	3.33	2.55	2.02	4.27	4.28	4.24	4.11	3.61	2.98
K <sub>2</sub> O	6.37	4.85	4.74	4.99	7.18	7.78	4.92	4.37	4.79	5.22	4.90	4.93
H <sub>2</sub> O+	0.17	0.19	0.22	0.79	0.23	0.17	0.53	0.64	0.57	0.39	0.76	1.38
H <sub>2</sub> O—	0.11	0.03	0.14	0.16	0.06	0.20	0.12	0.25	0.13	0.05	0.46	0.39
CO <sub>2</sub>	0.31	0.05	—	—	—	nil	—	—	—	—	—	—
TiO <sub>2</sub>	0.07	0.22	0.32	0.18	0.06	0.14	0.49	0.38	0.44	0.36	0.46	0.37
P <sub>2</sub> O <sub>5</sub>	0.01	0.03	0.05	0.05	0.08	Trace	0.14	0.03	0.09	0.03	0.10	0.19
MnO	0.02	0.02	0.02	0.02	0.01	0.03	0.03	0.05	0.02	0.06	0.19	0.14
Total	99.81	99.95	99.82	100.36	99.76	99.96	100.41	100.08	99.94	100.19	100.51	100.17

## Norms

Q	33.48	34.62	32.40	32.94	31.38	30.84	20.72	27.10	25.48	30.00	27.00	31.80
Or	37.81	28.91	27.80	29.47	42.81	46.15	29.03	25.80	24.75	30.58	28.91	28.91
Ab	25.15	29.34	28.82	28.30	20.96	16.77	36.10	36.15	35.84	31.44	30.39	25.15
An	1.10	3.34	5.84	5.00	—	0.83	4.17	2.06	3.47	—	5.28	5.84
C	—	0.41	0.10	—	—	—	—	—	—	—	—	0.71
Ac	—	—	—	—	0.46	—	—	—	—	2.77	—	—
Di	—	—	—	0.46	3.16	1.89	2.99	2.18	2.36	2.70	0.69	—
Hy	0.66	1.56	2.52	2.08	—	—	3.40	1.44	4.23	0.40	1.86	2.72
Wo	—	—	—	—	—	2.20	—	—	—	—	—	—
Mt	0.46	0.93	1.16	0.70	0.46	0.70	1.72	3.32	1.67	0.93	3.94	1.86
Il	0.15	0.46	0.61	0.46	0.15	0.30	0.93	0.71	0.84	0.76	0.91	0.76
Ap	—	—	—	—	0.34	—	0.34	0.07	0.20	—	—	—
Cc	0.70	0.10	—	—	—	—	—	—	—	—	—	—
H <sub>2</sub> O	0.28	0.22	0.36	0.95	0.29	0.37	0.65	0.89	0.70	0.44	1.22	0.56
Total	100.12	99.99	99.61	100.36	100.01	100.05	100.05	99.72	99.54	100.02	100.20	98.51

## Modes

Qtz	30.8	30.8	29.7	32.0	—	30.1	—	—	—	—	—	32.9*
Or	65.9	47.0	45.0	49.0	—	67.0	—	—	—	—	—	63.9
Pl	0.0	18.6	21.6	17.4	—	0.0	—	—	—	—	—	0.0
Others	3.3	3.6	3.7	1.6	—	2.9	—	—	—	—	—	3.2

\* Mode of specimen collected at the same outcrop as the analyzed specimen.

QUARTZ-ALKALI FELDSPAR-PLAGIOCLASE DIAGRAM (Q-Or-Pl): Variations in these three constituents are best illustrated by a ternary diagram (Fig. 55). Of the 10 specimens having less than 5 per cent plagioclase, 6 were from the Beinn an Dubhaich granite and were collected within 1 foot of the contact. The other 4 were from a small outcrop of a one-feldspar granite along the road from Sligachon Inn to Brad-

ford (3 miles from Sligachon Inn). According to Prof. L. R. Wager (Personal communication) this is the only granite of this character found in Skye. It is very coarse-grained, and the feldspar is coarse microperthite.

Distribution of the 44 modal analyses shown in Figure 55 is particularly inter-

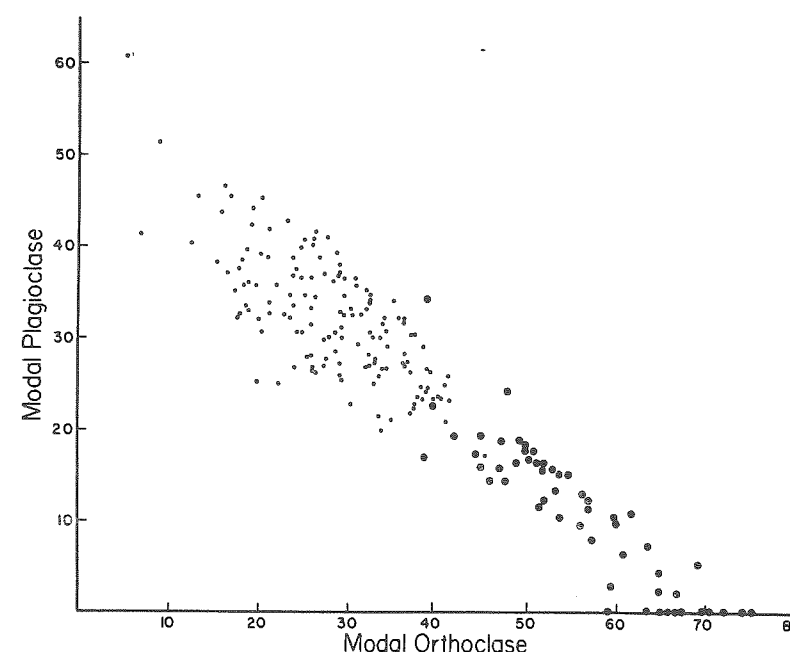


FIGURE 58.—Graph illustrating the relation between modal orthoclase and modal plagioclase in granites

Small circles represent eastern United States granites studied by Chayes (1952) and large circles are granites from Skye, Scotland, Drammen, Norway, Quincy, Massachusetts, Madoc, Ontario, and Pikes Peak, Colorado studied by the authors. The linear distribution is largely the result of the nearly constant quartz content of granites, together with the variable amount of sodium feldspar carried in solid solution in the potassium feldspar of granites.

esting when compared with Figure 56, which represents 260 modal analyses of granites in eastern United States (Chayes, 1951). Taken together they represent a continuous band extending from the orthoclase-quartz sideline to a little past the center of the diagram. This band does not represent a continuous change in chemical composition as the Skye granites, normatively, fall near the maximum for all granites (Fig. 57; Table 20). It represents to a very large extent nothing more than the variable amount of plagioclase in solid solution in the alkali feldspar. The alkali feldspars in the Skye granite carry a relatively large amount of plagioclase in solid solution, whereas the two-feldspar granites studied by Chayes must contain considerably less plagioclase in the alkali feldspar. Looked at in another way this band or trend from the orthoclase-quartz sideline toward the center of the diagram represents a falling temperature of final crystallization of granites; the Skye granites are



high-temperature, and those near the center of the diagram are low-temperature granites.

This relationship between potassium and plagioclase feldspar in granites is also illustrated in Figure 58, which is a plot of modal plagioclase versus modal orthoclase. The linear distribution is due largely to the nearly constant quartz content of the granites and to the variable amount of plagioclase held in solid solution in the potassium feldspar.

Experimental evidence presented earlier indicates that it is very unlikely that the two-feldspar granites (particularly those low in lime), as initially crystallized from a liquid, had two feldspars with the compositions normally found in these granites. More than likely, these granites completed crystallization from the liquid with modal compositions nearer the orthoclase-quartz sideline.

#### NORMATIVE ALBITE-ORTHOCLASE-QUARTZ OF SKYE GRANITES

The proportions of normative albite-orthoclase-quartz found in analyzed granites from Skye are illustrated in Table 20 and Figure 57. A comparison of this figure with Figure 42, which is a similar diagram for all granites in Washington's Tables (1917), shows that the Skye granites are "normal" granites—that is, they fall at or near the maximum for all granites. The three exceptions are contact facies of the Beinn an Dubhaich granite, which carry a relatively large amount of potassium feldspar. These three analyses are of specimens collected within 2 feet of the contact.

#### DISCUSSION

The Tertiary granites of Skye are normal granites, chemically, and to a large extent texturally; mineralogically they are surprisingly similar to rhyolitic rocks. The quartz, alkali feldspar, and plagioclase feldspar resemble in many respects the corresponding phenocrysts of extrusive rocks. These granites are intermediate between the extrusive and plutonic salic rocks. This, to the magmatist, is to be expected, as these young granites have been intruded into a high level in the earth's crust and consequently have cooled at a rapid rate compared to the deep-seated granites. This fast cooling has quenched in many of the mineralogical features normally associated with extrusive rocks. Those who wish to divorce the rhyolites from granites and the granites from magmas will find these young high-level granites something of a stumbling block. It is not difficult to imagine that, had these granites cooled somewhat more slowly, the alkali feldspars would have undergone further change to low-temperature modifications, the quartz would have recrystallized to give inversion temperatures similar to those found in quartz from older granites, and the plagioclase would have inverted to low-temperature types. If equilibrium were more nearly attained on cooling, a large proportion of the plagioclase now found in solid solution in the alkali feldspar would have unmixed to increase the modal plagioclase to a value corresponding more nearly to the normative plagioclase.

These studies on the feldspars of the Skye granites illustrate the importance of the sluggish inversions in silicates as a tool for deciphering the history of feldspar-bearing rocks. Perhaps we shall soon be able to decide with some certainty which granites owe their origin directly to magmatic processes and which are derived from pre-existing rocks by metamorphism and metasomatism. Certainly granites formed

by low-temperature processes without the aid of a liquid phase (if such granites exist) will record this fact in the feldspars. The problem is to find out in what fashion such information is stored in the feldspars.

#### GEOTHERMAL GRADIENTS AND GRANITE MAGMAS

##### INTRODUCTORY STATEMENT

Speculation concerning the origin of granitic and basaltic liquids has been rife for many decades, and even today little agreement can be reached among the students of the earth's interior as to a satisfactory mechanism for supplying these two liquids in large quantities and at all times during the earth's history. In recent years it has become popular to have all granitic liquids formed by the melting of sedimentary rocks, although many petrologists question this because, if there were no granites during the early history of the earth, where did the sediments come from which later melted to give granite liquid? It is impossible for sediments formed from the weathering of basalts to give granite liquids on melting; therefore the early granites must have been formed by some mechanism not requiring a sedimentary parent— thus fractional crystallization of more basic magmas is believed to have been operative. moon

The problem of supplying granitic and basaltic liquids at all times was solved by early geologists such as Bunsen (1851) and Durocher (1857) who advocated earth shells of liquid granite and liquid basalt which could be tapped at any convenient time. In later years when it was erroneously believed that granite melted at higher temperatures than basalt the liquid layer of granite was abandoned. From time to time the layer of basaltic liquid has been advocated and opposed by various petrologists. Seismologists have pointed out that liquid basalt does not have the requisite rigidity to give the earthquake-wave properties found at depths of 40 to 70 km. Daly (1914, p. 164) advocated an earth shell of basaltic liquid and suggested that the required rigidity is a result of the high hydrostatic pressures prevailing at depth.

The advantages of having an earth shell of basalt are not so great as they may appear at first thought as this requires a tremendous release of pressure to produce a liquid capable of moving to the earth's surface; such a release of pressure could equally well produce such a liquid directly from crystalline material.

In summary it appears that the general opinion among geologists and geophysicists at present is that there are no earth shells of liquids of any composition—granitic or basaltic—but that all magmas are produced locally as a result of orogenic disturbances and the periodic accumulation of heat from various sources.

The melting relations in the  $\text{NaAlSi}_3\text{O}_8\text{--KAlSi}_3\text{O}_8\text{--SiO}_2\text{--H}_2\text{O}$  (granite-water) system reported above can now be used to speculate on the existence of granitic liquids in the earth's crust. The presence or absence of granite liquid depends on the compositions, temperatures, and pressures. The appropriate anhydrous compositions can be found in sedimentary, metamorphic, or igneous rocks. However, the temperature and pressure at which melting will begin depend to a large extent on the presence of volatile materials which flux the more refractory silicates. Some melting will take place if the volatiles are present in only very small amounts, and it is only when complete melting at low temperatures is required that large quantities of these

fluxes are necessary. With the chemical requirements satisfied we can now turn to the temperatures and pressures in the earth's crust and see if they are appropriate for melting.

#### MEASURED GEOTHERMAL GRADIENTS

Figure 59 has been prepared to give a general picture of the thermal gradients measured in the earth's crust. The values were taken from the compilation by Spicer (1942).

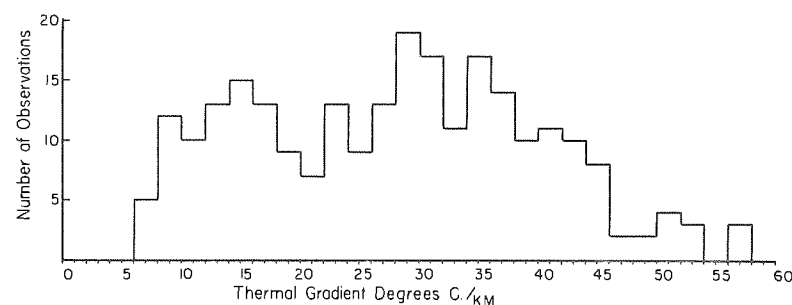


FIGURE 59.—Histogram showing the range and distribution of measured geothermal gradients in the earth's crust

Only values measured at depths greater than 610 m are shown. (All values taken from Birch *et al.*, 1942.)

Thermal gradients of 50°C./km are rare, gradients of 40°C./km are common, and gradients in the vicinity of 30°C./km are the most common.

Most of these gradients were measured in wells having a maximum depth of less than 1 km. We must now extrapolate these data to greater depths. First it would be desirable to know whether the geothermal gradient increases or decreases with depth. Spicer's data give this information directly. Figure 60 illustrates the relation between the rate of change of the gradient reduced to °C./km/km and the number of observations. These figures were obtained by assuming that the gradient in the depth range 30.5 to 305 m is characteristic of a depth half way between these two depths and that the gradient calculated for the range 610 m to the deepest observation is also characteristic of a depth intermediate between these two depths. These values can then be used to calculate the rate of change of the gradient with depth.

The data indicate that in general the gradient steepens with depth, and on the average the increase is on the order of 6°C./km. This is somewhat surprising as most published geothermal gradients show the initial gradient decreasing with depth (Gutenberg, Adams, Daly, Jefferys, and Holmes, *in* Gutenberg, 1951, p. 162). However, Van Orstrand (1951, p. 114) noted that most temperature-pressure curves are convex toward the depth axis, and Noble (1948) reported that the geothermal gradient steepens with depth at the Homestake mine. Noble suggested that the steepening gradient is due to the expulsion of moisture at depth, which would increase the insulating properties of the rocks. Apparently Van Orstrand did not explain his findings.

Many factors may influence the conductivity of the rocks at depth, and it is difficult to evaluate these quantitatively. In any single bore hole or well the change of the gradient with depth is of course determined largely by the local stratigraphy. If a well passes from shale to quartzite, the gradient will certainly decrease in the quartzite, whereas if the well passes from quartzite to shale the gradient will steepen

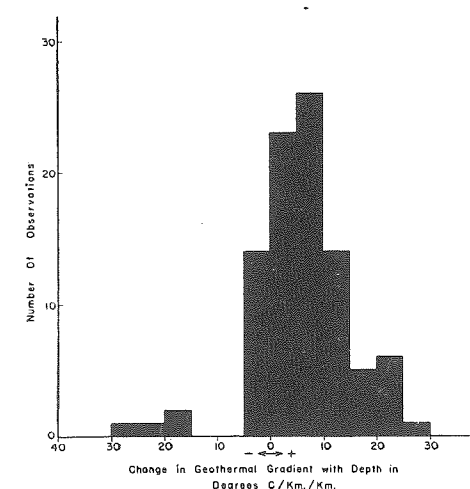


FIGURE 60.—Histogram showing the range and distribution of changes in the geothermal gradient with depth in degrees C./km/km

The + values signify that the gradient is steepening with depth. (Values computed from data in Birch *et al.*, 1942.)

as the shale is encountered. It is believed, however, that the compilation shown in Figure 60 indicates a general increase of the gradient with depth, and the local effects of the stratigraphy are believed to be "averaged out" by the relatively large number of observations.

Two possible explanations for this unexpected change in gradient with depth are: (1) the change is related to some thermal property of rocks which tends to decrease the conductivity at depth, and (2) the steepening is related to near-surface temperature changes in post-Pleistocene time. Possibility (2) appears unlikely because a large proportion of the measured gradients are in wells in southern United States where such an effect would not be expected to be pronounced. Possibility (1) appears to be the more likely explanation. The thermal conductivity can be influenced by chemical composition, mineral composition, textural properties, pressure, and temperature, all of which may change with depth.

The expulsion of moisture suggested by Noble (1948) as a possible cause of the steepening gradient is one type of compositional change which will tend to decrease the conductivity and hence steepen the gradient. This effect has been investigated experimentally (Clark, 1942, p. 258). The expected changes in other chemical properties—in mineralogy, in textural relations, and in pressure—all tend to increase thermal conductivity at depths and therefore can be assumed to be initially outweighed by other tendencies.

The most likely explanation of the increasing thermal gradient lies in the change in thermal conductivity of most rocks with increasing temperature. As the temperature increases the rocks become better thermal insulators, and therefore the thermal gradients increase. Figure 61 shows the relation between thermal conductivity and

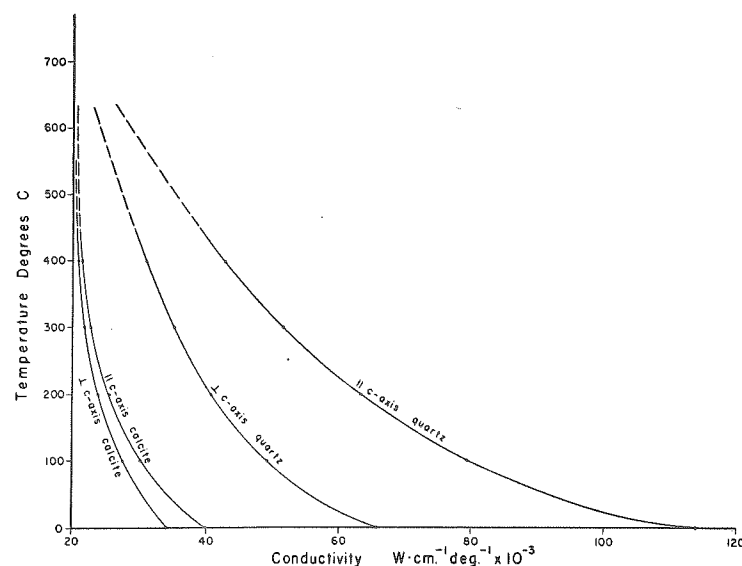


FIGURE 61.—Graph showing the effect of temperature on the thermal conductivity of quartz and calcite

Note that it is to be expected from this information that the geothermal gradient at a depth where the temperature is 600°C. will be at least twice as steep as the initial gradient near the earth's surface.

temperature for two common minerals. As quartz is one of the most common minerals in the sialic rocks, the conductivity as a function of temperature is particularly pertinent to the problem—the conductivity of quartz decreases from a mean of about 90 watts·cm<sup>-1</sup> deg.<sup>-1</sup> to 25 watts·cm<sup>-1</sup> deg.<sup>-1</sup> when the temperature is raised from 0° to 600°C. Unfortunately comparable data for other common rock-forming silicates are not available. In general the data indicate that the alkali feldspars behave as quartz does, but show less-pronounced drop in conductivity at elevated temperatures (judging from the effect of temperature on the conductivity of syenite, albitite, and granite). As quartz and alkali feldspars are the principal constituents of the sialic rocks it is to be expected that the thermal gradient in such rocks will increase with depth. Also, as quartz and carbonate are the principal constituents of many sedimentary rocks, it is expected that here, too, the gradient will increase with depth.

The conductivity of the lime feldspar (anorthite) increases with increasing temperature. This is the only common rock-forming mineral that behaves in this fashion. The “abnormal” increase in conductivity with increasing temperature of many

gabbros and diabbases is probably a reflection of the high anorthite content of these rocks.

The principal heat-producing radioactive substances are often considered to be concentrated in the sialic materials of the continental portions of the earth's crust, and it is therefore assumed that the measured thermal gradients will be influenced by this heat source. The recent heat-flow measurements in the oceanic basins where sialic material is sparse or absent indicate that in these areas the heat flow is comparable to that in continental regions. If these results are reliable, it seems unlikely that the principal source for the heat in the continental areas could be due to radioactive sources within the sial. More than likely most of the heat escaping in the continental areas comes from below the sial just as it must in the regions where sialic material is sparse. Conceivably a portion of the radioactive materials in the original subsialic layers of the continental areas has been abstracted during the formation of the crust, but it appears unlikely that all, or even a large proportion of, the heat-producing material would be so removed to the crust. It appears unlikely, therefore, that the change in geothermal gradient with depth shown in Figure 60 is related to the distribution of radioactive materials in the upper part of the earth's crust.

The initial steepening of the geothermal gradient at a rate of 6°C./km/km cannot, of course, be expected to continue indefinitely. It seems reasonable to assume that the gradient will steepen at a rate determined by the change in conductivity with increasing temperature (Fig. 61). Below a depth corresponding to a temperature somewhat less than 600°C. the gradient is expected to change sign and to decrease.

#### TEMPERATURE OF THE BEGINNING OF MELTING

In rocks whose compositions approach that the average granite melting will begin at 640°C. if sufficient water is present to more than satisfy the equilibrium requirements of the hydrous phases present (*i.e.*, micas or amphiboles) and if the pressure is on the order of 4000 kg/cm<sup>2</sup>. The minimum amount of water needed to begin melting under these circumstances will vary somewhat with variations in the anhydrous composition, but for a granite containing 10 per cent biotite as the only hydrous phase, for example, 0.5 per cent water would be adequate to give some liquid at 640°C. and 4000 kg/cm<sup>2</sup>. The water content of the liquid would be approximately 9 per cent by weight, and therefore the amount of liquid would be small under these conditions.

We have considered melting in rocks in which water is the only volatile material. What would be the effect of other volatile materials on the beginning of melting? Melting would probably begin at lower temperatures if other volatile materials capable of dissolving in the liquid phase are also present, but in view of the established preponderance of water as a volatile associated with volcanic activity and as a constituent of volcanic glass it is reasonable to assume that the presence of other volatiles would not lower the temperature of beginning of melting by any great amount.

The temperature of the beginning of melting can be drastically affected by the presence of alkalis in excess of that required to combine with alumina to form feldspars. The amount of liquid formed at temperatures below 640°C. as a result

of the presence of excess alkalis would be quantitatively small because the rocks do not carry large excesses of alkalis.

#### DEPTH OF THE BEGINNING OF MELTING

Using the value of  $640^{\circ}\text{C}.$  for the beginning of melting and a thermal gradient of  $30^{\circ}/\text{km}$ , melting will take place at a depth of approximately 21 km if the concen-

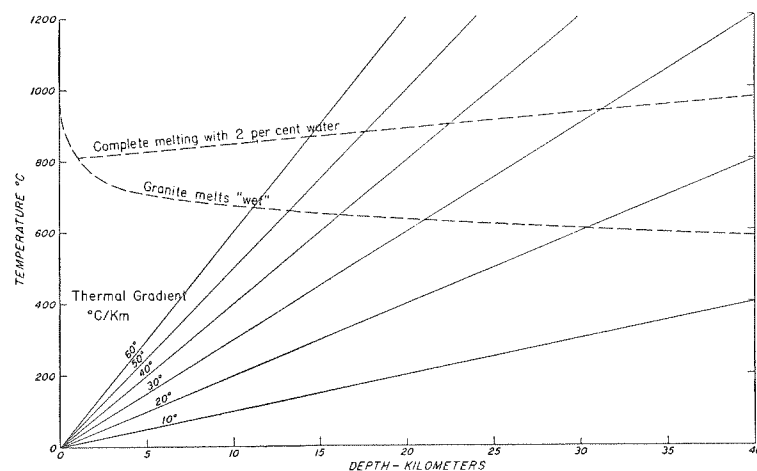


FIGURE 62.—Graph showing the relations between the melting of granite and various geothermal gradients assuming the gradients are linear

tration of volatile materials is adequate (Fig. 62). A thermal gradient of  $50^{\circ}\text{C}./\text{km}$ , on the other hand, would give a temperature of  $650^{\circ}\text{C}.$  at a depth of only 13 km. (As the pressure at a depth of 13 km is slightly less than  $4000 \text{ kg}/\text{cm}^2$  the temperature would have to be somewhat higher than  $640^{\circ}\text{C}.$  to produce melting under the assumed conditions—i.e.,  $655^{\circ}$ – $660^{\circ}\text{C}.$ )

If the geothermal gradient increases at a rate of  $6^{\circ}\text{C}./\text{km}/\text{km}$  to a depth where the temperature reaches the critical value for melting to begin then a gradient of  $30^{\circ}\text{C}./\text{km}$  results in melting at 12 km, and a gradient of  $50^{\circ}\text{C}./\text{km}$  results in temperatures at which melting would be expected at a depth of only slightly greater than 9 km. It is reasonable to assume that the rate of increase of the geothermal gradient will fall off with the rate of change of the thermal conductivity with temperature, and therefore the most probable depth at which melting is expected lies, at  $30^{\circ}\text{C}./\text{km}$  initial gradient, at a depth between 21 km and 12 km. Similarly the value for a  $50^{\circ}\text{C}./\text{km}$  initial gradient probably lies between 13 and 9 km depth.

#### DEPTH OF COMPLETE MELTING

The temperature of the beginning of melting will hold for a rather wide range in chemical compositions, whereas the temperature of the completion of melting varies greatly with changes in chemical composition. A much-simplified explanation of this relation can be given in terms of a binary system with no solid solution. Here any composition intermediate between two compounds *A* and *B* will show some liquid

when heated to the eutectic temperature. The temperature of complete melting, however, varies with composition, from a maximum at the melting point of the highest-melting end member to a minimum at the eutectic, and so it is in the most complex system which we are studying here—beginning of melting and complete melting will take place at the same temperature and pressure for only one anhydrous composition. Any adjacent anhydrous compositions may begin to melt at essentially the same temperature but will be completely melted only at some higher temperature. For the present discussion it will be assumed that the anhydrous composition is such that complete melting will take place at the temperature of beginning of melting if no volatiles are present.

Assuming, again, a thermal gradient of  $30^{\circ}\text{C}./\text{km}$ , melting will begin at 21 km, and if the water content is on the order of 9 per cent complete melting will ensue at this depth (Fig. 62). If the water content is less than 9 per cent melting will begin at 21 km but will not be completed until some higher temperature (greater depth) has been reached. For example, assuming a water content of 2 per cent, melting will begin at 21 km but will not be complete until a depth of 31 km has been reached. The amount of liquid in this 10-km zone will range from 0 at 20 km to 100 per cent at 30 km.

If the geothermal gradient is  $50^{\circ}\text{C}./\text{km}$  melting will begin at 12 km depth. If the water content is high enough complete melting will take place at this depth. With 2 per cent water melting would be complete at about 17 km depth. As the geothermal gradients increase with depth, the depth at which complete melting is to be expected with 2 per cent water is somewhat less than 17–30 km for initial gradients of  $50^{\circ}\text{C}./\text{km}$  and  $30^{\circ}\text{C}./\text{km}$  respectively—perhaps only 15 km for an initial gradient of  $50^{\circ}\text{C}./\text{km}$  and 20 km for an initial  $30^{\circ}\text{C}./\text{km}$  gradient.

Unlike the beginning of melting, the temperature of completion of melting is extremely sensitive to slight changes in chemical composition. The amount of water and other volatiles available to flux the silicates determines the amount of liquid formed at any depth at which the melting temperatures and pressures have been reached. Once melting has begun in granite compositions, the only obstacle to complete melting is the amount of volatile materials. The anhydrous chemical composition of the bulk of the granites (Fig. 42) is such that given the required quantity of volatiles they would melt completely, or nearly completely, at the temperature of the beginning of melting.

#### ZONE OF MELTING

If the water content of a segment of the earth's crust is on the order of 1–2 per cent by weight and the composition is approximately that of the average granite a zone of melting at least 10 km thick will result. In the upper portion of this zone where the amount of liquid is relatively small the principal effect of the melting will be to recrystallize the unmelted fraction. It is unlikely that this small amount of liquid could effect complete homogenization of initially layered sedimentary or volcanic rocks so that original textures would be preserved. Evidence for the former presence of a few per cent of liquid would be extremely difficult to establish. In other words a small amount of liquid would result in recrystallization of, say, a shale to a



schist or perhaps to a gneiss, but would not give rise to a degree of homogenization and recrystallization required to give a "granitelike" rock. The rocks in this portion of the zone of melting would have considerable strength and would fold and fracture much like a completely solid rock.

As the amount of liquid approaches the amount of crystalline material the rocks will lose a great deal of strength and therefore will not fail in the same fashion as in the region above. Failure by fracture will be impossible, and the rocks would be characterized by pygmatic folding and failure by flow. The coexistence of liquid and crystals in these proportions for long periods may result in segregation to some extent of the solid and liquid fractions, giving rise to banded or *lit-par-lit* gneiss.

When the amount of liquid exceeds the amount of crystalline material the opportunity for homogenization of gross banding and layering is present. Also, the unmelted portion can now sink into the hotter region below and thereby change the composition toward that of the liquid—the granite composition. It would appear that any initial composition capable of giving rise to a substantial amount of liquid under these conditions can be readily made over into compositions approaching that of the average granite by the settling out of the "nongranitic" unmelted fraction. The exact range of compositions which would develop the requisite amount of liquid under these conditions is not known, but it seems likely that rocks as basic as diorite as well as sedimentary and volcanic sections may be capable of developing large amounts of liquid under these circumstances.

The question now arises: Can granite liquids be abstracted from basaltic compositions under these circumstances? There have been no experimental studies that give direct information on the exact composition of the first liquid to form on melting of a basalt.

It is not unreasonable to expect that at depths of 35–40 km basalt could become partially liquid and that the liquid would have a composition not far from that of the andesitic rocks. If the unmelted portion then settled out, and the andesitic liquid, displaced upward, crystallized in an environment where an opportunity for settling of crystals still prevailed, liquids of granitic composition could result. This process of crystal fractionation by settling of crystals gives a progressively more salic liquid until granite liquids are produced—here the process stops. The liquid has now reached the bottom of petrogeny's residua system, and as crystallization of this granitic liquid proceeds the bulk composition of the crystals as well as the liquid has the composition of granite. Except for very special circumstances this is the end of the road for fractional crystallization, and consequently the composition of the liquid will remain essentially unchanged throughout crystallization.

*It is therefore suggested that this zone of melting, where temperatures are high enough to melt granite completely and more basic compositions at least partially, may offer a mechanism for producing large batholithic masses of granite.* The so-called room problem is nonexistent for granite batholiths formed in this fashion, as is also the heat problem. The contacts in an undisturbed region of the upper, low-liquid portion of the zone of melting would be gradational, whereas it is expected that the more fluid portions of the zone of melting would commonly be intruded into higher levels giving rise to sharp intrusive contacts. Rhyolitic lavas could be tapped off from the more

fluid portions of the zone of melting and could carry a large percentage of crystalline material or none at all. Basaltic liquids could be tapped off from the lower portions of the zone of melting, but such liquids would probably carry a fairly large amount of crystalline material.

#### SOME RESTRICTIONS ON THE MOVEMENT OF HYDROUS GRANITE MAGMAS

The first liquid to form at the top of the zone of melting will contain on the order of 7–9 per cent water; the exact amount will depend on the pressure and temperature. The amount of melting will depend to a large extent on the amount of water available. If 9 per cent water is available the rock will melt completely. If the amount available is only 0.1 per cent then only 1 per cent of the rock will melt. This liquid, regardless of the amount present, cannot move to higher levels in the earth's crust. If either the pressure or temperature falls slightly, crystallization must follow. For example, Figure 62 shows that a liquid formed at the pressure and temperature corresponding to the intersection of the 40°C./km thermal-gradient curve with the curve for melting of "wet" granite must crystallize on moving toward the temperature or pressure axis. Only when the pressure and temperature place the liquid above the melting curve for "wet" granites can the liquid move to higher levels in the earth's crust without crystallizing, and even under these circumstances the beginning of melting curve is an obstacle to any hydrous granite liquid on its way to the surface. Theoretically only a granite liquid whose temperature is 960°C. or higher could reach the surface as a liquid.

#### DISCUSSION

It is suggested that on the average the geothermal gradient initially steepens with depth largely as a result of the decreasing conductivity of the minerals with increasing temperature. The principal factors which tend to cause the geothermal gradient to fall with depth (*i.e.*, radioactive heat from within the crust and pressure) are apparently outweighed initially by other factors.

It is also suggested that the available information on geothermal gradients in the earth's crust indicates that temperatures at which partial melting will occur are expected at depths between 10 and 40 km in regions where the initial gradient is greater than approximately 20°C./km. As high geothermal gradients (*i.e.*, >40°C./km) are commonly found in the sedimentary rocks and the consistently low gradients of <20°C./km are common in shield areas, it appears probable that liquids of granitic composition will be more likely to be found in regions where a thick blanket of sediments is present.

In the upper part of the zone of melting where the proportion of liquid ranges from zero to approximately 50 per cent the liquid will not usually have an opportunity to free itself of crystalline material, and it is expected that large-scale homogenization may not take place. The principal effect of the liquid will be to recrystallize the nonmelted portion into crystalline phases in equilibrium with the liquid. If the initial material is granite it seems likely that the only effect would be the possible development of layering and/or foliation. If the initial material is of sedimentary origin probably short-range homogenization may take place under these circumstances, but large-scale layering such as alternating beds of quartzite and

→ coarse gr. gabbro  
conglomerate  
with  
megacrysts  
shale would not be homogenized. Under these circumstances only the shale would develop a significant amount of liquid, and it is suggested that the principal effect of the presence of a liquid phase would be the rather thorough recrystallization to a schist in the portion of the zone where only a small amount of liquid is developed, and perhaps recrystallization to a gneiss when the proportion of liquid is relatively large.

The proposed zone of melting which may be as much as 10 km thick (assuming a 30°C. gradient and 2 per cent volatiles) does not leave much room for high-grade regional metamorphism without the former presence of a magmatic liquid phase. Perhaps the liquid phase is an essential ingredient for the development of the high-grade metamorphic rocks? As melting may take place at temperatures as low as 600°C. in the presence of water vapor and at still lower temperatures when other volatiles are also present, it seems reasonable to consider partial melting as an important agent for promoting regional metamorphism. The former presence of such a liquid will be very difficult to establish as such rocks presumably always cool slowly, and the quenching necessary to preserve the evidence of the former presence of a liquid phase is not to be expected under these circumstances.

Some authors, e.g., Turner and Verhoogen (1951, p. 358) and Jefferies (1941, p. 834), have proposed geothermal gradients which give rise to a temperature of only 500°–600°C. at a depth of 40 km. Perhaps this is reasonable for an average gradient for the earth as a whole, but it is certainly unrealistic in so far as the granitic rocks and the generation of granitic liquids are concerned. Granitic liquids have been formed in great abundance in the earth's crust in the past, and it is unlikely that such liquids were generated at depths below 40 km. Granitic rocks are common in geosynclinal areas where a relatively thick blanket of sediments was present, but few, if any, geologists would suggest that the sediments ever attained a thickness of 40 km. We are not here concerned with average geothermal gradients for the earth as a whole, but with gradients in geosynclinal regions where thick blankets of sediments serve as thermal insulators. It is probable that granitic liquids exist at all times beneath these thick sedimentary sections if the chemical composition is appropriate.

Thus, once again laboratory studies point to the close genetic relationship between magmatism and metamorphism, and those who propose to separate these processes must be prepared to ignore the experimental studies. Granitization by solid diffusion can now be dismissed as being inconsistent with the temperatures and compositions found in the earth's crust, and granitization by low-temperature hydrothermal metasomatism can now assume the minor role long proposed for this process.

#### CLASSIFICATION OF SALIC ROCKS

Johannsen has said of the classification of rocks: "Although this may be an evil thing, it is, at least, the least of several evils." Much can be said against a rigid classification of igneous rocks such as Johannsen's (1917) quantitative mineralogical system, but there is little doubt that many rocks have been better described because of it—and this is surely ample justification for it. And so it is with the classification of salic rocks presented here; if a single salic rock is better described because of this classification it will have served a useful purpose.

In recent years it has become fashionable to discard the quantitative classifications

of the igneous rocks. There is some justification for this, but, once the quantitative aspect is discarded in favor of the qualitative, the spur to describe rocks precisely is lost, and the student is inclined to examine his granite or gabbro cursorily, give it an ill-defined name, and go on to the next problem. So we find numerous petrographic descriptions in the recent literature without a single quantitative determination of the minerals present in the rocks described, or with "calculated modes", or "approximate modes", or in the worst cases a rough mineralogical description with estimated mineral abundances and chemical analyses which have not been utilized in any fashion.

The inadequacy of modal classifications of granites can be illustrated by noting that a single chemical composition can give rise to the following rock types in Johannsen's mineralogical classification: (1) kaligranite, (2) sodalase granite, (3) granite, (4) sodalase adamellite, (5) adamellite, (6) sodalase granodiorite, and (7) granodiorite. The reason for this lies in the whereabouts of the sodium-feldspar component of the rock. If the sodium is tied up entirely in the potassium feldspar, the rock is a kaligranite, whereas if the sodium is present entirely as plagioclase together with the lime-feldspar component, the rock will fall in the granodiorite group. This is not a criticism of Johannsen's classification, but it merely points up the inadequacy of a mineralogical classification. The same can be said of chemical classifications. From modal analysis a kaligranite may fall into at least as many subdivisions of the C.I.P.W. classification as the above example in which the chemistry remains unchanged. Obviously a modal or normative classification is not suitable for all purposes.

It has often been said that rocks are completely gradational from one group to another, and therefore boundaries established between the various rock types must be entirely arbitrary. In the case of granitic rocks the frequency distribution offers an ideal and useful criterion for drawing certain class boundaries. For example, rocks which contain 80 per cent or more of the normative constituents, albite + orthoclase + quartz, give the distribution shown in Figure 63. The remarkable maximum at about one-third albite + one-third orthoclase + one-third quartz would appear to justify drawing the boundary *abc* as a classification division. Of the analyzed rocks containing 80 per cent or more normative albite + orthoclase + quartz, more than 75 per cent fall within this triangle which represents only 16 per cent of total area. It is proposed to call these rocks granites or rhyolites, whichever the texture and environment may require. Any rock whose composition falls outside this triangle should not be termed granite, and, in fact, in view of the frequency distribution, it is desirable to have names which clearly indicate that they differ from the bulk of the rocks containing quartz, potassium feldspar, and plagioclase. Rocks consisting essentially of quartz and albite or of quartz and orthoclase are not only rare, but it is questionable whether they are ever found among the unaltered glassy extrusive rocks. Unless they have a glassy equivalent, they differ from the granites in a much more fundamental fashion than do the syenites and quartz syenites and for this reason alone they should not be grouped with the granites. Genetically it is less important to distinguish the quartz syenites and syenites from the granites by a different name than to distinguish quartz-albite and quartz-orthoclase rocks.

In regard to adamellites and granodiorites, any classification which places a

boundary through the maximum of Figure 42 and 56 is unsound and tends to obscure the relations shown by the frequency distribution. Arithmetically it may be desirable to place a boundary at 50-50 potassium to plagioclase feldspars, but chemically and genetically it is ridiculous. The maximum of Figure 63 has important genetic

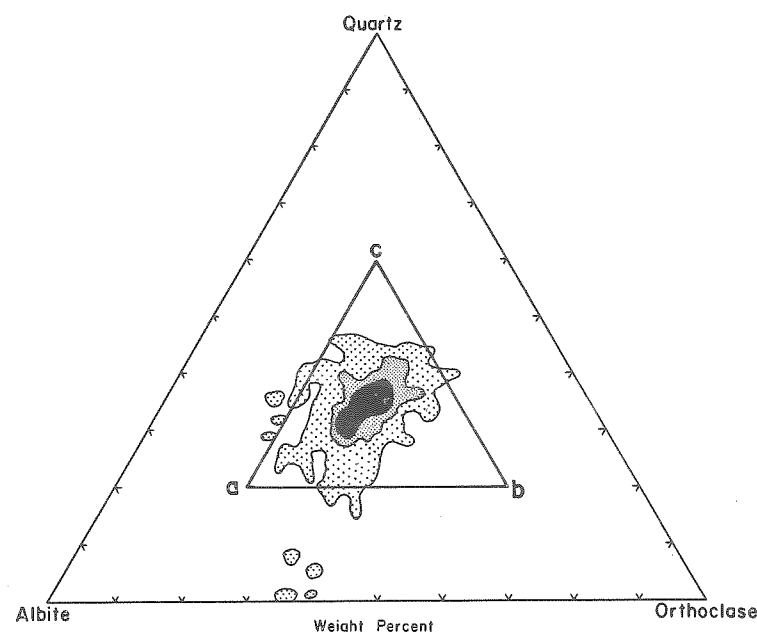


FIGURE 63.—Contoured triangular diagram showing the distribution of normative Ab-Or-Q in all analyzed rocks (1269) in Washington's Tables containing 80 per cent or more Ab + Or + Q

The triangle *abc* indicates the compositions considered to be granites (or rhyolites) in the present classification of salic rocks. It is suggested that rocks falling outside the area *abc* should be called something other than granite to indicate that they are rare compared with the "average" granite or rhyolite.

significance, and it is undesirable to camouflage this fact by dissecting this maximum with divisional boundaries.

The experimental results presented here suggest that granites, syenites, and nepheline syenites—rocks of "petrogeny's residua system" (Bowen, 1937)—may be classified on the basis of the distribution of the sodium feldspar between the plagioclase and potassium-feldspar components of these rocks. In some granitic rocks all the sodium feldspar is present as a component of perthite which has formed by unmixing during cooling, indicating that the rock crystallized at a temperature above the solvus in the binary system  $\text{NaAlSi}_3\text{O}_8$ – $\text{KAlSi}_3\text{O}_8$ . The temperature of crystallization was therefore higher than 660°C. and perhaps as high as 900°C. The survival of perthite in these granites also suggests either extremely rapid cooling or absence of volatile fluxes such as water vapor, because laboratory experiments show that un-

mixing of the sodium feldspar takes place in a few days if water vapor is present to flux the reaction. In those granites containing sodium feldspar in addition to potassium feldspar the albite content of the potassium phase is a measure of the temperature of final crystallization. However, as discussed in the following section, it is believed that many granitic rocks containing discrete plagioclase crystals recrystallized subsequent to magmatic crystallization, and the sodium content of the potassium feldspar is a measure of the final temperature at which recrystallization took place rather than the temperature of magmatic crystallization. The amount of solid solution is therefore a measure of the minimum temperature at which the feldspar could have formed under equilibrium conditions.

Turning now to the classification of the rocks whose compositions place them in or near "petrogeny's residua system", we can first divide these rocks into two broad groups:

(I) Hypersolvus granites, syenites, and nepheline syenites, characterized by the absence of plagioclase except as a component of perthite.

(II) Subsolvus granites, syenites, and nepheline syenites, characterized by both potassium feldspar and plagioclase feldspar.

Group (II) can be further divided into three subgroups on the basis of the albite content of the alkali feldspar:

(A) Ab of potassium feldspar >30 per cent by weight.

(B) Ab of potassium feldspar <30 and >15 per cent by weight.

(C) Ab of potassium feldspar <15 per cent by weight.

This is a genetic classification in the sense that Groups I and IIA can be considered high-temperature rocks (and therefore undoubtedly owe their origin to magmatic processes), whereas rocks in Group IIC completed crystallization or recrystallization at low temperatures. Group IIB occupies an intermediate position between IIA and IIC. Replacement or metasomatic rocks will undoubtedly fall in IIC, but, as has been pointed out elsewhere (Tuttle, 1952), the fact that a rock falls in this group is not evidence that it has not had a magmatic history because unmixing of plagioclase from potassium feldspar can and must go on if cooling has taken place in the presence of volatile materials which flux such a reaction.

It would appear that a diligent search for criteria for distinguishing IIC rocks having a magmatic history from IIC low-temperature replacement rocks will reveal diagnostic differences.

Obviously the above classification can apply only to rocks having the requisite composition—that is, in order to have 30 per cent albite in solid solution in the potassium feldspar the rock must contain at least this amount of sodium feldspar in the norm. Most granites, as here defined, have the appropriate composition (Fig. 42), and there is little doubt that most syenites and nepheline syenites also have the required amount of albite.

The above classes of salic rocks can be further subdivided on the basis of the alkali-feldspar modification. Only three subdivisions are considered here although many other combinations are known. For example, the following phases may be found in a single alkali feldspar crystal from the Beinn an Dubhaich granite: (1)

high albite, (2) low albite, (3) monoclinic potassium feldspar, and (4) triclinic potassium feldspar. Feldspars can be placed in or between the groups by measuring 2V and using the graph proposed by Tuttle (1952, p. 557).

- (I) Hypersolvus Granites, Syenites, and Nepheline Syenites
  - (1) sanidine-high-albite perthite
  - (2) orthoclase-high-albite perthite
  - (3) microcline-low-albite perthite
- (II) Subsolvus Granites, Syenites, and Nepheline Syenites
  - (A) potassium feldspar composition Ab > 30 per cent
    - (1) sanidine-high-albite perthite
    - (2) orthoclase-low-albite perthite
    - (3) microcline-low-albite perthite
  - (B) potassium feldspar composition Ab < 30 and > 15 per cent
    - (1) sanidine-high-albite perthite
    - (2) orthoclase-low-albite perthite
    - (3) microcline-low-albite perthite
  - (C) potassium feldspar composition Ab < 15 per cent
    - (1) orthoclase-low-albite perthite
    - (2) microcline-low-albite perthite
    - (3) microcline

The above classification requires that the petrographer examine the rocks in more than a cursory manner. It will be necessary in most cases to isolate the potassium feldspar and to analyze it chemically or by the X-ray method using the (201) spacing (Bowen and Tuttle, 1950). In some rocks a careful linear analysis and a chemical analysis of the rock will suffice. In any event, the classification requires both chemical and modal information.

This is a classification of salic rocks which contain 80 per cent or more normative quartz + albite + orthoclase + nepheline + leucite + kaliophilite with the relative amounts of these constituents, placing the total composition in or near Bowen's thermal valley (Bowen, 1937, p. 12). The general principle of the classification can perhaps eventually be extended to other compositions (rock types), but at present it is undesirable because the influence of lime on the solubility of sodium feldspar in the potassium feldspar is known only qualitatively.

#### FELDSPAR CRYSTALLIZATION IN RHYOLITES, TRACHYTES, AND PHONOLITES

##### FELDSPAR EQUILIBRIA

The suggestion that many two-feldspar granites may have gone through a sanidine-quartz or one-feldspar stage during initial magmatic crystallization has been questioned by some petrologists because rhyolites may carry two feldspars. This chapter demonstrates that the two feldspars found in rhyolites are not incompatible with this thesis.

The appearance of two feldspars during crystallization in rhyolitic, trachytic, and phonolitic magmas depends to a large extent upon the amount of solid solution between the feldspars and on the temperature of crystallization. If the potassium, sodium, and lime feldspars are completely miscible in each other at magmatic temperatures, then obviously only one feldspar, a ternary solid solution, will precipitate during crystallization. On the other hand, if solid solution is limited to the binary systems,  $\text{NaAlSi}_3\text{O}_8$ - $\text{CaAl}_2\text{Si}_2\text{O}_8$  and  $\text{NaAlSi}_3\text{O}_8$ - $\text{KAlSi}_3\text{O}_8$ , two feldspars will precipitate during crystallization if the magma carries all three in solution. The composi-

tional variations in the feldspars of these rocks indicate that the actual relations are intermediate between these two extremes—that is, limited ternary solid solution at high temperatures decreasing at lower temperatures.

It will be necessary to turn to the rocks and minerals for evidence because experimental studies have not been carried out on the appropriate compositions. The evidence does not permit a detailed discussion of the feldspar equilibria; nevertheless the general trend of crystallization and the position of the solidus in the ternary system  $\text{NaAlSi}_3\text{O}_8$ - $\text{KAlSi}_3\text{O}_8$ - $\text{CaAl}_2\text{Si}_2\text{O}_8$  can be located approximately for those extrusives carrying large amounts of normative alkali feldspars (trachytes).

##### SOLID SOLUTION IN THE SYSTEM $\text{NaAlSi}_3\text{O}_8$ - $\text{KAlSi}_3\text{O}_8$ - $\text{CaAl}_2\text{Si}_2\text{O}_8$

The extent of solid solution between albite, orthoclase, and anorthite depends largely upon the temperature of crystallization. It is expected that the maximum solid solution will be found in feldspars prepared at solidus temperatures in the dry system  $\text{NaAlSi}_3\text{O}_8$ - $\text{KAlSi}_3\text{O}_8$ - $\text{CaAl}_2\text{Si}_2\text{O}_8$ . In the igneous rocks the maximum solid solution will be found in the trachytic rocks in which compositions closely approach this system. Solid solution will be least extensive in the feldspars of low-temperature rocks such as hydrothermal veins or in those rocks which have recrystallized at low temperatures. The temperatures of crystallization of feldspars in the salic igneous rocks are expected to be highest in trachytes, and somewhat lower in rhyolites and phonolites where the liquidus temperatures are lowered by silica and nepheline, respectively. The presence of volatile constituents such as water and carbon dioxide, which may dissolve in the magma, may of course have a pronounced effect on the temperature of crystallization (Fig. 26).

The extent of solid solution between the feldspars may be estimated by noting their compositional variations in the igneous rocks. Figure 64 shows these variations; the analyses are those compiled by Vogt (1926) plus many recent analyses added by the writer. The curve  $LK_sP$  shows the approximate extent of solid solution in the feldspars of the extrusive rocks. Those points near the curve represent feldspars which have crystallized at high temperatures, probably in relatively dry trachytic and andesitic lavas. The extent of solid solution in the dry system  $\text{NaAlSi}_3\text{O}_8$ - $\text{KAlSi}_3\text{O}_8$ - $\text{CaAl}_2\text{Si}_2\text{O}_8$  will be somewhat greater than that given by the curve  $LK_sP$ .

##### CRYSTALLIZATION IN THE SYSTEM $\text{NaAlSi}_3\text{O}_8$ - $\text{KAlSi}_3\text{O}_8$ - $\text{CaAl}_2\text{Si}_2\text{O}_8$

As experimental studies of the compositions of coexisting liquids and crystals have not been carried out in this system, we must turn to the extrusive rocks for the information necessary to construct an equilibrium diagram. Such a diagram (Fig. 64) has been prepared from data in the literature on the composition of two coexisting feldspars and the host rock or the groundmass in extrusive rocks (e.g., Larsen *et al.*, 1938, p. 421; Vogt, 1926, p. 83). Although this information does not permit the drawing of a precise equilibrium diagram, the general relations are certainly correct and can be used to describe crystallization in the salic rocks. The diagram is characterized by a single-field boundary  $K_LD$  representing the composition of liquids in equilibrium with two feldspars (the incongruent melting of orthoclase is neglected). Perhaps the most novel feature of the diagram is that this field boundary crosses, in projection, the solidus curve  $LK_sP$  and ends at point  $K_L$ ; it does not extend to the



Ab-Or sideline. This relationship has important consequences and is the principal feature to be discussed here.

The curve  $LK_sP$  can be considered to represent the compositions of two feldspars ( $L$  to  $K_s$  and  $P$  to  $K_s$ ) coexisting with a liquid. (Point  $K_s$  represents the composition

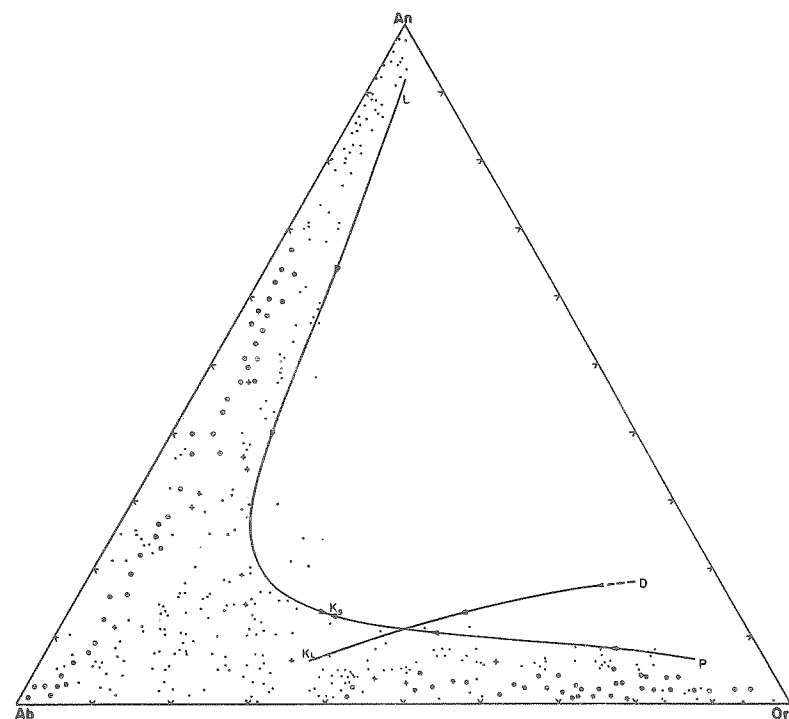


FIGURE 64.—Ternary diagram of the system  $\text{NaAlSi}_3\text{O}_8$ - $\text{KAlSi}_3\text{O}_8$ - $\text{CaAl}_2\text{Si}_2\text{O}_8$

Large dots represent the composition of seven analyzed feldspars having essentially the same compositions. The small dots represent single analyses of feldspars; the plus signs give the composition of analyzed feldspars examined by the authors. The approximate limit of solid solution under conditions expected in trachytic magmas is given by the curve  $LK_sP$ . Feldspars having compositions along the curves  $LK_s$  and  $PK_s$  are in equilibrium with liquids having compositions along  $DK_L$ . At the temperature of  $K_s$  a single feldspar is in equilibrium with the liquid at  $K_L$ . The arrows indicate the direction of falling temperatures.

of a single feldspar in equilibrium with liquid  $K_L$ ). The arrows indicate falling temperatures during crystallization. The curve  $K_LD$  is the boundary between the fields of potassium feldspar and plagioclase feldspar and represents the compositions of liquids in equilibrium with two feldspars whose compositions lie along the curve  $LK_sP$ . Figure 64 shows the approximate equilibrium relationships for trachytic rocks in which the proportion of constituents other than the three feldspars is not great and the temperature of crystallization is high.

Figure 65 illustrates crystallization in the system. If we consider the liquid of composition  $Y$ , the first crystalline phase to appear is a plagioclase feldspar having

a composition near  $C'$  but with an anorthite content somewhat greater than  $C'$ . As the temperature falls, the liquid changes composition toward the point  $C_L$ , and when the temperature reaches  $T_{cL}$  the plagioclase (now  $C'$ ) is joined by a potassium feldspar having the composition  $C$ . On further equilibrium crystallization the composi-

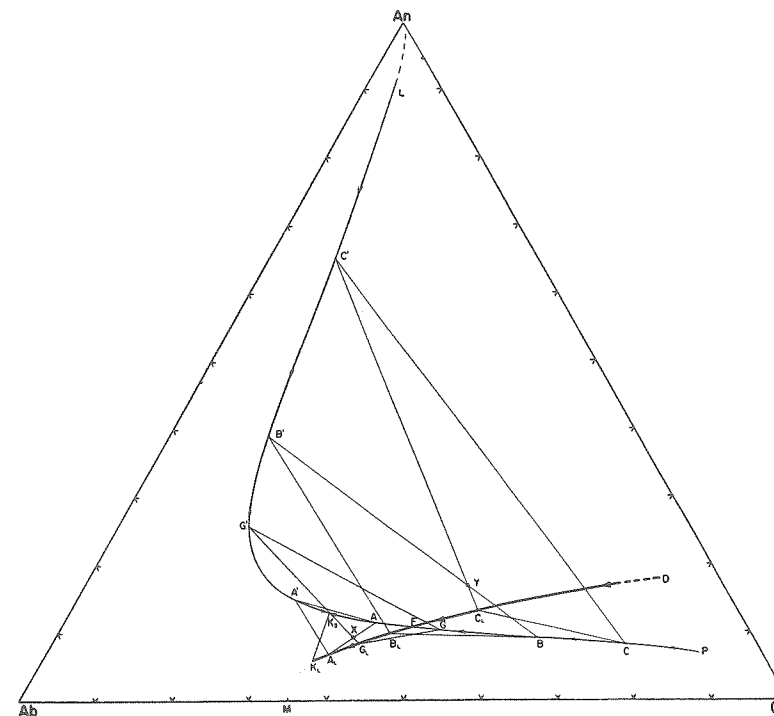


FIGURE 65.—Ternary diagram of the system  $\text{NaAlSi}_3\text{O}_8$ - $\text{KAlSi}_3\text{O}_8$ - $\text{CaAl}_2\text{Si}_2\text{O}_8$

Shows the approximate compositions of liquids coexisting in equilibrium with two feldspars. The temperatures represented by this diagram are relatively high and are believed to be comparable to those existing in the trachytic lavas. Arrows indicate direction of falling temperatures. The general trend of crystallization in trachytic, rhyolitic, and phonolitic magmas is discussed in the text with the aid of this diagram. The field boundary has been located by examining analyses of extrusive rocks in which the feldspar phenocrysts have also been analyzed and by noting the composition of two analyzed feldspars coexisting in extrusive rocks, in which the rock or the groundmass has also been analyzed. The general nature of the equilibrium relationships shown in this diagram were deduced by J. W. Greig (Personal communication).

tion of the liquid moves along the field boundary until it reaches  $B_L$ , at which time the last trace of liquid is used, and the crystals will have the composition  $B$  and  $B'$ . During crystallization the plagioclase crystals react with the liquid and change composition from  $C'$  to  $B'$ , and the potassium feldspar crystals from  $C$  to  $B$ . Throughout the area to the right of the solidus curve  $LK_sP$  equilibrium crystallization is of this type—that is, the initial feldspar crystallizes until the field boundary is reached, after which the second feldspar crystallizes along with the first, reacting with the liquid until all the liquid is used. Compositions in the area  $K_sK_LF$  have a consider-

ably more complicated crystallization history; the composition  $X$  illustrates this. A mixture having this composition crystallizes plagioclase having an anorthite content initially somewhat greater than  $G'$ ; the separation of these crystals changes the composition of the liquid along a curved path to  $G_L$  at which temperature the crystals have the composition  $G'$ . At this temperature potassium feldspar having the composition  $G$  begins to separate, and the liquid changes composition along the field boundary to  $A_L$  at which temperature the mixture consists of an alkali feldspar  $A$ , liquid  $A_L$ , and a trace of plagioclase crystals having the composition  $A'$ . During crystallization from  $G_L$  to  $A_L$  the plagioclase reacts with the liquid continuously and changes composition from  $G'$  to  $A'$ , while the alkali feldspar also reacts with the liquid and changes composition from  $G$  to  $A$ . At a temperature just below that of  $A_L$  all the plagioclase crystals have reacted with the liquid, and the mixture now consists of approximately equal amounts of an alkali feldspar having a composition very near  $A$  and a liquid whose composition is essentially that of  $A_L$ . Further crystallization will result in the liquid composition leaving the field boundary and moving toward the Ab-Or sideline while the crystals move in composition toward  $X$ . Crystallization will finally be completed when the crystals reach the composition  $X$  and the last trace of liquid has been used.

In the area  $K_sK_LF$  crystallization is characterized by the early separation of plagioclase followed by an alkali feldspar; the plagioclase reacts with the liquid and finally disappears leaving an alkali feldspar and liquid. Crystallization ends when the alkali feldspar crystals react with the liquid and attain the composition of the initial mixture. Thus all compositions below the curve  $G'A'K_sC$  will finish crystallization as a single homogeneous feldspar although some will crystallize two feldspars early in the crystallization history. *It is suggested that the plagioclase phenocrysts in many trachytes, phonolites, and rhyolites will react with the liquid in this fashion and give way to a single alkali feldspar during a later stage of crystallization; and therefore the presence of plagioclase and alkali feldspar phenocrysts is no proof that two feldspars will continue to crystallize throughout the crystallization history of the magma.*

The probability that crystallization will end with a single alkali feldspar separating from liquids of trachytic, phonolitic, and rhyolitic composition is much greater if there is an element of fractionation during crystallization. For example, during equilibrium crystallization the composition represented by  $Y$  (Fig. 65) completed crystallization at  $B_L$  with two feldspars. Now if the early plagioclase did not react with the liquid, say by zoning, the liquid would move on toward  $K_L$ , and at a point between  $G_L$  and  $A_L$  would leave the field boundary and change composition along a curved path to  $M$ , the minimum of the binary system Ab-Or. Thus, with fractional crystallization, compositions above the curve  $G'K_sP$  may, during final crystallization, precipitate a single alkali feldspar. Crystallization under these circumstances would produce a syenite, nepheline syenite, or granite in which some of the alkali feldspar crystals would have a core of plagioclase. Such a relationship has been noted by many petrologists. Alkali feldspars with cores of plagioclase are very common in the Adirondack igneous rocks, for example; Buddington (1939) described cores of plagioclase in granites, syenites, quartz syenites, and shonkinites. He reports (p. 79): "Plagioclase, forming the core of large feldspar crystals, varies from one-third to one-fifth of the

total feldspar. The plagioclase of the core of these large crystals is more calcic than that of the intergrowth in the microperthite . . ." and (p. 80) "Feldspar forms in general 70 to 79 per cent of the rock and consists of a core of plagioclase surrounded by a zone of microperthite. The plagioclase is commonly andesine and ranges from

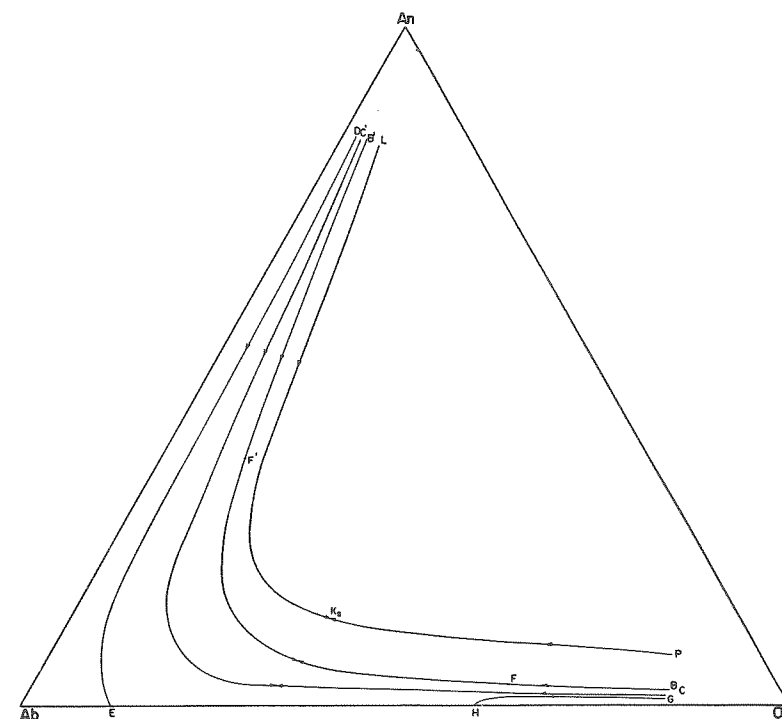


FIGURE 66.—Ternary diagram illustrating the probable extent of solid solution in the system  $\text{NaAlSi}_3\text{O}_8$ - $\text{KAlSi}_3\text{O}_8$ - $\text{CaAl}_2\text{Si}_2\text{O}_8$  at four different temperature ranges

The variations in temperature result from solution of materials in the liquid. The principal ingredients which cause a temperature lowering in the salic rocks are silica, nepheline, and water.

$\text{Ab}_{70}\text{An}_{30}$  to  $\text{Ab}_{62}\text{An}_{38}$ . . . ." (See also Buddington, 1939, p. 77, 81, 87, 104, 288, etc.) Similar relations have been noted by Iddings (1895, p. 940), Washington (1906, p. 431), Ito (1925, p. 105), Yagi (1953, p. 978), and others.

#### EFFECT OF COMPOSITION ON THE EXTENT OF SOLID SOLUTION

With some exceptions the general crystallization relations discussed above for high temperatures in the system  $\text{NaAlSi}_3\text{O}_8$ - $\text{KAlSi}_3\text{O}_8$ - $\text{CaAl}_2\text{Si}_2\text{O}_8$  will hold for the lower temperatures of rhyolites and phonolites. Figure 66 illustrates the relations expected at four different temperature ranges. Each curve represents the compositions of two feldspars which can coexist in equilibrium with a liquid. For example, curve  $B'F'FB$  represents the composition of two feldspars in equilibrium with a liquid at a lower temperature than that of the dry system; the temperature lowering could result from the solution of silica, nepheline, water, or other materials not taken

into solid solution in the feldspars. The points  $F'$  and  $F$  are, in fact, the compositions of two analyzed feldspars from an obsidian studied by Larsen (1938). Here the liquidus lowering is probably produced by silica, as the rock is a rhyolite. The curve  $CC'$  illustrates similar relationships at a still lower temperature, and  $DE-HG$  at tempera-

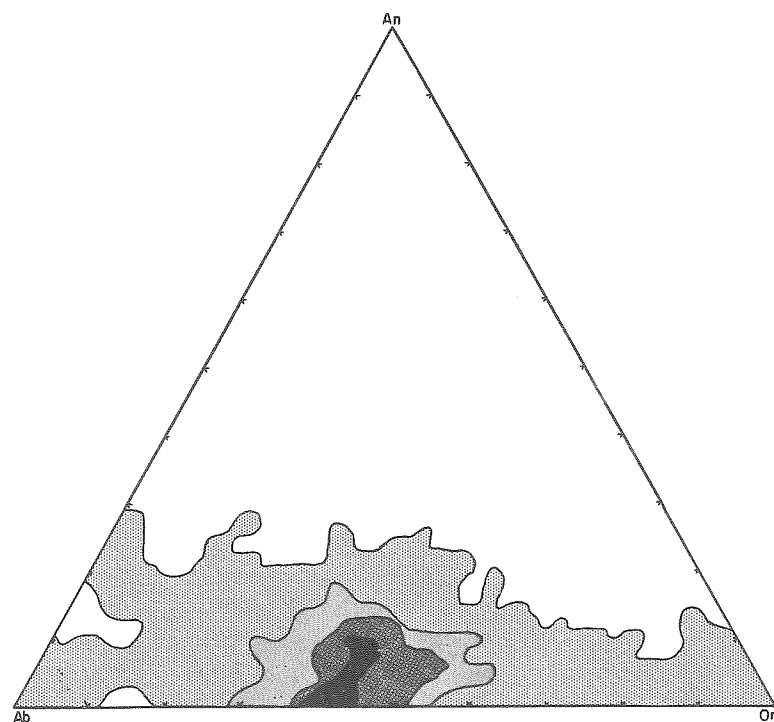


FIGURE 67.—Contour diagram illustrating the distribution of normative Ab, Or, An in all the analyzed rocks in Washington's Tables (1269) that carry 80 per cent or more normative Ab + Or + Q

Contours more than 1, 2, 3, 4, 5, and 6 per cent. 0.25 per cent counter

tures where two feldspars can coexist in equilibrium with liquid when no anorthite is present. The latter relationship was found in synthetic granites at water-vapor pressures above about 3500 kg/cm<sup>2</sup>.

The solid-solution relations depicted by curve  $LK_sP$  represents temperatures expected in dry trachytic magmas, curve  $B'F'FB$  in relatively dry rhyolites or phonolites, and perhaps trachytes carrying large amounts of water; curve  $CC'$  in rhyolites and phonolites with high water contents; and curves  $DE$  and  $HG$  in rhyolites and phonolites with very high water content.

The appearance of plagioclase early in the crystallization history of granites, syenites, and nepheline syenites is strongly dependent upon the amount of lime present in the magma. If there is little lime the possibility of plagioclase appearing during crystallization is highly improbable, whereas if the lime content is high plagioclase

will certainly be one of the earliest phases to begin crystallizing. Figure 67 shows the normative anorthite content of 1269 analyzed rocks containing 80 per cent or more normative quartz + albite + orthoclase (this represents all the rocks in Washington's Tables (1917) that have 80 per cent or more normative quartz + albite + orthoclase). The diagram is contoured to show the distribution of analyses as in Figures 41 and 42. More than 40 per cent of all the analyses have anorthite values that place them to the left and below curve  $B'F'FB$  of Figure 66. All these rocks have compositions which are expected to finish crystallization with a single alkali feldspar, with or without a core of plagioclase. The normative anorthite in 80 per cent of the 1269 analyses places them to the left and below curve  $LK_sP$ . Trachytic rocks having contents of normative anorthite which place them between the curves  $LK_sP$  and  $B'F'FB$  are expected to finish crystallization with a single alkali feldspar if the water content is low or if there has been some fractional crystallization. The rhyolites and phonolites falling in this compositional range are expected to finish crystallization with two feldspars unless fractionation has taken place.

#### SUMMARY

The presence of phenocrysts of two feldspars in the salic extrusive rocks cannot be considered proof that two feldspars will continue to crystallize throughout magmatic crystallization. The equilibrium relations deduced from a study of the feldspars of extrusive rocks indicate that plagioclase phenocrysts may react with the liquid and leave a single alkali feldspar. If fractionation takes place during crystallization, the possibility of completing crystallization with only a single feldspar is greatly enhanced.

#### EVOLUTION OF THE GRANITIC TEXTURE

The principal differences between hypersolvus and subsolvus (Type IIC) granites are: (1) the sodium feldspar is or was held in solid solution with the potassium feldspar in hypersolvus granites, whereas in the subsolvus granites the bulk of the sodium feldspar is present as discrete grains of albite or albite-oligoclase; (2) most or all hypersolvus granites carry an amphibole which is commonly a sodium-iron species, and the subsolvus granites (Type IIC) rarely or never carry a sodium-iron amphibole; (3) many hypersolvus granites carry a pyroxene which is in most cases a sodium-bearing variety, while few or no subsolvus granites carry such a pyroxene; (4) most of the hypersolvus granites are rather small intrusives, whereas the subsolvus granites may occur as small intrusive stocks and as large batholithic masses as well; (5) the contacts of most hypersolvus granites indicate that little metamorphism has been produced by the intrusives despite the high temperature of crystallization required by the feldspars, while the subsolvus granites may show evidence of profound contact metamorphism and granitization or little evidence of contact effects; (6) hypersolvus granites apparently do not carry the large zoned pegmatites which are characteristically found in subsolvus granites or in the adjacent contact rocks; (7) the hypersolvus granites do not carry muscovite, except perhaps as an alteration product of the feldspar, whereas the subsolvus granites commonly hold muscovite along with biotite; (8) the hypersolvus granites may or may not carry quartz which has inversion properties characteristic of the quartz of rhyolite, while the subsolvus granites

of Group IIC carry quartz whose inversion properties suggest a low temperature of crystallization or recrystallization; and (9) the hypersolvus granites may or may not carry feldspar having properties of high-temperature types, whereas subsolvus IIC granites do not carry such feldspars.

In general, these differences suggest that the hypersolvus granites have crystallized at a relatively high temperature, whereas the subsolvus granites of Group IIC have crystallized, or recrystallized, at a somewhat lower temperature and have certain characteristics which are not found in rhyolites yet which would be expected if these granites are magmatic with no subsequent recrystallization.

Our experimental studies suggest that properties of the hypersolvus granites indicate that they have crystallized at high temperatures from a magma. The laboratory studies also suggest that it is unlikely that the two feldspars having the compositions of the plagioclase and microcline of the IIC granites could have crystallized from a silicate melt. These differences immediately suggest that the hypersolvus granites are magmatic, whereas the IIC granites are metasomatic. This would indeed be a happy solution to the granite problem; however, the situation is somewhat more complicated, and the final answer to the problem is not yet in sight.

It has been proposed (Tuttle, 1952) that the granites of Group IIC were initially much like the hypersolvus granites and that unmixing of plagioclase from the potassium feldspar has taken place during cooling. If this is correct then all IIC granites must be considered possible magmatic granites that have changed their mineralogy and texture during cooling or by later metamorphism.

Equilibrium relations demand considerable unmixing, and the driving force for the change is the decreasing solubility between the sodium feldspar and the potassium feldspar with falling temperature. We now know that this driving force exerts itself in all but the most quickly cooled feldspars, for all natural feldspars having compositions near  $Ab_{50}Or_{50}$  consist of mixtures of nearly pure albite and pure potassium feldspar. To be sure, feldspars from extrusive rocks are optically homogeneous, but the X ray clearly shows that the unmixing has taken place. These finely unmixed feldspars can be made homogeneous by heating to about  $660^{\circ}C.$ ; they can then be quenched without unmixing by rapid cooling. If such homogeneous feldspars are heated at temperatures below the binary solvus in the presence of water vapor under pressure they will again unmix in a few days. Unmixing in these labora-

#### PLATE 1.—INTERGROWTHS IN SULFIDES AND FELDSPARS

FIGURES 1, 2.—Chalcopyrite-bornite specimens from Bisbee, Arizona. (1) Heated 41 hours at  $700^{\circ}C.$  and cooled in air.  $\times 100$ . (2) Heated to  $600^{\circ}C.$  and cooled slowly for 24 hours.  $\times 50$ . This specimen showed the texture of (1) before the slow cooling. Note that in (1) unmixing has taken place along grain boundaries as well as within the grains. Unmixing in (2) has completely separated the two phases leaving no evidence of the former intergrowth. It is believed that many and perhaps all two-feldspar granites have undergone similar recrystallization and unmixing during cooling. After G. M. Schwartz (1931, p. 195).

FIGURE 3.—Granite from Quincy, Massachusetts. Photograph of thin section of granite in which unmixing in the alkali feldspars has taken place within the grains and along grain boundaries. This texture is analogous to Figure 1. This is believed to represent an intermediate stage between a perthite-quartz granite illustrated in Plate 2 and a granite made up of discrete grains of microcline, plagioclase, and quartz. Potassium feldspar stained.

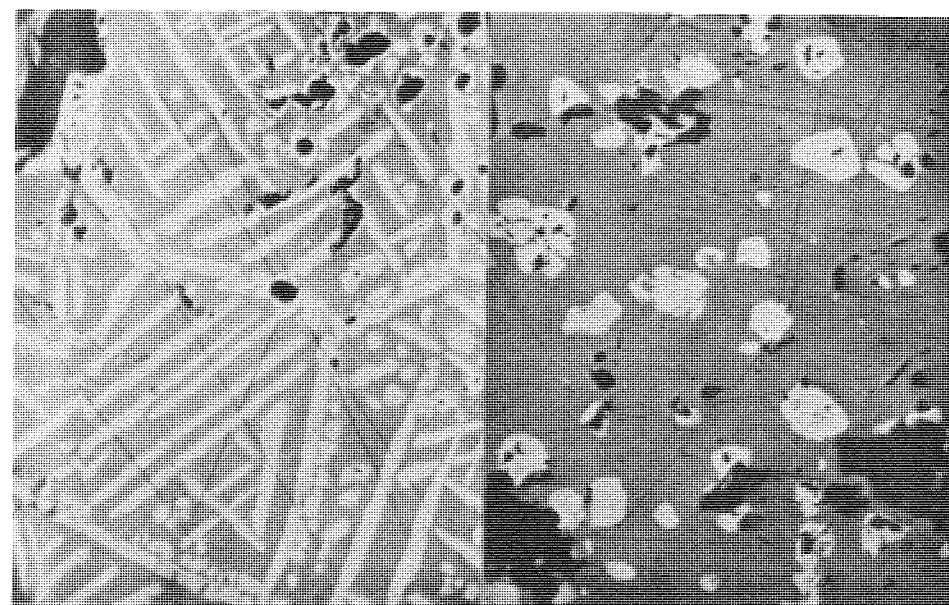


FIGURE 1

FIGURE 2

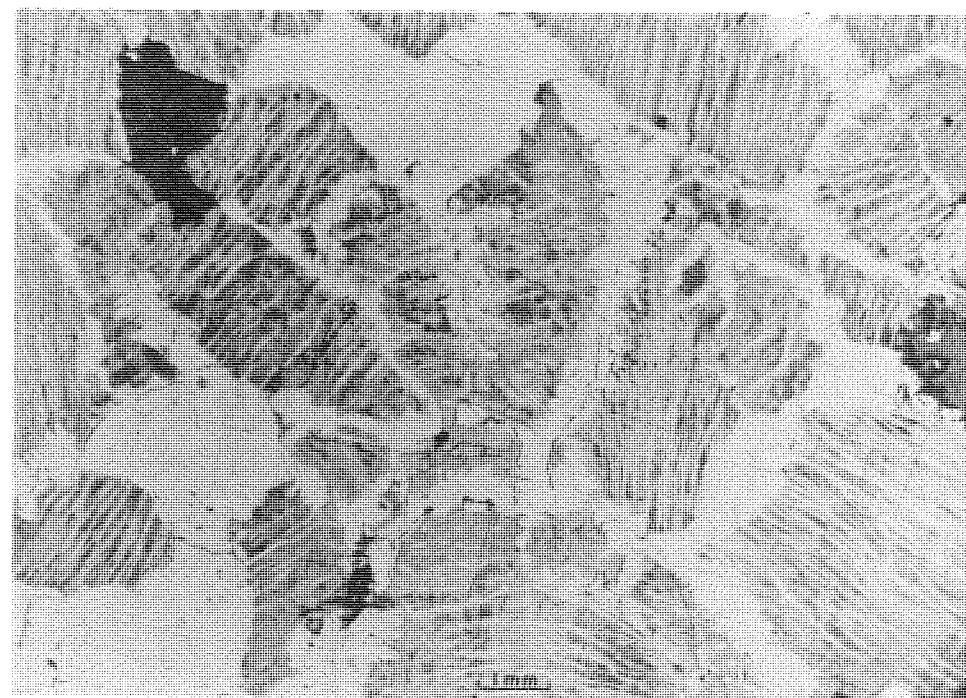
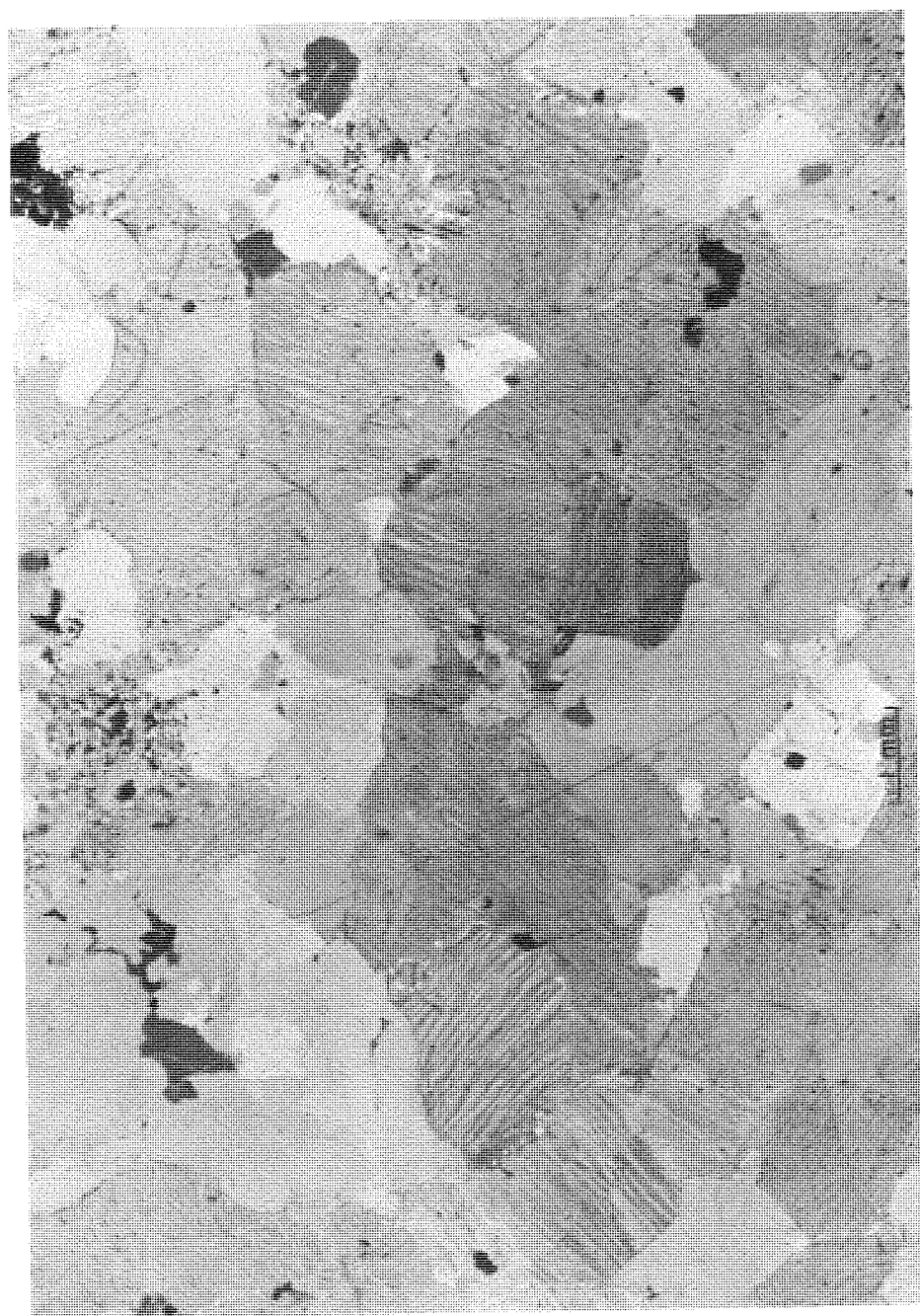


FIGURE 3

#### INTERGROWTHS IN SULFIDES AND FELDSPARS





GRANITE FROM MADOC, ONTARIO

tory experiments is surprisingly rapid, and it appears impossible for granites to retain any suggestion of the initial homogeneous feldspar. When one considers that a granite may require several millions of years to cool it is not difficult to accept unmixing in most granites; rather, it is difficult to understand how the hypersolvus granites managed to escape further unmixing and recrystallization. The fluxing power of volatile materials provides an answer to this quandary. If a granite cools in the presence of a copious supply of volatile materials unmixing will take place readily, and it is expected that potassium and sodium feldspar will separate completely under these circumstances with no evidence that the rock began its subsolidus history as a quartz-sandine rock containing little or no plagioclase feldspar as discrete grains. On the other hand if all the volatile materials are used, or escape, during crystallization, slow cooling will not produce complete unmixing. Unmixing will proceed to the cryptoperthite or perthite stage, but the hypersolvus character of the granite will be preserved.

It will be very difficult if not impossible to produce unmixing of the first type (segregation of plagioclase into discrete grains with no perthitic texture) in silicates because laboratory experiments cannot duplicate the time factor which is so important in such a sluggish process. Unmixing can however be readily produced in the sulfides, and the experimental studies of Schwartz (1931) on bornite-chalcopyrite solid solutions produced both types of unmixing with a striking difference depending on the cooling rate. Schwartz writes (p. 196):

*"Unless the solid is drastically quenched, however, it breaks down and segregates with amazing rapidity into a crystallographic intergrowth of the subordinate mineral in the predominant one. A cooling time of five minutes from 600°C to room temperature allows sufficient segregation so that the intergrowth may be observed at a magnification of 75 diameters. Cooling in one hour allows segregation of some of the subordinate mineral to grain boundaries (see Pl. 1, fig. 1), and 24 hours in some cases results in complete segregation into grains (Pl. 1, fig. 2)."* (Italics added).

The crystallographic intergrowths which form on rapid cooling may segregate into discrete grains of one substance in another, directly analogous to the intergrowths of feldspars in the perthites of hypersolvus granites and the isolated plagioclase and microcline in the Group IIC subsolvus granites.

Schwartz was surprised to find that two phases could develop from a solid solution in such a fashion that no textural evidence of the former single phase could be discovered, and consequently he took special pains to check this point. He writes (p. 192):

*"The complete segregation of the minor constituent into grains is most surprising and bring out a fact which has been very little considered in geologic theory; that is, that even more or less granular mixtures of two constituents may represent a breakdown of a solid solution that existed at higher temperatures."* (Italics added).

PLATE 2.—GRANITE FROM MADOC, ONTARIO

Photograph of thin section of a granite in which the feldspar has unmixed to a fine intergrowth of sodium feldspar and potassium feldspar. Unmixing has taken place entirely within the original grains and the more advanced state of recrystallization shown in Figure 3 of Plate 1 has not been reached. Some thin sections of this granite, however, do show fine-grained albite at the borders. Unmixing and recrystallization in feldspars of this composition in the laboratory is extremely rapid when water vapor under pressure is present, and it is concluded that granites of this type must have cooled in a very dry environment.

The general nature of the unmixing process is well illustrated by these sulfides. The solid solution which produced the intergrowth of Figure 1 of Plate 1 was a homogeneous single phase on quenching in water, and on cooling rapidly in air a fine unmixing texture could be readily seen. In other words, it was necessary to cool in a few seconds to prevent the unmixing, and cooling in a few minutes produced the results shown in Figure 1 of Plate 1. The principal difference between rapid cooling in air and cooling in 5 minutes is that the faster cooling gave no unmixing along grain boundaries such as is shown in Figure 1 of Plate 1, and the lamellae are considerably thinner in the faster quench. Cooling in 24 hours gave the results illustrated in Figure 2 of Plate 1. Here there is complete segregation of the two phases with no textural evidence of the former presence of a single phase.

The perthitic intergrowths illustrated in Plate 2 from the Madoc, Ontario, granite are in many respects similar to the intergrowths in the bornite-chalcopryrite (Schwartz, 1931, Figs. 1, 2) which was cooled rapidly in air. For example, the unmixing has taken place entirely within the grains in both examples, and the intergrowths are uniformly fine-grained. The intergrowths illustrated in Figure 3 of Plate 1, a photograph of a thin section of the Quincy, Massachusetts, granite, are similar to Figure 1 of Plate 1, in that both show lamellar intergrowths as well as unmixing along grain boundaries. The Westerly granite shown in Plate 3 is analogous to the sulfide texture illustrated in Figure 2 of Plate 1.

The variations in the textures of the feldspars cannot be simply and directly related to cooling rates because of the influence of fluxes on these sluggish silicate reactions. However, the analogy with the sulfides is valuable in that it points up the fact that unmixing can occur within grains and along grain boundaries, and it is possible for the process to proceed until all textural evidence of unmixing disappears.

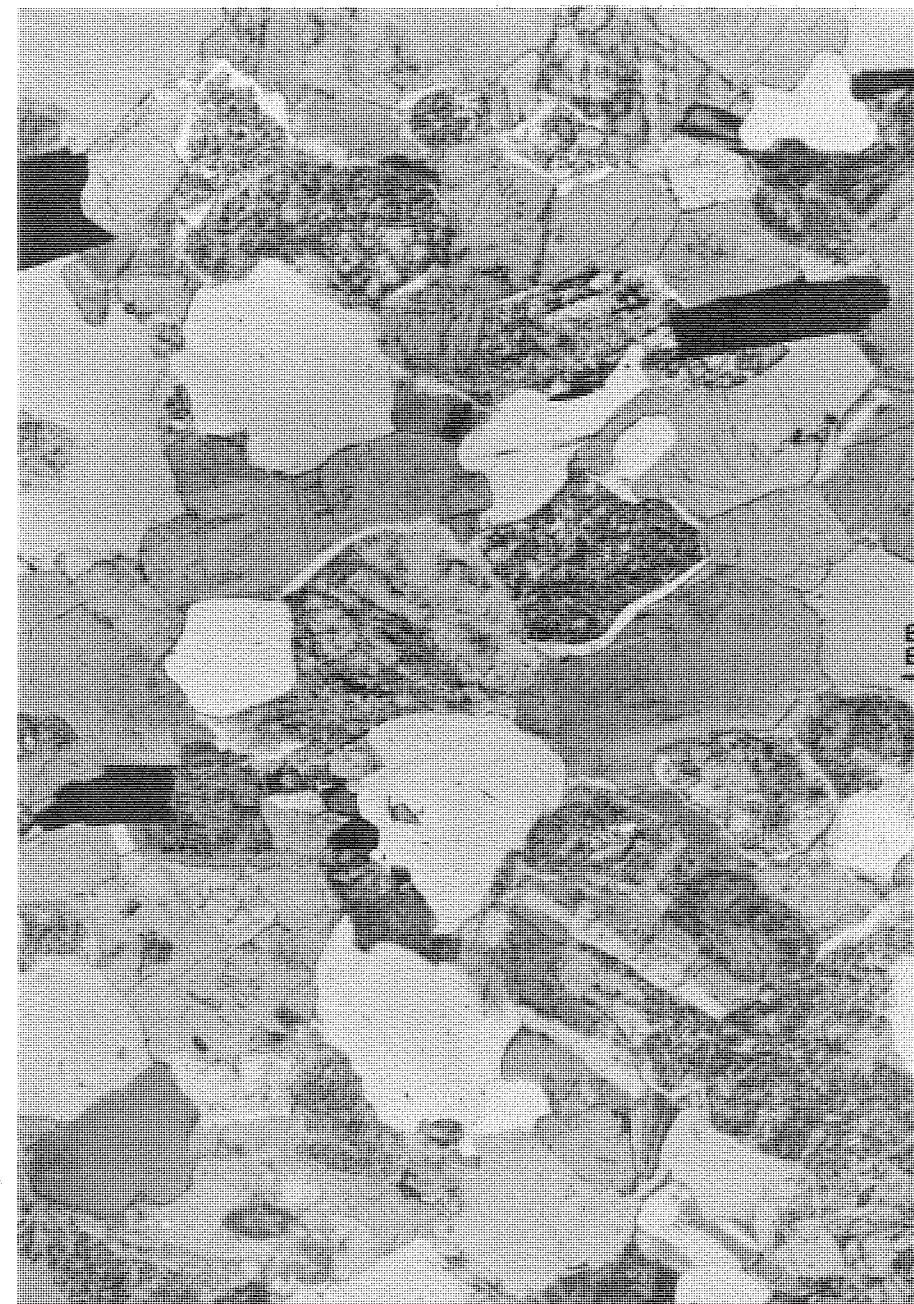
It is believed that the initial texture of all magmatic granites was much like that illustrated in Plates 2 and 6. Figure 1 of Plate 6 shows a thin section of the Beinn an Dubhaich granite, Island of Skye, Scotland. All the plagioclase is in solid solution in the alkali feldspar. The texture is granular and may be called granitic or saccharoidal. This texture is changed as unmixing proceeds and irregular plagioclase makes its appearance, particularly at the intersection of a number of grains. Plates 4 and 5 are photographs of a section of the Beinn an Dubhaich granite in which

#### PLATE 3.—GRANITE FROM WESTERLY, RHODE ISLAND

Photograph of thin section of the Westerly, Rhode Island, granite. This is a subsolvus (H.C.) granite believed to have originally carried much of, and perhaps all, the plagioclase in solid solution in the potassium feldspar. The clear rims between plagioclase and microcline are believed to represent late-stage unmixing. These have been described in detail elsewhere (Tuttle, 1952b). Potassium feldspar stained.

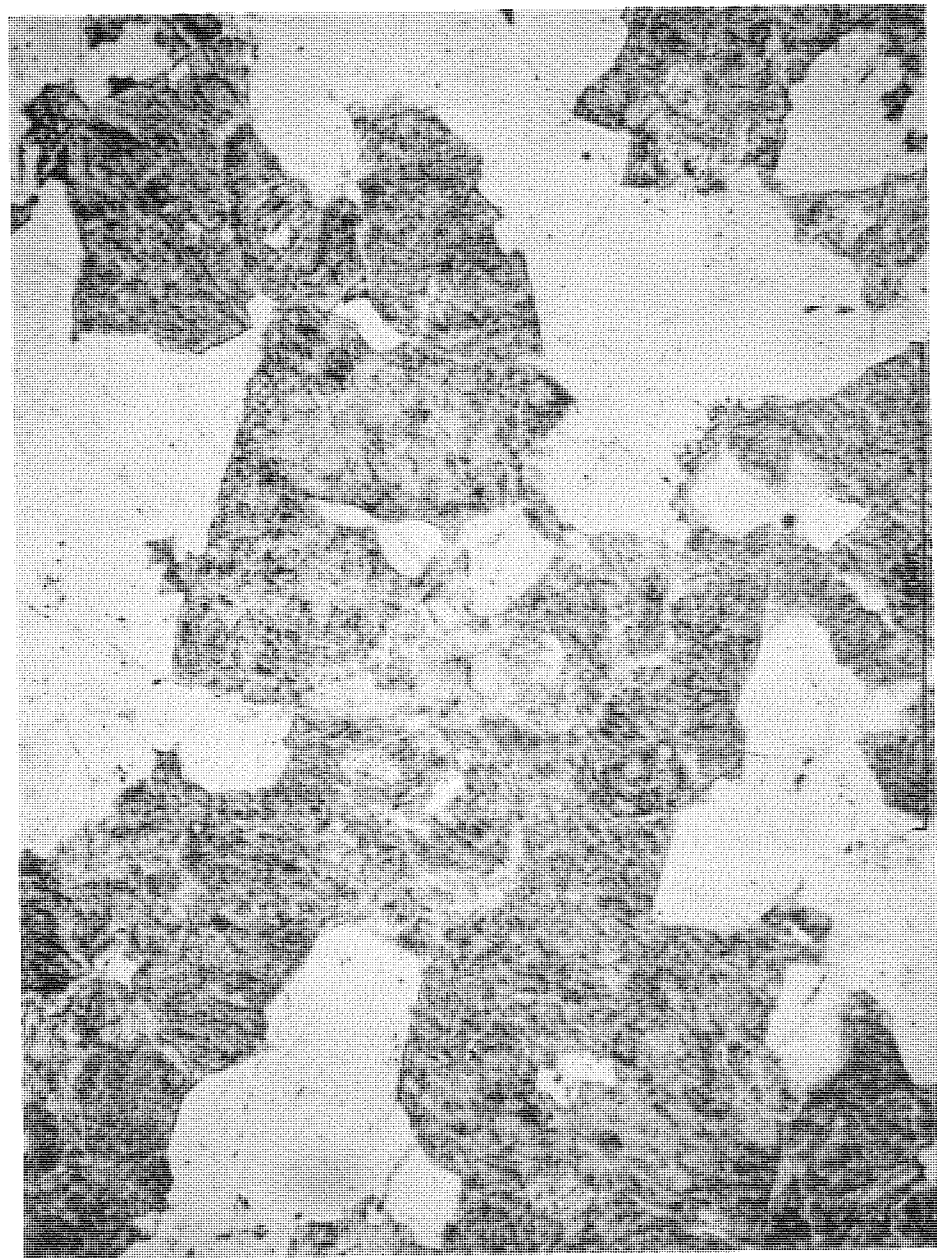
#### PLATE 4.—BEINN AN DUBHAICH GRANITE, SKYE, SCOTLAND

Photograph of a thin section of the Beinn an Dubhaich granite in which 12 per cent of the 33 normative per cent plagioclase is present as irregularly shaped grains which are believed to have unmixed from the potassium feldspar during cooling. Here the unmixing has not taken the form of perthite but has produced irregular plagioclase grains within the original sanidine grains. The potassium-rich feldspar still contains more than 35 per cent plagioclase as suboptical cryptoperthitic intergrowths. Plagioclase grains have been outlined in Plate 5.

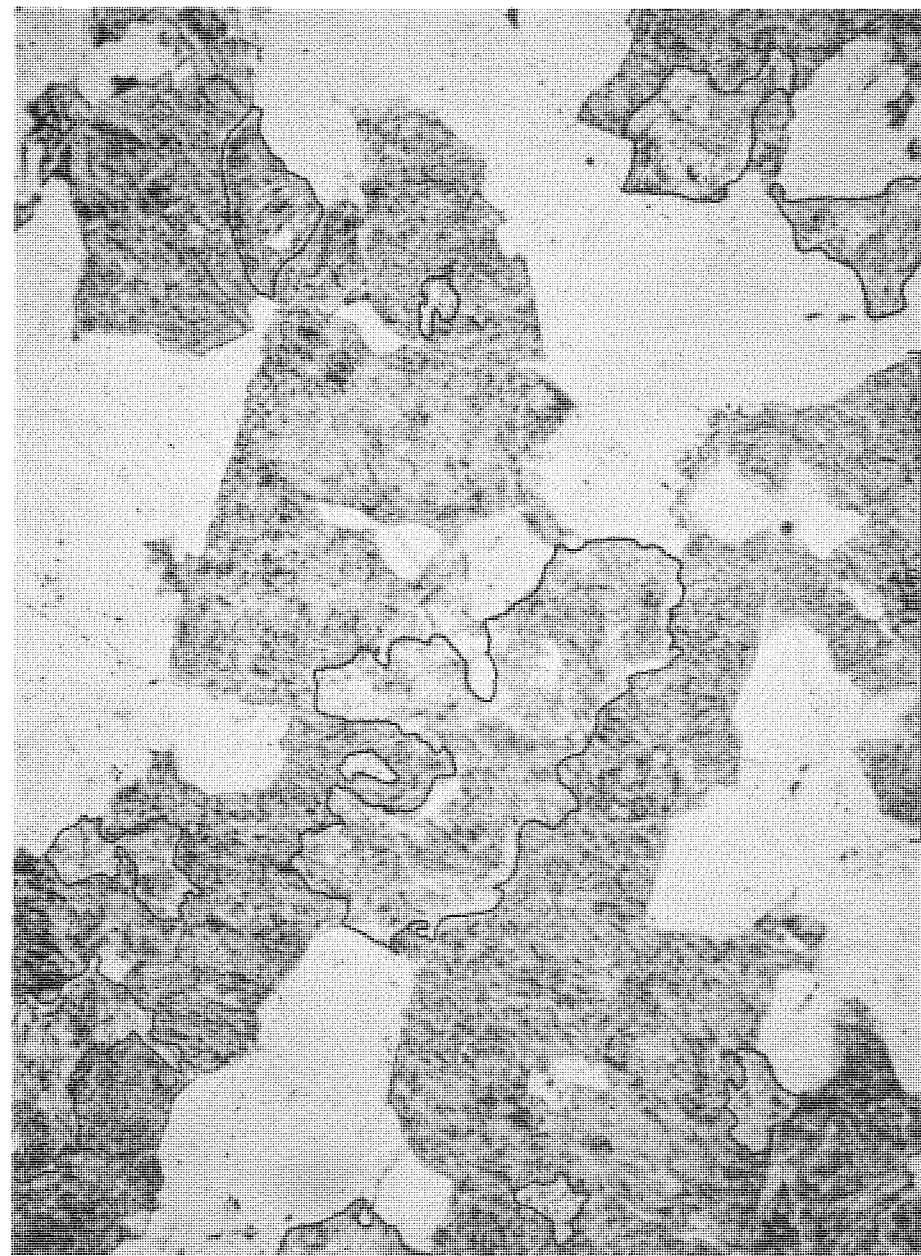


GRANITE FROM WESTERLY, RHODE ISLAND





BEINN AN DUBHAICH GRANITE, SKYE, SCOTLAND



BEINN AN DUBHAICH GRANITE, SKYE, SCOTLAND

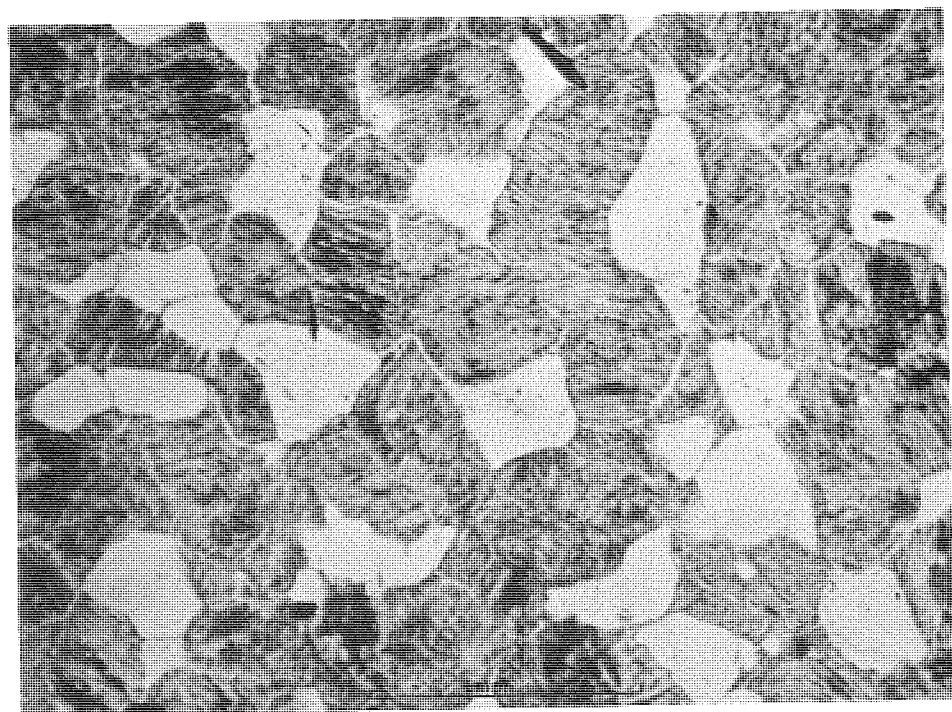


FIGURE 1

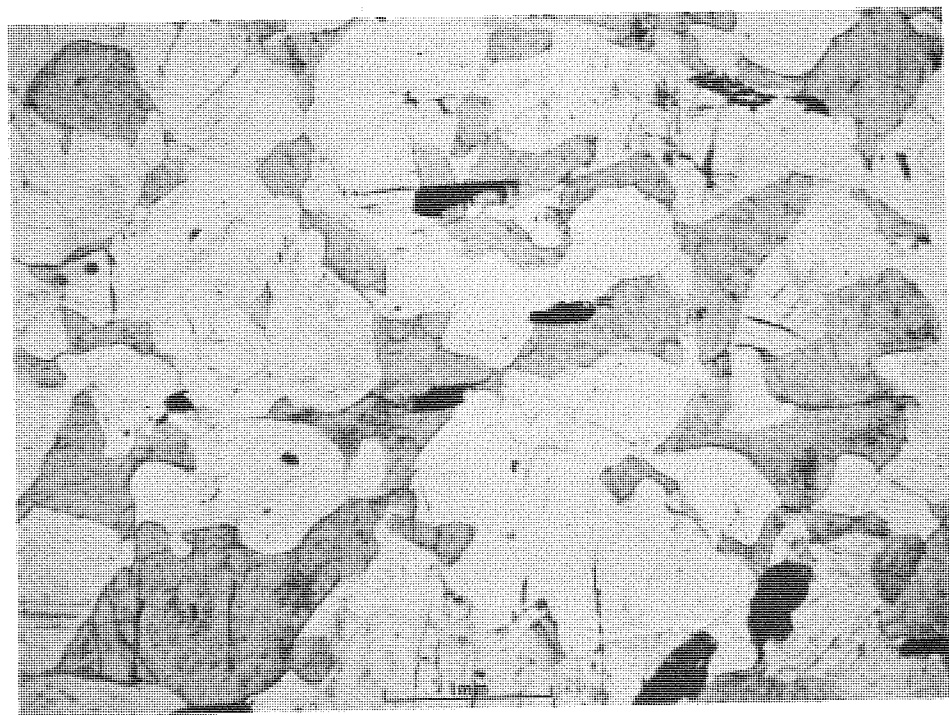


FIGURE 2

## HYPER SOLVUS AND SUBSOLVUS GRANITES

considerable plagioclase is present (12 per cent by volume). It is believed that this plagioclase has unmixed during cooling in the solid state. The alkali feldspar, however, still contains nearly 35 per cent albite in solid solution. Plate 5 illustrates the irregular shape of the plagioclase grains (in Plate 5 the plagioclase areas are outlined, whereas Plate 4 is the original photograph). The sinuous nature of the contact between the plagioclase and the alkali feldspar is believed to indicate that the plagioclase has unmixed from the alkali host by solid diffusion, perhaps aided by volatile fluxes, during the cooling of the Beinn an Dubhaich granite. It is not unusual to find an alkali feldspar grain with a Carlsbad twin in which the twin plane continues into the unmixed plagioclase feldspar. In such cases the plagioclase on one side of the twin plane under crossed nichols will be extinguished simultaneously with the perthitic plagioclase of the alkali feldspar on the same side of the twin plane, whereas the plagioclase on the opposite side of the twin plane will behave in a like manner toward the perthitic plagioclase on that side of the twin plane. The crystallographic continuity between the plagioclase and alkali feldspar of perthite is apparently also present between plagioclase grains which are not intergrown in perthite and a neighboring alkali feldspar grain, suggesting a possible method of determining whether or not the plagioclase of a IIC type granite has unmixed from the alkali feldspar.

At this stage the plagioclase may appear as large subhedral crystals, and it is suggested that these large plagioclases may also have grown by solid diffusion, but it is always possible that these crystals represent phenocrysts originally grown from the liquid. In some border facies of the Beinn an Dubhaich granite plagioclase and alkali feldspars appear as phenocrysts set in a fine-grained groundmass. These "phenocrysts" may owe their origin to magmatic crystallization, but the possibility of post-magmatic growth must also be considered.

Plates 1-6 represent some of the changes believed to be brought about in the texture of granites by unmixing and recrystallization. Figure 2 of Plate 6 is a photograph of a variant of the Pikes Peak granite. Here the microcline appears to fill the interstices between the plagioclase and quartz. For this reason Harker (1939) placed microcline at the bottom of the crystalloblastic series. The micas in this granite are well oriented and give the rock a distinct foliation. Many geologists would perhaps call this a metamorphic rock, but the general field relations plus the fact that it contains approximately equal amounts of plagioclase, microcline, and quartz strongly

## PLATE 5.—BEINN AN DUBHAICH GRANITE, SKYE, SCOTLAND

Same as Plate 4 except plagioclase grains have been outlined to show their irregular shapes.

## PLATE 6.—HYPER SOLVUS AND SUBSOLVUS GRANITES

FIGURE 1.—Photograph of thin section of the Beinn an Dubhaich granite, Skye, Scotland. This is a hypersolvus contact facies. No plagioclase feldspar is present except as lamellae in potassium feldspar. Potassium feldspar stained.

FIGURE 2.—Photograph of a thin section of granite from Colorado (a variant of the Pikes Peak granite). This is a subsolvus IIC granite in which a conspicuous foliation has developed as a result of alignment of the micas. The potassium feldspar in this rock shows no suggestion of crystal outlines such as can be seen in the hypersolvus granites of Figure 1. The potassium feldspar appears to fill the interstices between the plagioclase and quartz grains. This is believed to represent an advanced stage of recrystallization in granites. Potassium feldspar stained.



suggest that this is a normal magmatic granite which has experienced considerable recrystallization in addition to the unmixing of the feldspars.

Most granites apparently fall in the subsolvus IIC group and texturally lie between those illustrated in Plate 5 and Figure 2 of Plate 6.

In summary, the experimental results presented here demonstrate that many changes have taken place in: (1) the compositions of the minerals, (2) the polymorphic forms of the minerals, and (3) the textural relations among the minerals of the granites, syenites, and nepheline syenites between the time of final magmatic crystallization and observation under the petrographic microscope. A few of these changes have been described here, but many more complex reactions undoubtedly remain to be discovered. For example, probably the myrmekitic intergrowths, the altered cores of plagioclase, and the development of muscovite will be found to owe their origin to these post-crystallization reactions.

## REFERENCES CITED

- BAKKEN, RUTH, AND ROSENQVIST, I. TH. (1952) Note on different modifications of alkali feldspar, *Research*, vol. 5, p. 1-3.
- BIRCH, FRANCIS, *et al.*, Editors (1942) Handbook of physical constants, Geol. Soc. Am. Sp. Paper no. 36, 325 p.
- BOWEN, N. L. (1928) The evolution of the igneous rocks, Princeton, Princeton University Press, 332 p.
- (1937) Recent high-temperature research on silicates and its significance in igneous geology, *Am. Jour. Sci.*, vol. 33, p. 1-21.
- (1941) Certain singular points on crystallization curves of solid solutions, *Proc. Nat. Acad. Sci.*, vol. 27, p. 301-309.
- BOWEN, N. L., AND TUTTLE, O. F. (1949) The system  $MgO-SiO_2-H_2O$ , *Geol. Soc. Am., Bull.*, vol. 60, p. 439-460.
- (1950) The system  $NaAlSi_3O_8-KAlSi_3O_8-H_2O$ , *Jour. Geol.*, vol. 58, p. 489-511.
- BUDDINGTON, A. F. (1939) Adirondack igneous rocks and their metamorphism, *Geol. Soc. Am. Memoir* 7, 354 p.
- BUERGER, M. J. (1947) The relative importance of the several faces of a crystal, *Am. Min.*, vol. 32, p. 593-606.
- (1948) The role of temperature in mineralogy, *Am. Min.*, vol. 33, p. 101-121.
- BUNSEN, R. (1851) Ueber die Prozesse der vulkanischen Gesteinsbildungen Islands, *Pogg. Ann.*, vol. 83, p. 197-272.
- CHAYES, F. (1949) A simple point counter for thin-section analysis, *Am. Min.*, vol. 34, p. 1-11.
- CHAYES, F. (1950) Composition of some New England granites, *Trans. N. Y. Acad. Sci.*, ser. 2, vol. 12, p. 144-151.
- (1950) On the relation between anorthite content and  $\gamma$ -index of natural plagioclase, *Jour. Geol.*, vol. 58, p. 593-595.
- (1951) Modal composition of granites, *Carnegie Inst. of Washington Year Book*, no. 50, p. 41.
- (1951) A test of the precision of thin-section analysis by point counter, *Am. Min.*, vol. 36, p. 704-712.
- (1952) The finer-grained calcalkaline granites of New England, *Jour. Geol.*, vol. 60, p. 207-254.
- CLARK, H. (1942) Effect of wetting and of simple compression on the thermal conductivity of certain rocks, in Birch, Francis, *et al.*, Editors, Handbook of physical constants, Geol. Soc. Am. Sp. Paper no. 36, p. 258.
- COES, L. (1953) A new dense crystalline silica, *Science*, vol. 118, p. 131.
- CROSS, C. W., IDDINGS, J. P., PIRSSON, L. U., AND WASHINGTON, H. S. (1902) A quantitative chemico-mineralogical classification and nomenclature of igneous rocks, *Jour. Geol.*, vol. 10, p. 555-690.
- DALY, R. A. (1914) *Igneous rocks and their origin*, New York, McGraw-Hill, 563 p.
- DONNAY, GABRIELLE, AND DONNAY, J. D. H. (1952) The symmetry change in the high-temperature alkali-feldspar series, *Am. Jour. Sci.*, Bowen vol., p. 115-132.
- DUROCHER, J. (1857) *Essai de petrologie comparee*, *Ann. des Mines*, vol. 11, p. 217-259.
- ESKOLA, PENTTI (1939) in Barth, Correns, and Eskola, *Die Entstehung der Gesteine*, Part III, p. 263-407, Berlin, Julius Springer.
- FAIRBAIRN, H. W., AND SCHAIRER, J. F. (1952) A test of the accuracy of chemical analysis of silicate rocks, *Am. Min.*, vol. 37, p. 744-757.
- FLASCHEN, S. S., AND OSBORN, E. F. (1953) The system  $FeO-SiO_2-H_2O$  (Abstract), *Geol. Soc. Am., Bull.*, vol. 64, p. 1423.
- FRIEDMAN, IRVING (1950) Immiscibility in the system  $H_2O-Na_2O-SiO_2$ , *Jour. Am. Chem. Soc.*, vol. 72, p. 4570-4574.
- GORANSON, R. W. (1931) The solubility of water in granite magmas, *Am. Jour. Sci.*, vol. 22, p. 481-502.
- (1932) Some notes on the melting of granite, *Am. Jour. Sci.*, vol. 23, p. 227-236.
- (1938) Silicate-water systems: Phase equilibria in the  $NaAlSi_3O_8-H_2O$  and  $KAlSi_3O_8-H_2O$  systems at high temperatures and pressures, *Am. Jour. Sci.*, vol. 35-A, p. 71-91.

- GREIG, J. W., SHEPPARD, E. S. AND MERWIN, H. E. (1931) Melting temperatures of granite and basalt, Carnegie Inst. of Washington Year Book, no. 30, p. 75-78.
- GUTENBERG, B. (1951) Internal constitution of the earth, New York, Dover, 439 p.
- HARKER, A. (1939) Metamorphism, London, Methuen & Co., Ltd., 362 p.
- HOLMQVIST, P. J. (1901) Rapakivstruktur och granitstruktur, *Föredr. Geol. För. Stockh. Förh.*, Bd. 23, p. 150-161.
- IDDINGS, J. P. (1895) Absarokite-shoshonite-banakitite series, *Jour. Geol.*, vol. 3, p. 940-942.
- ITO, T. (1925) Zonal growth of plagioclase and soda-orthoclase in syenitic magma, *Jour. Faculty Sci. Tokyo*, sect. 2, vol. 1, p. 105-109.
- JAHNS, RICHARD H. (1955) The study of pegmatites, *Econ. Geol.*, Fiftieth Anniv. vol., p. 1025-1130.
- JEFFRIES, H. (1941) The thermal state of the earth, *Am. Jour. Sci.*, vol. 239, p. 825-835.
- JOHANNSEN, A. (1917) Suggestions for a quantitative mineralogical classification of igneous rocks, *Jour. Geol.*, vol. 25, p. 63-97.
- KEITH, M. L., AND TUTTLE, O. F. (1952) Significance of variation in the high-low inversion of quartz, *Am. Jour. Sci.*, Bowen vol., p. 203-280.
- KOZU, S., AND ENDO, Y. (1921) X-ray analysis of adularia and moonstone and the influence of temperature on the atomic arrangement of these minerals, *Tohoku Imp. Univ. Sci. Repts.*, ser. 3, vol. 1, no. 1, p. 1-17.
- LARSEN, E. S., IRVING, J., GONYER, F. A., AND LARSEN, E. S., III (1938) Petrologic results of a study of the minerals from the tertiary volcanic rocks of the San Juan Region, Colorado, *Am. Min.*, vol. 23, p. 417-429.
- LAVES, F. (1952) Phase relations of the alkali feldspars, *Jour. Geol.*, vol. 60, p. 436-450, 549-574.
- MACKENZIE, W. S. (1952) The effect of temperature on the symmetry of high-temperature soda-rich feldspars, *Am. Jour. Sci.*, Bowen vol., p. 319-342.
- (1952) Optical and X-ray studies of alkali feldspars, *Carnegie Inst. of Washington Year Book*, no. 51, p. 50.
- (1954) The orthoclase microcline inversion, *Min. Mag.*, vol. 30, p. 354-366.
- MOREY, G. W., AND FENNER, C. N. (1917) The ternary system  $H_2O-K_2SiO_3-SiO_2$ , *Jour. Am. Chem. Soc.*, vol. 39, p. 1173-1229.
- MOREY, G. W., AND INGERSON, EARL (1937) The pneumatolytic and hydrothermal alteration and synthesis of silicates, *Econ. Geol.*, vol. 32, p. 607-760.
- MOREY, G. W., AND INGERSON, EARL (1938) The system, water-sodium disilicate, *Am. Jour. Sci.*, vol. 35-A, p. 217-225.
- MOSESMAN, M. A., AND PITZER, K. S. (1941) Thermodynamic properties of the crystalline forms of silica, *Am. Chem. Soc. Jour.*, vol. 63, p. 2348-2356.
- NOBLE, J. A. (1948) Evidence for a steepening of geothermal gradients in some deep mines and drill holes, *Am. Jour. Sci.*, vol. 246, p. 426-440.
- OSBORN, E. F., AND SCHAIRER, J. F. (1941) The ternary system pseudowollastonite-akermanite-gehlenite, *Am. Jour. Sci.*, vol. 239, p. 715-763.
- POPOFF, B. (1903) Über Rapakivi aus Russland, *Trav. Soc. St. Petersburg*, vol. 31, p. 175-266.
- RAMBERG, H. (1952) The origin of metamorphic and metasomatic rocks, Chicago, Univ. of Chicago Press, 317 p.
- RICCI, JOHN E. (1951) The phase rule and heterogeneous equilibrium, New York, D. van Nostrand, 505 p.
- SAHAMA, TH. G. (1945) On the chemistry of the East Fennoscandian rapakivi granites, *Compt. Rend. Soc. Geol. Fin.*, no. 18, p. 15-64.
- SCHAIRER, J. F. (1950) The alkali-feldspar join in the system  $NaAlSi_3O_8-KAlSi_3O_8-SiO_2$ , *Jour. Geol.*, vol. 58, p. 512-518.
- SCHAIRER, J. F., AND BOWEN, N. L. (1935) Preliminary report on equilibrium relations between feldspathoids, alkali-feldspars, and silica, *Trans. Am. Geophy. Union*, Sixteenth Annual Meeting, p. 325-328.
- (1947) Melting relations in the systems  $Na_2O-Al_2O_3-SiO_2$  and  $K_2O-Al_2O_3-SiO_2$ , *Am. Jour. Sci.*, vol. 245, p. 193-204.

- SCHWARTZ, G. M. (1931) Intergrowths of bornite and chalcopyrite, *Econ. Geol.*, vol. 26, p. 186-201.
- SEDERHOLM, J. J. (1928) On orbicular granites, spotted and nodular granites, and on the rapakivi texture, *Bull. Com. Geol. Fin.*, no. 83, 105 p.
- SPENCER, E. (1930) A contribution to the study of moonstone from Ceylon and other areas and of the stability relations of the alkali-feldspars, *Min. Mag.*, vol. 22, p. 291-367.
- (1937) The potash-soda-feldspars. I. Thermal stability, *Min. Mag.*, vol. 24, p. 453-494.
- (1938) The potash-soda-feldspars. II. Some applications to petrogenesis, *Min. Mag.*, vol. 25, p. 81-118.
- SPICER, H. C. (1942) Observed temperatures in the earth's crust, in Birch, Francis, *et al.*, *Editors*, Handbook of physical constants, *Geol. Soc. Am. Spec. Paper* 36, p. 279-292.
- TILLEY, C. E. (1949) An alkali facies of granite at granite-dolomite contacts in Skye, *Geol. Mag.*, vol. 86, p. 81-93.
- (1951) The zoned contact-skarns of the Broadford area, Skye, *Min. Mag.*, vol. 29, p. 621-666.
- TURNER, F. J., AND VERHOOGEN, J. (1951) Igneous and metamorphic petrology, New York, McGraw-Hill, 602 p.
- TUTTLE, O. F. (1948) A new hydrothermal quenching apparatus, *Am. Jour. Sci.*, vol. 246, p. 628-635.
- (1949) Two pressure vessels for silicate-water studies, *Geol. Soc. Am., Bull.*, vol. 60, p. 1727-1729.
- (1951) Studies in feldspar equilibria at the Geophysical Laboratory, Washington, *Min. Mag.*, vol. 29, p. 757-758.
- (1952) Origin of the contrasting mineralogy of extrusive and plutonic salic rocks, *Jour. Geol.*, vol. 60, p. 107-124.
- (1952) Optical studies on alkali feldspars, *Am. Jour. Sci.*, Bowen vol., p. 553-567.
- TUTTLE, O. F., AND BOWEN, N. L. (1950) High temperature albite and contiguous feldspars, *Jour. Geol.*, vol. 58, p. 572-583.
- TUTTLE, O. F., AND ENGLAND, J. L. (1955) Preliminary report on the system  $SiO_2-H_2O$ , *Geol. Soc. Am., Bull.*, vol. 66, p. 149-152.
- TUTTLE, O. F., AND FRIEDMAN, I. (1948) Liquid immiscibility in the system  $H_2O-Na_2O-SiO_2$ , *Jour. Am. Chem. Soc.*, vol. 70, p. 919-926.
- TUTTLE, O. F., AND KEITH, M. L. (1954) The granite problem: Evidence from the quartz and feldspar of a tertiary granite, *Geol. Mag.*, vol. 91, p. 61-72.
- VAN ORSTRAND, C. E. (1951) Observed temperatures in the earth's crust, in Gutenberg, B., *Editor*, Internal constitution of the earth, New York, Dover, p. 107-149.
- VOGT, J. H. L. (1906) Physikalisch-chemische Gesetze der krystallisations-folge in eruptivgesteinen, *Tsch. Min. Pet. Mitt.*, vol. 25, p. 402-403.
- (1926) The physical chemistry of the magmatic differentiation of igneous rocks. II. On the feldspar diagram  $Or:Ab:An$ , *Skrifter Utgitt av Det Norske Videnskaps-Akademi I Oslo*. I. Mat. Naturvid. Klasse, no. 4, 101 p.
- WAGER, L. R., STEWART, F. H., AND KENNEDY, W. Q. (1948) Guide to Excursion C 14: Skye and Morar: XVIII Intern. Geol. Cong., Great Britain, 26 p.
- WAHL, W. (1925) Die Gesteine des Wiborger Rapakivgebietes, *Fennia*, vol. 45, no. 20, p. 105-126.
- WARREN, C. H. (1913) Petrology of the alkali granites and porphyries of Quincy and the Blue Hills, Massachusetts, *Proc. Am. Acad. Arts and Sci.*, vol. 49, p. 203-230.
- WASHINGTON, H. S. (1906) The Roman-Comagmatic region, *Carnegie Inst. of Washington*, pub 57, 199 p.
- (1917) Chemical analyses of igneous rocks, *U. S. Geol. Survey Professional Paper* 99, 1201 p.
- YAGI, K. (1953) Petrochemical studies on the alkalic rocks of the Morotu District, Sakhalin, *Geol. Soc. Am., Bull.*, vol. 64, p. 769-810.
- YODER, H. S. (1950) High-low quartz inversion up to 10,000 bars, *Am. Geophy. Union Trans.*, vol. 31, p. 827-835.
- (1952) Change in melting point of diopside with pressure, *Jour. Geol.*, vol. 60, p. 364-374.
- (1952) The  $MgO-Al_2O_3-SiO_2-H_2O$  system and the related metamorphic facies, *Am. Jour. Sci.*, Bowen vol., p. 569-627.

# INDEX

- Absence of prism faces on synthetic quartz, 28
- Adiabatic crystallization, 69
- Albite
  - content of natural orthoclase feldspar by (201) spacing, 11
  - high, 14, 15, 17
  - hydrothermally crystallized, 14
  - inversions in, 16, 38
  - low, 14, 16
  - monoclinic, 16, 39
  - optic axial angle, 14
  - pressure-temperature relations, 16
  - triclinic, 15, 16
- Albite-water (*See* System  $\text{NaAlSi}_3\text{O}_8\text{-H}_2\text{O}$ ), 35, 46
- Alkali-alumina ratio of granitic rocks, 88
- Alkali feldspar
  - composition of by (201) spacing, 10, 11, 42
  - high albite in, 107
  - in Skye granite, modal analyses, 112, 115
  - low albite in, 107
  - optic axial angle, 105
  - single crystal X-ray studies, 107
  - size of, 105
  - transitional optics, 105, 106
  - 201 spacing, 106
- Alumina-silica order-disorder in potassium feldspar, 5, 26
- Amphibole from Quincy granite, 92
- stability, 92, 93
- Analyses, modal
  - alkali feldspar in Skye granites, 112, 115
  - plagioclase feldspar in Skye granites, 113, 115
  - quartz in Skye granites, 112, 115
  - Skye granites, 112, 113, 115
- Anthophyllite, 91
- Apparatus, hydrothermal quenching, 8, 35
- Bakken, Ruth, 15, 16
- Batholith, origin, 124, 180
- Beginning of melting
  - earth's crust, 121, 122
  - feldspar, 39
  - Quincy granite, 82
  - synthetic mixtures, 83
  - Westerly granite, 80, 83
- Biotite
  - primary phase in granites, 83
  - Skye granites, 109
- Birch, F., 119
- Bowen, N. L., 5, 10, 14, 15, 17, 18, 64, 80, 86, 91, 94, 99, 107, 128, 139
- Buddington, A. F., 135
- Buerger, M. J., 95
- Bunsen, R., 117
- Chayes, F., 77, 79, 80, 98, 100, 101, 108, 109, 111, 112, 113, 115
- Clark, H., 119
- Classification
  - granites, syenites, and nepheline syenites, 127-130
  - rocks, 126
- Coes, L., 33
- Cold-seal pressure vessel, 10, 11
- Composition
  - feldspars, 131
  - perthite using (201) spacing, 20, 22
  - discrepancies, 22, 23
  - sanidine cryptoperthites, 20
  - orthoclase cryptoperthites, 22
  - vapor in equilibrium with hydrous granitic melts, 89-91
- Compositional variations
  - rhyolite, 77
  - trachyte, 77
- Control of fractionation by viscosity, 77
- Crystallization
  - feldspar, in rhyolites, trachytes, and phonolites, 130-136
  - in system  $\text{NaAlSi}_3\text{O}_8\text{-KAlSi}_3\text{O}_8\text{-H}_2\text{O}$ , 46, 47
  - equilibrium, 46-48
  - fractional, 47
  - isobaric, 46, 48
  - in system  $\text{NaAlSi}_3\text{O}_8\text{-KAlSi}_3\text{O}_8\text{-SiO}_2\text{-H}_2\text{O}$ , 5, 66-68
  - adiabatic, 69
  - as control of granite compositions, 77
  - equilibrium, 66, 67
  - fractional, 64, 66
  - isobaric, 63-67
  - isothermal, 67-69
  - relation to viscosity, 77
  - sluggishness, 6
  - trend, 77
  - in "dry" system  $\text{NaAlSi}_3\text{O}_8\text{-KAlSi}_3\text{O}_8\text{-SiO}_2$ , 5
  - glass, 39
- Core of plagioclase, 134
- Cristobalite, 29, 32
- field, 29
- liquidus, 31
- Cross, C. W., 88

- Crucibles  
open, 6, 7  
platinum, 6  
method of fabricating, 7
- Cryptoperthites  
low sanidine-high albite, 19-21  
microcline, 26  
orthoclase, 16, 21-23, 35
- Crystalline material, experimental methods for use of, 11
- Curve, pressure-temperature  
tridymite-cristobalite, 29, 32  
tridymite-quartz, 29, 39, 40
- Daly, R. A., 117
- Depth to complete melting in earth's crust, 122
- Determination of  
liquidus, experimental methods, 11  
solidus, experimental methods, 11, 12  
solvus  
high sanidine-high albite, 18, 40  
low sanidine-high albite, 19  
metastable, 25  
microcline-low albite, 26  
orthoclase-low albite, 26  
water content of glasses, 13, 31, 54, 58
- Diagram, isobaric, 40, 50, 54-56
- Discrepancies in composition of perthite using  $(\bar{2}01)$  spacing, 22, 23
- Donnay, G., 15, 38
- Donnay, J. D. H., 15, 38
- Dry melting, 5
- "Dry" system  $\text{NaAlSi}_3\text{O}_8\text{-KAlSi}_3\text{O}_8\text{-SiO}_2$ , 5  
crystallization, 5  
preparation of glasses, 5
- Durocher, J., 117
- Earth's crust  
beginning of melting, 121, 122  
depth to complete melting, 122  
geothermal gradients in, 121, 122  
granitic magma, 117, 118, 126  
zone of melting, 123  
significance, 124-126
- Effect of bubbles on water content of glasses, 14
- Effect of particle size on water content, 14
- Endo, Y., 44
- England, J. L., 31, 92
- Equilibrium crystallization, 46-48, 66, 67
- Equipment  
experimental, 8-10  
hydrothermal, 9-11
- Eskola, P., 84
- Eutectic, isobaric "ternary", 75  
position of at 4000 bars pressure, 74
- Evolution of granitic texture, 137-141  
comparison to sulfide textures, 139  
influence of volatiles, 39
- Experimental equipment, 8-10
- Experimental methods, 8-14  
determination of liquidus, 11  
determination of solidus, 11, 12  
use of crystalline material, 11
- Fairbairn, H. W., 6
- Feldspar  
alkali, 103  
composition of by  $(\bar{2}01)$  spacing, 10, 11, 42  
high albite, 107  
low albite, 107  
optic axial angle, 105  
single crystal X-ray studies, 107  
size, 105  
transitional optics, 105, 106  
 $\bar{2}01$  spacing, 106  
as geologic thermometer, 28  
environment for unmixing, 42, 50, 128, 139, 142  
liquidus, 39  
mantled, 96  
metastable solvus, 43  
minimum, 40  
natural, content of orthoclase by  $(\bar{2}01)$  spacing, 11  
ovoid alkali, 95  
order-disorder, 26  
plagioclase, 107  
high-temperature modification, 107  
low-temperature modification, 107  
X-ray determination, 109  
potash, order-disorder, 26  
potassium, 17  
inversions, 109
- Fenner, C. N., 84
- Field  
cristobalite, 29  
leucite, 37, 41
- Field studies, 5, 101-104
- Flaschen, S. S., 92
- Fractional crystallization, 47, 64, 66
- Friedman, I., 85, 86
- Gap, miscibility, 26
- Geothermal gradient, 117, 118, Fig. 59  
change with depth, 118  
factors influencing, 118-121

- influence of thermal conductivity at elevated temperatures, 120
- Glass  
crystallization, 39  
use of in determining liquidus and solidus, 11, 12  
ignition loss, 13  
preparation of in "dry" system  $\text{NaAlSi}_3\text{O}_8\text{-KAlSi}_3\text{O}_8\text{-SiO}_2$ , 5
- Goranson, R. W., 8, 31, 36, 37, 41, 46, 84
- Gradient, geothermal, 117, 118, Fig. 59  
change with depth, 118  
factors influencing, 118-121  
influence of thermal conductivity at elevated temperatures, 120
- Granite  
beginning of melting of Westerly, Rhode Island, and Quincy, Massachusetts, 80, 83  
classification, 129, 130  
hypersolvus, 129  
magma, 117  
movement of hydrous, 125  
water content, 78  
one-feldspar, 98  
relations to other granites, 99
- Rapakivi, 93-98  
genesis, 93-95  
mantled feldspars, 97, 98  
ovoid feldspars, 95, 96  
two generations of feldspars, 97, 98  
views on origin, 93, 94
- Skye, 98  
alkali feldspar, 112, 113  
modal analysis, 110-112  
normative Ab-Or-Q content, 113, 116  
plagioclase feldspar content, 113  
quartz content, 112  
subsolvus, 129
- textures, 137-142  
evolution, 137-142  
two-feldspar, 130  
Westerly, Rhode Island, 99-101
- Granitic magma in earth's crust, 117, 118, 126
- Granitic rocks, alkali alumina ratio, 88
- Granitic texture  
comparison to sulfide textures, 139  
evolution, 137-141  
influence of volatiles, 139
- Greig, J. W., 83
- Grunerite, 92  
stability, 92
- Gutenberg, B., 118
- Harker, A., 141  
Heat production by radioactivity, 121  
High albite, 14, 15, 17  
High quartz, 28  
High sanidine, 17, 18  
Holmqvist, P. J., 93  
Homogenization  
perthite, 23  
orthoclase cryptoperthite, 23  
sanidine cryptoperthite, 20
- Hydrothermal  
crystallization of albite, 14  
equipment for experimentation, 9-11  
quenching apparatus, 8, 35  
Hydrous granitic magmas, 125  
movement, 125  
Hydrous minerals, 5  
Hypersolvus granite, 129
- Iddings, J. P., 88, 135
- Ignition loss of glasses, 13
- Inversion  
albite, 16, 38  
quartz-tridymite, 29  
studies of quartz, 101-103
- Isobaric diagram, 40, 50, 54-56
- Isobaric "ternary" eutectic, 25  
position at 4000 bars pressure, 74
- Isobaric "ternary" minimum  
control of composition, 77  
importance of in magmatic composition, 77  
location, 74  
position of as a function of pressure, 75
- Isothermal crystallization, 67
- Ito, T., 135
- Jahns, R. H., 93
- Jefferies, H., 126
- Johannsen, A., 126
- Kalsilite, 5
- Keith, M. L., 101, 103
- Kozu, S., 44
- Laboratory studies, importance, 5
- Larsen, E. S., 131, 136
- Laves, F., 17, 25, 26, 35, 36
- Leucite, field, 37, 41
- Liquids, viscosity of, 76
- Liquidus  
cristobalite, 31  
determination of relations, 15  
feldspar, 39



- Liquidus—(Cont'd.)  
 silica, 32, 43  
 stability fields, 70–73, 96–98  
 cause of changing, 70
- Low albite, 14, 16
- Low quartz, 28, 32
- Low sanidine, 17
- Low sanidine-high albite cryptoperthites, 19–21  
 microcline, 26  
 orthoclase, 16, 21–23, 25
- MacKenzie, W. S., 15, 16, 17, 38, 73
- Magma, granite, 117  
 in earth's crust, 117, 118, 126  
 movement of hydrous, 125
- Mantled feldspar, 96
- Measurement and control  
 pressure, 8  
 temperature, 8
- Melting  
 beginning of, 121, 122  
 depth of complete, 122, 123  
 dry, 5  
 granite, 80–84, Fig. 43  
 Quincy, Massachusetts, 80, Fig. 43  
 Westerly, Rhode Island, 80, Fig. 43  
 metastable, 5  
 zone of, 123–125
- Merwin, H. E., 83
- Metamorphism, regional, 126
- Metastable melting, 5
- Metastable mixing, 25
- Metastable solvus of feldspar, 43
- Method of fabricating platinum crucibles, 7
- Microcline, 17
- Microperthites, 43
- Minerals, hydrous, 5
- Minimum  
 feldspar, 40  
 isobaric "ternary"  
 control of composition, 77  
 importance of in magmatic compositions, 77  
 location, 74  
 position of as function of pressure, 75
- Miscibility  
 complete in sanidine-albite series, 20  
 gap, 26  
 incomplete in orthoclase cryptoperthites, 26
- Mixing, metastable, 26
- Mixtures, preparation, 6  
 chemicals used for, 6  
 materials used, 6  
 possible errors introduced during, 6
- Modal analyses  
 alkali feldspar in Skye granites, 112, 115  
 plagioclases in Skye granites, 113, 115  
 quartz in Skye granites, 112, 115  
 Skye granites, 112, 113, 115
- Modifications of plagioclase, 108
- Monoclinic albite, 16, 39
- Moonstone, 19, 44
- Morey, G. W., 33, 84, 86
- Mosesman, M. A., 28, 31
- Nepheline, 5
- Nepheline syenites, 5
- Noble, J. A., 118, 119
- One-feldspar granites, 98  
 relation to other granites, 99
- Open crucibles, 6, 7
- Optic axial angle of albite, 14
- Optical studies on plagioclase, 108
- Order-disorder in feldspar, 26
- Origin of batholiths, 124
- Orthoclase, 16, 17, 22
- Orthoclase cryptoperthite  
 homogenization, 23  
 incomplete miscibility, 26
- Osborn, E. F., 64
- Oscillatory zoning, 69
- Perthite, 43, 44, 49–51, 140, 141  
 composition of using (201) spacing, 20, 22  
 discrepancies in, 22, 23  
 orthoclase cryptoperthites, 22  
 sanidine cryptoperthites, 20  
 homogenization, 23
- Phenocrysts, reaction of plagioclase, 134
- Phonolites, 5
- Pirsson, L. V., 88
- Pitzer, K. S., 28, 31
- Plagioclase  
 core, 134  
 early, dependent on lime content, 136, 137  
 feldspar, 107  
 high-temperature modification, 107  
 low-temperature modification, 107  
 X-ray determination, 109  
 modifications, 108  
 optical studies, 108  
 Skye granites, modal analyses, 113, 115  
 X-ray studies, 109
- Platinum crucibles, 6  
 method of fabricating, 7
- Popoff, B., 94

- Position of thermal trough, 75, 76, Fig. 23
- Potash feldspar, order-disorder, 26
- Potassium feldspar, 17  
 inversions, 118
- Preparation of mixtures, 6  
 chemicals used for, 6  
 materials used, 6  
 possible errors introduced during, 6
- Pressure  
 effect of on thermal trough, 78, Fig. 23  
 measurement and control, 8
- Pressure-temperature relations in albite, 16
- Pressure vessel, 10, 11  
 cold seal, 9  
 internally heated, 31
- Primary phase in granites, biotite, 83
- PTX diagram for silica, 31
- Pyroxene  
 primary phase in granites, 84, 85  
 Skye in, 109
- Quartz  
 absence of prism faces on synthetic, 28  
 high, 28  
 inversion studies, 101–103  
 low, 28, 32  
 (1010) spacing of as standard, 12, 13  
 Skye granites, modal analyses, 112, 115  
 stability, 28, 29
- Quartz-cristobalite, 31
- Quartz-tridymite  
 heat of transformation, 30  
 inversion, 29  
 melting, 30  
 slope of PT curve for, 29
- Quincy granite  
 amphibole, 92  
 stability, 92, 93  
 beginning of melting, 82
- Radioactivity, heat production, 121
- Ramberg, H., 84
- Rapakivi granite, 93–98  
 genesis, 93–95  
 mantled feldspar, 97, 98  
 ovoid feldspar, 95, 96  
 two generations of feldspars, 97, 98  
 views on origin, 93, 94
- Reaction of plagioclase phenocrysts, 134
- Regional metamorphism, 126
- Relations, determination of liquidus and solidus,  
 11, 12
- Residual solution, 84, 89  
 formed by crystallizing granite magma, 88, 89
- Rhyolite  
 compositional variation, 77  
 water content, 78
- Ricci, J. E., 33
- Riebeckite, 92  
 stability, 92
- Rocks, salic, 5  
 classification, 126
- Rosenqvist, I. Th., 15, 16
- Sahama, Th. G., 93, 95
- Salic rocks, 5  
 classification, 126
- Sanidine, 16, 19  
 high, 17, 18  
 low, 17
- Sanidine-albite series, complete miscibility in, 20
- Sanidine cryptoperthites, 20
- Schairer, J. F., 5, 6, 17, 38, 64, 86
- Schwartz, G. M., 139
- Sealed-tube technique, 8
- Sederholm, J. J., 94, 95, 96, 97, 98
- Shepherd, E. S., 83
- Silica  
 liquidus of, 32  
 PTX diagram for, 31  
 solubility in water vapor, 31  
 stable forms of, 29  
 water determination, 31
- Silica glass, water content, 31
- Skye, granites, 98–117  
 alkali feldspar, 103, 104  
 biotite, 109  
 mineralogy, 102–108  
 modal analyses, 12, 113, 115  
 normative Ab-Or-Q content, 113, 116  
 plagioclase feldspar content, 113  
 pyroxene, 84, 85  
 quartz content, 112
- Solidus, determination of relations, 11–13
- Solubility of silica in water vapor, 31
- Solution, residual, 84, 89  
 formed by crystallizing granite magmas, 88, 89
- Solvus  
 determination, 39  
 high sanidine-high albite, 18, 40  
 low sanidine-high albite, 19  
 metastable, 25  
 microcline-low albite, 26  
 orthoclase-low albite, 26
- Spencer, E., 16, 17, 20–26, 44, 105
- Spicer, H. C., 118
- Stable forms of silica, 29

- Stability of  
 amphiboles, 91, 93  
 anthophyllite, 91  
 grunerite, 92  
 Quincy granite, 92, 93  
 riebeckite, 92
- Stability fields on the liquidus, 70-73  
 cause of changing, 70
- Studies, field, 5, 101-104
- Subsolvus granite, 129
- Sulfides, unmixing, 139-141
- Syenite, 129  
 classification, 127-130  
 nepheline, 129  
 classification, 127-130
- Synthetic compositions, water content of, 57
- Synthetic mixtures, beginning of melting, 83
- System  $K_2O-Na_2O-Al_2O_3-SiO_2$ , 87  
 residual solutions, 87
- System  $K_2O-Al_2O_3-SiO_2-H_2O$ , 85  
 residual solutions, 86
- System  $KAlSi_3O_8-H_2O$ , 36
- System  $KAlSi_3O_8-SiO_2-H_2O$ , 53
- System  $Na_2O-Al_2O_3-SiO_2-H_2O$ , 86
- System  $NaAlSiO_4$ (nepheline)- $KAlSiO_4$ (kalsilite)- $SiO_2$ , 5
- System  $NaAlSi_3O_8-H_2O$ , 35, 36  
 beginning of melting in, 36  
 liquidus, 35  
 PT relations, 36  
 range of melting, 36
- System  $NaAlSi_3O_8-KAlSi_3O_8$ , 17  
 anorthoclases, 17, 19
- System  $NaAlSi_3O_8-KAlSi_3O_8-H_2O$ , 37, 46, 54  
 albite field, 52  
 beginning of melting, 40  
 complete series of solid solution, 38  
 critical phenomena, 48  
 crystallization, 46  
 of mixtures, 39, 46, 47  
 determination of solvus, 42  
 effect of water-vapor pressures on minimum, 40  
 equilibrium crystallization, 46  
 effect of pressures, 87  
 fractional crystallization, 47  
 influence of pressure, 48  
 inversion in crystals, 39  
 leucite field, 41, 42  
 minimum, 41  
 composition, 41  
 determination, 40  
 mixing and unmixing, 43
- solidus, 40  
 determination, 43
- solvus, 42  
 determination, 43  
 metastability of portion, 43
- tridymite field, 50
- System  $NaAlSi_3O_8-KAlSi_3O_8-CaAl_2Si_2O_8$ , 131  
 crystallization, 131  
 solid solution, 131
- System  $NaAlSi_3O_8-KAlSi_3O_8-SiO_2$ , "dry", 5  
 crystallization, 5  
 preparation of glasses, 5
- System  $NaAlSi_3O_8-SiO_2-H_2O$ , 50  
 albite-quartz boundary, 52  
 albite-tridymite boundary, 52  
 appearance of low quartz, 52  
 TX diagram, 52
- System  $NaAlSi_2O_8-KAlSi_3O_8-SiO_2-H_2O$ , 61  
 adiabatic crystallization, 69  
 determination of minimum, 63, 74  
 equilibrium crystallization, 63, 66, 67  
 fractional crystallization, 63-67  
 isobaric crystallization, 63, 64  
 boiling of liquid, 64  
 equilibrium, 63, 67  
 fractional, 63, 64  
 isothermal crystallization, 67-69  
 heat of crystallization, 67  
 liquidus determinations, 61  
 location of isobaric "minimum", 75  
 "ternary" eutectic, 72  
 "ternary" minimum, 71  
 three-phase triangles, 62  
 tie lines, 58  
 unique "invariant" point, 72  
 zoning in plagioclase, 69
- System  $SiO_2-H_2O$ , 31  
 cristobalite stability, 32  
 liquidus, 32  
 liquidus lowering, 31  
 PTX relations, 34  
 quadruple points, 34  
 tridymite stability, 32  
 triple points, 33  
 water determination of glass, 31
- Technique, sealed-tube, 8
- Temperature, measurement and control, 8
- Ternary "eutectic", 71
- Ternary "minimum", 74  
 relation of water content to, 98  
 relation of water content of rhyolite to, 79

- Textures of granite, 137-142  
 evolution, 137-142
- Thermal conductivity, 120
- Thermal gradient, 120
- Thermal trough, 75  
 effect of pressure, 78, Fig. 23  
 importance, 76, 77  
 position, 75, 76, Fig. 23
- Tilley, C. E., 109
- Trachyte, compositional variation, 77
- Transport, vapor, 6, 90, 91
- Triclinic albite, 15, 16
- Tridymite, 28, 29, 32  
 stability, 29
- Turner, F. J., 84, 126
- Two-feldspar granites, 130
- Tuttle, O. F., 8, 10, 13, 14, 17, 18, 19, 24, 26, 28, 31, 85, 91, 93, 99, 101, 103, 104, 107, 129, 130, 138, 144, 145, 150, 151, 154, 191, 192, 208
- Unmixing  
 feldspars, environment, 42, 50, 128, 139, 142  
 sulfides, 139-141
- Van Orstrand, C. E., 118
- Vapor  
 in equilibrium with hydrous granitic melts, composition of, 89-91  
 prevention of transport, 6  
 transport, 90, 91
- Verhoogen, J., 84, 126
- Vessel, pressure, 9
- cold seal, 10, 11  
 internally heated, 31
- Viscosity  
 control of fractionation, 77  
 liquid, 76
- Vogt, J. H. L., 94, 131
- Volatiles, 5
- Wager, L. R., 115
- Wahl, W., 93, 94
- Warren, C. H., 92
- Washington, H. S., 77, 88, 116, 135, 137
- Water content  
 determination of in glasses, 13, 31, 54, 58  
 effect of bubbles, 14  
 effect of particle size, 14  
 granite magmas, 78  
 relation to "ternary minimum", 79  
 rhyolite, 78  
 silica, 31  
 silica glass, 31  
 synthetic compositions, 57
- Westerly granite, 99-101  
 beginning of melting, 83
- X-ray studies of plagioclase, 109
- Yagi, K., 135
- Yoder, H. S., 28, 69
- Zone of melting in earth's crust, 123  
 significance, 124-126
- Zoning, oscillatory, 69

